CRANFIELD INSTITUTE OF TECHNOLOGY

SCHOOL OF MECHANICAL ENGINEERING

PhD Thesis

A.M.Y. RAZAK

Dynamic Simulation of Centrifugal Compressors in a Process Environment

Supervisor: Dr. R.L. Elder

October 1984

To My Mother I Dedicate This Work

SUMMARY

The recent developments in process plant design have made it desirable that a better understanding of transient compressor performance within the process plant be gained. The model outlined in this thesis is capable of representing most types of process plants. Further the number of degress of freedom, plus the dynamic flexibility of a polytropic analysis allow any system transient to be simulated, including compressor surge. A computer program has been developed from the model and validated using a small centrifugal compressor. The results showing successful simulation of compressor transient behaviour (including surge) are given. The model was then applied to study the transient behaviour of a natural Gas Transmission station. The model successfully highlighted compressor surge problems under certain operative conditions. This surge phenomenon is present in the transmission station and a possible solution to the problem was suggested due to the better understanding of dynamic response of station.

ACKNOWLEDGEMENTS

The author would like to thank the various members of the School of Mechanical Engineering at Cranfield Institute of Technology who have given help and advice during this project. In particular Dr. R.L. Elder and Mrs. M.E. Gill for their advice and Mr. C.J. Austin of British Gas Corporation for releasing the necessary information for use in this project, and for their continuing interest.

CONTENTS

LIST OF FIGURES

NOTATION

A	Area	(m^2)
Cp	Specific Heat at Constant Pressure	(J/kgK)
Cv	Specific Heat at Constant Volume	(J/kgK)
c	Velocity	(m/s)
d	Diameter	(m)
e	Polytropic Efficiency	(-)
E	Energy	(J)
E_{net}	Net Input of Energy into an Element	(J)
f	Pipe Resistance Coefficient	(-)
fp	Polytropic Head Factor	(-)
F	Body Force	(Pa)
F_{net}	Net Body Force Acting Within an Element	(Pa)
h	Integration Time-Step Length	(s)
H	Stagnation Enthalpy	(J/kg)
KE	Kinetic Energy	(J)
Ks	Static Pressure Coefficient	(-)
L	Length	(m)
m	Schultz Polytropic Index	(-)
M	Mach Number	(-)
M_W	Molecular Weight	(kg)
n	Polytropic Index	-)
N	Compressor Shaft Speed	(r.p.m.)
P_t	Stagnation Pressure	(pa)
P_s	Static Pressure	(Pa)

Q	Volumetric Flow Rate	(m^3/hr)
R	Gas Constant	(J/kgK)
Re	Reynold's Number	(-)
s	Surface Area	(m^2)
S	Compressor Speed	(m/sec)
t	Time	(s)
T_t	Stagnation Temperature	(K)
T_s	Static Temperature	(K)
U	Pipe Resistance Function	(-)
v	Volume	(m^3)
W	Mass Flow	(kg/s)
Wp	Polytropic Head	(J/kg)
Ws	Shaftwork	(J/kg)
x	Axial Direction	(-)
X	Compressibility Function	(-)
y	Pipe Resistance Function	(-)
Y	Compressibility Function	(-)
Z	Compressibility Factor	(-)
Δx	Element Length	(m)
ϵ	Surface Roughness	(m)
γ	Ratio of Specific Heats	(-)
ρ	Stagnation Density	(kg/m^3)

CHAPTER 1

1.0 INTRODUCTION

Until recently, relatively little attention has been paid to the prediction of transient behaviour of dynamic compressors, and the response rate of such compressors was established empirically during testing. Now, however, the transient behaviour is often predicted by mathematical models and a detailed knowledge of the dynamic response at the design stage is becoming increasingly important for the design and development of control systems. This is particularly the case in the aero gas turbine industry where it is common practice for manufacturers to be asked to guarantee the transient behaviour of their products when negotiating contracts.

A full analytical model considering all the aerodynamic factors are considered not practical, and much simplified one dimensional models based on the conservation of linear momentum and continuity have been developed for aero space industry. In spite of the limitations such a model has (i.e. element length) very promising results have been obtained. The steady state compressor characteristics have been used to introduce effects of the blading or impeller depending on the type of compressor being considered. (I.e. axial or centrifugal).

This trend has now been reflected in the process plant industry where the transients may be introduced by the operation of many process plant controls and/or the change in gas composition. Within such industry the use of large centrifugal compressors in application such as the compression of process gas, and especially natural gas transmission, is wide spread. Unlike the steady state performance of these machines the transient response are, as yet, little understood. Still less well understood is the interaction of these machines with plant controls during rapid transients such as compressor surge, sudden start up/shut down, and sudden operation of valves. Therefore the design of control systems to govern the behaviour of the plant during such transient

operation is difficult, and in many cases results in inefficient design due to, on the one hand, over specification, and on the other, under estimation which can lead to catastropic failure of critical plant components leading to high operation cost and/or repair.

The development of such computer models for the process industry must be more general and therefore such models should have the capability of simulating compressors operating in parallel and precise modelling of plant controls where transients are likely to be introduced. The transient effect due to change in gas composition must also be a feature. Further to this the model must have the ability of simulating compressor surge and have sufficient thermodynamic flexibility in order that various gases, that are commonly used in process industry, may be represented.

To gain this much needed understanding of the installed dynamic response of the compressor a research program was carried out involving British Gas Corporation and ICI Agricultural Division Ltd., which developed a mathematical model capable of simulating compressor transient performance, including compressor surge within the process environment. The model was originally developed for an aero-space application, and has been extensively modified for an industrial user where the working fluid need not necessarily be air. In addition to this transient data has been acquired using a small high speed centrifugal compressor (of a turbo-charger) for model validation purposes.

The availability of such models also enable the simulation of existing process plants where the plant may have suffered from compressor instabilities in the past, particularly those plants where a satisfactory solution to the instability problem was not found. Further to this, when plant modifications are planned the simulation of the transient response of the proposed system may highlight operational problems and remedies may be found at the planning stage. When compressor instabilities result in plant failure the model may be used to investigate the cause of failure.

The model was applied to study the dynamic response of a British Gas transmission station. The plant was selected as an

example because it offered both an engineering challenge sought and was a plant which had demonstrated operational problems which were associated with plant dynamics. The model has evolved to a state where many other process plants may be considered.

The model has the following potential uses:

(1) As a design tool so that a better understanding of the dynamic behaviour of process plants may be determined at the design stage.

(2) Improving the control systems of existing plants and highlighting operational problems associated with plant dynamic behaviour due to any modifications to the existing plant.

(3) Accident investigation associated with plant dynamics (particularly compressor surge).

(4) The model is also well equipped to handle both industrial axial and centrifugal compressor systems.

Further applications of the model may be considered in the field of turbo-charging of reciprocating engines. Although the method of characteristics has been used the technique described in this thesis is considered much simpler to use. Another example, is the transient effects due to the augmenting of thrust, by after-burning, low by-pass ratio fan engines. In the past such engines have suffered from low pressure compressor surge problems. It is felt that two dimensional models are required to fully analyse the transient behaviour of such engines. The potential to extend the current one-dimensional model to a two-dimensional model exist and are briefly discussed here under the heading Discussion and Suggestion For Further Work (chapter 7).

CHAPTER 2

2.0 THE MATHEMATICAL MODEL

The successful simulation of compressor transients requires that the model used must have sufficient flexibility to simulate compressor surge and the ability to represent non-ideal gases. The wide availability of steady state compressor characteristics describing compressor performance between upstream and downstream stations suggests the use of such data in any model. This also suggests the use of a one dimensional model neglecting the detailed modelling of secondary flow, rotating stall and other related three dimensional phenomenon.

Numerous compressor models have been developed to study the transient behaviour of industrial compressors although none (Ref.1-6) have the capability of simulating compressor surge. Fasol Ref. (5,6), however, has produced good results when simulating rapid transfers between stable compressor operator points and applies the model to a blast furnace plant where the flow may branch into other systems. In this respect the system considered there is similar, (to the problem considered in this thesis), but the ability to combine flows as in recycle loops was not considered (a feature available in the proposed model). The applicability of the techniques proposed in this thesis are considered to be more general than those of Fasol and the capability of simulating compressor surge is an added feature of the proposed model.

To achieve a concise model the flow has been assumed to be one dimensional. The transient basis of the model is achieved by considering the conservation relations in their dynamic form. Models of this type have been proposed previously, for instance the work of Kulberg et al (7), Willoh and Seldner (8), and Elder (9, 10, 11) suggests models which are capable of simulating compressor surge and Greitzer (12) has used similar models to that proposed here to simulate

post stall behaviour of compressors. These models, however, did not consider parallel flow path systems such as those described here.

The thermodynamic flexibility to model non-ideal gases has been much less generally considered although Davis (1) (in a simple dynamic model) used the quite powerful Bendict-Webb-Rubin equation of state. A more manageable method, however, is presented by Schultz (13), and is employed in the proposed model. The compressibility charts x, y and z referred to by Schultz are plotted in terms of reduced pressures and reduced temperatures. These charts are very much the same for all gases, therefore making it much easer to use.

2.1 Derivation of the Basic Dynamic Equation

The equations below result from an application of the continuity and momentum equations to the general element shown in fig. 2.1.

2.2 Continuity Equation

Writing the continuity equation in the integral form

$$-\int_{c.v} \frac{\partial \rho_s}{\partial t}\, dv = \int_{c.s} \rho\, c \,.\, d\, A \qquad \ldots.(2.1)$$

where A is the mean element area.

$$dv = A\, dx \qquad \ldots.(2.2)$$

and

$$\int_{c.s} \rho_s\, c\, dA = W_2 - W_1 \qquad \ldots.(2.3)$$

Substituting equations (2.2) and (2.3) in (2.1) gives

$$\int_{X_1}^{X_2} A \frac{\partial \rho_s}{\partial t} \,.\, dx = W_1 - W_2 \qquad \ldots.(2.4)$$

2.3 Momentum Equation

Writing the momentum equation in the integral form

$$-\int_{c.v} \frac{\partial(\rho_s c)}{\partial t} \cdot dv = \int_{wall} p_s \, dA - \int_{c.s} \rho_s c(c.dA) + F \qquad \ldots.(2.5)$$

where F ≡ total surface forces.

Now

$$\int_{c.s} \rho_s c(c.dA) = (p_s A + \rho_s c^2 A)_2 - (p_s A + \rho_s c^2 A)_1 \qquad \ldots.(2.6)$$

It is assumed the terms $\int_{wall} p_s \, dA + F$ in equation (2.5) may be expressed as a pressure force x mean flow area. Therefore

$$\int_{wall} p_s \, dA + F = - F_{net} \times A \qquad \ldots.(2.7)$$

Substituting equations (2.2), (2.5) and (2.7) in equation (2.6) gives

$$-\int_{X_1}^{X_2} A \frac{\partial(\rho_s c)}{\partial t} \cdot dx = (p_s A + \rho_s c^2 A)_2 - (p_s A + \rho_s c^2 A)_1 - F_{net} A \qquad \ldots.(2.8)$$

Substituting a mean element area A

$$\int_{X_1}^{X_2} \frac{\partial W}{\partial t} dx = A \left[(P_{t_1} - P_{t_2}) + F_{net} + (\tfrac{1}{2} \rho_s c^2)_1 - (\tfrac{1}{2} \rho_s c^2)_2 \right]$$

or

$$\frac{1}{A} \int_{X_1}^{X_2} \frac{\partial W}{\partial t} dx = P_{t_1} - P_{t_2} + F_{net} + \Delta KE \qquad \ldots.(2.9)$$

The change in kinetic energy (ΔKE) across a compressor stage is small. Therefore

$$\frac{1}{A}\int_{X_1}^{X_2}\frac{\partial W}{\partial t}\,dx = P_{t_1} - P_{t_2} + F_{net} \qquad \ldots.(2.10)$$

2.4 Lumped and Linearly Distributed Parameter

The solution of equations (2.4) and (2.10) present difficulties involving the partial derivative terms $\partial\rho_s/\partial t$ and $\partial w/\partial t$. An assumption about how the variables ρ and $\dot{w}$ vary across the element length is required in order to overcome this problem. Two such assumptions are considered, firstly that these parameters remain constant across the element and secondly these parameters vary linearly across the element. These assumptions give rise to the concept of lumped and linearly distributed parameter models respectively.

2.5 Lumped Parameter Model

Applying the lumped parameter concept;

$$\int_{X_1}^{X_2} A\frac{\partial\rho_s}{\partial t}\,dx = A\frac{d\rho_{s_2}}{dt}\Delta x \qquad \ldots.(2.11)$$

and

$$\frac{1}{A}\int_{X_1}^{X_2}\frac{\partial W}{\partial t}\,dx = \frac{1}{A_m}\frac{dw_1}{dt}\Delta x \qquad \ldots.(2.12)$$

Substituting equations (2.11) and (2.12) in equations (2.9) and (2.10) gives

$$\Delta x\, A\frac{d\rho_{s_2}}{dt} = W_1 - W_2 \qquad \ldots.(2.13)$$

$$\Delta x\frac{dw}{dt} = A\ (P_{t_1} - P_{t_2} + F_{net}) \qquad \ldots.(2.14)$$

2.6 Linearly Distributed Parameter Model

By applying the linearly distributed concept gives:

$$\int_{X_1}^{X_2} A\frac{\partial\rho_s}{\partial t}\,dx = \left(A_1\frac{d\rho_{s_1}}{dt} + A_2\frac{d\rho_{s_2}}{dt}\right)\frac{\Delta x}{2} \qquad \ldots.(2.15)$$

and

$$\frac{1}{A}\int_{X_1}^{X_2}\frac{\partial W}{\partial t}\,dx = \left(\frac{dW_1}{dt} + \frac{dW_2}{dt}\right)\frac{\Delta X}{2A_2} \qquad \ldots.(2.16)$$

Substituting equations (2.15) and (2.16) in equations (2.9) and (2.10) gives

$$A_1\frac{d\rho_{s_1}}{dt} + A_2\frac{d\rho_{s_2}}{dt} = \frac{2}{\Delta x}(W_1 - W_2) \qquad \ldots.(2.17)$$

and

$$\frac{dw_1}{dt} + \frac{dw_2}{dt} = \frac{2A_2}{\Delta x}(P_{t_1} - P_{t_2} + F_{net}) \qquad \ldots.(2.18)$$

2.7 Choice of Model

Table 2.1 summarises the model development so far considered. Ref. 9 reports that the simulated results for the lumped and linearly distributed parameter models were in good agreement but that the linearly distributed model requires 2.3 times the computing time relative to the lumped distributed model. Due to the lower computer time requirement of the lumped distributed model, it was chosen for the simulation.

2.8 Dynamics of the Energy Equation

The dynamics of the energy equation was considered in Ref. 9

$$A\frac{\partial}{\partial t}\left(\rho_s\,(c_v\,T_s + \tfrac{1}{2}\,c^2)\right)dx = Cp\,(W_1\,T_{t_1} - W_2\,T_{t_2} + E_{net}) \qquad \ldots.(2.19)$$

The incorporation of the dynamic response of the energy equation did little to improve the accuracy of the simulation, but again increased the computer run time required to 2.8 times that required by the simple lumped distribution parameter model. Therefore the steady state energy equation in conjunction with the equations for the lumped distributed parameter model were used, to determine the energy changes in the element. The steady state energy equations being

$$H_2 = H_1 + \frac{E_{net}}{W_1} \qquad \ldots.(2.20)$$

or

$$T_2 = T_1 + \frac{E_{net}}{CpW_1} \qquad \ldots.(2.21)$$

2.9 Thermodynamic Relationships to Account for Real Gases

To keep computational requirements down to a reasonable level while retaining good accuracy under normal process plant operations the Schultz method was used (Ref. 13), where the following compressibility factors are derived.

$$X = \frac{T}{V}\left(\frac{\partial v}{\partial T}\right)_P - 1 \qquad \ldots.(2.22)$$

$$Y = -\frac{P}{V}\left(\frac{\partial v}{\partial P}\right)_T \qquad \ldots.(2.23)$$

These functions introduce effects to account for real gases in the polytropic analysis given below. The equation of state used for this model is the simple relationship:

$$PV = ZRT \qquad \ldots.(2.24)$$

Schultz introduces a further term, f_p - the polytropic head factor, to take into account the difference between the true work and the calculated work from the polytropic relationships discussed below. Differences may occur when large change in state variables are present. The analysis presented here neglects such refinements ($f_p = 1$). Since the state variable changes are relatively small, the following equations are then obtained.

$$m = \frac{ZR}{Cp}\left(\frac{1}{e} + X\right) \qquad \ldots.(2.25)$$

$$Wp = \frac{Cp\ T_1\ f_p}{\left(\frac{1}{e} + X\right)}\left((P_2 / P_1)^m - 1\right) \qquad \ldots.(2.26)$$

$$W_s = \frac{W_p}{e} + \Delta KE \qquad \ldots.(2.27)$$

$$T_2 = T_1 \left(\frac{P_2}{P_1} \right)^m \qquad \ldots.(2.28)$$

Using these equations allow the calculations of the steady state outlet gas states given the inlet gas states and the gas properties (Z, R, X, Cp), together with the compressor characteristic which will usually define the polytropic head and efficiency as a function of volume flow rate. This analysis is discussed further in the next chapter where the F_{net} and E_{net} terms are determined for a compressor element.

2.10 Calculation of Element Variables

One further simplification is required for the chosen model equations, which will overcome the need to calculate densities so that these equations may determine the element pressures directly.

For an adiabatic process

$$\frac{p_s}{\rho_s^m} = k \qquad \text{where } k \equiv \text{constant}$$

or

$$p_s = k\, \rho_s^m$$

$$\frac{dp_s}{dt} = k\, m\, \rho^{m-1} \frac{d\rho_s}{dt}$$

$$\frac{dp_s}{dt} = \frac{p_s m}{\rho_s} \frac{d\rho_s}{dt}$$

Substituting $\frac{p_s}{\rho} = ZRT_s$

$$\frac{dp_s}{dt} = ZRTm \frac{d\rho_s}{dt}$$

or

$$\frac{d\rho_s}{dt} = \frac{1}{ZRTm} \frac{dp_s}{dt} \qquad \ldots.(2.29)$$

Substituting in the model equation (2.4)

$$\frac{\Delta x\ A}{ZRTm} \cdot \frac{dp_s}{dt} = (W_1 - W_2)$$

$$\frac{dp_s}{dt} = \frac{ZRT_s m}{V} (W_1 - W_2) \qquad \ldots.(2.30)$$

where $V = A \cdot \Delta x$.

It is preferred to have total pressures and total temperatures because compressor characteristics are expressed in terms of totals or some function of totals (depending if the characteristic is represented in pressure ratios or polytropic head).

Using:

$$\frac{P_t}{P_s} = \left(1 + \frac{\gamma-1}{2} m^2\right)^{\frac{\gamma}{\gamma-1}}$$

and

$$\frac{T_t}{T_s} = \left(1 + \frac{\gamma-1}{2} m^2\right)$$

$$\frac{dP_t}{dt} = \frac{dp_s}{dt} \left(1 + \frac{\gamma-1}{2} m^2\right)^{\frac{\gamma}{\gamma-1}} \qquad \ldots.(2.31)$$

Substituting in equation (2.30)

$$\frac{dP_t}{dt} = (W_1 - W_2) \frac{ZRT_s m}{V} \left(1 + \frac{\gamma-1}{2} m^2\right)^{\frac{\gamma}{\gamma-1}} \qquad \ldots.(2.32)$$

including T_s as a function T_t and m

$$\frac{dP_t}{dt} = (W_1 - W_2) \frac{ZRmT_t}{V} \frac{\left(1 + \frac{\gamma-1}{2} m^2\right)^{\frac{\gamma}{\gamma-1}}}{\left(1 + \frac{\gamma-1}{2} m^2\right)}$$

or simplifying

$$\frac{dP_t}{dt} = (W_1 - W_2) \frac{ZRmT_t}{V} \left(1 + \frac{\gamma-1}{2} m^2\right)^{\frac{1}{\gamma-1}} \qquad \ldots.(2.33)$$

expanding $\left(1 + \frac{\gamma-1}{2} m^2\right)^{\frac{1}{\gamma-1}}$ using the binomial theorem

$$\left(1 + \frac{\gamma-1}{2} m^2\right) = 1 + \tfrac{1}{2} m^2 + \frac{(2-\gamma)(\gamma-1)}{8} m^4 + \text{higher orders of } m$$

Since it is assumed that $m < 0.3$ then $m^2 \approx 0$. Therefore equation (2.33) becomes

$$\frac{dP_t}{dt} = \frac{ZRmT_t}{V} (W_1 - W_2) \qquad \ldots.(2.34)$$

Expressing the model equations in terms of station numbers:

$$\frac{dP_{t_2}}{dt} = \frac{ZRmT_{t_2}}{V} (W_1 - W_2) \qquad \ldots.(2.35)$$

$$\frac{dw_1}{dt} = \frac{A}{\Delta x} (P_{t_1} - P_{t_2} + F_{net}) \qquad \ldots.(2.36)$$

2.11 Branch Elements (Flows Combining and Dividing)

Fig. 2.2 shows such elements. The branch flow, W_3, is assumed to be at right angles to the main flow and therefore the momentum of these flows do not take part in the momentum analysis. Writing the integral form of the continuity equation

$$-\int_{c.v} \frac{\partial \rho}{\partial t} dv = \int_{c.s} \rho c dA \qquad \ldots.(2.37)$$

In this case

$$\int_{c.s} \rho c dA = (\rho cA)_1 - (\rho cA)_2 \pm (\rho cA)_3 = W_1 - W_2 \pm W_3 \qquad \ldots(2.38)$$

where the positive sign is for flows combining and negative sign is for flows dividing. W_3 is the flow rate during combination or dividing (fig. 2.2).

Assuming a mean area for the element and using the lumped parameter model assumption equation (2.38) becomes

$$\frac{d\rho_s}{dt} = \frac{1}{A\Delta x}(W_1 - W_2 \pm W_3)$$

Expressing in terms of total pressures and temperatures as discussed in section 2.11

$$\frac{dP_{2_t}}{dt} = \frac{MRZT_{t_2}}{V}(W_1 - W_2 \pm W_3) \quad \ldots.(2.39)$$

The momentum equation for these types of elements are unaltered and equation (2.36) is used.

2.12 Conclusions

The generalised flow element has been developed for one-dimensional flow and although the model will not cope with complex three dimensional compressor flows this limitation does not prevent the model being used to simulate such elements if the element boundaries are chosen sufficiently far upstream and downstream of the compressor and relevant body force terms are available. This requirements also tends to imply that the low Mach number assumption (in the model derivation) is satisfied since the Mach numbers at these stations are generally below 0.3.

The choice of the lumped parameter model which neglects the dynamics of the steady state energy equation was justified on the basis of saving computational efforts and because the frequency restrictions so implied did not present any problem. The terms which still need to be defined are the force term, F_{net}, and the energy term E_{net}. The following chapter discusses the evaluation of these terms for a series of elements.

CHAPTER 3

3.0 APPLICATION OF THE MODEL

During this chapter both the restrictions imposed by such assumptions and the techniques used to model the various items of a process plant (i.e. compressor, valves, pipework, etc.) will be considered.

Several assumptions have been made in the derivation of the model equations. The internal compressor flows where the flow direction is complex cannot be modelled, and therefore in modelling such elements it is necessary to chose station points sufficiently upstream and downstream of the compressor. The assumptions of low Mach number, discussed in chapter 2, hold true only if the element boundaries are chosen to avoid high velocity regions. For instance this assumption does not hold if the element boundaries are chosen at the compressor impeller, but holds at boundaries sufficiently upstream and downstream of the impeller, (say at the compressor inlet and outlet flanges). The assumptions of the lumped parameter distribution to overcome the difficulties of the integral terms, $\left(\int A \frac{\partial \rho}{\partial x} dx \text{ and } \int \frac{\partial W}{\partial t} dx\right)$ in chapter 2, impose frequency limitations. If a frequency (ν) and a velocity (c) is considered then the basic wavelength (assuming $c \ll a$, the velocity of sound) is $\lambda = a/\nu$ and it was assumed that the element length $\Delta x \ll \lambda$ i.e. if the frequency was 10Hz and the velocity of sound 340 ms^{-1} then $\Delta x \ll 34m$.

It is assumed an element length of 3m ($\ll$ 34m) enables a longitudinal wave to traverse the length of the element several times during a transient, and therefore capable to simulation such longitudinal wave forms.

3.1 Frequency Parameter Model

To account for the frequency of pre-surge oscillations, a certain geometrical distribution was thought necessary. Too large an element length for the compressor element results in an unrealistic

response of the compressor surge. Too short an element length gives an unsatisfactory pre-surge compressor response.

Earlier work of Elder, Ref. (11) related a frequency parameter to the phase change across an element in terms of an expected error when comparing the lumped parameter model with the true solution to the partial differential equations. For a reasonable error (less than 5%) this suggests that:

$$2\pi f_x \Delta x < \sqrt{\gamma RT} - \frac{WRZT}{AP} \quad \ldots.(3.1)$$

$$2\pi f_x \Delta x < a - Vx \quad \ldots.(3.2)$$

$$2\pi f_x \Delta x < a\ (1 - Mx) \quad \ldots.(3.3)$$

where P and T are the mean pressures and temperatures for the element.

The expected frequency of interest, f_x, is used in the inequality (3.1) to determine the element length Δx. The Mach number, Mx, is taken to be about 0.3 or less. This yields the suitable element length for the compressor. This compressor length should be less than that imposed by the frequency limitation discussed in section 3.0.

3.2 Equalised Model

Although the above analysis improves simulated results it was found that the elements do not "communicate" in a realistic manner if the volumes of adjacent elements were significantly different. In order that these elements interact with each other in a realistic manner, a criterion of approximately equal volumes is used, in conjunction with the frequency parameter concept. This ensures that the elements take proper account of events occuring upstream and downstream. Furthermore if adjacent element volumes are significantly different the numerical solutions to the model equations become stiff.

3.3 Definition of Element Types

All the terms in the model equations

$$\frac{dP_2}{dt} = \frac{MZRT_2}{V} (W_1 - W_2) \quad \ldots.(3.4)$$

$$\frac{dW_1}{dt} = \frac{Am}{\Delta x} (P_1 - P_2 + F_{net}) \quad \ldots.(3.5)$$

$$H_2 = H_1 + \frac{E_{net}}{W_1} \quad \ldots.(3.6)$$

are calculable with the exception of the energy term, E_{net}, and the force term F_{net} (E_{net} represents the energy input into an element, and F_{net}, the force exerted by the element on the flow). The assumption is made that the E_{net} and F_{net} terms may be calculated using the instantaneous steady state values for the entry element parameters (e.g. inlet mass flows, pressures and temperatures). Evaluation of F_{net} and E_{net} terms for the different types of elements ocurring in a process plant are considered below.

3.4 Compressor Element (TYPE=1)

In the case of the compressor element the force term (F_{net} in (3.5)) is obtained from the stored compressor characteristic which is of the form

$$e, Wp = f(Q)$$

To obtain F_{net} the characteristics are interpolated to give the polytropic head (Wp) and the polytropic efficiency (e). These are used in the polytropic relations

$$Wp = \frac{Cp\ T_1}{\left(\frac{1}{e} + X\right)} \left[\left(\frac{P_2}{P_1}\right)^m - 1 \right] \quad \ldots(3.7)$$

$$\text{where} \quad m = \frac{ZR}{Cp} \left(\frac{1}{e} + X\right) \quad \ldots(3.8)$$

and X is the Schultz factor which like the Z factor, represents the real gases effects (also see Schultz, ref. (13).

Since the force term, F_{net}, is defined as the pressure rise in

steady state for the instantaneous flow rates then the F_{net} term in equation (2.36) for the compressor element is equated to

$$F_{net} = P_2 - P_1 = P_1 \left[\left[\frac{Wp}{Cp\ T_1} \left(\frac{1}{e} + X \right) + 1 \right]^{1/m} - 1 \right] \quad \ldots.(3.9)$$

The shaft work W_s for a given polytropic efficiency, e, is given as

$$W_s = \frac{Wp}{e} \quad \ldots.(3.10)$$

Substituting W_s in the energy equation (3.6) we have the compressor outlet temperature.

$$T_2 = T_1 + \frac{W_s}{Cp} \quad \ldots.(3.11)$$

or $$T_2 = T_1 + \frac{Wp}{e.Cp} \quad \ldots.(3.12)$$

3.5 Duct with Loss Element (DWL)

In this type of element the force term, F_{net}, is equated to the pressure drop due to friction loss along the duct. The pipe resistance factor, f, is given by

$$f = \frac{P_1 - P_2}{\rho c_1^{\,2}} \cdot \frac{d}{2L} \quad \ldots.(3.13)$$

Royal Aeronautical Society Ref. (14) gives:

$$f = \left[16 \left(y + \log_{10} \frac{Re}{5.02} - \log_{10} U \right)^2 \right]^{-1} \quad \ldots.(3.14)$$

and $$U = \frac{\varepsilon}{d} \cdot \frac{Re}{18.57} + \log_{10} \frac{Re}{5.02} \quad \ldots.(3.15)$$

and y is defined in the following table:

U	y	U	y
2	0.057	100	0.087
10	0.044	1000	0.0013
20	0.029	100,000	0.00008
40	0.018		

from equation 3.13:

$$F_{net} = \frac{2fL}{d} \cdot \rho c_1^2$$

or

$$F_{net} = \frac{2fL}{d} \cdot \frac{c_1}{A} \cdot W_1 \quad (\text{TYPE} = -2) \qquad \ldots.(3.16)$$

Furthermore, adiabatic conditions are assumed and zero work input. Therefore element outlet temperature equals inlet temperature.

$$T_2 = T_1 \qquad \ldots.(3.17)$$

3.6 Diffusing or Contracting Element (DWL)

Using the assumptions made in section (3.5) above, the following equations give the force term for the respective cases.

For a diffusing element

$$F_{net} = \left[\left(1 - \frac{A_1^2}{A_2^2} \right) - \frac{4fL}{\bar{d}} \right] \cdot \frac{c_1}{2A_1} \cdot W_1 \quad (\text{TYPE} = -5) \ldots.(3.18)$$

For a contracting element

$$F_{net} = -\left[\left(1 - \frac{A_1^2}{A_2^2} \right) + \frac{4Lf}{\bar{d}} \right] \cdot \frac{c_1}{2A_1} \cdot W_1 \quad (\text{TYPE} = -6) \ldots.(3.19)$$

where $4fL/\bar{d}$ represents the equivalent straight pipe static pressure loss. Pipe friction factor, f, may be calculated as in (3.14).

3.7 Curved Duct Element (DWL) (TYPE = -8)

The treatment of this element is similar to that of a diffuser. Ref. 15 quotes the following equation and contains the necessary information for the calculations to be performed.

$$F_{net} = \left(k_s + \frac{4fL}{d} \right) \frac{c_1}{2A_1} \cdot W_1 \qquad \ldots.(3.20)$$

The application of this equation is as for (3.5) above. Where k_s is the factor to account for the additional pressure loss in the curved element.

3.8 Recycle Valve Element

The mass flow rate through the valve is determined by the following equation.

$$W = 4.4113716 \times 10^{-6} \sqrt{\frac{M_w}{TZ}}\ Cg\ P_1\ \sin\left(\frac{3427}{Cp}\ .\sqrt{\frac{P_1 - P_2}{P_1}}\right)_{deg} \quad ....(3.21)$$

where P_1 and P_2 are the upstream and downstream pressures and the valve coefficient Cg is a function of the valve characteristic and valve travel given below.

$$Cg = Cg_{max} \cdot f(x) \quad ....(3.22)$$

f(x) ≡ valve characteristic (linear, step, parabolic, etc. with time).

Further details are discussed by Nisenfeld (Ref. 16). The dynamics of this element were neglected.

$$E_{net} = 0$$
$$T_2 = T_1$$

3.9 Branching Element

In this element equation (2.35) is modified by the flows combining or separating. The rates of change in outlet pressure for the respective cases are given by:

For combining flows

$$\frac{dP_{t_2}}{dt} = \frac{A_m}{\Delta x}\ (W_1 - W_2 + W_3) \quad ....(3.23)$$

For separating flows

$$\frac{dP_{t_2}}{dt} = \frac{A_m}{\Delta x} (W_1 - W_2 - W_3) \qquad \ldots.(3.24)$$

where W_3 is the flow in the branch.

The expression for the rates of change in the entry mass flow is unaltered (equation 2.36) and the F_{net} term is calculated as discussed in section 3. above.

3.10 Blow Off Valve Element

This type of element may be used to introduce a transient into a system by splitting the flow into two parts (i.e. the case of opening the blow off valve) or introducing a transient by combining the flows by closing the blow off valve. One part of the divided flow exhaust to the ambient and the other part continues downstream of the valve element.

The branch element discussed above may also be used to divide the flow and a valve similar to the recycle valve discussed in section 3.8 attached to the flow leaving the main system. The blow off valve element was developed before the branch element and was used to introduce the transients in the experimental validation system discussed in chapter 5.0.

The dynamic response of this element was neglected because it was assumed to be too small for there to be any rates of change in pressure and mass flows across it. A simple mass balance gives:

$$W_{TOT} = W_{out} + W_{Res}$$

where W_{out} is the flow through the valve determined from the nozzle relationship discussed later (section 3.14). The pressure to which the valve exhaust is set to the ambient. W_{Res} is the residual mass flow continuing downstream of the valve. The valve characteristic for this element are

Valve closing $\frac{A}{ABOV} = 1 - (t_o - t_v)/T_{CON}$ ....(3.25)

T_{CON} = 0.25 seconds.

Valve opening $\frac{A}{ABOV} = (t_o - t_v)/T_{CON}$ ....(3.26)

T_{CON} = 0.5 seconds.

t_o ≡ simulated time
t_v = valve movement time
T_{CON} = valve stroke time.

The pressure loss across this element was neglected and adiabatic conditions were assumed. Therefore

$F_{net} = 0.0$
$E_{net} = 0.0$

Hence $T_2 = T_1$.

3.11 Non-Return Valve

The force term, F_{net}, for this element was equated to the pressure loss across the valve. This data was obtained from the valve manufacturer.

$$\Delta P = 0.055749 \cdot ABS\ (Q)^{1.326} \quad ....(3.27)$$

Again adiabatic conditions were assumed. Hence

$T_2 = T_1$

The dynamic response of the valve movement is discussed in chapter 6 where it was treated as a spring mass system. The flow rate through the valve was determined by the expression used for the recycle valve. The valve movement was obtained from the solution to the equation of motion for this valve (discussed in chapter 6).

3.12 Boundary Conditions

The model equations discussed in chapter 2 do not determine the system entry pressure and system exit mass flow. The different criterion used in evaluating the parameters at the system boundary are discussed below.

3.13 Impedance ("near infinite volume") Boundary Condition

This type of boundary condition is used in a system where the upstream pipe work and/or the downstream pipe work extend continuously to near infinity (i.e. the pipe work upstream of element 1 and downstream of element 48 in fig. 6.3).

It is assumed that due to the large (near infinite) volume of the upstream pipe work the acoustic impedance upstream of element (1) and up stream of element (2), in fig. 6.3, are identical. Similarly it is assumed the impedance downstream of element 48 and downstream of element 47 are identical.

(i) for the upstream condition we have, by definition of acoustic impedance,

$$I_1 = \frac{\Delta P}{\Delta W} = \frac{P_1 - P_2}{W_1 - W_2} = \frac{P_2 - P_3}{W_2 - W_3} \qquad \ldots.(3.28)$$

or

$$P_1 = P_2 - \left(\frac{P_3 - P_2}{W_3 - W_2}\right) \times (W_2 - W_1) \qquad \ldots.(3.29)$$

(ii) downstream condition

$$I_{48} = \frac{P_{47} - P_{48}}{W_{47} - W_{48}} = \frac{P_{46} - P_{47}}{W_{46} - W_{47}} \qquad \ldots.(3.30)$$

$$W_{48} = W_{47} - \left(\frac{W_{46} - W_{47}}{P_{46} - P_{47}}\right) \times (P_{47} - P_{48}) \qquad \ldots.(3.31)$$

3.14 Nozzle Boundary Condition

This type of boundary condition is used to determine the mass flow rate leaving a system assuming the flow is exhausted into a near infinite chamber. From an isentropic analysis of nozzle flow the mass flow through a nozzle is given by

$$W_{noz} = \frac{\gamma \cdot A_{noz} \cdot P_{noz}}{\sqrt{2\ Cp\ T_{noz}}} \left[(PR)^{-\frac{2}{\gamma}} - (PR)^{-\frac{\gamma+1}{\gamma}} \right]^{\frac{1}{2}} \quad \ldots.(3.32)$$

where PR ≡ nozzle pressure ratio.

Either equations 3.31 or 3.32 have been used as downstream conditions.

3.15 Butt Boundary Condition

The butt boundary condition is the simplest of all the boundary conditions discussed above. It is used to represent a closed end of a pipe. For instance the flow rate leaving the systems CE and Bf, fig. 3.1, are zero because the ends E and f are flanged off. Therefore, referring to fig. 3.1

$$W = 0.0$$
$$W_f = 0.0$$

3.16 Conclusions

The definition of the force term, F_{net}, and the energy term, E_{net}, in the model equation, for different types of elements have been discussed. Not previously considered the recycle valve element could be modelled in a similar fashion if the definition of the force term, F_{net}, was available. This term may be obtained experimentally by plotting the force term against mass flow rate for a series of valve settings. The volume of this element compared with the system is too small to have a significant rate of change in pressure and mass flow rate.

Detailed analysis of intercoolers and heat exchangers has yet to be performed. The force term, F_{net}, for this type of element may be determined using the method discussed in section 3.5. The outlet temperature may be obtained from the heat exchanger characteristic (i.e. the effectiveness of the heat exchanger plotted against the number of transfer units for a series of thermal capacity ratios).

The ability for the model to simulate pre-surge oscillations has been incorporated via the frequency parameter and the equalised volume concept.

All the terms in the model equations have been defined. These equations are first order non-linear equations, and therefore require a numerical technique to solve them. Different numercial techniques are now discussed in order that these non-linear equations may be solved.

CHAPTER 4

4.0 REVIEW OF NUMERICAL METHOD

The primary objective of numerical integration (also called quadrature) is the evaluation of integrals which are either impossible or else very difficult to evaluate analytically. Analytical solutions to differential equations have many advantages over numerical evaluations, so numerical techniques should not be employed without first making a serious effort at analytical evaluation.

The advantages of an analytical expression includes the exactness (as there is no concern about errors of an analytical expression) and freedom from induced stabilities inherent in numerical methods. Nevertheless, numerical integration is indispensible in many complex cases (as with the equations in Chapter 2) due to the non-linear nature of these equations, since it can be the only method available to obtain a solution.

4.1 Taylor-Series Method

This is not strictly a numerical method, but it is sometimes used in conjunction with the numerical schemes, is of general applicability, and serves an introduction to the other techniques that will be discussed. Consider the equation

$$y' = \frac{dy}{dx} = f(x, y) \qquad \ldots.(4.1)$$

By developing the relation between y and x by finding the coefficients of the Taylor series in which the expansion of this series is about a point $x = x_i$, we have

$$y(x) = y(x_0) + y'(x_0)(x-x_0) + \frac{y''}{2!}(x_0)(x-x_0) + \frac{y'''(x_0)}{3!}(x-x_0) + \ldots\ldots$$

and substituting $h = (x-x_0)$, where h is called the step size, we get

$$y(x) = y(x_0) + y'(x_0)h + \frac{y''(x_0)}{2}h + \frac{y'''(x_0)}{6}h + \qquad \ldots.(4.2)$$

Applying the initial condition, and successively differentiating equation (4.1) until the second and higher-order derivatives are obtained, and substituting these values in equation (4.2), the solution to equation (4.1) may be obtained.

This Taylor series is awkward to apply if the various derivatives are complicated, and the error estimation is difficult to determine. An even more significant criticism in this computer age is that taking derivatives of arbitrary functions cannot be easily evaluated. We therefore look for another approach that is not subjected to these disadvantages.

4.2 Euler and Modified Euler Method

One thing we do know about the Taylor series, is that the error will be small if the step size h (the interval beyond x_0 where the series is evaluated) is small. In fact, if this step size is small enough, only a few tems in the Taylor series are needed for good accuracy.

4.2.1 Euler Method

The Euler method may be thought of as following this idea to the extreme for first order differential equations. Suppose h is chosen to be small enough that it is possible to truncate the Taylor Series after the first derivative term. Then we may write:

$$y(x_0+h) = y(x_0) + h\, y'(x_0)$$

Adopting a subscript notation for the successive y-values, the algorithm for the Euler may be written as:

$$y_{n+1} = y_n + h\, y'_n \qquad \ldots.(4.3)$$

Since truncation of the Taylor series will generally produce an error in the integration for each step, this error per step is called the local truncation error. All practical application of numerical methods involve many steps, and the accumulation of these local errors is called the global truncation error. The Euler method has a local truncation error of the order of h^2 and a global truncation error of the order of h.

4.2.2 Modified Euler Method

The trouble with the method described in the previous section is its requirement of small step size for accurate computation. Fig. 4.1 gives a graphical representation of the simple Euler method. It can be seen (from fig. 4.1) that the simple Euler method determines y_{n+1} by adding the area of the rectangle ABCD to the initial value y_n. A more accurate estimate of y_{n+1} may be found if the area of the trapizium ABCE (in Fig. 4.1) is added to the initial value of y_n. From fig. 4.1 this modified Euler method has the algorithm

$$y_{n+1} = y_n + h \left[\frac{y'_n + y'_{n+1}}{2}\right] + \quad h^3 \text{ error} \qquad \ldots.(4.4)$$

The method has a local truncation error of the order of h^3 and a global error of the order of h^2.

However, it is not possible to apply equation (4.4) immediately, because the solution is a function of x_n, y'_n and y'_{n+1} , since we cannot evaluate y'_{n+1} without knowing y_{n+1}. The modified Euler method (or sometimes known as the trapizoidal method) overcomes this difficulty by estimating or predicting a value of y_{n+1} by using the simple Euler relationship (in equation 4.3) and using this to compute y'_{n+1}, hence giving an improved estimate (corrected value) for y_{n+1} using equation (4.4). Since the value of y'_{n+1} was computed using the predicted value of less than perfect accuracy, the value of y_{n+1} may be recorrected until the difference in y_{n+1} is insignificant. If more than two or three recorrections are required, it is more efficient to reduce the step size.

The use of large step size may cause the solution to become oscillatory and diverge. The modified Euler method is less sensitive to this "induced instability" when compared with the simple Euler method. The modified Euler may use a step size twice as large as that employed by simpler Euler, without going unstable. Although the modified Euler method is more accurate this improvement in error may not be sufficient and there are more accurate and more efficient numerical methods available. One such method that is very popular is the Runge-Kutta formula.

4.3 Runge-Kutta Second Order Method

To obtain some idea of how Runge-Kutta methods are developed, the increment of y is written as a weighted average of two estimates of Δy, of k_1 and k_2 below. For the equation (4.1) $y' = f(x,y)$

$$k_1 = hf(x_n, y_n)$$

$$k_2 = hf(x_n + \alpha h,\ y_n + \beta k_1)$$

and

$$y_{n+1} = y_n + ak_1 + bk_2$$

It can be said that the values of k_1 and k_2 are the estimates of the change in y when x advances by h because they are the product of the change in x and a value for the slope of the curve, y'_n. The Runge-Kutta methods always use the first estimate of Δy by the simple Euler estimates. The other estimates are taken with x and y stepped up by the fractions α and β of h. The solutions to α, β, a and b may be found in ref. 17 and only the final results are quoted here.

$$y_{n+1} = y_n + \frac{2}{3} k_1 + \frac{1}{3} k_2 \qquad \ldots\ (4.5)$$

$$k_1 = hf(x_n, y_n)$$

$$k_2 = hf(x_n + \tfrac{3}{2} h,\ y_n + \tfrac{3}{2} h)$$

If one takes $a = \frac{1}{2}$, and the other variables are $b = \frac{1}{2}$, $\alpha = 1$, $\beta = 1$ gives the modified Euler algorithm that was previously discussed. The modified Euler method is a special case of the second-order Runge-Kutta method.

4.4 Runge-Kutta Fourth Order Method

Fourth-order Runge-Kutta methods are the most widely used and are derived in a similar manner. The most commonly used set of values to define the coefficients k_1, k_2, k_3 and k_4 leads to the algorithm:

$$y_{n+1} = y_n + \frac{1}{6} (k_1 + 2k_2 + 2k_3 + k_4) \qquad \ldots\ (4.6)$$

$$k_1 = hf(x_n, y_n)$$

$$k_2 = hf(x_n + \tfrac{1}{2}h,\ y_n + \tfrac{1}{2}k_1)$$

$$k_3 = hf(x_n + \tfrac{1}{2}h,\ y_n + \tfrac{1}{2}k_2)$$

$$k_4 = hf(x_n + h,\ y_n + k_3)$$

The local and global errors are of the order of the step size h^5 and h^4 respectively. It is computationally more efficient than the modified Euler method because, while four evaluations of the functions are required per step rather than two, the step size can be many folds larger for the same accuracy.

It is easy to see why Runge-Kutta technique is so popular. Since going from the second order to the fourth order was so beneficial, because for a given accuracy criterion a larger step size may be employed by resorting to a higher order Runge-Kutta method.

A standard way to determine whether the Runge-Kutta values are sufficiently accurate is to recompute the values at the end of each interval with the step size cut in half. If this makes a change of negligible magnitude, the results are accepted. If not, the step size is halved again until the results are satisfactory. This is very expensive because the additional sets of function evaluations are made just to estimate the accuracy. There are several schemes proposed to minimise the effort to determine error in a Runge-Kutta method computation. They all demand some additional effort, but fewer than the method discussed above. One such method that is widely used is the Runge-Kutta-Merson method.

4.5 Runge-Kutta-Merson Method

The Runge-Kutta-Merson method computes five estimates of Δy in the next step. The required formulae are:

$$k_1 = hf(x_n, y_n)$$

$$k_2 = hf(x_n + h/3,\ y_n + k_1/3)$$

$$k_3 = hf(x_n + h/3,\ y_n + k_1/6 + k_2/6\ )$$

$$k_4 = hf(x_n + h/2,\ y_n + k_1/8 + 3k_3/8)$$

$$k_5 = hf(x_n + h, y_n + k_1/2 - 3k_3/2 + 2k_4)$$

The solution:

$$y_n + 1 = y_n + \frac{k_1 + 4k_4 + k_5}{6} \quad \ldots\ldots (4.7)$$

$$\text{Error} = 1/30\ (2k_1 + 8k_4 - k_5) \quad \ldots\ldots (4.8)$$

The order of global and local truncation error are similar to that of the Runge-Kutta fourth order method. By halving or doubling the step size the required accuracy may be maintained using equation (4.8).

4.6 Runge-Kutta-Fehlberg Method

For better accuracy the Runge-Kutta-Fehlberg method is becoming increasingly popular. The technique is similar to Runge-Kutta-Merson. The required formulae are:

$$k_1 = hf(x_n, y_n)$$

$$k_2 = hf(x_n + h/4,\ y_n + k_1/4)$$

$$k_3 = hf(x_n + 3h/8,\ y_n + 3k_1/32 + 9k_2/32)$$

$$k_4 = hf(x_n + 12h/13,\ y_n + 1932k_1/2197 - 7200k_2/2197 + 7269k/1297)$$

$$k_5 = hf(x_n + h,\ y_n + 439k_1/216 - 8k_2 + 3680k_3/513 - 845k_4/4104$$

$$k_6 = hf(x_n + h_2,\ y_n - 8k_1/27 + 2k_2 - 3544k_3/2565 + 1859k_4/2565 + 2197k_4/4104 - k_5/5)$$

$$\text{Error} = k_1/360 - 128k_3/4275 - 2197k_4/75240 + k_5/50 + 2k_6/55$$

The method has a local and global error of the order of h^6 and h^5 respectively. The step size control is similar to that discussed under Runge-Kutta-Merson.

4.7 Multi-Step Method

Runge-Kutta, Euler and Modified Euler methods are called single step methods because they only use the information from the last step computed. In this they have the ability to perform the next step with different step size and are ideal for beginning the solutions where only the initial conditions are available. After the solution has begun there is additional information available, and this may be stored in the memory of a computer. A multi-step method is one that takes advantage of this information.

The principal behind multi-step method is to utilize the past values of y and y' to construct a polynomial that approximates the derivative function, and extrapolates this to the next step. Most multi-step methods use equispaced past values to make the construction of the polynomial easy. Adams method is typical of this.

4.8 Adams Method

The derivation of this method may be found in ref. 18. The formula required to determine y_{n+1} from the equation (4.1) is

$$y_{n+1} = y_n + \frac{h}{12} [\, 23y'_n - 16y'_{n-1} + 5y'_{n-2}]$$

The local and global errors are of the order of h^4 and h^3 respectively. The Adams method resembles the single step formula previously discussed in that the increment in y is a weighted sum of the derivatives times the step size, but differs in that past values are used rather than the estimates in the forward direction.

Higher order Adams formulae may be considered but there are better alternatives. The errors of an extrapolated polynomials are larger than when one interpolates. These alternative methods use the first calculated values of y_{n+1} as a predicted value and then correct it before going on to the next interval. The technique is similar to the strategy of the modified Euler method when y'_n is a function of x_n, y_n and y'_{n+1}.

4.9 Milnes Method

The Milnes method is a multi-step method that first predicts a value for y_{n+1} by extrapolating the values for the derivatives. It differs from the Adams method in that it corrects this predicted value before going on to the next interval. The Milnes formulae are:

Predictor:

$$y_{n+1} = y_{n-3} + \frac{4}{3} h [2y'_n - y'_{n-1} + 2y'_{n-2}]$$

Corrector:

$$y_{n+1} = y_{n-1} + \frac{h}{3} [y'_{n+1} + 4y'_n + y'_{n-1}]$$

The local and global errors for Milnes are similar to the Runge-Kutta fourth order method (i.e. they are of the order of h^5 and h^4 respectively). The number of evaluations for the Milnes method are only two instead of four as required in Runge-Kutta fourth order method. Therefore the Milner method is twice as fast as the corresponding Runge-Kutta method. However, the Milner method is subjected to an instability problem in certain cases. As the step size is reduced the errors do not tend to zero. Due to this unexpected phenomenon the Milnes method is not widely used.

4.10 Adams-Moulton Method

A method that does not have the same instability problem as the Milnes method and is about as efficient, is the Adams-Moulton method. Again it is assumed that a set of starting values are already calculated by some self starting method technique such as the Runge-Kutta methods. The equations used by Adams-Moulton are:

Predictor:

$$y_{n+1} = y_n + \frac{h}{24} [55y'_n - 59y'_{n-} + 37y'_{n-2} - 9y'_{n-3}]$$

Corrector:

$$y_{n+1} = y_n + \frac{h}{24} [9y'_{n+1} + 19y'_n - 5y'_{n-1} + y'_{n-2}]$$

When the predicted and corrected values agree to as many decimals as the desired accuracy, considerable computational effort may be saved by increasing the step size. After seven equispaced

values are available the step size may be conveniently doubled. When the difference between the corrected and predicted value reaches or exceeds the accuracy criterion the step size should be reduced. In order to obtain the intermediate values when the step size is halved the following equation may be used where the local error is still of the order of h^5.

$$y_{n-\frac{1}{2}} = \frac{1}{128} \left[35y_n + 140y_{n-1} - 70y_{n-2} + 28y_{n-3} + 3y_{n-4} \right]$$

$$y_{n-\frac{3}{2}} = \frac{1}{64} \left[-y_n + 24y_{n-1} + 54y_{n-2} - 16y_{n-3} + 3y_{n-4} \right]$$

It is clear that step size control using predictor corrector methods are not as easy when compared with Runge-Kutta Merson or Fehlberg methods. The disadvantages of these predictor corrector methods are that they are not self-starting and the relative difficulty in step size adjustment in order to satisfy a specified error criterion. Nevertheless, the Adams-Moulton method is popular mainly because of its better computational efficiency.

4.11 Hamming's Method

Another predictor corrector method that has been widely accepted is due to Hamming. The equations employed are:

$$y_{n+1,p} = y_{n-3} + \frac{4}{3} h \left[2y'_n - y'_{n-1} + 2y'_{n-2} \right]$$

$$y_{n+1,m} = y_{i+1,p} - \frac{112}{121} \left[y_{n,p} - y_{n,c} \right]$$

$$y_{n+1,c} = \frac{1}{8} \left[9y_n - y_{n-2} + 3h(y'_{n+1,m} + 2y'_n - y'_{n-1}) \right]$$

$$y_{n+1} = y_{n+1,c} + \frac{9}{121} (y_{n+1,p} - y_{n+1,c})$$

The predictor equation is the Milner predictor. Before correcting the estimated value, $Y_{n+1,p}$ it is modified using the difference between the predicted and corrected values of the previous

interval, $y_{n+1,m}$. Although two additional equations appear in each step compared with the other predictor-corrector methods discussed, only two evaluations of the derivative functions are needed as before. Therefore the Hemming's method is as computationally efficient as the Milnes and Adams-Moulton methods.

The special merits of the Hammings method are good stability combined with good accuracy. Like the Adams-Moulton and the Milnes, the method has a local and global error of the order of h^5 and h^4 respectively.

4.12 Gears Method

Gears (ref. 19) has proposed a predictor-corrector method that has a local error of the order of h^6 using only three previous steps rather than four as employed by Adams-Moulton and Milnes. It obtains its high accuracy by recorrecting values for the function and derivatives. The formulae employed are:

$$y_{n+1,p} = -18y_n + 9y_{n-1,c} + 10y_{n-1,c_2} + 9hy'_n$$
$$+ 18hy'_{n-1} + 3hy'_{n-2}$$

$$hy'_{n+1,p} = -57y_n + 24y_{n-1,c_1} + 33y_{n-2,c_2}$$
$$+ 24hy'_n + 57hy'_{n-1} + 10hy'_{n-2}$$

$$F = hy'_{n+1,p} - hf\,(x_{n+1},\ y_{n+1,p})$$

$$y_{n+1} = y_{n+1,p} - \frac{95}{288} F$$

$$y_{n,c_1} = y_n + \frac{3}{160} F$$

$$y_{n-1,c_2} = y_{n-1,c_1} - \frac{11}{1440} F$$

$$hy'_{n+1} = hy'_{n+1,p-F}$$

The method is stable and is particularly recommended for differential equations whose general solution has an exponential term such as $C_1 e^{bx}$ where b is positive. Under certain conditions (such as rounding of errors in the numerical solution) b may have large values, and this situation gives rise to a special stability problem. Such differential equations are called 'stiff' equations.

4.13 Conclusions

Of all the methods discussed the Euler, modified Euler, and the second order Runge-Kutta methods are very rarely used, mainly due to their large inaccuracy for a given step size. Another method that is not recommended is the Milnes. Here the reason is not due to the inaccuracy but to a special instability at small step size.

The single step methods have the advantage of being self-starting and the ease of control to satisfy a given error criterion. However the multi-step methods are computationally more efficient. Generally multi-step methods are not self-starting because they use information from the previous steps in evaluating the next solution. When multi-step methods are not self-starting they use a single step method such as Runge-Kutta-Merson to generate the necessary information required by these methods.

The method used for solving the differential equations in Chapter 2 was Runge-Kutta-Merson. The reason for this choice was good accuracy and ease of step-size control. A fixed step size, Adams-Moulton method, has also been included in the program as an alternative Table 4.1 shows the respective merits and disadvantages of the techniques discussed.

CHAPTER 5

5.0 EXPERIMENTAL VALIDATION OF THE MATHEMATICAL MODEL

An experimental program was undertaken to validate the mathematical model developed in Chapter 2.0. The experiment was conducted using a turbo-charger.

5.1 Description of Test Rig and Instrumentation

In order to obtain useful results a very simple system was chosen for the experimental study. The test rig is shown in fig. 5.1.

The compressor was a small (100mm impeller diameter), single stage, centrifugal compressor. The compressor speed selected for the test was 90,000 rpm. The characteristic of the compressor at the chosen speed is shown in fig. 5.2.

The duct work upstream of the compressor consisted of a straight pipe and an inlet bell mouth. The downstream ducting had two right angle bends and a branch to which a fast acting blow-off valve was mounted. (The valve stroke times for the opening and closing of the blow-off valve were 0.25 seconds and 0.5 seconds respectively.) The blow-off valve was a repeatable poppet actuator type, and fast transients were introducted into the system by the operation of this valve. The compressor delivery air exhausted through a throttle valve, and the compressor steady state operating point on its characteristic was determined by the actuation of this throttle valve.

High performance pressure transducers were mounted at the system inlet, impeller inlet, compressor outlet and blow-off valve stations respectively. The type of transducers used is given in Appendix A. These transducers were calibrated and the expression for pressure as a function of voltage is also given in Appendix A. Due to the relative small changes in pressure ratios during the transients considered and the slowness of the temperature changes the

effect of temperature on the pressure readings were neglected. All the data from the transducers were stored on magnetic tape using the system shown in fig. 5.3.

The duct work upstream of the turbine section was a straight pipe via a combustion chamber connecting to the high pressure air supply. The exhaust from the turbine was discharged via a straight vertical pipe to the ambient. The combustion chamber becomes operational if insufficient energy is available in the high pressure air (cold) driving the compressor at the required speed and pressure ratio (preheating using the combustion chamber was required for operating conditions above 60,000 RPM).

5.2 Compressor Test

A series of validation tests were conducted. Firstly, by adjusting the flow through the throttle valve (fig. 5.1) a steady state compressor operating point on the compressor was chosen, point A in fig. 5.2. A this operating point the flow through the compressor was measured to be 0.54 kg s^{-1} at a pressure ratio of 3.3. The blow off valve was set to the closed position.

5.3 Compressor Transients between Stable Points

By the actuation of the blow-off valve a fast transient was introduced into the system. The repeated opening and closing of the blow-off valve transients between the corresponding two stable points were obtained. Sufficient time was given between the opening and closing of the valve so that the post transient steady state operating point could be obtained. During the transient the compressor speed remained nominally constant. The stable points due to the opened and closed position of the blow-off valve are shown by point A and B respectively in fig. 5.2.

5.4 Surge Tests

The blow-off valve was returned to the opened position, and by adjusting the flow through the throttle valve in fig.1 the compressor was made to operate at point A (fig. 5.2) on the characteristic. The

transient due to the closing of the blow-off valve was sufficient to take the compressor into surge. The compressor remained under surge conditions for only approximately 15 seconds so that no damage was done to the test rig. This surge test was repeated twice.

5.5 Data Analysis

The analogue signals from the pressure transducers during the transient were stored on magnetic tape. A separate channel on the tape recorder was used for each transducer. The tape recorder also stored a trigger pulse which was produced whenever a transient was initiated.

The stored signal was passed through an oscilloscope so that the beginning of a transient could be defined. From the oscilloscope the signal was sent to a DATA-LAB DL905 transient recorder. The digitised output from the transient recorder was stored on floppy disk via a PET 2001 micro computer (see fig. 5.3). The program package used in the micro computer known as "DATA" is described in ref. (20).

Having determined the beginning of the transient, the magnetic tape was played back again, however, on this occasion the transient recorder was armed and the computer program executed. In this condition the transient recorder waits for the trigger pulse. When the transient recorder received the trigger pulse and starts digitising (the analogue signal from the tape recorder) the micro computer waits until all data has been accepted by the transient recorder. The micro computer then goes into the final stages of transfering the digitised data from the transient recorder into its memory and then on to the floppy disk. This was repeated for each data channel on the recorder.

The compressor transients considered were very fast. The section of the magnetic tape which represented ten seconds after the transient was initiated was taken for digitisation. To achieve this a sweep time of ten seconds was set on the DATA-LAB transient recorder. In this time period the analogue signal was digitised into 1024 parts which range from 0 to 255 in value. The nature of the signal being digitised may give rise to the situation where this range is exceeded, hence introducing an overflow condition in the micro computer. To overcome this, an off-set and a scaling of the voltage was introduced to provide the

correct level of signal. An offset of 124 and a scaling of the voltage of 2 volts was sufficient to ensure that the signal was within the given range. A flow chart explaining how the transient recorder and the micro computer interact is shown in fig. 5.4.

The next task was to convert the digitised data into pressure readings. A computer program was developed using the micro computer incorporating the characteristics of the pressure transducers. The program was structured into different subroutines where each sub-routine determined the pressures from the digitised data that originated from a particular transducer. Such a structure was chosen so that further transducers may be incorporated into the program with ease. A flow chart describing this is shown in fig.5.5.

The output from this program may be in a printed format of pressure readings and time, or a simple graphical output. To obtain the graphical output the TAB function was used. The variable incorporated in the TAB function was the digitised number rather than the pressure value. The reason for this being that the TAB function is only accurate to the nearest integer and therefore the full transient may be captured using the digitised number. The scale of the graph was, however, calibrated in pressure units (pa) using the characteristics of the transducer. The graphical output enabled one to select an interesting transient to simulate with relative ease.

5.6 Simulation of Compressor Transients

The mathematical model described in Chapter 2 was implemented in a Fortran IV program using a PDP 11/34 machine. The system shown in Fig. 5.1 was discretised into elements using the frequency parameter and approximately equal volume concept discussed in Chapter 3. The element geometry was selected such that the system had a frequency response of 200 Hz, although the frequency response expected during the transient need not exceed about 150 Hz. The system is schematically represented in Fig 5.6 and the geometry of the elements within the system is given in appendix B.

5.7 Setting Up of Data for Simulation

The simulation program is in two parts. The first, whose name

is "SETUP", sets up the data files required for the second program "TRANS", where the simulation is performed. The program SETUP is divided into five sections. The first part reads the gas properties such as the gas constant R, gamma γ, specific heat Cp, system entry pressure, temperature and various times (eg. valve stroke time, valve movement time etc.). The next part reads the number of elements in the system, number of compressor stages and compressor speed.

The third part of the program, SETUP, enables the simulation program TRANS to distinguish one type of element from another, by associating a number to each type of element that exists in the system. Appendix (B) shows the different types of elements that are involved in representing the system. The meaning of these elements are as follows.

a) Duct-with-loss (TYPE = -2)

This element is used to represent pipe work which only introduces a pressure loss. The pressure loss is determined using pipe resistance coefficients and the technique used to determine the pressure loss is given in Chapter 3.

b) Blow-off-valve (TYPE = -3)

This element is used to introduce a transient into the system. The dynamic response of this element was neglected as it was considered to be sufficiently small. The relationship for the valve movement are given in Chapter 3 and this information may be obtained from the valve manufacturer.

c) Compressor (TYPE = 1)

This is the only element that inputs work into the system. The pressure rise across this element is determined from its pressure rise characteristic. During the development of the program it was decided that the compressor characteristic should be of the form of polytropic head against volume flow rate. The reason being that most industrial compressors have characteristics expressed in this form.

These were the only type of elements needed for the simulation of the test rig. However, other elements which represent recycle valves, non-return valves, branch, bends etc. are also available (Appendix C).

The next selection of the program reads the geometry of each element and loss constants as the pressure drop in the element were to be defined by experimental values (ie. element type -4 duct with experimental loss DWEL in Appendix C).

The compressor stage characteristics are input to the program followed by the compressor speed time history. This speed time history accounts for any variation in compressor speed during the transient. However, the compressor speed remained nominally constant during this test but any such variation in speed may be included without analysing the dynamic response of the driver (in this case, the turbine). The data is stored on floppy disks by generating two data files. The first stores the system variable and the other stores the speed history only. This choice was made so that if a few variables need changing in the system this could be achieved by editing the system variable data file using the computer command codes. It is also possible to make the necessary changes to the file by executing the data program SETUP. A flow chart describing SETUP is given in Fig. 5.7. A typical data file is given in Table 5.1 with a guide to the meanings of the variables in that file, in Appendix D).

5.8 The Simulation Program TRANS

The simulation program consists of a main routine which calls the necessary subroutines defining the type of elements that exist in the data files generated by SETUP. Further to this the integrating section has been included as a separate subroutine. Such a structure enables the inclusion of other integrating algorithms and new types of elements with relative ease.

A flow chart describing program TRANS (fig. 5.8) shows that it is split up at point 'A' into two sections. The first section reads in all the data, performs a curve fit upon any element characteristic using a natural cube spline fit, and sets up the initial valves of the

element variable to give steady state running conditions. These tasks are performed once per program run.

The second section of the program contains the call for the integrating routine (subroutine RKM, see Appendix E) where the bulk of the calculations are performed during a program run. Most of the calculations necessary to simulate the transients occur with subroutines RKM, SUBØ1 and DYBDX.

The program path is determined by two 'If' statements. The first of these enables the change of certain variables (eg. pressure, temperature, mass flow and gas properties of any element within the system) using subroutine SUBØ6 (see appendix E), at a simulated time specified by the initial input data variable XTIM (see typical data file Table 5.1). Since XTIM may be reset within subroutine SUBØ6 it is possible to simulate a sequence of transient inducing events.

The second 'If' statement determines whether an output should occur. In order to reduce computer output and hence computer run times an output occurs if the fixed output interval (OUTDEL, defined in the data file, Appendix D) is reached, or if the ratio of the compressor entry mass to the time changes sign. This enables all the oscillatory response during a transient to be captured.

5.9 Program Performance

The main problem encountered is one of program run times and hard copy times, where a single simulation may take several hours. Fortunately, this problem is to a large extent dependent on the type of computer used and its peripheral equipment. The reduction of computer time is in some ways a simple matter of employing a more powerful computer. To test this theory the TRANS program was executed using a VAX 11/780 machine. The CPU time was reduced by some 85%.

The problem of run time is also a function of the number of elements used to define the system. Generally the computer runtime increases proportionally with the number of elements within a system. Only five elements were required for the validating simulation, however if a real process plant were to be considered, and indeed the case of the gas transmission station considered in Chapter 6, the number of elements may run into hundreds. Under these conditions the impressive

reduction in computer run times achieved using the VAX 11/780 machine still represents a run time of over an hour.

Another line of attack on computer run times is to use a faster integrating algorithm. The method used in program TRANS is the Runge-Kutta-Merson. The main reason for the use of this method of integration is the ease of integrating step size control to keep the error within some pre-set limit. However, Runge-Kutta-Merson is by no means the fastest method numerical integration. Another desirable feature of Runge-Kutta -Merson is that the method is self-starting unlike predictor-corrector methods such as Adam-Moulton, Hamming and Gears. This disadvantage of starting predictor-corrector methods is not inherent in this case, the reason being that the system considered for simulation is initialised to give steady state response. Therefore, the previous values for the rates of change may be conveniently put to zero and hence the previous solutions are also known. Generally, these predictor;corrector methods are some 60% faster than Runge-Kutta-Merson but the change in step size , so that the integration error will be below a pre-determined limit, is not that easy. The reason being that the previous values needed for most predictor-corrector methods must be of equal step. Therefore, one must interpolate and extrapolate to ensure good accuracy. The general rule is that if stable solutions are found then the integrating error is relatively small, hence making such predictor-corrector methods attractive in achieving small computer run times. Another attractive property of prediction-correction methods such as Hamming and Gears, are that they are well suited for so-called stiff equations, discussed in Chapter 4.0.

An altogether different approach in reducing large computer run times is the application of the concept of parallel or array processing. Basically, this approach enables the computer to evaluate a sequence of events by one instruction. Therefore if 'n' elements were involved in defining a system, array processing will be able to complete the task in approximately 1/nth the time required by conventional computers that operate on a sequential basis. However, this technique is only useful when many hundreds of elements are involved in the system. Ref. 21 and 22 give details on array processing.

5.10 The Simulation of Measured Transients

The following transients were simulated to provide a comparison between the experimental data obtained and the model prediction.

(i) Point to Point Simulation

a) The model was set up so that the compressor operated at point 'A' on the compressor characteristic (fig. 5.2). After 0.2 seconds of steady state running a transient was introduced by opening the blow off valve. The post transient steady state compressor operating point is also shown in fig.5.2 by point 'B'.

b) Next the operating of the compressor on its characteristic was set at point 'B', (fig.5.2) with the blow off valve in the opened position. Again after 0.2 seconds of steady state running a transient was initiated by the closure of the blow off valve element, and therefore reproducing the two steady state compressor operating points 'A' and 'B' on the compressor characteristic.

(ii) Surge Simulation

Compressor surge, the periodical reversal of flow within the compressor, is by far the most dangerous aspect of compressor operation. Therefore its prediction is of vital importance within the simulating model.

For successful simulation of compressor surge the unstable part of the compressor characteristic is required. The reasons being that the force terms, Fnet, in equation (3.5) in chapter (3) are determined by the interpolation of the compressor characteristic. However, the unstable part of the characteristic is exceedingly difficult to obtain by experimental means. By understanding how surge cycles are formed the shape of the unstable part of the compressor characteristic may be estimated.

Fig. 5.9 shows a typical form of a compressor characteristic operating at constant speed. Using this diagram the behaviour of a dynamic compressor delivering gas through a pipe downstream operating under surge conditions can be explained. The unstable region where the characteristic has a positive slope lies between points A and C. As the operating point moves from D to A, a reduction in gas flow is

met by an increase in discharge pressure. This has a stabilizing effect since the increase in discharge pressure attempts to increase the gas flow in the delivery pipe work which counteracts the reduction in gas flow from D to A. However, if the gas flow is reduced beyond A a momentary reversal of flow in the compressor occurs and the operating point is now located at B. The reversal of flow tends to lower the pressure in the discharge pipeline to the point C on the characteristic where the gas flow is increased to D. At this point normal compression is resumed and the cycle is repeated.

With the so-called 'inverted' characteristic included to the stable part, the compressor was taken into surge by the closure of the blow-off valve when the compressor was operating at point A on its characteristic (fig.5.10). Again, this transient was introduced after 0.2 seconds of steady state running. The restriction introduced downstream of the compressor due to the closing of the blow-off valve was sufficient to introduce surge conditions.

5.11 Comparison of Measured and Simulated Results

The simulated results for the series of validation tests are compared with the measured transients in fig.11 at the compressor delivery at blow off valve station. The general agreement between the experimental and simulated results are very good. The slight discrepancies are largely due to the inaccuracies in the representation of the "poppet" blow-off valve action. The action of the valve was assumed to be linear with respect to time. However, it would be expected that the valve movement initially would be rapid compared with the movement towards the end of the valve stroke. Due to the small valve stroke times, the inaccuracies introduced due to the assumption of linear response of the valve will be small and indeed highlighted in the results (fig. 5.11).

In these tests no post transient oscillatory motion was observed. This lack of oscillatory action was attributed largely to the relative response capability of the system and valve stroke times of the valve. These conclusions were supported by a theoretical study (Fig.5.12), in which the valve action was considered to be infinitely fast, in which case settling oscillations will be noted.

It is interesting to note that a similar conclusion was reached in ref. 7

The simulated and experimental results for the surge cycles are shown in Fig. 5.13 at the compressor delivery and blow-off valve station. The discrepancy in frequency between the experimental and simulated values are small, and the periodic time of the oscillation for both cases are equal to the time taken for a pressure wave to propagate the length of the system and back. The slight difference in time to surge between the simulated and experimental results can again be attributed to the inaccuracy in the blow-off valve relation. Fig 5.14 shows the resultant surge cycle on the compressor characteristic.

A series of further surge cycle simulation was repeated, however the compressor volume was changed by ± 20% in steps of 5%. These simulated results when compared with the experimental tests showed small errors up to ± 10% change in compressor volume. This feature is very valuable as it is not always possible to obtain the compressor geometry very accurately, due to the tortuous path the gas follows within the compressor. Therefore, if an accuracy in compressor geometry of ± 10% is obtained it could be concluded that the simulation is still largely valid.

5.12 Conclusions

The simulated results compare favourably with those of the experimental tests. The small discrepancies are mainly attributed to the inaccuracies in the representation of the poppet valve action. The travel of the poppet valve was assumed to be linear with time. In reality the valve action is likely to be of the form

$$\text{displacement} \propto (\text{time})^n$$

where $n > 1$

This valve information was exceedingly difficult to obtain and a linear response of the valve was assumed. Due to small valve stroke times of the poppet valve the error introduced due to this linear

assumption is small.

Surge tests gave good results. The frequency response of the system between simulated and experimental results were good.

With satisfactory validation results, the model was then applied to a British Gas transmission station. This plant was selected because it had operational problems associated with plant dynamics. The simulation of the gas transmission station was discussed in chapter 6.0.

CHAPTER 6

6.0 APPLICATION OF THE MODEL TO SIMULATE THE DYNAMIC RESPONSE OF THE GAS TRANSMISSION STATION

The operation of the transmission station suffered compressor stability problems and it was a problem that manifested itself when new compressor wheels and non-return valves were installed. The model was used to investigate the problem and suggest solution in order that the system may operate satisfactory. The first part of this chapter discusses the extention and validation of the program so that the gas transmission may be considered.

6.1 Further Development of Program

The program developed to this point was only capable of simulating the dynamic response of compressor systems used in series, (i.e. flow enters at station 1 and leaves from the last station). Many practical examples, however, use compressor systems which are connected in parallel, (with parallel flow paths) and therefore the computer model had to be able to simulate such systems. To achieve this the program was modified such that any number of "series" systems may be connected together to simulate parallel paths. This was achieved using a patching routine.

Consider the compressor system shown in Fig. 6.1 where three compressors may operate in parallel and each compressor discharges to a common outlet. Firstly, by applying the frequency and equal volume concepts, discussed in Chapter 3, the whole system is divided into elements whose geometry is defined by the frequency response of the system. Secondly the element types are assigned to each element (e.g. duct with loss, bend, compressor, tee-section, etc.). Since the procedure for connecting the series systems are only required at a branch junction (or tee section), the patching routine is invoked only when this element is located. To achieve this the patching routine is included in the subroutines describing the pressure loss in the tee-piece.

6.2 Patching Procedure

The system shown in Fig. 6.1 is divided into three series paths AB, CED and EF, where AB is considered the main system and CED, EF

as sub-system. The model equations discussed in Chapter 2 determine the entry mass flow rate and exit pressure within any element. In this example the entry pressure to the main system is equated to the ambient pressure (it is assumed that the system is opened to the ambient, but this pressure condition may be determined by the equal impedance boundary condition discussed in Chapter 3). The exit flow from all the sub-systems (i.e. at B, F and D) are determined by nozzle relationship discussed in Chapter 3. The entry pressures to the sub-systems CED and EF are determined by the mean pressure in the branch (1) and (2) in Fig. 6.1 respectively. The patching routine determines these entry pressures to the sub-systems. The system entry mass flows are determined by the steady state studies for each system.

The above example considered the case where the flows at the branch are dividing. In many parallel systems the occurrence of combining flows is equally common. Consider another example where a compressor has an anti-surge recycle valve (Fig. 6.2). The system is again divided into systems where AB is considered as the main system and CDE as a sub-system. The entry pressure to the sub-system CDE is equated to the mean pressure in the branch (1) in Fig. 6.2 similar to that of the example discussed above. The exit mass flow leaving the sub-system is again determined by the nozzle relationship, however the pressure ratio across the nozzle is equated to the ratio of the pressure in the last element in the sub-system to the mean pressure in the branch (2) in Fig. 6.2. The entry mass flow to the sub-system is put to zero as it is assumed that the recycle valve is in the closed position during the steady state response.

In a similar manner the dynamic response of many different compressor systems may be studied.

6.3 Patching Procedure for the Gas Transmission Station

The section of the pipe work associated with the compressor station initially modelled is shown in Fig. 6.3. A second case where further downstream ducting was considered will be discussed later.

The initial gas circuit (Fig. 6.3) was first discretized into shorter elements by applying the equalised volume and the frequency parameter concept. The element volumes, areas and lengths derived were $0.32m^3$, $0.29m^2$ and 1.1m respectively. In using such a (geometrical) distribution it was implied that the model was capable of simulating a wave of frequency up to 70 Hz.

This system was then divided into a main system and three sub systems as follows.

System (1) from element 1 to element 48 (main system).

System (2) from element 49 to element (the recycle loop) 58 (1st sub-system).

System (3) element 59 (2nd sub-system).

System (4) from element 60 to element 63 (3rd sub-system).

6.4 System Boundary Conditions

(a) Main system

The impedance ("near infinite volume") boundary condition was used to define this system entry pressure and system exit mass flow. It was assumed that due to the large (near infinite) volume of the upstream pipe work the acoustic impedance upstream of element (1), and upstream of element (2) were identical. Similarly it was assumed the impedance downstream of element 48 and element 47 were identical. Applying the impedance boundary condition described in Chapter 3 the system entry pressure and system exit mass flow rate are given by

$$P_1 = P_2 - \left(\frac{P_3 - P_2}{W_3 - W_2}\right) x \ (W_2 - W_1)$$

and

$$W_{48} = W_{47} - \left(\frac{W_{46} - W_{47}}{P_{46} - P_{47}}\right) x \ (P_{47} - P_{48})$$

(b) System (2)

The entry pressure to this system is equated to the mean pressure in the branch element 41 (in Fig. 6.3).

The exit mass flow from this system is obtained by the nozzle relationship given in Chapter 3. The pressure ratio across the nozzle is determined by the ratio of the pressure in the last element of the system to the mean pressure in the branch to which the system is exhausting (i.e. pressure ratio RP = $P_{58}/\overline{P}_{25}$, where $\overline{P}_{25}$ is the mean pressure in element 25). Therefore the system exit mass flow rate is

$$W_{58} = \frac{\gamma . A_{noz} . P_{58}}{\sqrt{2\ Cp\ T_{58}}} \left[(RP)^{-\frac{2}{\gamma}} - (RP)^{-\left(\frac{\gamma+1}{\gamma}\right)} \right]^{\frac{1}{2}}$$

(c) Systems (3) and (4)

Initially the non-return valve element 63 (Fig. 6.3) was assumed closed irrespective of the pressure difference across this element. Therefore the exit mass flow rate leaving systems (3) and (4) were put to zero, (it should be noted that this assumption is not a limitation as the system has been modelled whereby the valve may open and this will be discussed later).

The entry pressure to these two systems are determined by the mean pressure in the branch elements 21 and 45.

The different types of elements used in describing the complete system are given in Appendix F.

6.5 Simulation Results

The compressor characteristic provided was reproduced on the basis of polytropic head against volume flow rate (Fig. 6.4). The selected speed for the simulation was 6,500 RPM and, for the first set of tests, assumed constant.

A series of validation tests were conducted as follows.

6.6 Action of Recycle Valve

A transient was introduced by opening the recycle valve (element 55 in Fig. 6.3) with the compressor operating at point (1) on the compressor characteristic (see Fig. 6.4). The steady state operating point with the recycle valve open is indicated by point (2) on the compressor characteristic (Fig. 6.4). To reduce computing time the action of the recycle valve was considered infinitely fast. The stagnation pressure variation at the compressor inlet and outlet station (Fig. 6.5a) prompt the following comments

(1) The compressor outlet pressure fall (due to the opening of the recycle valve) was not very large because of the relatively flat compressor characteristic.

(2) During the transient the compressor inlet pressure decreased a little. This is apparently due to increased losses in the intake system associated with increase in mass flow through that system. Operation at both points (1) and (2) on the compressor characteristic (Fig. 6.3) were quite stable.

6.7 Effect on Non-Return Valve due to the action of Recycle Valve

It was suspected that during the actuation of the recycle valve the non-return valve could open or flap. To determine whether the pressure difference across the non-return valve (element 63 in Fig. 6.3) could cause this valve to become active the pressure time history for this element was investigated (Fig. 6.5b). It can be seen that the pressure difference across this valve is always large ensuring that it remains closed during the transient.

6.8 Transient Response due to Perturbation

The operating point on the compressor characteristic was moved to point (3) (see Fig. 6.4) and the recycle valve to the closed position. The system was then perturbed by altering the pressure instantaneously

in element 48 (Fig. 6.3) by 2% above its steady state value, and then returned (instantaneously) to its original value. The pressure time history for the compressor element (Fig. 6.6a) shows that the mean pressure remains approximately constant and indeed returns back to its initial value once steady state conditions were reached.

A similar test was performed with the compressor operating closer to surge, points (4) and (1) on the compressor characteristic (Fig. 6.4). The pressure time history, at compressor inlet and outlet stations for the respective tests are shown in Figs. 6.6b and 6.6c. A similar conclusion may be drawn for these tests, although it would be expected that the transient would take longer to settle as the compressor operates closer to surge; (the compressor being less stable as surge is approached). This phenomenon does not manifest itself well on the pressure time history (Figs. 6.6a, 6.6b and 6.6c). This is apparently due to the relatively flat compressor characteristic which tends to minimise pressure fluctuations arising from variations in mass flow. Examining the corresponding mass flow variations, Fig. 6.7, when the system was perturbed at points (3), (4) and (1) highlights this phenomenon very clearly (close to surge there are larger oscillations for the same initial excitations).

To investigate this phenomenon further the very first transient test, (i.e. case 6.6 when the transient was introduced by the opening of the recycle valve), was repeated, however, after 2 seconds of simulated time the recycle valve was closed so that the compressor operating point on the characteristic may return back to its initial point (i.e. the compressor operating point moves from (1) to (2) and back to (1) in Fig. 6.4). Figs. 6.8a and 6.8b show the compressor inlet and outlet pressure and entry mass flow time history respectively.

Again, by examining the mass flow time history, (Fig. 6.8b), it can be deduced that the compressor is less stable when operating nearer surge (that is, the excursion taking the compressor closer to surge, lower mass flow, provides the larger perturbations).

6.9 Surge Simulation

The compressor operating point was reset to its initial condition on the compressor characteristic (point (1) in Fig. 6.4) and the recycle valve returned to its closed position. With the inverted characteristic surge conditions were produced by introducing a transient into the system by, again, perturbing element 48 (Fig. 6.3) with a pulse whose strength was 10% above the steady state pressure. The strength of the pulse was sufficiently large to cause the compressor operating point to move into surge.

The resultant surge cycles are shown in Fig. 6.9 where the compressor outlet and inlet pressure were plotted against time. It is noted that the mean compressor outlet pressure falls. This is associated with the compressor characteristic being non-linear near surge. To explain this phenomenon further, consider an operating point close to surge (see Fig. 6.10). If a sinusoidal variation in mass flow is assumed, then by interpolating this mass flow variation of both linear and non-linear characteristic the mean outlet pressure in the case of the non-linear characteristic will be lower. Surge cycles behave similarly to a sinusoidal perturbation, hence the fall in mean pressure. Furthermore the incorporation of the inverted characteristic will result in a further fall in mean pressure. Details regarding this phenomenon may be found in Ref. 23.

A fast fourier transform was performed in order to obtain the frequency content of these surge cycles. Figs. 6.11a and 6.11b show the modulus of the fourier transform against frequency for the inlet and outlet station of the compressor element. It can be seen that in both cases the dominant frequency is about 50 Hz.

6.10 Antisurge Simulation

The surge test was repeated, this time, however, when the simulated time reached 0.5 seconds the recycle valve was opened attempting to remove the compressor from surge. From the pressure time history, Fig. 6.12a for the compressor element it is clear that

the model is capable of operating successfully in the stable and unstable parts of the compressor characteristic, (although the inverted characteristic is needed for satisfactory simulation in the unstable part of the characteristic). The post transient operating point on the characteristic coincided with point (2) in Fig. 6.4. This is to be expected because it was known that point (2) on the characteristic was the steady state operating point with the recycle valve in the opened position. Fig. 6.12b shows the corresponding pressure time history across the non-return valve element. Again it can be concluded that the pressure difference across the non-return valve is insufficient to cause it to become active.

6.11 Antisurge Controller Simulation

The antisurge test was repeated where the action of the recycle was controlled by a constant speed antisurge controller. The position of the surge limit on the polytropic head against volume flow rate characteristic occurs at the point where the compressor pressure ratio is a maximum. Ref. 24 and Ref. 25 have shown that this point occurs where the polytropic head is maximum. At a constant speed, constant composition of the gas and constant suction temperature the following control law will ensure that the polytropic head developed by the compressor will not exceed the critical head at surge.

$$P_2/P_1 < \text{constant}$$

where $P_2/P_1 \equiv$ compressor pressure ratio and the constant is determined from the critical polytropic head at surge.

With the constant speed controller included in the model the system was perturbed in element 48 to introduce surge conditions. The pressure time history for the compressor and non-return valve are shown in Fig. 6.13a and 6.13b respectively. Comparing the results for the compressor element (Fig. 6.13a) with the previous antisurge cycle test, the recycle valve in this case responded much earlier (approximately 0.1 s) avoiding such severe surge conditions.

Examining the simulated pressure differences across the non-return valve (Fig. 6.13b) it would appear that it is unlikely to open or flap. Further studies have shown that some 16% change in outlet pressure is required before the non-return valve becomes active. Such changes in pressures are unlikely and it is therefore concluded that this element remains inactive and is not excited by the action of the recycle valve.

6.12 Reproduction of the Compressor Characteristic

The next task was to reproduce the compressor characteristic by introducing a transient due to the opening of the recycle valve. Two such transients were considered. Firstly the valve was opened to half its fully opened area and secondly, the case when the valve was fully opened. The results for the respective transients are shown on the compressor characteristics (Fig. 6.14a and 6.14b). It can be seen that the compressor characteristic is closely reproduced. It should also be noted that the operating point may depart from the compressor characteristic, a feature not present in other models.

6.13 Non-Return Valve

The non-return valve (element 60 in Fig. 6.3) up to now was assumed closed irrespective of the pressure difference across this valve. This assumption in quite valid up to now since the pressure difference across the valve during the transients discussed indicate that it will remain closed. However, should this valve become active, due to any perturbations introduced in the vicinity of this valve, the dynamic response of this valve must be represented.

6.14 Alteration to the Patching Procedure due to the Inclusion of the Dynamic Response of the Non-Return Valve

The sub-systems (2) and (3) discussed in section 4.2 was replaced by one sub-system (i.e. the flow direction is from element 60 to 59 in Fig. 6.3. The sub-system entry pressure is again determined from the mean pressure in the branch element 21. The sub-system

exit mass flow is now determined from the nozzle relationship (Chapter 3) where the pressure ratio is determined by the ratio of the exit pressure in the last element in this system to the mean pressure in the branch element 45 (in Fig. 6.3).

6.15 The Equations of Motion for Non-Return Valve

The non-return valves used in the transmission station are of the spring-mass type with some damping and a drawing of the valve is shown in Fig. 6.15a represented schematically by Fig. 6.15b.

The forces acting on this valve are the restoring spring force, damping force (viscous damping) and driving or external force. The equation of motion is obtained by applying Newtons second law of motion and is given by

$$\frac{d^2x}{dt^2} + 2\,\xi\,\frac{dx}{dt} + \omega_n{}^2\,x = \frac{f(t)}{m} \qquad \ldots.(4.1)$$

where ξ = damping ratio

$\omega_n{}^2$ = (s/m) square of the natural radiancy of the system

and $f(t)$ = external driving force.

The external forcing function $f(t)$ is obtained from the pressure difference across the valve at any instant in time multiplied by the normal valve area

$$f(t) = \Delta P.A_N$$

$$\frac{d^2x}{dt^2} + 2\,\xi\,\frac{dx}{dt} + \omega_n{}^2\,x = \frac{\Delta P.A_N}{m} \qquad \ldots.(4.2)$$

The valve displacement is obtained by integrating equation (4.2) twice and employing the displacement in equation (3.21) in Chapter 3 to determine the mass flow rate through the valve, similar to that employed by the recycle valve.

6.16 Validation of Non-Return Valve

A transient was introduced into the system by perturbing the high pressure side of the non-return valve (element 63 in Fig. 6.3), such that the pressure in the high pressure side was reduced instantly to 400 kpa after 0.02 seconds of steady state running with constant compressor speed operation. This perturbation was sufficient to open the non-return valve and the resultant pressure time history across the non-return valve is shown in Fig. 6.16. Since this pressure restraint on the high pressure side of the valve is only instantaneous and the compressor continuing to deliver gas at a higher pressure the tendency is to close the non-return valve. When the pressure difference across the non-return valve is sufficient to keep it closed the system returns to the initial conditions, and this can be seen in Fig. 6.17, where the pressure time history for the non-return valve is plotted on a smaller time scale.

The corresponding valve movement and the mass flow rate through the non-return valve is shown in Figs. 6.18a and 6.18b respectively. It is interesting to note that the mass flow rate does not reach a maximum when the valve is fully opened. The natural frequency of the spring-mass system in the non-return valve is some 3 Hz. The perturbing or forcing function frequency is some 50 Hz. This condition gives rise to a phase shift between the valve movement and the forcing function. Therefore the pressure difference across the valve will be a minimum when the valve movement is a maximum. Since the mass flow through the valve is a product of some function of the pressure difference across the valve and the valve movement, (equations 3.21 and 3.22 in Chapter 3, this unexpected phenomenon occurs. This phase shift is not quite π radians and is due to the initial transient response of the valve movement.

6.17 Variable Speed Simulation

The compressor characteristic at different speeds are of similar shape, Fig. 6.4. This feature enables the lower speed characteristics to be obtained by assuming that the polytropic head and the volume flow

rate vary according to the square of the compressor speed and linear to the compressor speed respectively. This assumption is valid for compressors that operate at low pressure ratios, typically up to 2.0. The pressure of the compressor never exceeds this value and therefore above assumption is valid for the compressor employed in the transmission station.

The speed transients were introduced by reducing the compressor speed linearly. The deceleration was taken as 500 rpm per second (as opposed to a more usual rate of deceleration of 5 rpm per second) in order to keep computing time to a reasonable level.

The compressor operating point was set at point (4) on the characteristic, Fig. 6.4, and the speed transient was introduced after 0.02 seconds of steady state running. Fig. 6.19a and Fig. 6.19b show the variation of inlet, outlet pressure and entry mass flow rate for the compressor element respectively. The operating point on the compressor characteristic during this transient is also shown in Fig. 6.20.

The transient running line on the compressor characteristic is almost horizontal, and is imposed largely by a near infinite capacity of the downstream duct work.

Another speed transient test was also simulated, however in this case the impedance boundary condition in element 48 (Fig. 6.3) was replaced by a nozzle condition. The system discharges through this nozzle to a fixed pressure equal to that of the system entry pressure at time equal to zero. The pressures across the compressor element and the corresponding entry mass flow rate time history are shown in Figs. 6.21a and 6.21b respectively. The compressor transient running time on the compressor characteristic is also shown in Fig. 6.20.

Unlike the impedance boundary condition the running line in this case is much steeper. This is due to the reduction in nozzle pressure ratio in order to accommodate a lower mass flow rate that has resulted due to the reduction in compressor speed.

Another speed transient was also considered where the deceleration was reduced to 250 RPM per second, with the impedance boundary condition. The simulated results for the compressor element, where the compressor pressures and entry mass flow time history, are shown in Figs. 6.22a and 6.22b. The response of the compressor is similar to that of the previous case (i.e. the case with the higher deceleration rate, -500 RPM per second). The time to surge is, as expected, larger due to the slower deceleration rate.

6.18 Variable Speed Simulation with Further Duct Work Downstream

Further duct work was included in the simulation, however some of the upstream duct work was removed. This was necessary in order to have sufficient computer memory available. Furthermore the simulation with further duct work downstream was considered to be of much interest as it was here that transients were likely (in Fig. 6.23) to occur. A schematic representation of this larger system is shown in Fig. 6.23. The patching of the stub pipes shown is similar to the case when the non-return valve was assumed closed irrespective of the pressure difference across it.

Again the deceleration was maintained at 500 RPM per second and the speed transient was introduced after 0.02 seconds of steady state running. The simulated results, where the pressure across the compressor element and the corresponding entry mass flow during the transient are shown in Figs. 6.24a and 6.24b respectively. The transient running line of the compressor characteristic is shown in Fig. 6.25. It can be seen that the compressor outlet pressure drop during the transient is larger when compared with the smaller system (Fig. 6.19a). The transient running line on the compressor characteristic is also steeper for this case (Fig. 6.25). This is due to the increased frictional loss that has resulted by the addition of further duct work downstream.

6.19 Single and Double Discharge Operation

The gas leaving the pumping station may be discharged through

one or two pipe lines (see Fig. 6.23). The simulated results due to the speed transient when one and both discharge lines are operating are shown in Figs. 6.26a and 6.26b.

Fig. 6.26a shows the variation of the compressor outlet pressure with time when the single and double discharge lines are operating. The pressure drop in the case of the double discharge is smaller and encounters surge before the single discharge case. The reason for this being the velocity in the pipe line when operating with the double discharge is smaller due to the flow area being doubled. Therefore the frictional loss will be less when the double discharge is operating, hence the compressor outlet pressure drop is smaller in this case.

Due to the lower pressure drop in the double discharge line the transient running line is less steep on the compressor characteristic when compared with the single discharge case. Therefore surge will result earlier with double discharge operation. The transient running line on the compressor characteristic for the double discharge case is shown in Fig. 6.27. The corresponding entry mass flow for each case is shown in Fig. 6.26b.

Figs. 6.28a and 6.28b are the simulated results for the compressor element where the deceleration rate was reduced to 250 RPM per second. Again the double discharge case surges earlier than the single discharge case.

6.20 Transient Response due to Perturbations and Speed Decelerations

The only non-return valve considered in the simulations completed so far is the non-return valve (element 63 in Fig. 6.3). There are two further non-return valves in the downstream discharge line (Fig. 6.23). For these tests is was assumed that these valves were not present and a duct with friction loss (i.e. element type =-2) was used in their place. This assumption enables the response of the system due to perturbations to be studied. The case with these non-return valves in position will be considered later.

The speed transient for these tests were set to 250 RPM per second and introduced after 0.02 seconds of steady state running. The perturbation was introduced after 1.5 seconds of simulation time and at the position of the last non-return valve downstream of the compressor, Fig. 6.23. The perturbation was such that the mass flow was reduced instantly to zero and then this constraint removed immediately (putting this mass flow to zero effectively throttles the gas flow).

The compressor pressures and mass flow variation with time are shown in Figs. 6.29a and 6.29b. The oscillatary response does not appear to be damped to the same degree when compared with the perturbation tests already performed with the compressor speed remaining constant. The reason for this response is that the compressor stability is continuously reduced as surge is approached.

The above tests was repeated, however, on this occasion the mass flow perturbation was such that the mass flow was reduced to zero for a period of 0.1 seconds of simulated time. The test gave rise to surge conditions very much earlier when compared with the previous case, and is largely due to the increased throttling effect of the downstream gas flow. The simulated results are shown in Figs. 6.30a and 6.30b where the pressures and mass flow are plotted against time for the compressor element. This situation may arise in the real case should the non-return valves downstream of the compressor close due to a speed transient. The corresponding transient running line on the compressor characteristic is shown in Fig. 6.31.

6.21 Variable Speed Anti-Surge Controller

The variable speed transient was introduced to give surge conditions, however, in order to make the system more general a variable speed anti-surge controller law was included into the computer model. The speed transient was such that the compressor deceleration rate was set to 250 RPM per second and was introduced after 0.02 seconds of steady-state running.

The anti-surge controller law assumes that the surge polytropic head varies with the square of the compressor speed. Ref. 26 quotes that the polytropic head at low compressor ratio (up to 2.0) the polytropic head may be represented by:

$$H_p = \frac{P_2 - P_1}{\rho S^2}$$

and therefore

$\frac{P_2 - P_1}{\rho S^2} \lesssim (H_p^*/U^2)$ to prevent surge (where H_p^* is the surge polytropic head).

The action of the recycle valve was considered to be infinitely fast in order to reduce computer run times.

The pressure time history for the compressor element at the inlet and outlet stations are shown in Fig. 6.32a. It can be seen that the compressor outlet pressure falls at about 2.5 seconds of simulated time. This was due to the recycle valve opening in order to avoid surge. The corresponding entry mass flow time history is shown in Fig. 6.32b. Comparing these values with the previous speed transients (Fig. 6.24a) surge is delayed by over one second. If the mass flow through the recycle valve is increased further the compressor operating point on the characteristic could be moved further from surge such that surge could be avoided altogether. The transient running line on the compressor characteristic is also shown in Fig. 6.33.

The above anti-surge test was repeated but on this occasion the critical value of H_p^*/U^2 was reduced such that the anti-surge controller assumes the surge line has moved into the stable part of the compressor characteristic to the position shown by the line 'AA' on the characteristic, Fig. 6.35. The simulated results for this test is shown in Figs. 6.34a and 6.34b where the pressures and entry mass flow time history for the compressor elements were produced. The corresponding transient running line of the compressor is shown on its characteristic, Fig. 6.35.

6.22 Surge Problems Associated with the Operation of the Compressor Plant

During the deceleration of the compressor the non-return valves in the downstream discharge line may close and it was reported by British Gas that the operation of these valves could indeed be heard. Furthermore, just after these non-return valves start operating the compressor would surge. This surge phenomenon only occurred when the pressure in the discharge line was high. This surge problem was more profound when the double discharge lines were operational. The flow rate through the compressor just prior to surge was large enough to position the operating point of the compressor on the stable part of the compressor characteristic. To an observer this implied that the surge line of the compressor had moved further into the stable part of the characteristic. This surge problem appeared since new compressors and non-return valves were installed.

The recycle valve was unable to cope with this surge problem suggesting that a fast transient associated with the operation of the non-return valve was responsible for the surge problem. To support this explanation British Gas conducted a fast fourier transform on the signals measured downstream of the compressor, and it was found that the transform had a frequency component of 3 Hz. This frequency was associated with the non-return valves since these valves had a resonance frequency of about 3 Hz. The origin of this frequency could not have come from another source because this will result in the non-return valves resonating. As this resonance phenomenon was not observed it was concluded that these non-return valves were active thereby introducing this frequency component in the signal measured.

6.23 Speed Transient Simulation with the Downstream Non-Return Valves

With the two non-return valves included in the downstream duct work the speed transient was introduced after 0.02 seconds of steady state running. The deceleration rate of the compressor was set to 250 RPM per second. The compressor pressures and entry mass flow time history are shown in Figs. 6.36a and 6.36b. It can be seen that

the compressor outlet pressure falls off to a larger degree when compared with the case when no non-return valves were present in the downstream duct work. This was due to the additional pressure loss incurred by the presence of these non-return valves. The corresponding transient running line is shown in Fig. 6.37.

It can be seen in Figs. 6.36 and 6.37 that the sudden surge problem is (see section 6.22) not apparent and during this simulation the downstream non-return valve did not operate. The pressure losses quoted by the valve manufacturers are generally the maximum loss in order to satisfy guarantee requirements. However, such valves may have lower pressure losses and the effect of lower pressure losses will be considered later in section 6.27.

6.24 Effect of Active Downstream Non-Return Valves on Compressor Surge

The above defined speed transient was again introduced. At the time the speed transient was introduced (i.e. after 0.02 seconds of steady state running), the pressure downstream of the last down-stream non-return valve was instantaneously increased by 5% above its initial value, and maintained for 0.1 seconds of simulated time. This increase in pressure was sufficient to close the downstream non-return valves.

The pressures across the compressor element and the entry mass flow time history is shown in Figs. 6.38a and 6.38b respectively. Examining the compressor entry mass flow time history, Fig. 6.38b, it can be seen that surge occurs quite quickly, furthermore the compressor surges in approximately 0.075 seconds. The anti-surge recycle valve having a stroke time of some 10 seconds will be unable to cope with such fast transients. This condition is very similar to that observed in the gas transmission station where such a sudden surge condition occurs. This surge condition is produced by the throttling of the gas flow due to the closure of the downstream non-return valves.

The non-return valve movements in the downstream discharge line are shown in Figs. 6.39a and 6.39b respectively. The pressure difference

across each non-return valve and the corresponding mass flow rate are given in Figs. 6.40a, 6.40b and Figs. 6.41a, 6.41b respectively. The pressure difference across the isolating non-return valve (element 63 in Fig. 6.3) is shown in Fig. 6.42 again the pressure difference across this valve is always sufficiently positive to ensure that this valve remains closed during the transient.

A further test was conducted where the above pressure transient was introduced after 1.5 seconds of simulated time. The speed transient was identical to that mentioned above. The results for this test are shown in Figs. 6.43a and 6.43b where the pressures and entry mass flow time history are shown for the compressor element. Again as in the previous case surge was encountered in a similar manner, however it occurred much faster. This is due to the reduced compressor stability since the compressor operating point on the characteristic was much closer to surge when the non-return valve was closed, (due to the delayed introduction of the pressure transient downstream of the last non-return valve). Therefore the stability of the compressor may have a significant effect on this sudden surge problem, and will be investigated later.

6.25 Effect of One Non-Return Valve on Compressor Surge

The last non-return valve in the downstream duct work was removed and replaced by a straight pipe having only friction loss (element type = -2). The above pressure and speed transient were both introduced after 0.02 seconds of steady state running. The compressor inlet, outlet pressure and entry mass flow time history are shown in Figs. 6.44a and 6.44b respectively. Compressor surge was again encountered but very much delayed, after some 1.75 seconds of simulated time. The above tests indicated that the activation of the number of downstream non-return valves also has a strong influence on compressor surge due to the resultant throttling of the gas flow associated with closing of the downstream non-return valves.

6.26 The effect of the Operation of the Anti-Surge Valve on Compressor Surge

It was mentioned that during such fast transients the anti-surge recycle valve was unable to cope resulting in compressor surge. To test this theory the speed transient and the delayed pressure transient test was repeated with both downstream non-return valves in position, (i.e. the speed transient was introduced after 0.02 seconds of steady state running and the pressure down stream of the last non-return valve in the discharge line was increased after 1.5 seconds of simulated time), with the variable speed anti-surge controller included in the compressor model. The recycle valve action was assumed to be infinitely fast.

The simulated compressor pressures and entry mass flow time history are shown in Figs. 6.45a and 6.45b. By examining the compressor entry mass flow results (Fig. 6.45b) it can be seen that surge did occur for approximately 0.25 seconds of simulated time before the system recovered sufficiently to remove the compressor from surge. It is also noticed that the compressor response, after the opening of the recycle valve, is very oscillatory. This oscillatory response is largely due to the continued slamming of the two non-return valves in the discharge line. Here the slamming of the non-return valves are due to the fall in compressor outlet pressure resulting from the opening of the anti-surge recycle valve.

6.27 The Effect of Reduced Pressure Loss in the Non-Return Valves

The precise pressure drops to apply to the NRV was uncertain and the manufacturers pressure loss data was reduced by $^1/_{50}$th and the speed transient only repeated. The deceleration was again fixed at 250 RPM per second and this transient introduced after 0.02 seconds of steady state running.

On this occasion the non-return valves did indeed close and eventually gave rise to compressor surge conditions. This can be seen in Figs. 6.46a and 6.46b where the compressor element pressures and entry mass flow time history are shown. The corresponding non-return valve movements are shown in Figs. 6.47a and 6.47b. These valve movement results show that the last non-return valve (Fig. 6.47a) in the discharge line moved first. The compressor mass flow decreased from about 250 kg s^{-1} (well into the stable part of the compressor

characteristic) into the surge part about 20 kg s^{-1} in some 0.17 seconds of simulated time, hence confirming that such fast transients may be produced the surge problem observed in the transmission station. The slamming of the downstream non-return valves were due to the change in pressures across these valves, during the transient, was larger than the valve pressure loss.

6.28 Slower Speed Transients Simulation

The speed transients considered up to now were unrealistically high. This was necessary in order to keep computer run times reasonable. However it was considered necessary to conduct a few speed transient tests at a more realistic deceleration rate. The computer program was transferred to a faster VAX 11/782 machine so that such slow speed transients may be considered.

The first system considered for the slow speed transient had no non-return valves in the downstream discharge line. The speed transient was introduced after 0.02 seconds of steady state running and the compressor speed deceleration rate was set to 25 RPM per second. The simulated results for the compressor element where the pressures and entry mass flow time history are shown in Figs. 6.48a and 6.48b respectively. These transient results are similar to those of the, previous, faster speed transients considered with the expectation that the simulated time to surge was considerably larger, nearly ten times that of the fast speed transient.

The above slow speed transient was then repeated with the two downstream non-return valves in the system. The pressure loss in those valves were reduced to $^{1}/_{50}$th the manufacturers data. The simulated results for this test are shown in Figs. 6.49a and 6.49b where the compressor element pressures and entry mass flow time history are shown. The corresponding valve movements for the respective values are shown in Figs. 6.50a and 6.50b. By examining the mass flow time history for the compressor element, Fig. 6.49b, the sudden compressor surge phenomenon is present. This can also be seen on the compressor characteristics, Fig. 6.51 , where the transient running line is shown.

6.29 Comparison of Speed Transient Simulation with the old Compressor Characteristics

It was mentioned that this surge phenomenon, present in the gas transmission station, started after the compressor had new impellers and non-return valves installed. Comparing the old and the new compressor characteristics show that the new wheel has a flatter characteristic, and therefore the stability of the new compressor was less.

To determine the effect of the reduction in compressor stability, the slow speed transient was repeated with the old compressor characteristic. The pressure loss in the non-return valves was still maintained at $^1/_{50}$th of the manufacturers data.

The slamming of the non-return valves were again present during this transient. The simulated results for the compressor element where the pressures and entry mass flow for this element were plotted against time are shown in Figs. 6.52a and 6.52b respectively. It can be seen (Fig. 6.52b) that surge due to the slamming of the downstream non-return valves, was considerably delayed, (see Figs. 6.46a and 6.46b where the flatter characteristic was used in producing these results).

6.30 Conclusion

The system behaviour with respect to stable operation, transients from one stable point to another have been successfully simulated. Other transients such as perturbations introduced into the system have also been reasonably simulated. The phenomenon where the compressor becomes less stable as the compressor operating point approaches surge is clearly illustrated. The ability for the transient operating point to leave the steady state characteristic was also demonstrated (a feature not available in most models).

The surge cycle simulations gave encouraging results. The fall in the compressor outlet mean pressure, due to a non-linear characteristic was well represented. The model also showed the ability to incorporate anti-surge controllers, and may be used to test the

efficiency of control systems used in process plants.

The development of the boundary condition for use in an "in finite" system appear to have been very successful. The infinite boundary condition highlights compressor surge problems during shut down.

Increasing the number of elements downstream tends to help avoid surge conditions and is mainly due to the increase in loss in the system. The double and single discharge header was also simulated, and the results indicate that the double discharge system is likely to reach compressor surge before the single discharge system. This is in line with experience in the real system.

All the tests conducted on the non-return valve 3, (fig. 6.23), show that the pressure difference across this valve is always large enough to ensure that this element remains inactive (closed). The necessary pressure difference required to open this valve is unlikely to be attained under operating conditions simulated in this thesis.

The case when the steeper characteristic was used surge occurred but somewhat delayed. The non-return valve did slam in this case too. The surge resulted due to the operation of these downstream non-return valves where the gas flow through these valves are throttled when the valves close.

The slamming of these downstream non-return valves appears to be the real cause of the problem since the operation of these valves throttle the compressor discharge gas making the compressor surge prone. A reduction of the number of non-return valves will help the system as was illustrated in figs. 6.44a and 6.44b where only one of the downstream return valves was present (the non-return valve closest to the compressor in the discharge line), due to the reduced throttling effect. However, increasing the pressure loss on each valve will prevent the valve slamming but the system will operates less efficiently.

A system that may have such an arrangement having only one non-return valve in the discharge line irrespective of the number of compressor units present in the station is shown in fig. 6.53. The limitation of such a system is that only parallel operation of the compressor units is possible. However this transmission station has never used the compressor units in series. Furthermore, when any one unit is operational, (the proposed system Fig. 6.53), the gas has to flow through only one non-return valve unlike two valves with the current system. This will result in lower pressure loss hence making the station more efficient. Alternatively the pressure loss in the non-return valve may be increased sufficiently to prevent the non-return valve slamming hence over coming the surge problem.

CHAPTER 7

7.0 DISCUSSION AND SUGGESTION FOR FURTHER WORK

Increasing the losses in the gas transmission system will result in a steeper transient running line on the compressor characteristic. However, surge encountered due to a relatively flat transient running line may be satisfactorily overcome by the anti-surge recycle valve since this transient is relatively slow. The throttling of the gas flow in the downstream discharge line, due to the slamming of the non-return valve, introduce rapid transients, and the recycle valve is unable to cope resulting in compressor surge operation. Reducing the number of non-return valves in the discharge line helps this surge problem due to the reduction of the throttling effect and therefore giving the recycle valve a better chance to cope.

7.1 Non-Return Valve

In order to simulate the case when these downstream non-return valves may operate during a speed transient it was necessary to reduce the pressure losses in these valves. The pressure loss was reduced in steps of $^1/_{25}$th of the valve manufacturers data until the valve movements occurred (i.e. a pressure loss of $^1/_{100}$th of the pressure loss data was necessary in order to obtain the valve movement). A better estimation of the pressure loss may be obtained by undertaking an experimental investigation on these non-return valves. Furthermore the valve mass and spring stiffness data were not readily available and these values were obtained by approximate calculation of valve volume and density of the material. The reasonable valve stiffness was (225 Nm^{-1}) assumed. The above information from the valve manufacturer will enable a more accurate simulation.

7.2 Boundary Condition

The impedance boundary condition requires that the pressures upstream of the system boundaries (i.e. upstream of element 1 and downstream of element 48 in fig. 6.4) must be largely constant. This condition satisfies the assumption that the acoustic impedance upstream of elements 1 and 2 (fig. 6.4) are equal, and similarly downstream of elements 48 and 47 are also equal. However, the pressures in the pipeline may vary considerably as the pipeline serves a secondary function of gas storage.

The satisfactory manner to account for such pressure variations is to model the pipeline all way down to the consumer. Should such a simulation be attempted, the number of elements may run into tens of thousands and the computer run times of such a simulation will be prohibitively high. If a simulation accounting for such pipeline pressure variation were required a reasonable approximation may be to use the nozzle relations discussed in Chapter 3. The plenum pressure to which the nozzle exhausts to may be determined by performing an instantaneous mass balance of a given control volume, V_p, downstream of the system considered. Using the value of the mass, m, within this control volume the approximate instantaneous plenum pressure, p_s, may be determined via the equation of state $p_s V_p = mRt_s$. A similar method may be used to determine the system entry pressure.

7.3 Intercoolers

Intercoolers are common occurrence in process plants. Detailed analysis of this type of element has yet to be performed. It is expected that such an element may be modelled similar to that of a duct with loss type element discussed in Chapter 3, and the exit temperature determined from the intercooler effectiveness equation.

7.4 Computer Run Times

A significant problem uncovered during this project has been the very long computer program executing times, particularly when many elements are involved in defining a system. Although using a powerful

computer and a faster integrating technique helps matters, a substantial reduction in executing times may be obtained by using parallel or array processing.

7.5 Additional Application for the Technique

The application of the model may be considered for many systems where one-dimensional flow analysis is required. There are instances where two dimensional flow considerations are required. One such example is the effect of after-burning, in low-by pass ratio turbo-fan engines, on low pressure compressor surge.

The problem may be attacked by dividing the low pressure compressor into two parallel systems along the by pass splitter axially. The flows between the compressor stages and at the splitter may be patched using the patch procedure discussed in Chapter 6. The steady state compressor characteristic for the two systems is required, (i.e. below and above the splitter line), in order to determine the required body force terms. The respective system entry pressures may be found by studying the radial equilibrium criteria used (i.e. free vortex or constant reaction etc.).

The disadvantage of the above method is that flows crossing the systems within the stages are not accounted for. However, the radial pressure gradient that exists within the compressor stage will ensure that most of the flow crossing the system dividing line will occur within stages hence reducing any error due to the assumption that no flows crossing the dividing line with the stage.

CHAPTER 8

8.0 CONCLUSIONS

This project, in the main, has been concerned with the application of a mathematical model which can simulate process plant system transients, in particular centrifugal compressor transients used in natural gas transmission systems. After the development of the model it was considered necessary to undertake an experimental validation programme.

8.1 The Model

The derivation of the mathematical model has involved several assumptions. Firstly, the one-dimensional flow assumption, although this appears to be a drastic simplification of the complex flow structure known to exit it does not appear to be a limiting factor as proven by the results obtained in this study. Furthermore such assumptions have been made in many other models and good results have been obtained. The model employed here is considered to be much easier to apply compared with those described in Ref. 8, and where again momentum and continuity equations were used in the derivation.

Secondly the assumption of low Mach number at the boundaries of the discretisation process (less than 0.3) implies that the element boundaries should be chosen to comply with this requirement. Thirdly, the justification for neglecting the dynamic effects of the energy equation is simply that results are little effected and the computational effort is much reduced (Ref. 10,11). Finally, the lumped parameter and the quasi-steady state assumptions impose frequency limitations on the model. These limitations are not serious so long as care is taken and the element length is much less than the wave length of the flow perturbations.

General application rules for the geometric distribution of element have been formulated. The first, relating element length with a frequency parameter, is based upon the work of Elder (Ref. 11), and is derived from the comparison of the lumped and true partial differential solutions. The critical frequency parameter obtained from this study is set such that the error between these two solutions is small (less than 5%). The second criteria, namely approximately equal volumes, is necessary to ensure that the elements will interact with each other to a larger extent.

8.2 Experimental Validation

The mathematical model was validated using transient data obtained from a small centrifugal compressor of a turbo-charger. The general agreement between the simulated and experimental results is very good. The slight discrepancies are very largely attributed to the inaccuracies in the representation of the poppet valve action. The surge validation test gave equally encouraging results.

It is not reasonable to expect a model of this type to simulate full compressor surge cycles without accurate knowledge of the post surge compressor characteristic. If such characteristics are available it is thought that the model is capable of simulating complete surge cycles.

8.3 Simulation of Natural Gas Transmission System

The behaviour of the natural gas transmission system during transient changes between two stable operating conditions has successfully been simulated. The system response to perturbations introduced into the system have also been reasonably simulated. The reduced stability of the compressor when surge is approached has been clearly illustrated.

Compressor surge simulation gave encouraging results. The fall of the mean compressor outlet pressure, due to the non-linear nature of the compressor characteristic near surge, was well represented.

The ability to test the efficiency of anti-surge control systems is also possible. Pre surge and post surge simulation has also been performed (i.e. the case when the anti-surge recycle are opened after the compressor had surged).

The development of the "infinite volume" boundary condition appear to be successful and this boundary condition indicated compressor surge problems during shut down. The single and double discharge operation simulation showed the compressor surge delayed when the single discharge system was operational. This was due to the higher velocities in the discharge pipe during single discharge operation resulting in higher pipe pressure loss which tends to delay surge.

The model was also successful in highlighting compressor surge problems associated with the operation of the downstream discharge line non-return valves. The activation of these valves throttles the gas flow in the discharge line resulting in compressor surge. This throttling effect introduces rapid transients into the system to make the recycle anti-surge valve ineffective. Even when the re-cycle valve time constant was put to zero compressor surge occurred. This sudden surge phenomenon is present in the plant and apparently the non-return valves are the cause of this surge problem.

The operation of these downstream non-return valves could be prevented if the pressure loss associated with these valves were in-creased, and therefore overcoming the surge problem. However, this will result in the plant becoming inefficient and a higher operating cost. The model was used to study the effect of one non-return valve in the down stream discharge line. This study indicated compressor surge to be delayed, due to the reduced effect of the throttling of the gas flow in the discharge line. Since only one non-return valve is present the pressure loss may be increased in this valve without suffering a significant loss in plant efficiency hence help overcome this unexpected compressor surge problem.

The steeper compressor characteristic also gave surge conditions although delayed compared with the case of the flatter characteristic. However stable the characteristic is made, sufficient throttling of the downstream gas flow (due to the activation of the non-return valves) will give surge condition.

8.4 Numerical Method

Single step methods are generally self starting and the estimation of the integration error is relatively easy. Of the many single step methods available, that of Runge-Kutter-Merson is very efficient. To this effect the Runge-Kutta-Merson method was used to solve the non-linear differential equations derived in Chapter 2. Another efficient method that is becoming increasingly popular is the Runge-Kutta-Fehlberg method.

Multi-step methods are computationally more efficient but they have the disadvantages of not being self starting and the estimation of the integration error is awkward. A multi-step method that is stable, accurate and particularly recommended for so called stiff equations is Gears method. Other multi-step methods worth considering are Adam-Moulton and Hammings methods.

8.5 Numerical Instabilities

Numerical instabilities were incurred where the volumes of elements in the vicinity of branches and butts (or stub) are very similar. These instabilities are apparently due to flows pulsating in branches (and butts) exciting oscillations in the main stream elements in the neighbourhood.

It was found that such instabilities may be avoided if the element volumes near branches (and butts) were staggered. A ± 10% change in these element volumes are possible without introducing a

significant error in the simulation. Another approach to these instabilities is to increase the friction force in elements in the neighbourhood of branches (and butts) so that these oscillations may be damped to a larger degree. However, this may result in an unrealistic pressure loss in these elements. Apart from these problems the model proved relatively simple to use.

CHAPTER 9

9.0 SUMMARY OF CONCLUSIONS

A mathematical model capable of simulating centrifugal compressor transient performance within a process system has been developed and implemented in a Fortran computer program. The model is applicable to any type of process plant, and can deal with non-ideal gases. The analysis is limited to one dimensional flow consideration. A comparison of simulated and measured compressor transients has shown that:

(1) Simulation of transients between stable operating points has been performed with reasonable accuracy.

(2) Satisfactory compressor surge simulation has been performed in terms of variable time history.

(3) The computer code has been prepared in a modular fashion to permit different studies to be easily made. In addition to this project described here, multi-stage axial and centrifugal compressors may be considered.

The model was successfully applied to a natural gas transmission system, having operational problems associated with plant dynamics. The model highlighted compressor surge problems due to the interaction of the compressor with plant controls. Through these studies a possible solution to the compressor surge problem was suggested.

The model has the potential to be used as a design tool to study plant dynamic problems or improving the dynamic performance of existing plants. Another application for the model is the accident investigation of process plants.

REFERENCES

1. Davis, F.T.
   Corripio, A.B.
   Dynamic Simulation of Compressor using a Real Gas Equation of State.

2. Dean, R.C.
   Young, L.R.
   The Time Domain of Centrifugal Compressor and Pump Stability, Stall and Surge. March 1976.

3. Rothe, P.H.
   Runstadler, P.W.
   First Pump Surge Behaviour. J. Fluid Eng. Dec. 1978. p.439-466.

4. Fasol, Kitt,
   Tuip, L.
   Identification of Blast Furnace Air Supply System. Paper 8.6, 4th IFAC Symposium on Identification and System Parameter Estimation, Tbi Usi, Sept. 1976.

5. Fasol, Kitt,
   Gironau, M.
   Tuip, L.
   Possibilities of Theoretical and Experimental Identification of Blast Furnace Air Supply System, VDI Berichte, 276, 1977, p.18-85.

6. Fasol, K.H.
   Gironau, M.
   Modelling and Simulation of a Chemical Process Plant Blast Furnace System. IMACS Symposium on Simulation of Control Systems, Vienna, Sept. 1978.

7. Kulberg, J.F.
   Sheppard, D.E.
   King, E.O.
   Baker, J.R.
   The Dynamic Simulation of Turbine Engine Compressors. AIAA 69-486, AIAA 5th Propulsion Conference.

8. Willoh, R.G.
   Seldner, K.
   Multistage Compressor Simulation Applied to the Prediction of Axial Flow Instabilities. NASA TMX-1880. Sept. 1969.

9. Corbett, A.G. / Elder, R.L. — Stability of an Axial Flow Compressor with Steady Inlet Condition. J.Mech.Eng.Sci. Vol. 16, No. 6, 1975.

10. Corbett, A.G. / Elder, R.L. — Mathematical Modelling of Compressor Stability in Steady and Unsteady Flow Conditions. Unsteady Phenomena in Turbomachinery, AGARD p177, 1976.

11. Elder, R.L. / Macdougal, I. — Simulation of Centrifugal Compressor Transient Performance for Process Plant Application. ASME paper, 1983.

12. Greitzer, E.M. — Surge and Rotating Stall in Axial Flow Compressor Part II - Experimental Results and Comparisons with Theory. J. Eng. for Power, April, 1978, p.199.

13. Schultz, J.M. — The Polytropic Analysis of Centrifugal Compressors. J. Eng. for Power, Jan 1962, p.62-82.

14. Royal Aero. Soc. — Friction Losses for Fully Developed Flow in Straight Pipes. Eng. Sci. Data Sheet 66027, 1966.

15. Royal Aero. Soc. — Pressure Losses in Curved Ducts: Single Bends. Eng. Sci. Data Sheet 77008, 1977.

16. A. Eli Nisenfeld — Centrifugal Compressor Principals of Operation and Control. ISA 67, Alexander Drive, P.O. Box 12277, Research Triangle Park, NC 27706.

17. Curtis F. Gerald / Patrick O. Wheatley — Applied Numerical Analysis Third Edition, Addison Wesley 11577.

18. Robert W. Hornbeck — Numerical Methods. QPI Series, Quantum.

19. Gear, C.W. — The Numerical Integration of Ordinary Differential Equations, Mathematics of Computation, 21, p.146-156.

20 Jaroszkiewicz, G. Strange, J.H. — DL900 Series Transient Recorder (MK11 Binary Interface). Interface and Software for PET 2001 Microcomputer.

21. Hockney, R.W. — Characterisation of Parallel Computers and Algorithms. University of Reading, March 1981.

22. Hockney, R.W. — The Large Parallel Computer and University Research. Section A, No. 22. British Association for the Advancement of Science Annual Meeting. Bath University, Sept. 1978.

23. Elder, R.L. — Mathematical Modelling of Axial Compressors. Ph.D. Thesis, Leicester University, 1972.

24. Kemp. U. — The Control of Turbo-Compressor. Sulzer Technical Report, 1963, Vol. 45, part 2.

25. Brown, R.N. — Control Systems for Centrifugal Gas Compressors. Chemical Engineering 1964, Feb. 17.

26. Roberts, P.D. — Methods for Anti-Surge Control of Centrifugal Compressors. Inst. M.C. Symposium, Turbine and Compressor Control, April 1979.

APPENDIX A

The following fast response Kulite transducers were used to take transient measurements during the compressor test.

Station	Type	Pressure Convertion Expression
System inlet	4376-1-10	$P_{sig} = \frac{43}{45} \times (mV)$
Impeller inlet	4376-1-4	$P_{sig} = \frac{70}{71} \times (mV)$
Compressor outlet	7056	$P_{sig} = \frac{22200}{87} \times (mV) - \frac{19}{87}$
Blow-off valve	7055	$P_{sig} = \frac{430}{17} \times (mV) - \frac{3}{17}$

APPENDIX B

VALIDATION MODEL SYSTEM GEOMETRY

Element	Volume	Area	Length	Type
1	0.00109	0.007	0.152	-2
2	0.00181	0.002	0.761	1
3	0.00278	0.005	0.610	-2
4	0.00012	0.005	0.025	-3
5	0.00278	0.005	0.761	2

APPENDIX C

ACTIVE ELEMENT TYPES

The desired system may be obtained by the combination of some or all of the types of elements discussed below.

Non-Active Element (Type = -1)

This element does not introduce any pressure loss or work input. Adiabatic conditions are assumed (ideal duct).

Duct with Loss Element (Type = -2)

Simple pipe friction used to calculate pressure loss. No work input and adiabatic conditions are assumed.

Throttle Valve Element (Type = -3) or Blow Off Valve Element

This element introduces transients into the system. The variation of valve area with time and valve time constants is required.

Compressor Element (Type = 1)

This element inputs work into the system. The characteristic must be of the form of polytropic head (J kg^{-1}) vs volume flow rate (m^3 h^{-1}), together with corresponding value of the compressor polytropic efficiency, at the desired operating speed.

Duct with Experimental Loss Element (Type = -4)

This element determines the pressure loss to evaluate F_{net} from experimental values. A linear fit is obtained from the experimental data.

Therefore

$$\Delta P = A * \text{slope} + \text{constant}$$

Diffuser Element (Type = -5)

This element is used to represent an expanding duct.

Nozzle Element (Type = -6)

As the name suggests this element represents a converging duct.

Valve Element (Type = -7)

A recycle valve is represented by this element. It may be used as an isolating valve or a means of introducing a transient into the system. The valve area variation with time and the valve stroke time is required.

Bend Element (Type = -8)

This element is used to represent a right angle bend.

Branch Element (Type = -9)

Combining and dividing flows are represented by this element. This element also patches sub-system when parallel systems are considered.

Non-Return Valve Element (Type = 6 and 7)

This element represents a valve that is operated by the pressure difference across it. If TYPE = 6 it is assumed the valve is initially closed. When TYPE = 7 the valve is initially opened.

Nozzle Boundary Condition (Type = 2 and 4)

This element determines the exit mass flow leaving a system by the nozzle relationship discussed in chapter 3. If type = 2, then the nozzle discharges to a fixed plenum pressure specified by pamb in Table 5.1. If type = 4, the discharge pressure is determined by the mean pressure in the branch to which the system is exhausting.

Butt Element (Type = 3)

This element sets the exit mass flow of a system to zero. It represents a flanged pipe.

Near Infinite Volume Boundary Condition (Type = 5)

This element determines the system exit mass flow by the equating of the acoustic impedence downstream and upstream of the exit of the system. See chapter 3.0.

APPENDIX D

QUICK REFERENCE GUIDE TO TRANS

The required data for the simulation programme (Trans) is stored in a file and accessed through an edit programme (Setup). Fig. 5.7 shows a flow chart which explains how the edit programme operates.

There are two data files formed by the execution of Setup. The first file stores compressor speed data, and this file is named SPEED. The second file has the remaining data (i.e. input system geometry, gas characteristics, compressor characteristics) required to run the simulation programme Trans.

This arrangement enables the user to edit the second data file either using the programme Setup or by editing the data file directly (using the computer command codes). If many changes are required it is usually more convenient to use the programme Setup which has a question answer format, however, if only a few changes are required it is often simpler for the experienced operator to edit the file directly.

Table 5.1 shows a typical data file, used for the simulation programme Trans, called Test 2. The meanings of the variables in this file are as follows:

VARIABLE	NAME	MEANINGS	UNITS
1	GASCON	Gas constant (R)	(J kg^{-1} K^{-1})
2	GAMMA	Ratio of specific heats ($\gamma = C_p/W$)	(-)
3	COMFAC	Compressibility factor (Z)	(-)
4	XFAC	Schultz "X" factor	(-)
5	VISK	Kinematic Viscosity (V)	(m^2 s^{-1})
6	ETA	Pipe surface roughness	(-)

VARIABLE	NAME	MEANINGS	UNITS
7	PAMB	Ambient pressure	Nm^{-2}
8	TAMB	Ambient temperature	K
9	P_1	System inlet total press	Nm^{-2}
10	W_1	System inlet mass	kg s^{-1}
11	T_1	System inlet temperature	K
12	AREA	Nozzle Area	m^2
13	ABOV	Valve fully opened area	m^2
14	TCON	Valve time constant	(sec)
15	VTIM	Valve movement start time	(sec)
16	VIND	Valve start position indicator	(-)
17	XTIM	Variable change time	(-)
18	DELT	Initial time step	(sec)
19	FINTIM	Stop time	(sec)
20	OUTDEL	Fixed output interval	(sec)
21	ERRT	Upper Integration error limit	(-)
22	ERRB	Lower Integration error limit	(-)
23	ITURB	Turbine Indicator	

All the above variables are self-explanatory except the variables 16 and 17. The variable 16, VIND, is provided as a transient indicator. In the case of "blow off valve" transients it is usual to use VIND to indicate the initial position (open or closed) of the blow off valve. (VIND = +1 implies the valve to be initially open and VIND = -1 the valve to be initially closed). The use of variable 17, XTIM, is given below.

Interactive Input

The variable change time, XTIM, 17, enables the user to change the following variables at a time originally specified by XTIM. These variables are:

1 MASS FLOW (any element)
2 PRESSURE (any element)
3 TEMPERATURE (any element)

4	GAMMA (γ)
5	GAS CONSTANT (R)
6	COMFAC (Z)
7	XFAC (X)

Furthermore, future variable changes are possible without altering the previously chosen value of XTIM (i.e. XTIM may be altered through the simulating program (Trans), when the accumulated time is equal to or greater than the initial value of XTIM).

APPENDIX E

SUBROUTINES

Subroutine DYBDX

As the name implies, this routine calculates rates of change (at the present time) of pressure and mass flow with respect to time just prior to integration (using equations

Subroutine RKM

This routine solves ordinary differential equations using the Runge-Kutta-Merson method.

Subroutine SUB06

Enables the user to change certain variables during the program execution at a specified time (XTIM) (i.e. interactively).

Subroutine INOUT

Reads input data from disk and write output data to the specified device (i.e. line printer, VDU or disk file).

Subroutine CHANGE

This routine inputs the system geometry and speeds of the respective elements. (It also enables the user to increase the number of elements in an existing data file).

The programme Trans operates quite simply once the necessary data files SPEED and (for example) TEST 2 have been defined. (The actual name of the second file is requested as the running of Trans is initiated).

Both data files can be defined using the programme Setup. Running of this programme has a question-answer system which is self explanatory. The second file (for example TEST 2) must be provided for the successful operation of Trans but the file is only required if the compressor shaft speed fluctuates.

Subroutine SUB01

This routine calls the subroutines defining the type of elements present in the system (i.e. duct with loss, compressor, valves, etc as discussed in Appendix A).

APPENDIX F

Element Types Used for the Simulation of Gas Transmission Station

Element	Type	Element	Type
1 - 10	-2	41	-9
11	-6	42 - 44	-2
12	-8	45	-9
13 - 18	-2	46 - 47	-2
19	-6	48	5
22	-2	59	-2
21	-9	60 - 62	-2
22 - 26	-2	63	-3
27	-8	49	-2
28	-8	50	-9
29	-2	51	-2
30	-8	52	-9
31 - 32	-2	53	-2
33	1	54	-8
34 - 35	-2	55	-7
36	-8	56	-2
37	-2	57	-9
38 - 39	-8	58	-2
40	-2	59	-2
		60	-2

Basic Flow Relations Across Element

Continuity

$$\int_{X_1}^{X_2} A \frac{\partial \rho_s}{\partial t} dx = W_1 - W_2$$

Momentum

$$\int_{X_1}^{X_2} \frac{\partial W}{\partial t} dx = A\ (P_1 - P_2 + F_{net})$$

Lumped Distribution Assumption

$$A \frac{d\rho_{s_2}}{dt} = \frac{1}{\Delta x} (W_1 - W_2)$$

$$\frac{dW_1}{dt} = \frac{A}{\Delta x} (P_1 - P_2 + F_{net})$$

Linearly Distributed Parameter

$$A_2 \frac{d\rho_2}{dt} + A_1 \frac{d\rho_1}{dt} = \frac{2}{\Delta x} (W_1 - W_2)$$

$$\frac{dW_2}{dt} + \frac{dW_1}{dt} = \frac{2A}{\Delta x} (P_1 - P_2 + F_{net})$$

Table 2.1

Method	Type	Local Error	Global Error	Function Evaluation Step	Stability	Ease of Changing Step Size	Recommend-ation
Modified Euler	Single-step	$O(h)^3$	$O(h)^2$	2	Good	Good	No
Fourth Order Runge-Kutta	Single-step	$O(h)^5$	$O(h)^4$	4	Good	Good	Yes
Milnes	Multi-step	$O(h)^5$	$O(h)^4$	2	Poor	Poor	No
Adams-Moulton	Multi-step	$O(h)^5$	$O(h)^4$	2	Good	Poor	Yes
Hamming's	Multi-step	$O(h)^5$	$O(h)^4$	2	Very Good	Poor	Yes
Gears	Multi-step	$O(h)^6$	$O(h)^5$	2	Very Good	Poor	Yes

Table 4.1 Comparison of Methods for Differential Equation

SURGE.DAT

VAR	NAME	VALUE	VAR	NAME	VALUE
1	GASCON	287.0	13	ABDV	0.00060
2	GAMMA	1.400	14	TCON	0.25
3	COMFAC	1.000	15	VTIM	0.20
4	XFAC	0.000	16	VIND	1.0
5	VISK	0.000016	17	XTIM	0.00
6	ETA	0.0025	18	DELT	0.0010
7	PAMB	101300.00	19	FINTIM	2.00
8	TAMB	288.1	20	OUTDEL	0.10
9	P1	101300.00	21	ERRT	0.0100
10	W1	0.54	22	ERRB	0.0001
11	T1	288.1	23	ITURB	0
12	AREA	0.00456			

SPEED = 6500.

ELEMENT	TYPE	STAGE
1	-2	0
2	1	1
3	-2	0
4	-3	0
5	-2	0
6	2	0

	VOLUME	AREA	LENGTH	NDS	SLOPE	CNST
1	0.00109	0.00700	0.152	0.0	0.00	0.0
2	0.00181	0.00200	0.761	6500.0	0.00	0.0
3	0.00278	0.00500	0.610	0.0	0.00	0.0
4	0.00012	0.00500	0.025	0.0	0.00	0.0
5	0.00278	0.00500	0.761	0.0	0.00	0.0
6	0.00058	0.00500	0.127	0.0	0.00	0.0

*** STAGE 1

VOLFLOW	POLYHEAD	EFFICIENCY
1100.0	130000.0	0.6000
1150.0	127000.0	0.6000
1200.0	125000.0	0.6500
1250.0	122500.0	0.6700
1300.0	120000.0	0.7000
1350.0	122500.0	0.7200
1400.0	124000.0	0.7250
1450.0	125500.0	0.7350
1500.0	126000.0	0.7400
1550.0	125500.0	0.7440
1600.0	125000.0	0.7550
1650.0	124000.0	0.7420
1700.0	122500.0	0.7370
1750.0	120500.0	0.7300
1800.0	117000.0	0.7250
1850.0	115000.0	0.7150
1900.0	110000.0	0.6950
1950.0	60000.0	0.4200

ILE ENDFILE ENDFILE ENDFILE ENDFILE ENDFILE ENDFILE ENDFILE ENDFILE ENDFILE ENDFI

TABLE 5.1 TYPICAL DATA FILE

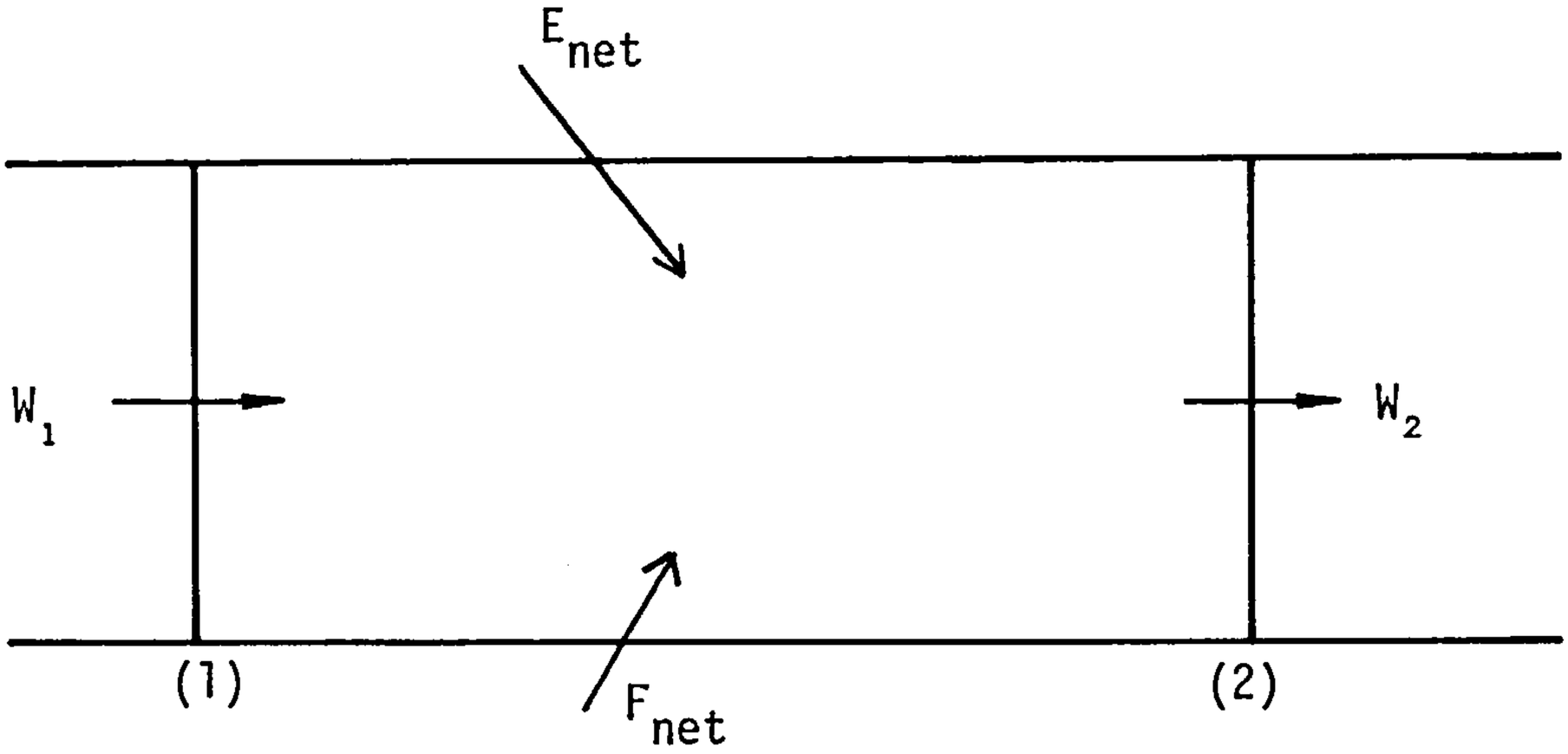

Figure 2·1 Generalised One Dimensional Flow Model

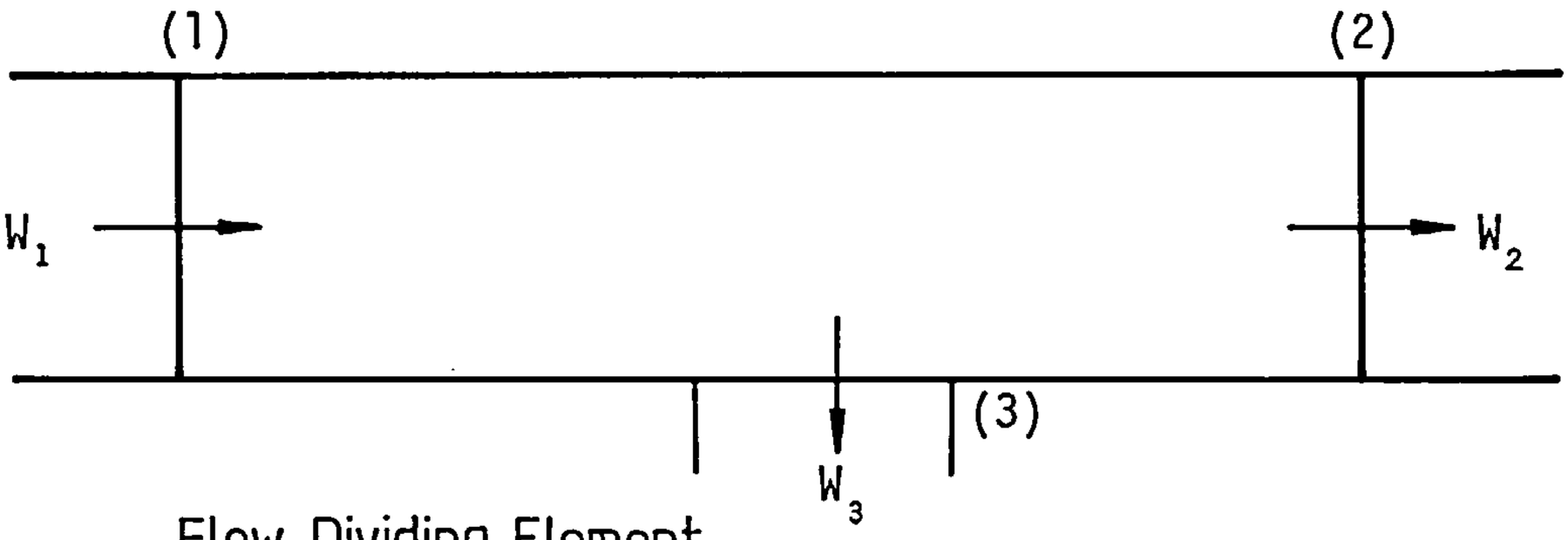

Flow Dividing Element

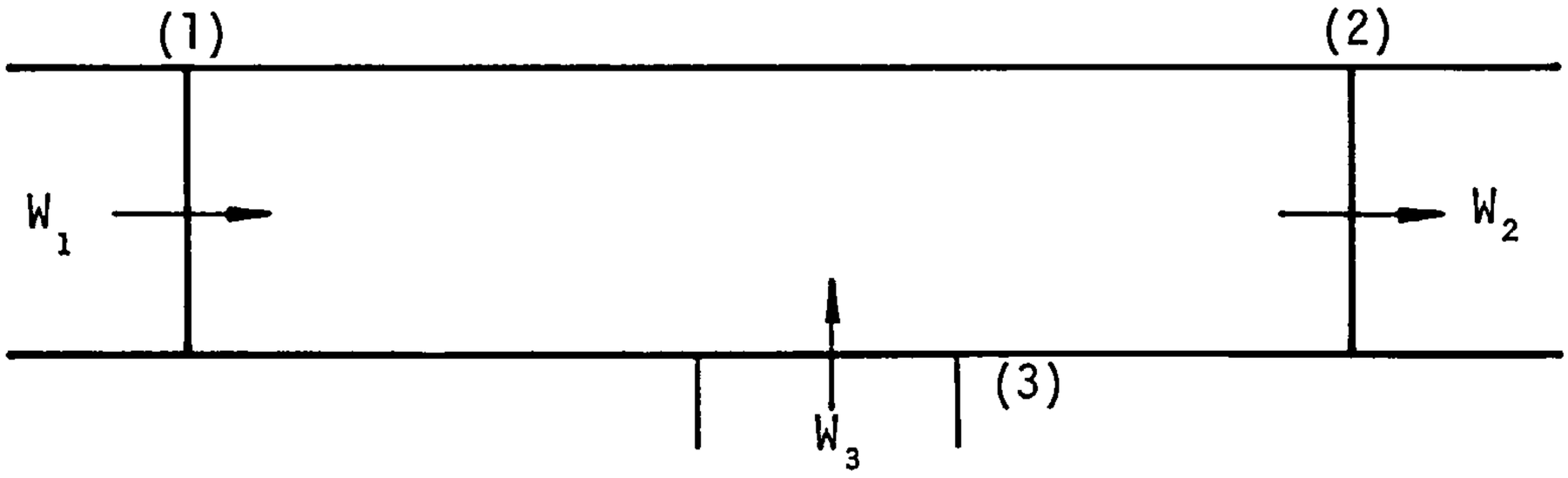

Combining Flow

Figure 2·2 Branch Element

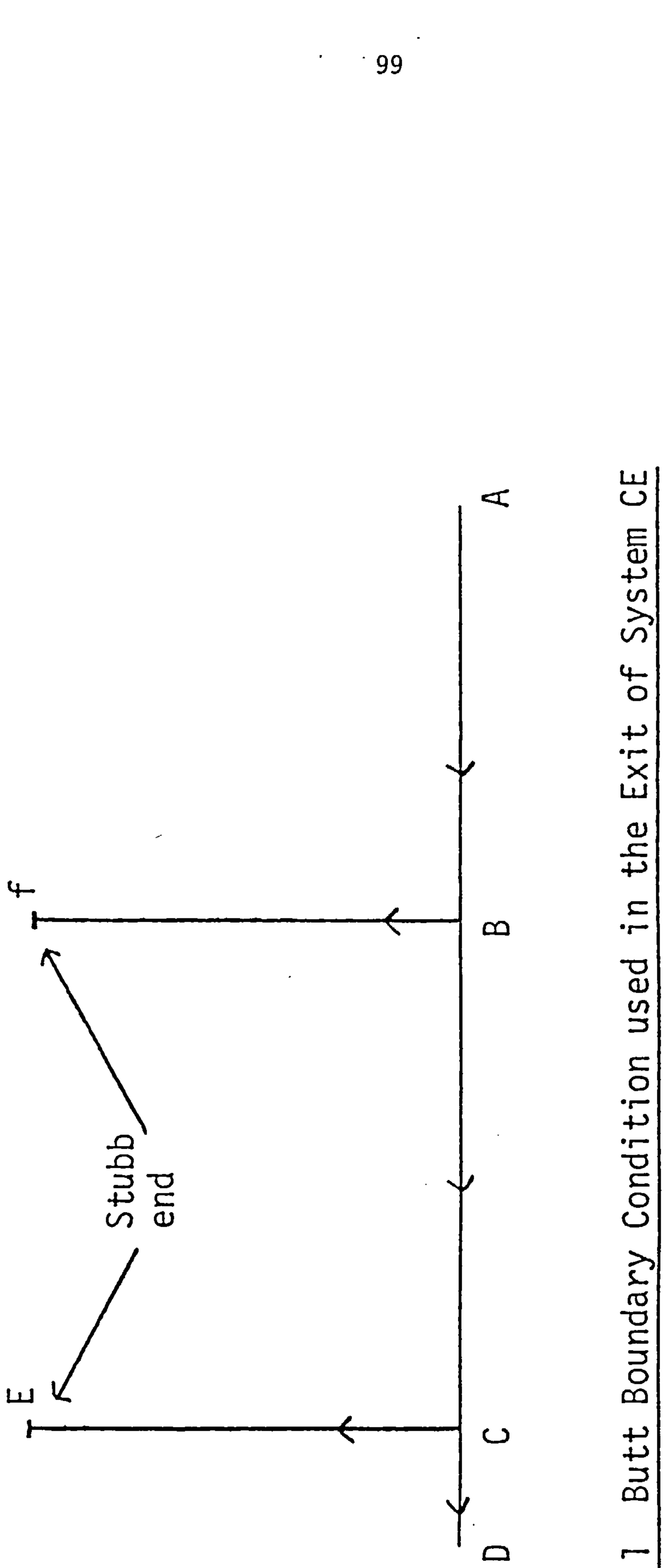

Figure 3.1 Butt Boundary Condition used in the Exit of System CE and Bf above

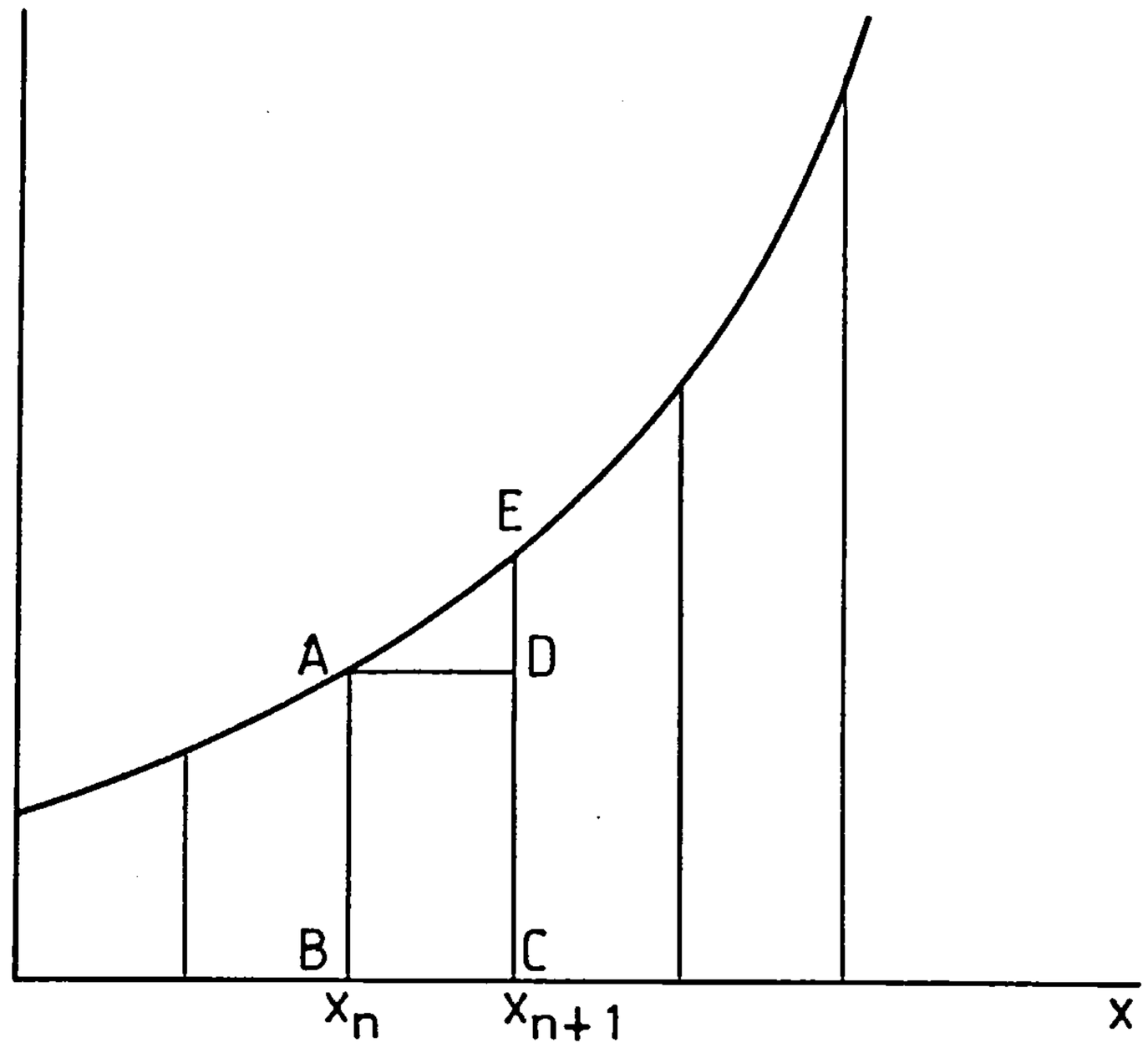

$$Y_{n+1} \quad Y_n + n\left(\frac{dy}{dx}\right)_n \longleftarrow \text{SIMPLE EULER}$$

$$Y_{n+1} = Y_n + n\left[\frac{\left(\frac{dy}{dx}\right)_n + \left(\frac{dy}{dx}\right)_{n+1}}{2}\right] \longleftarrow \text{MODIFIED EULER}$$

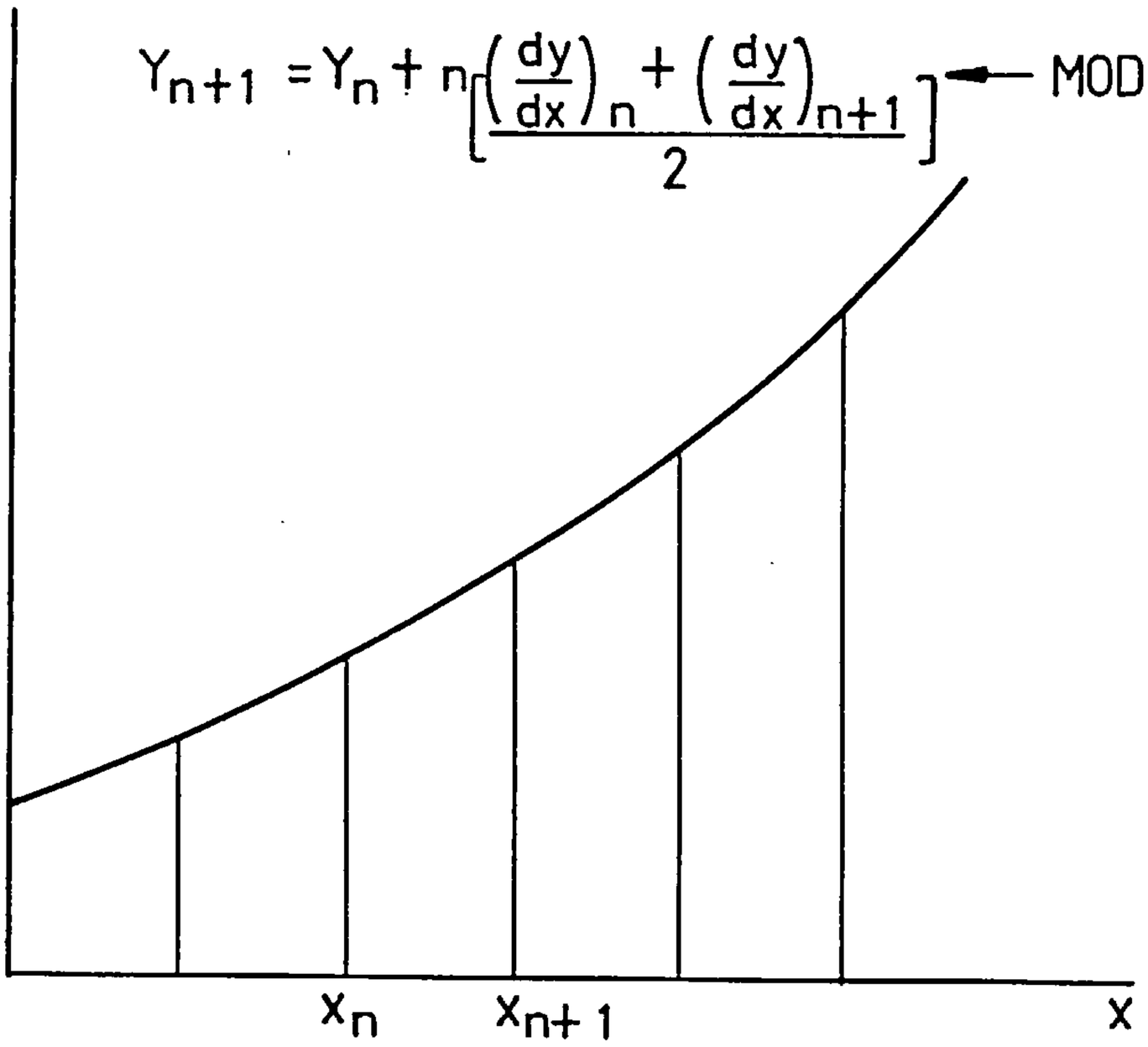

FIG. 4.1 GRAPHICAL REPRESENTATION OF SIMPLE EULER AND MODIFIED EULER METHODS

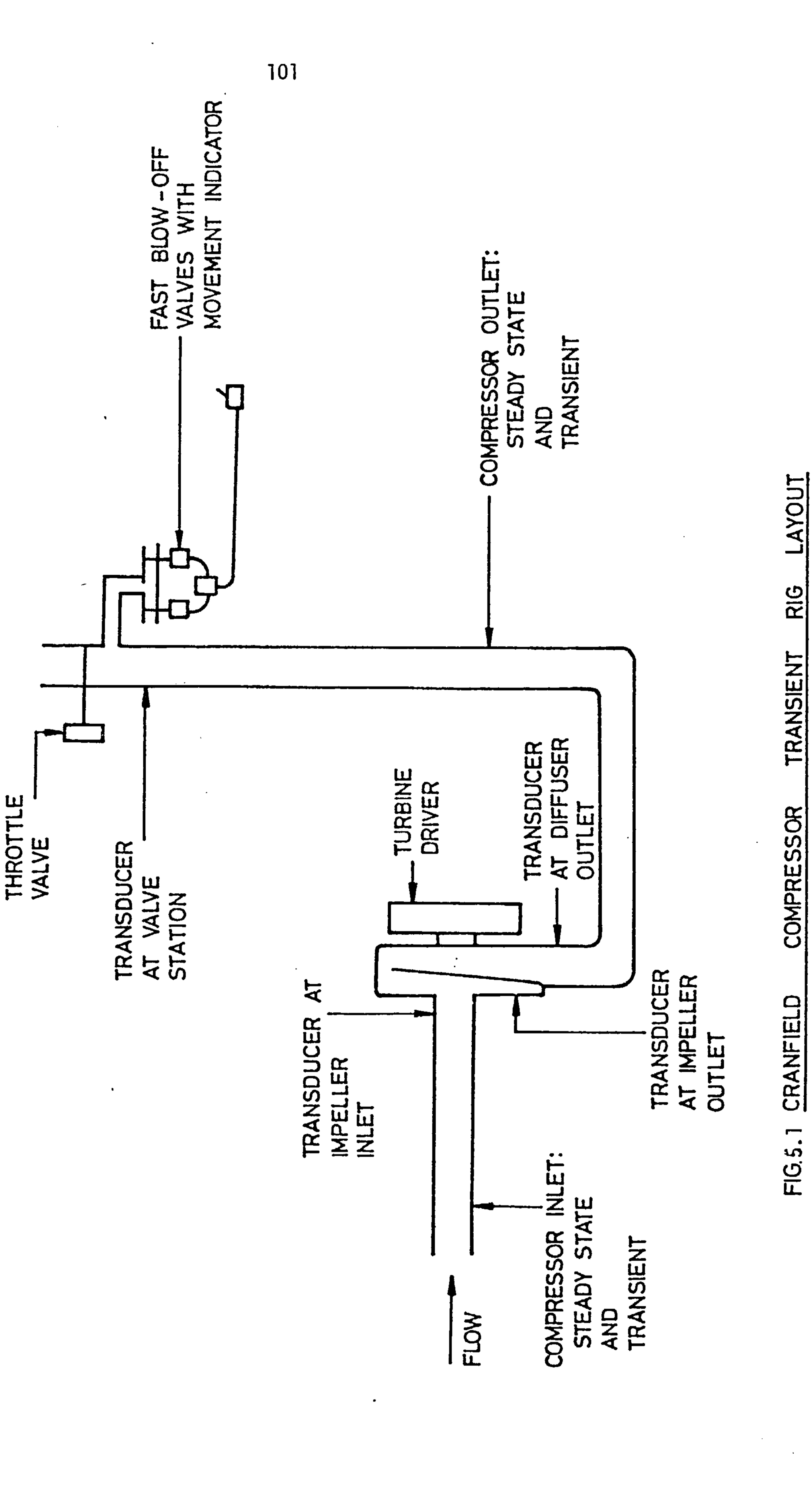

FIG.5.1 CRANFIELD COMPRESSOR TRANSIENT RIG LAYOUT

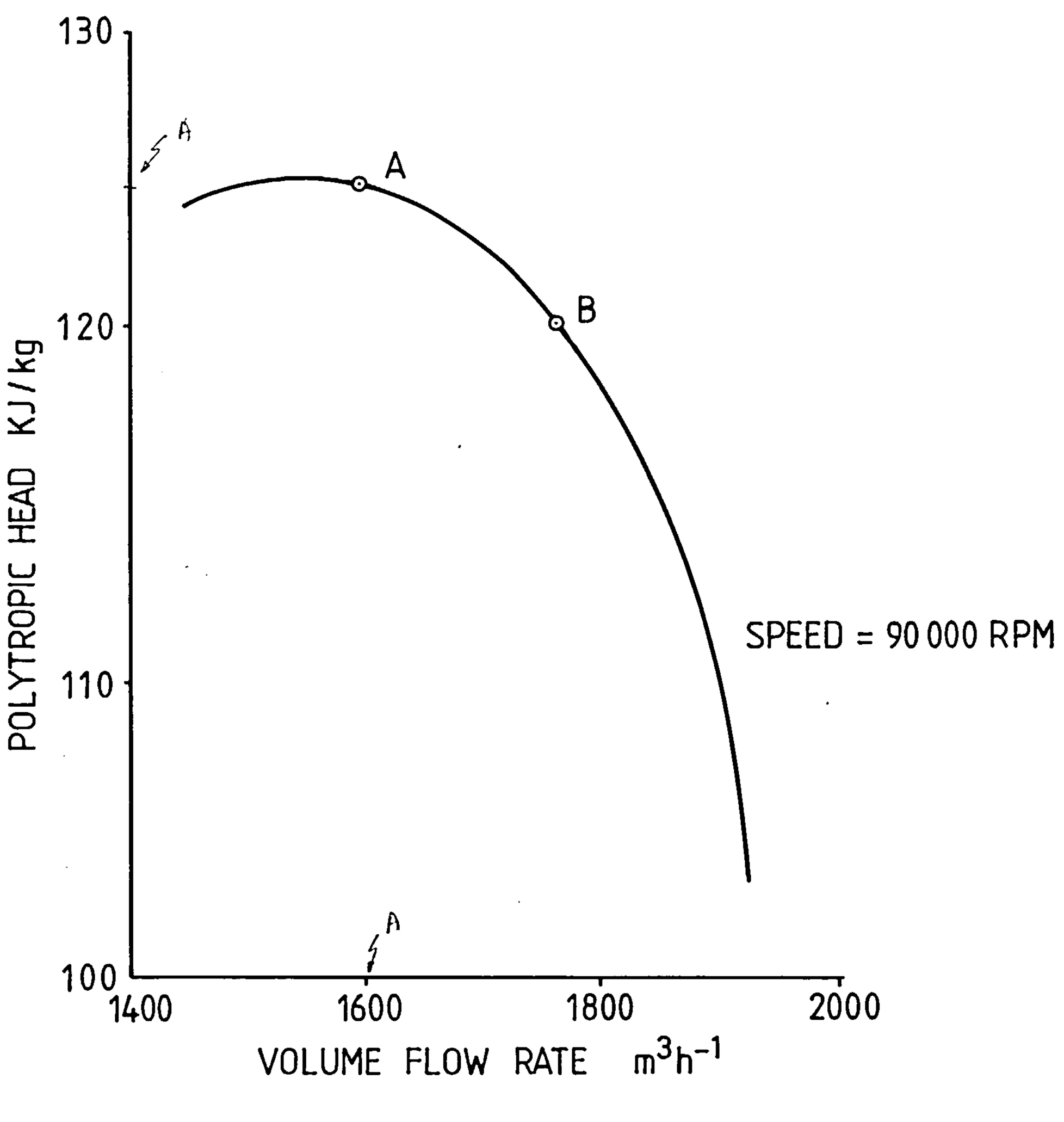

FIG. 5·2 CHARACTERISTIC OF COMPRESSOR USED FOR VALIDATION OF MATHEMATICAL MODEL

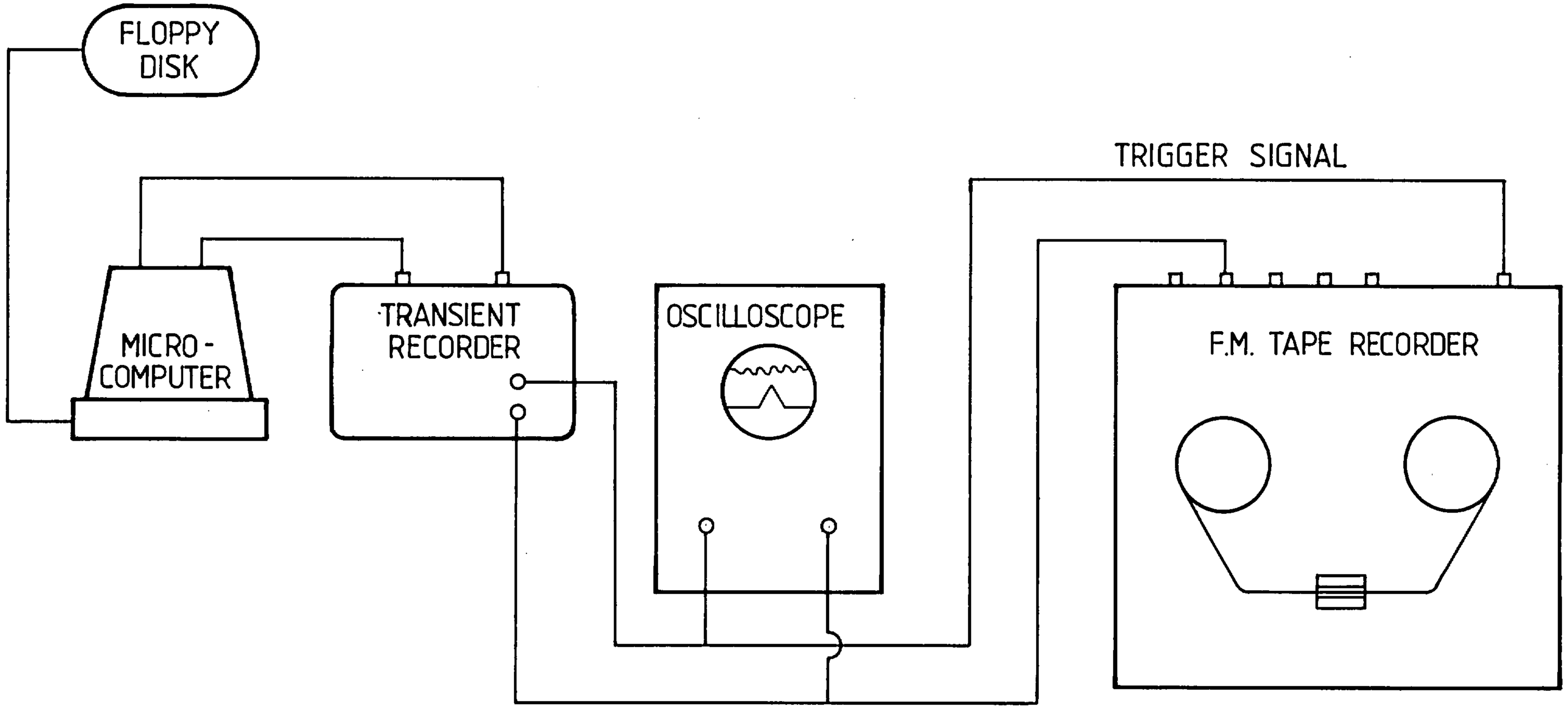

FIG. 5.3 EQUIPMENT LAYOUT FOR DIGITISATION OF ANALOG SIGNAL

FIG. 5.4

Digitisation Program Flow Chart

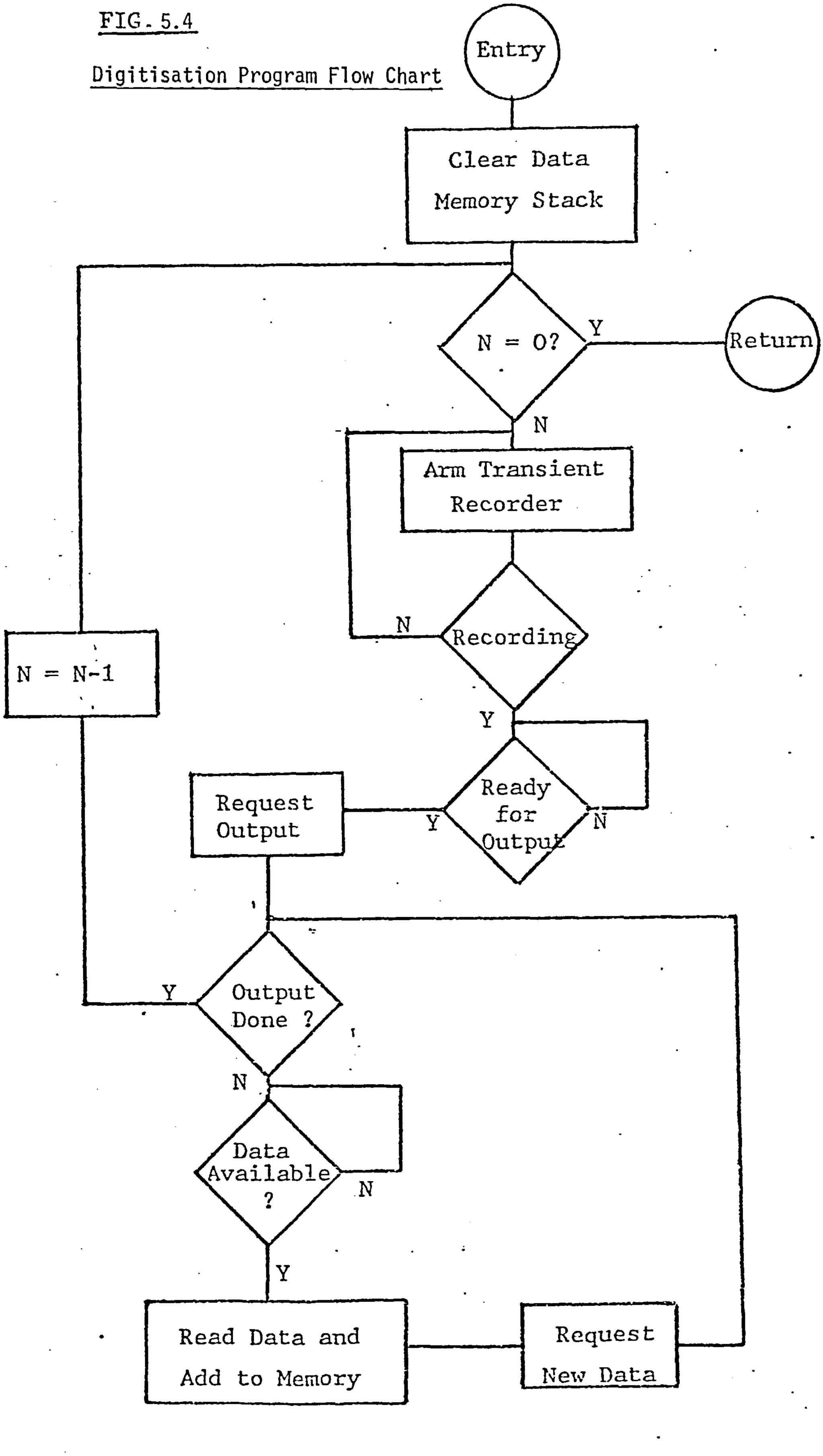

FLOW CHART DIGITISED DATA ANALYSING PROGRAM

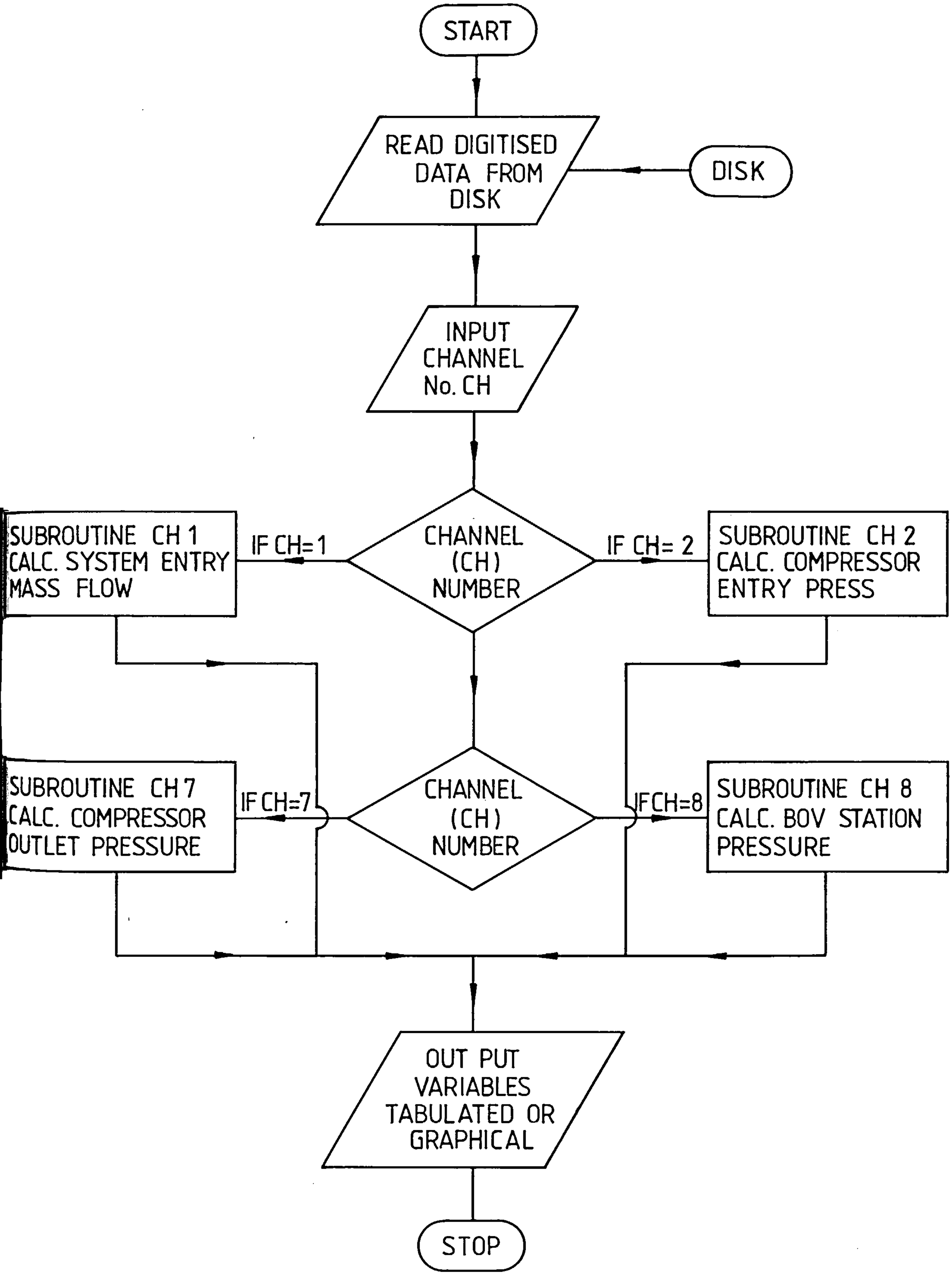

FIG. 5.5

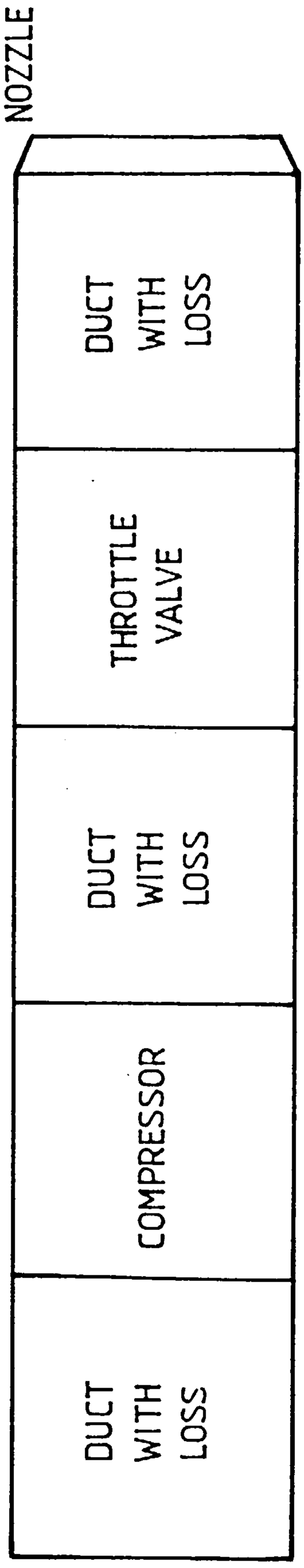

FIG. 5.6 ELEMENT DISTRIBUTION

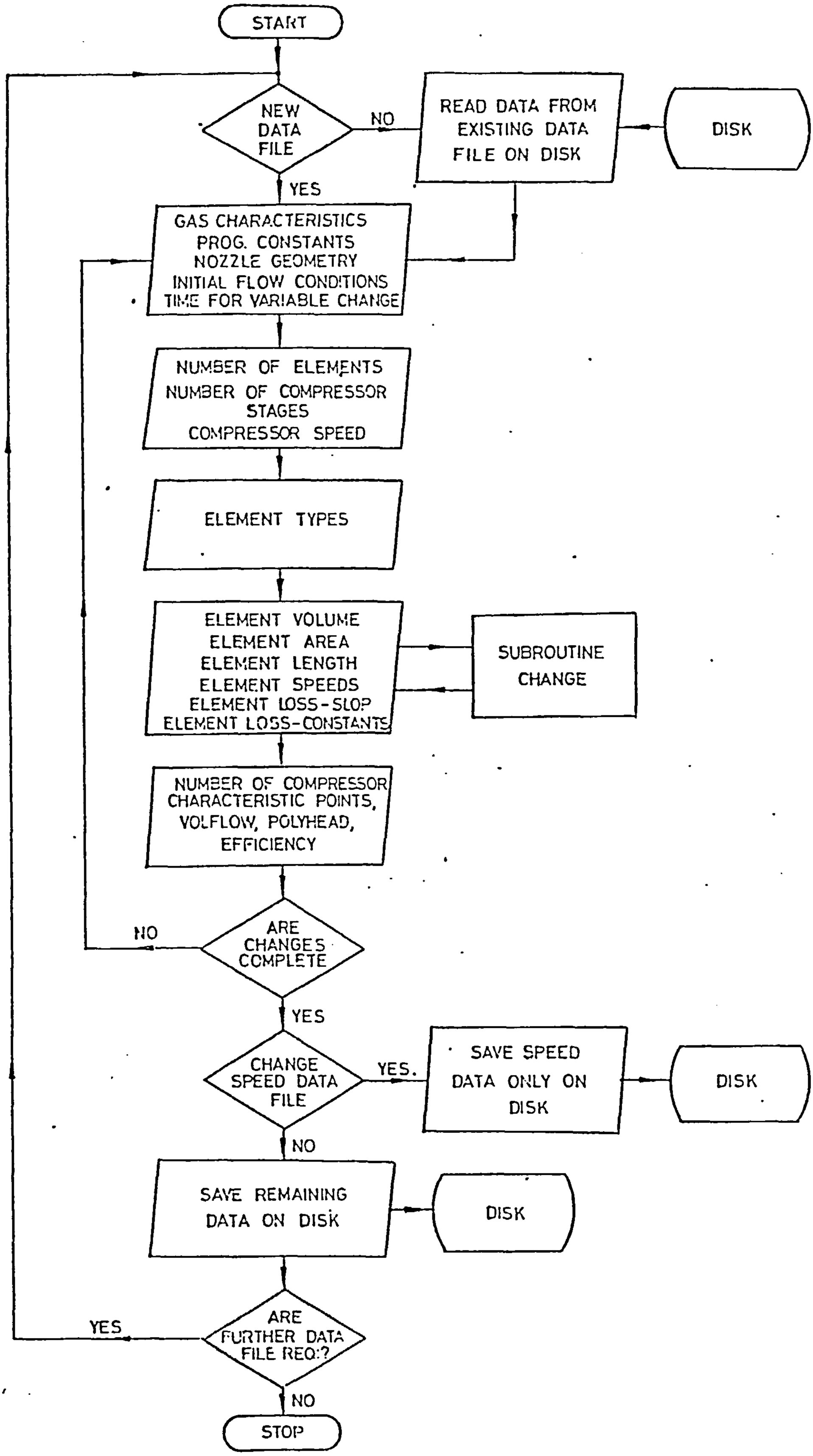

FIG. 5.7 PROGRAM STEP UP FLOW CHART

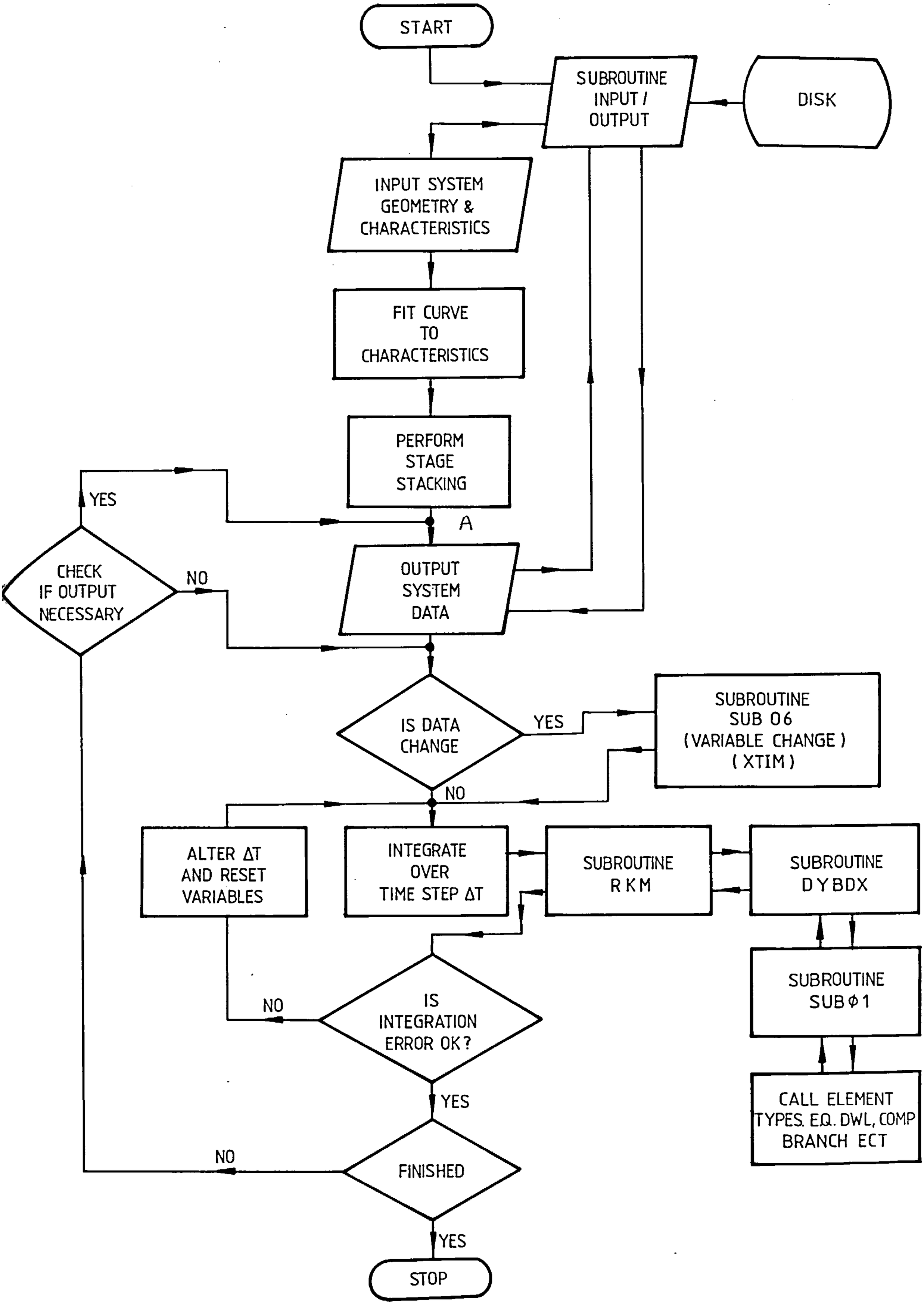

FIG. 5·8 SIMPLIFIED FLOW CHART FOR 'TRANS'

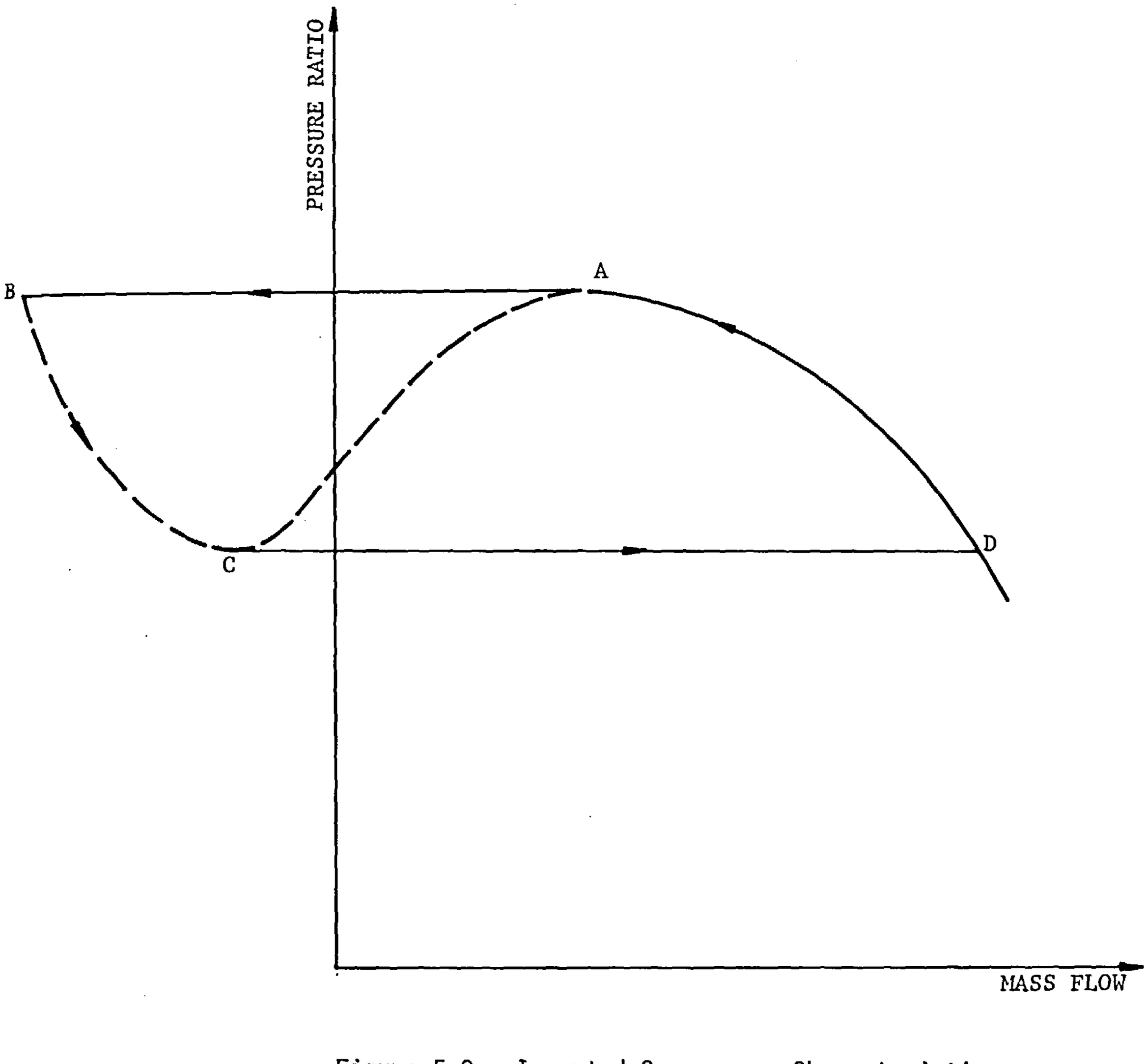

Figure 5.9 Inverted Compressor Characteristic

COMPRESSOR CHARACTERISTIC WITH THE INVERTED CHARACTERISTIC

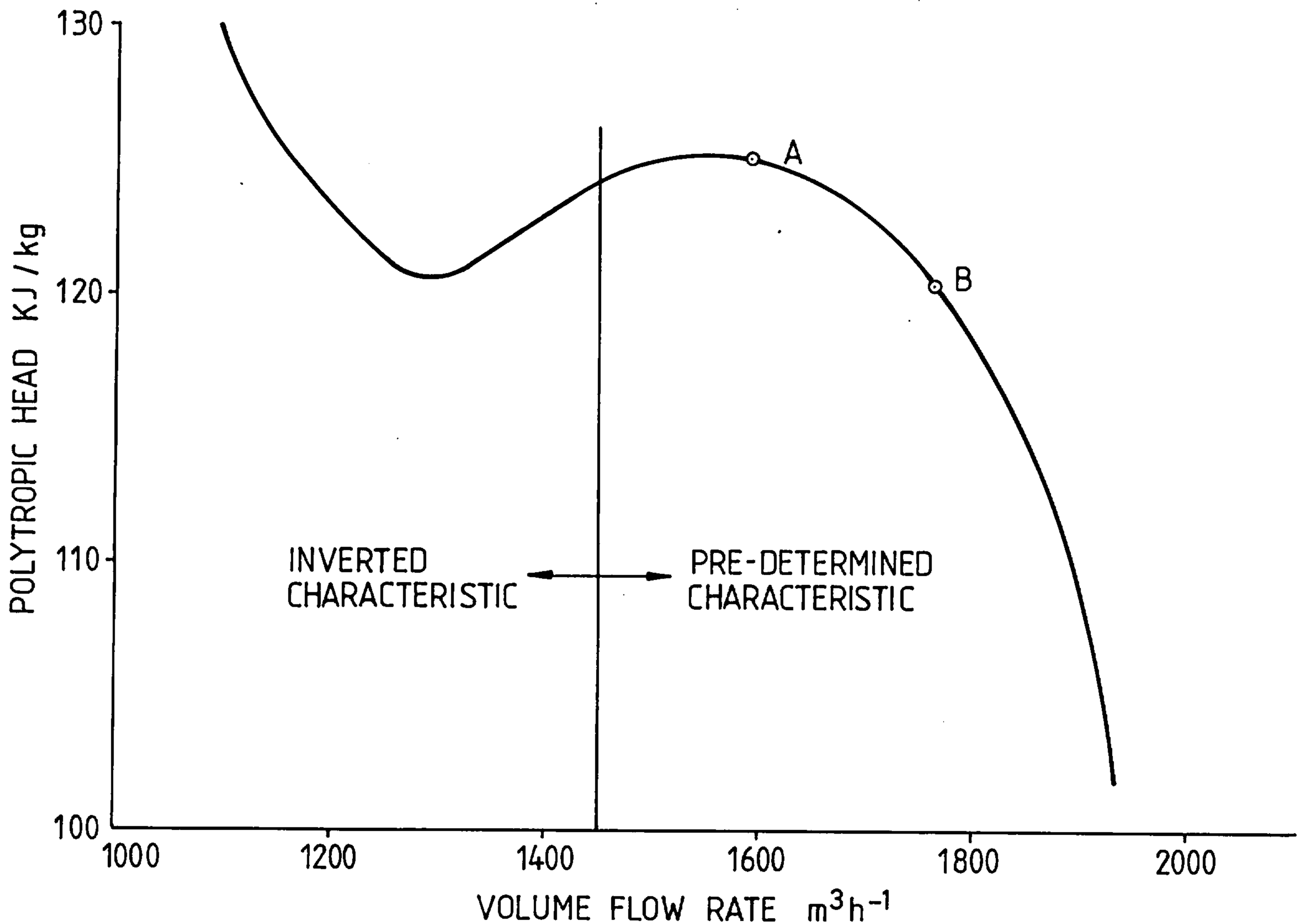

FIG. 5·10

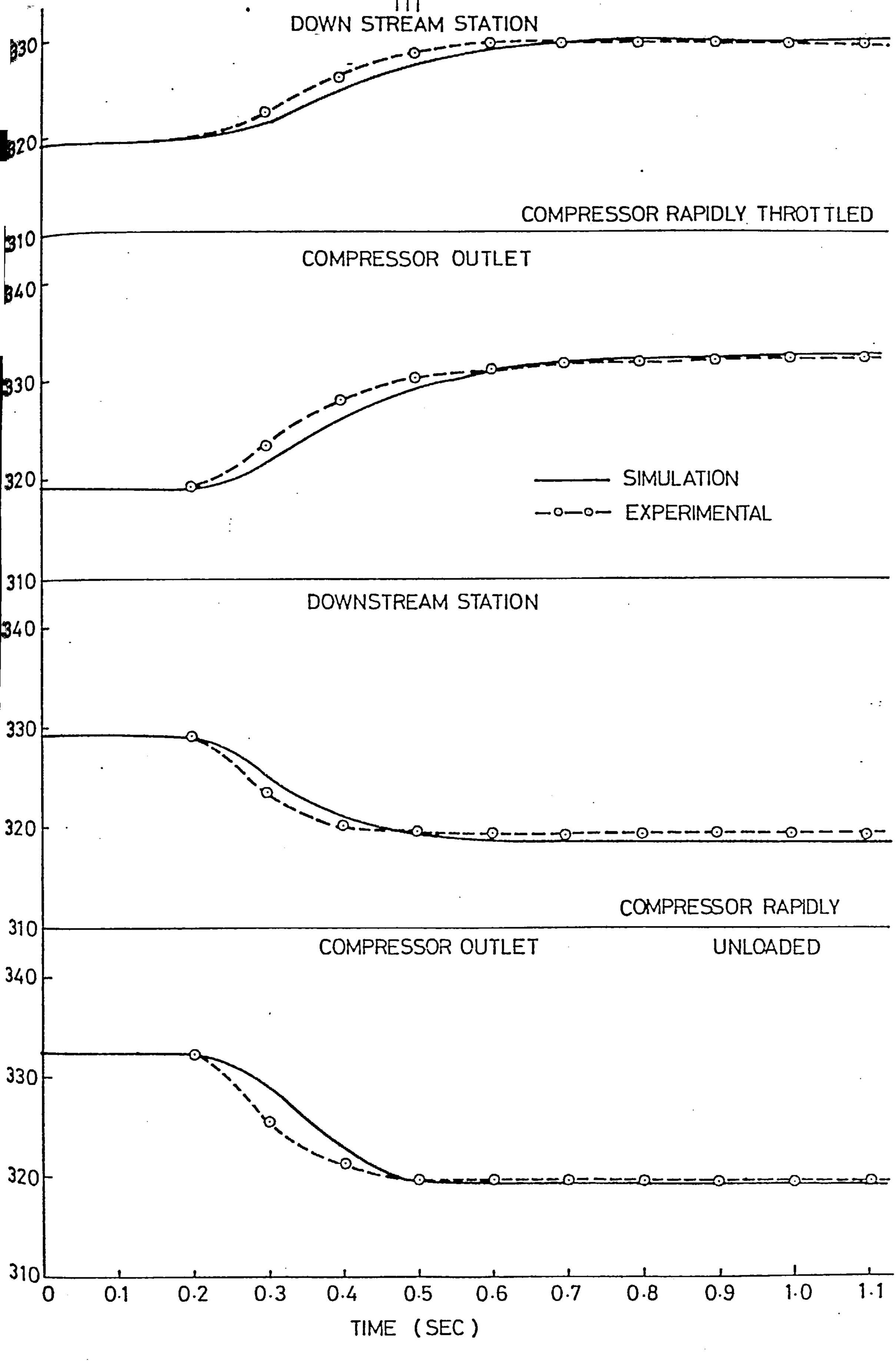

FIG. 5.11 COMPRESSOR SIMULATION FOR THE SECOND TEST COMPRESSOR

SIMULATED RESULTS FOR STEP CHANGE IN B.O.V. AREA

B.O.V. = Blow Off Valve

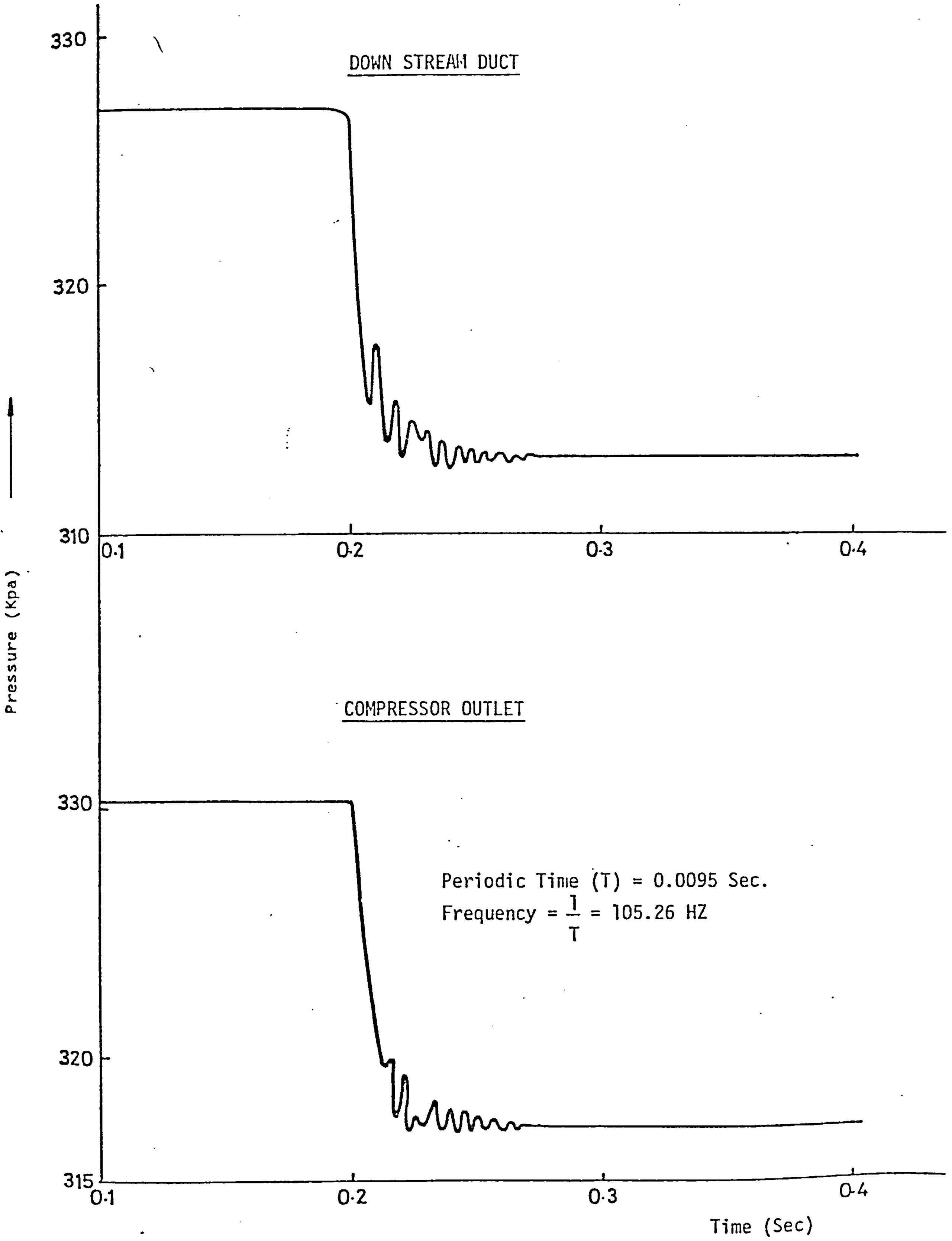

Periodic Time (T) = 0.0095 Sec.

Frequency = $\frac{1}{T}$ = 105.26 HZ

FIG. 5.12 SIMULATION OF INSTANTANEOUS BLOW OF VALVE ACTION FOR THE SECOND SET OF COMPRESSOR TESTS

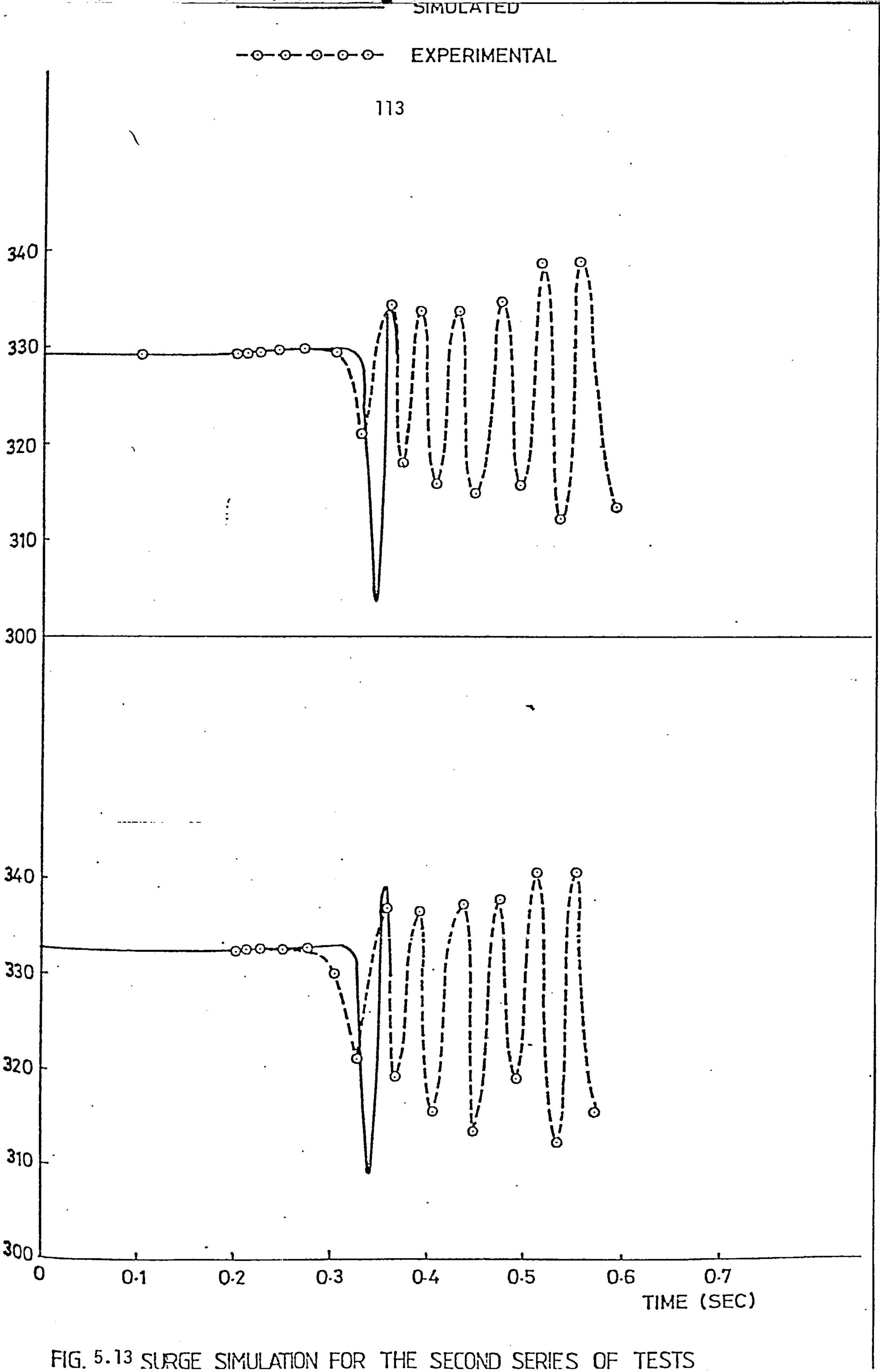

FIG. 5.13 SURGE SIMULATION FOR THE SECOND SERIES OF TESTS

SURGE SIMULATION ON COMPRESSOR CHARACTERISTIC

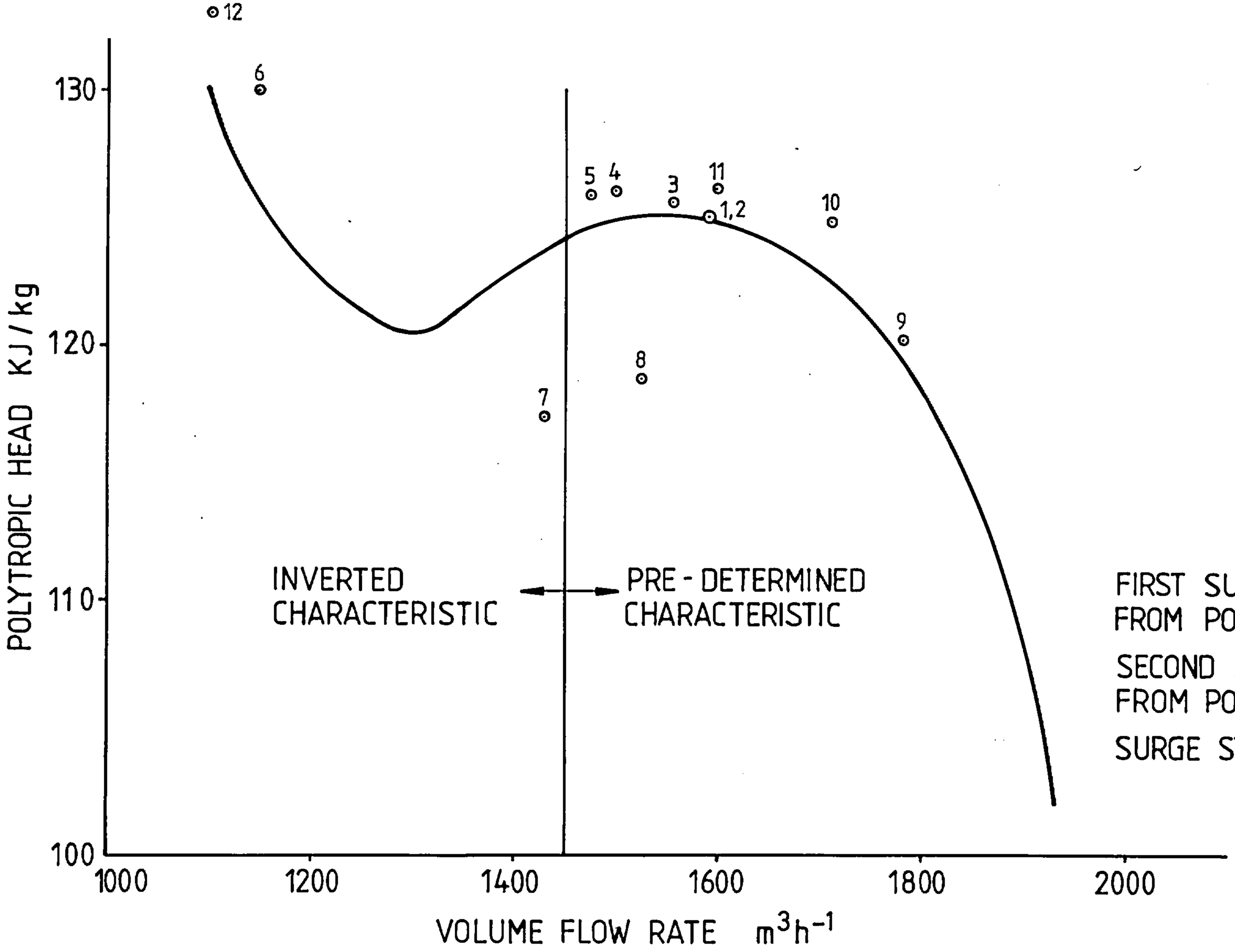

POINT	TIME (S)
1	0·000
2	0·200
3	0·235
4	0·288
5	0·326
6	0·345
7	0·354
8	0·356
9	0·361
10	0·362
11	0·378
12	0·380

FIRST SURGE CYCLE IS FROM POINT 1 TO 9

SECOND SURGE CYCLE IS FROM POINT 9 TO 12

SURGE START AT POINT 5

FIG. 5·14

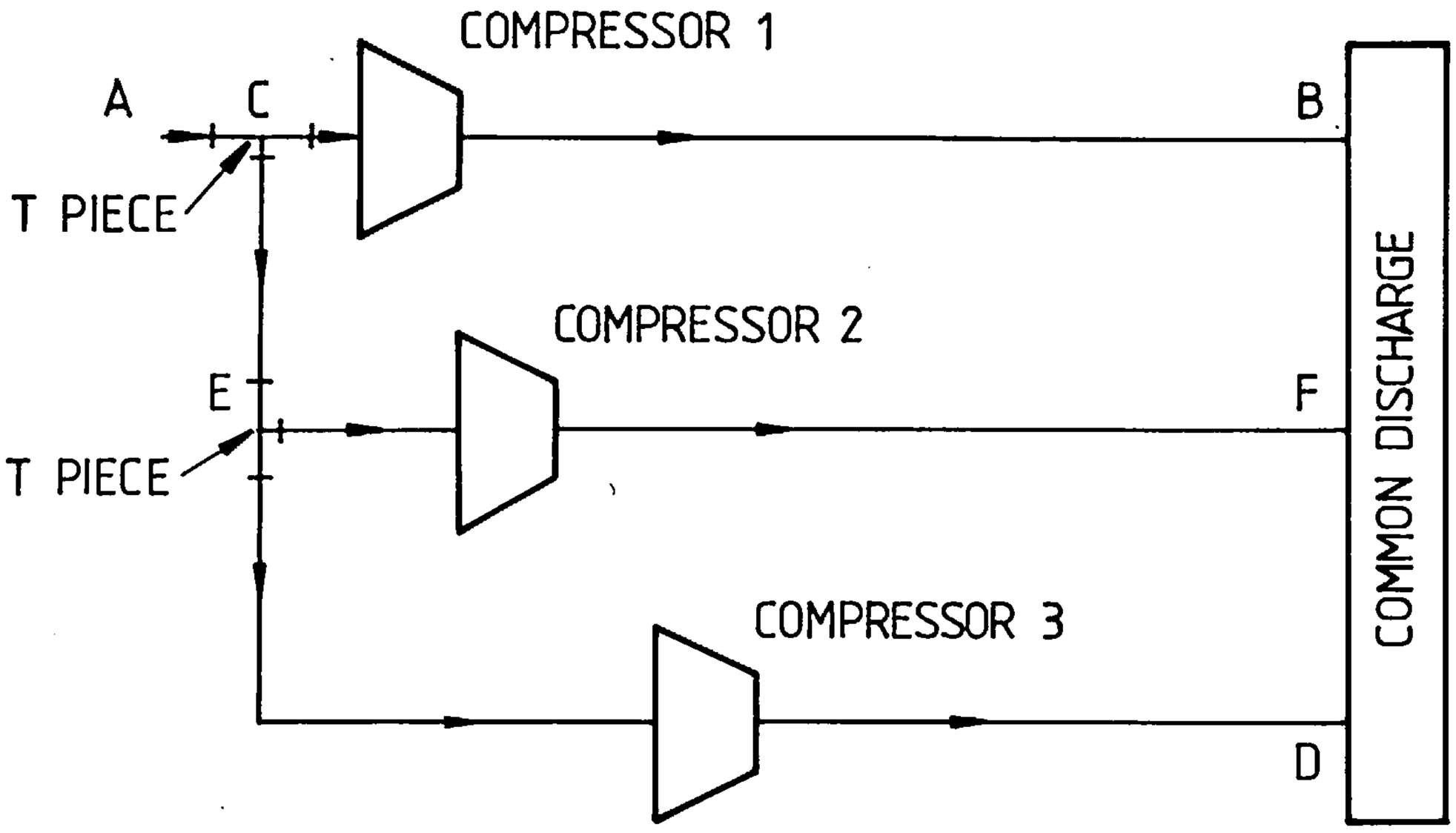

FIG. 6.1 Patching Procedure Example 1

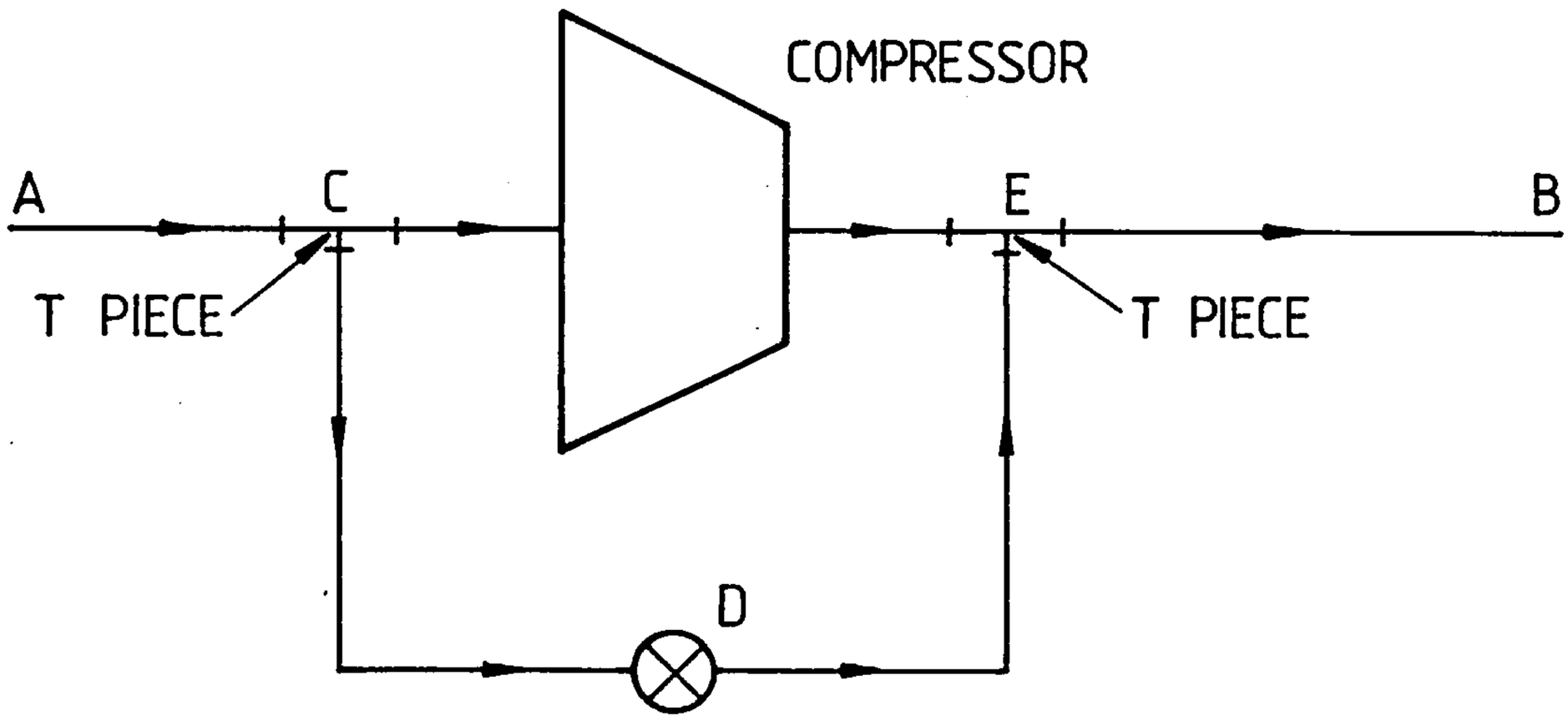

FIG. 6.2 Patching Procedure Example 2

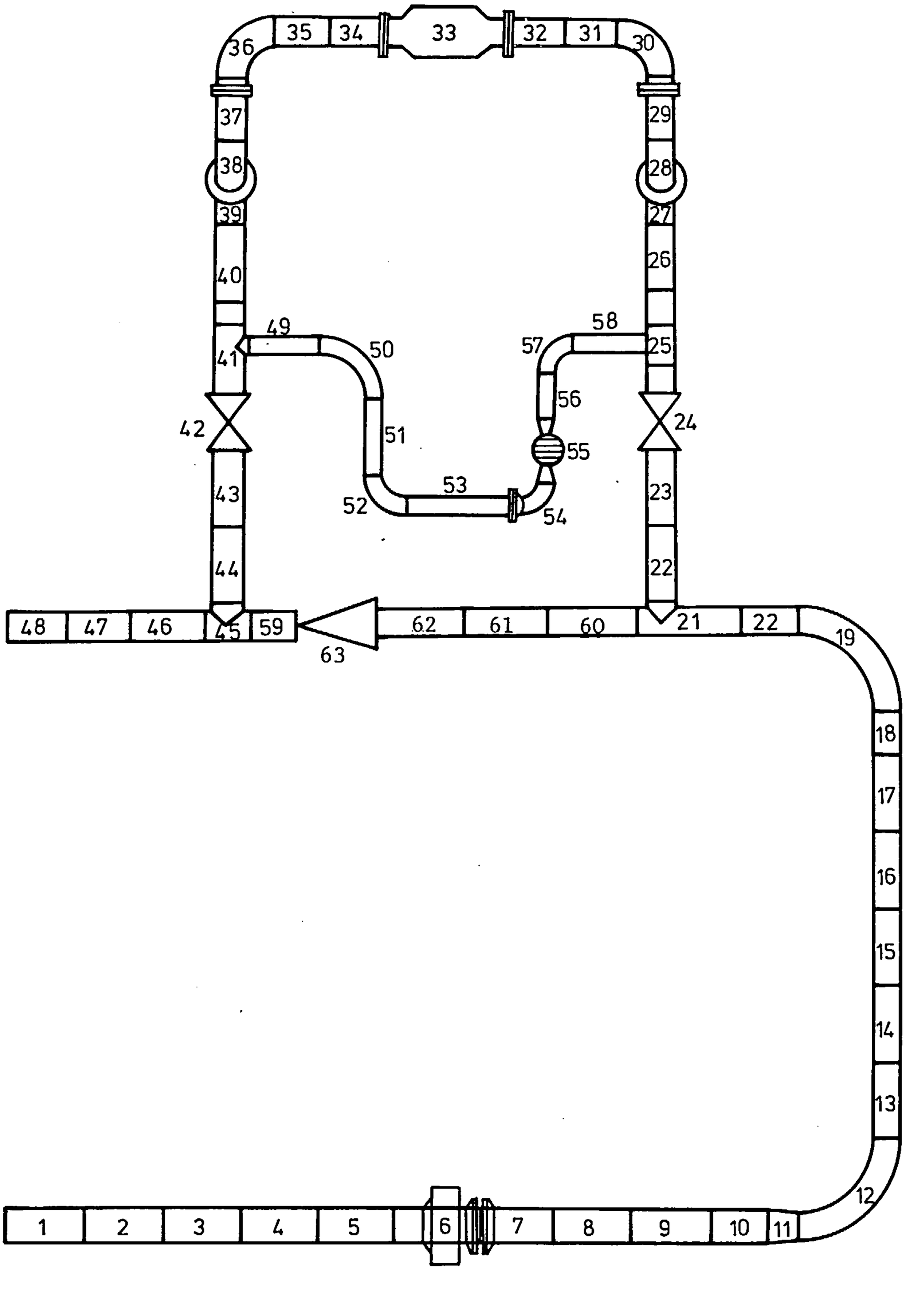

FIGURE 6.3 ELEMENT DISTRIBUTION

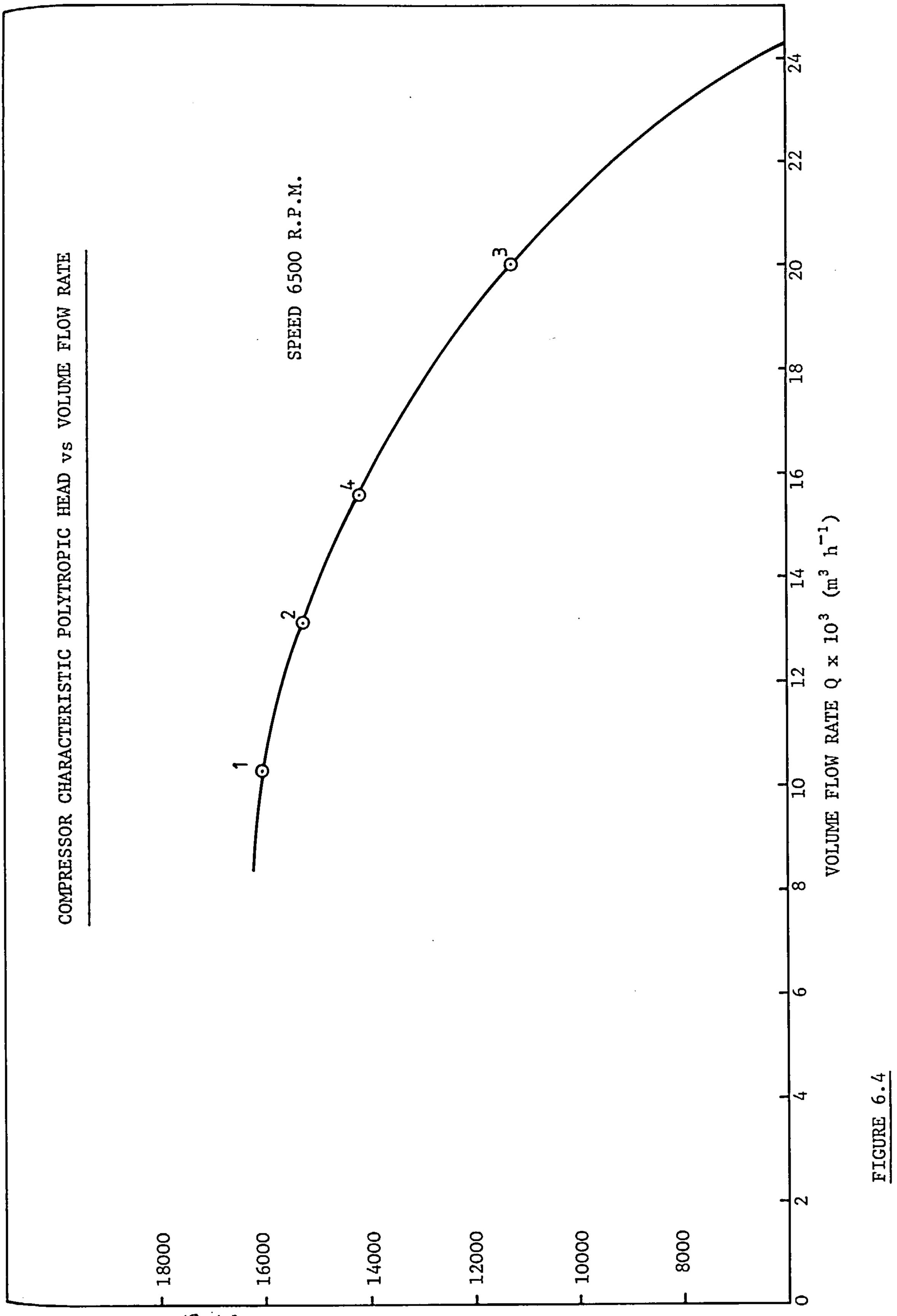
COMPRESSOR CHARACTERISTIC POLYTROPIC HEAD vs VOLUME FLOW RATE
SPEED 6500 R.P.M.
1
2
3
4
POLYTROPIC HEAD Wp (J/kg)
18000
16000
14000
12000
10000
8000
0
2
4
6
8
10
12
14
16
18
20
22
24
VOLUME FLOW RATE Q x 10³ (m³ h⁻¹)

FIGURE 6.4

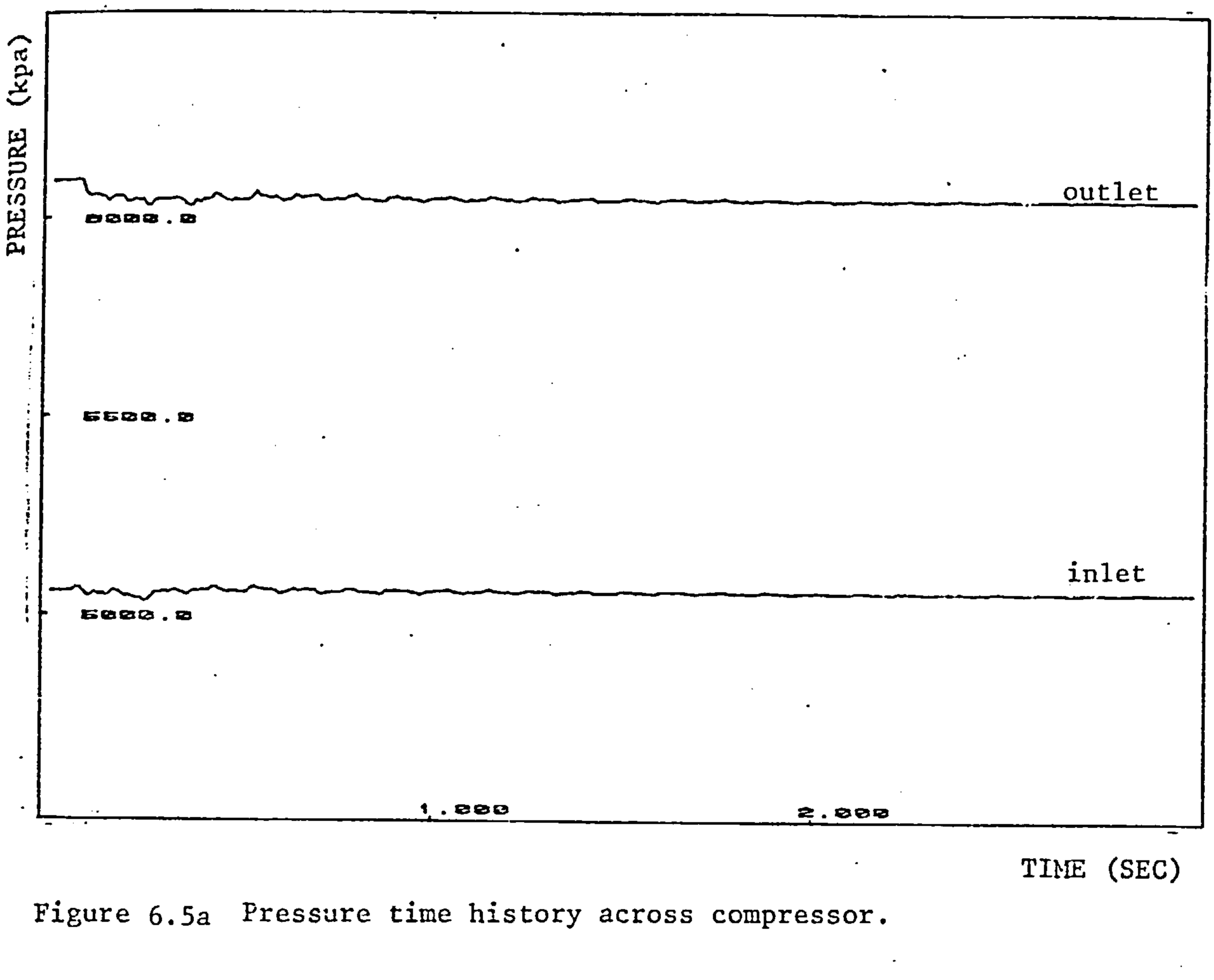

Figure 6.5a Pressure time history across compressor.

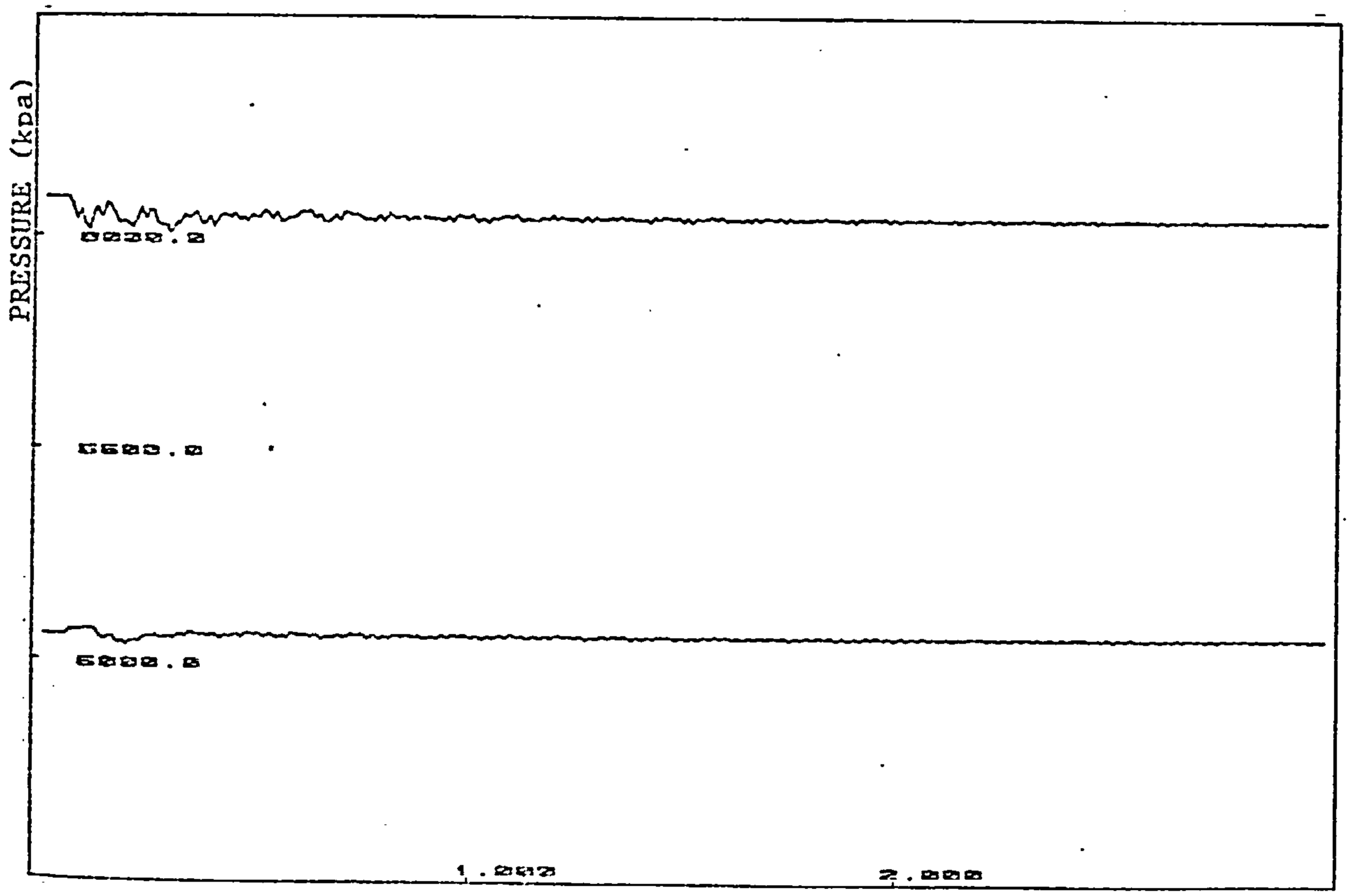

Figure 6.5b Pressure time history across non-return valve (element 60, see fig. 1) due to opening of recycle valve.

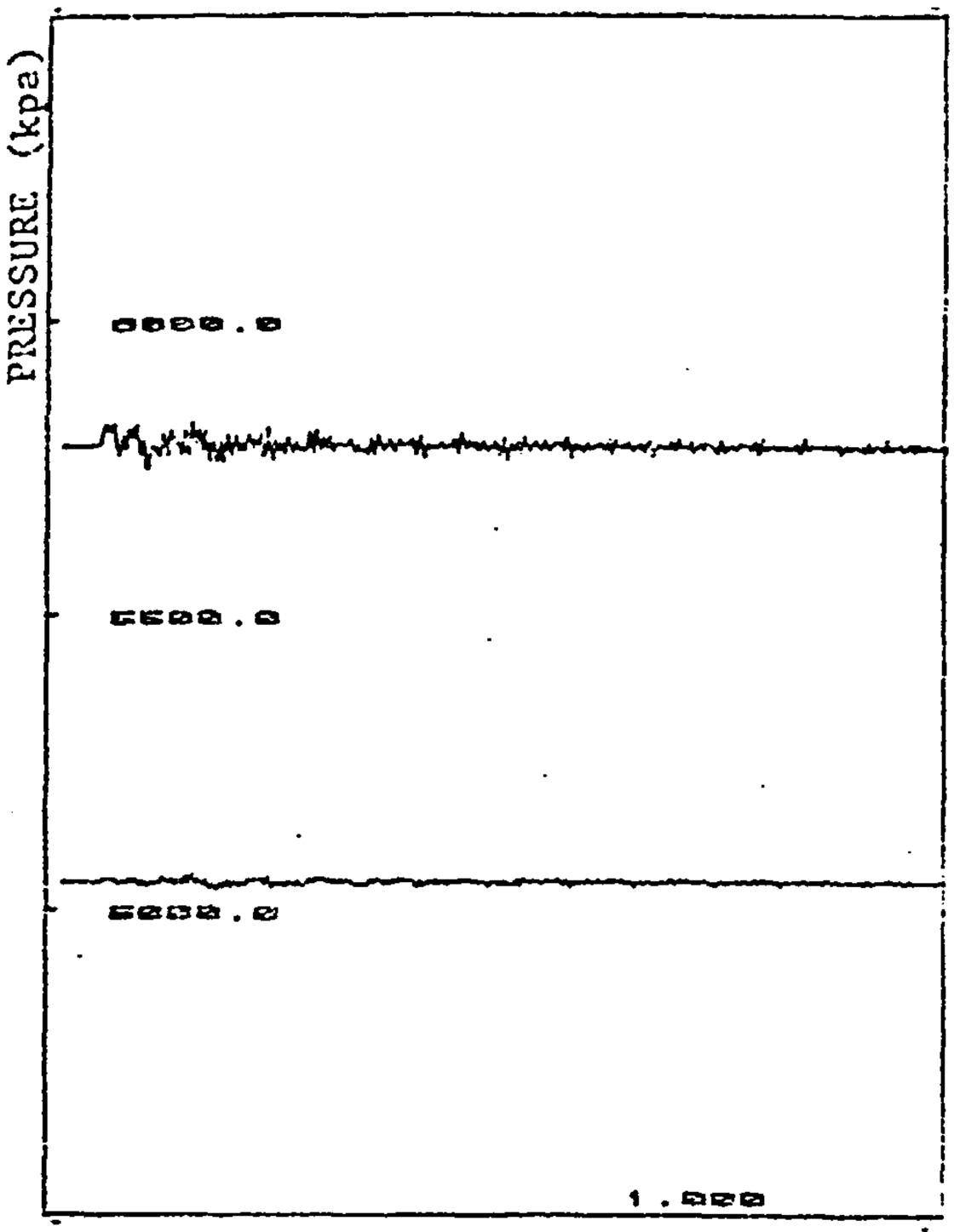

(a) when compressor is operative at point (3) on compressor characteristic.

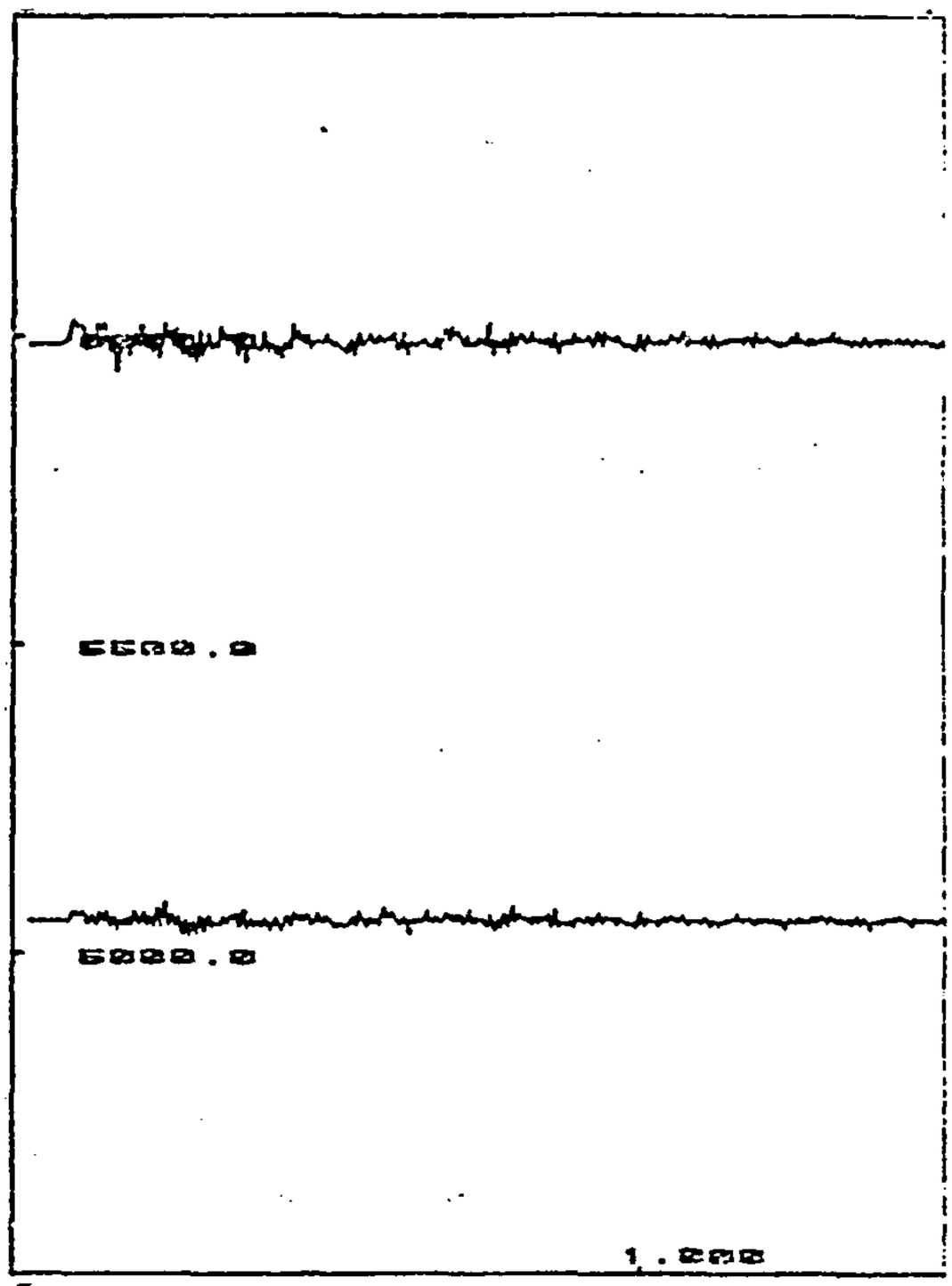

(b) when compressor is operative at point (4) on compressor characteristic.

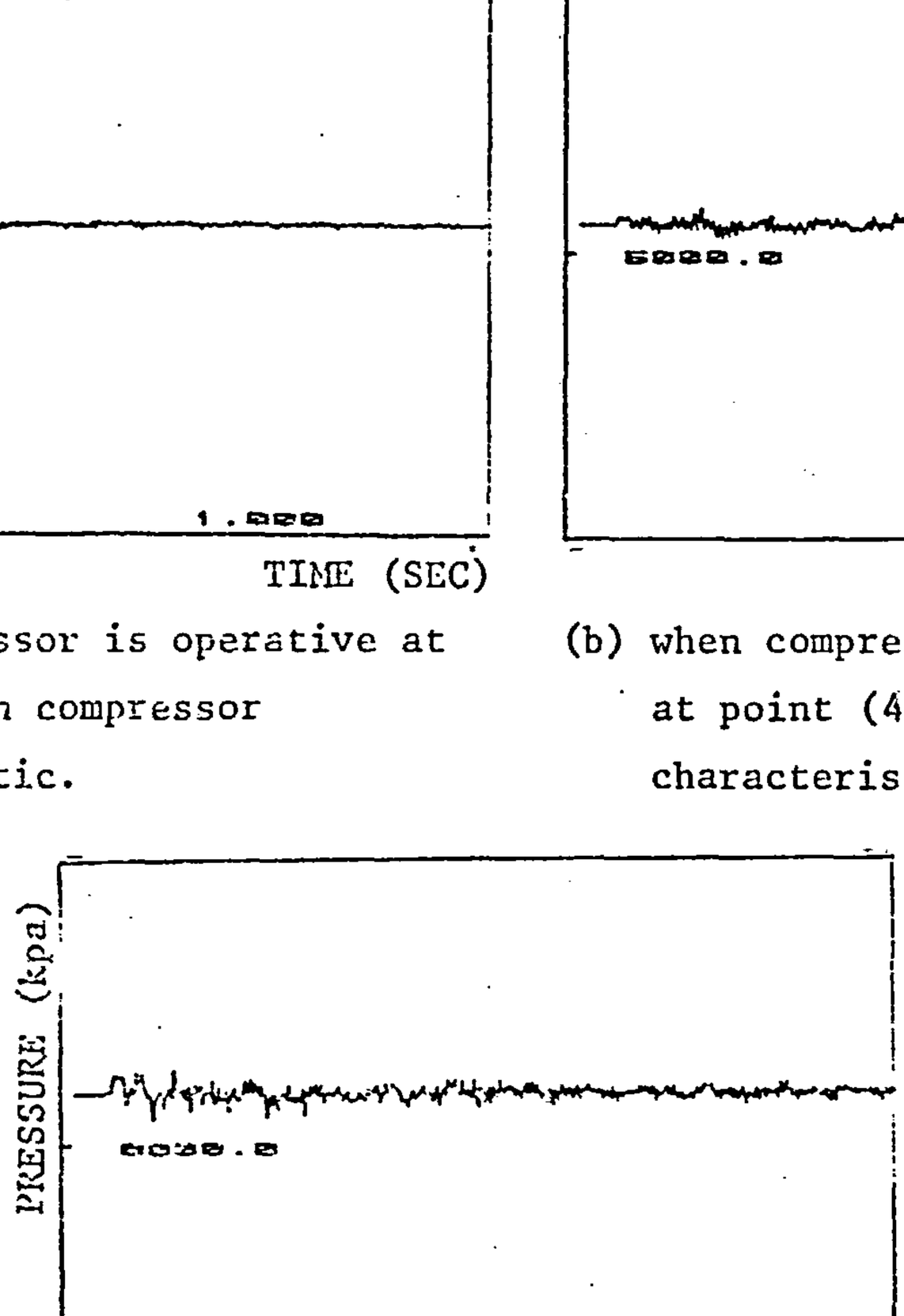

(c) when compressor is operative at point (1) on compressor characteristic.

Figure 6.6 Pressure time history across compressor due to perturbation in downstream element.

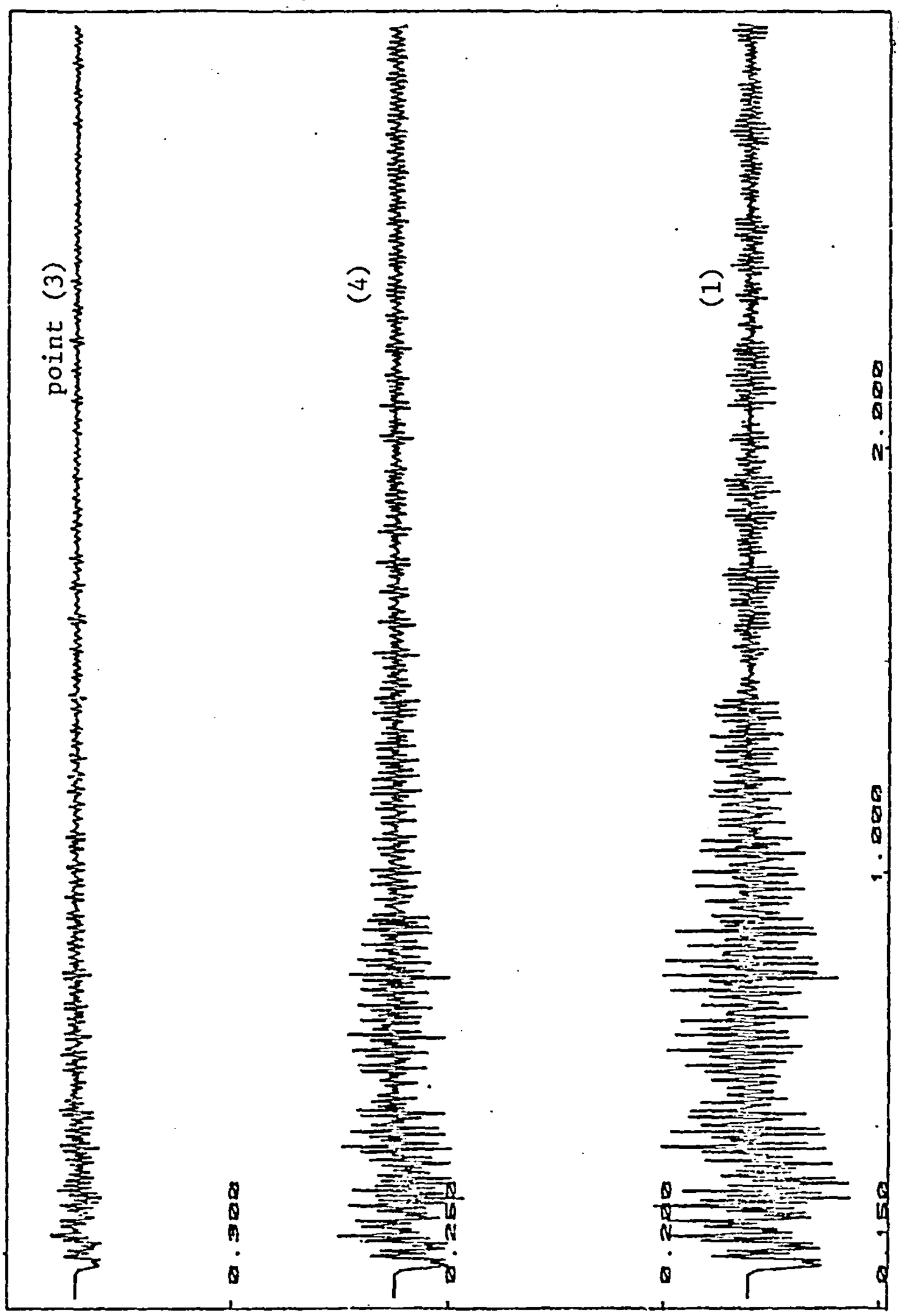

Figure 6.7 Compressor entry mass flow time history due to perturbation introduced at point 4, 3 and 1 on characteristic when compressor is operating at

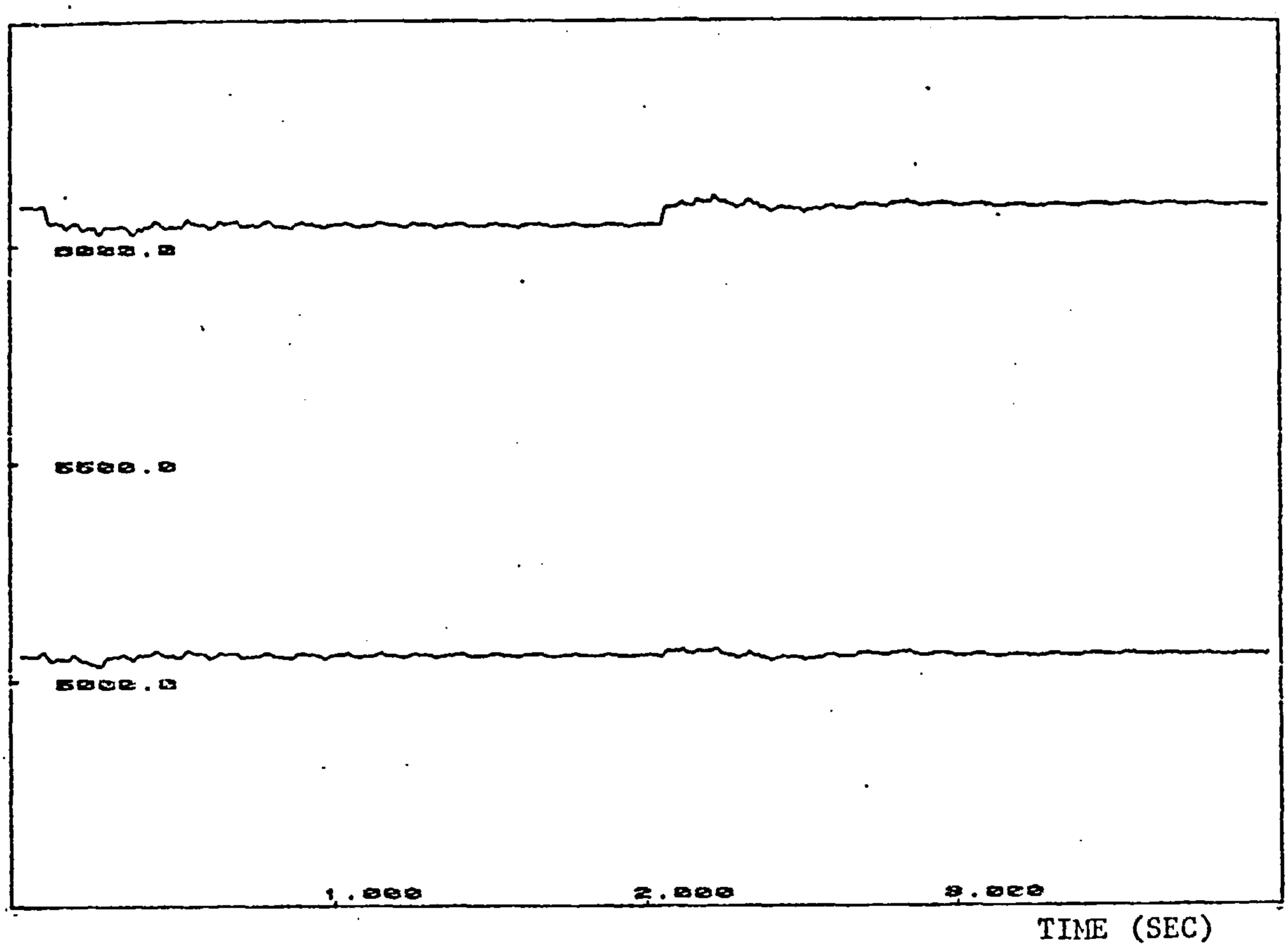

Figure 6.8a Inlet and Outlet Pressure Time History Across Compressor

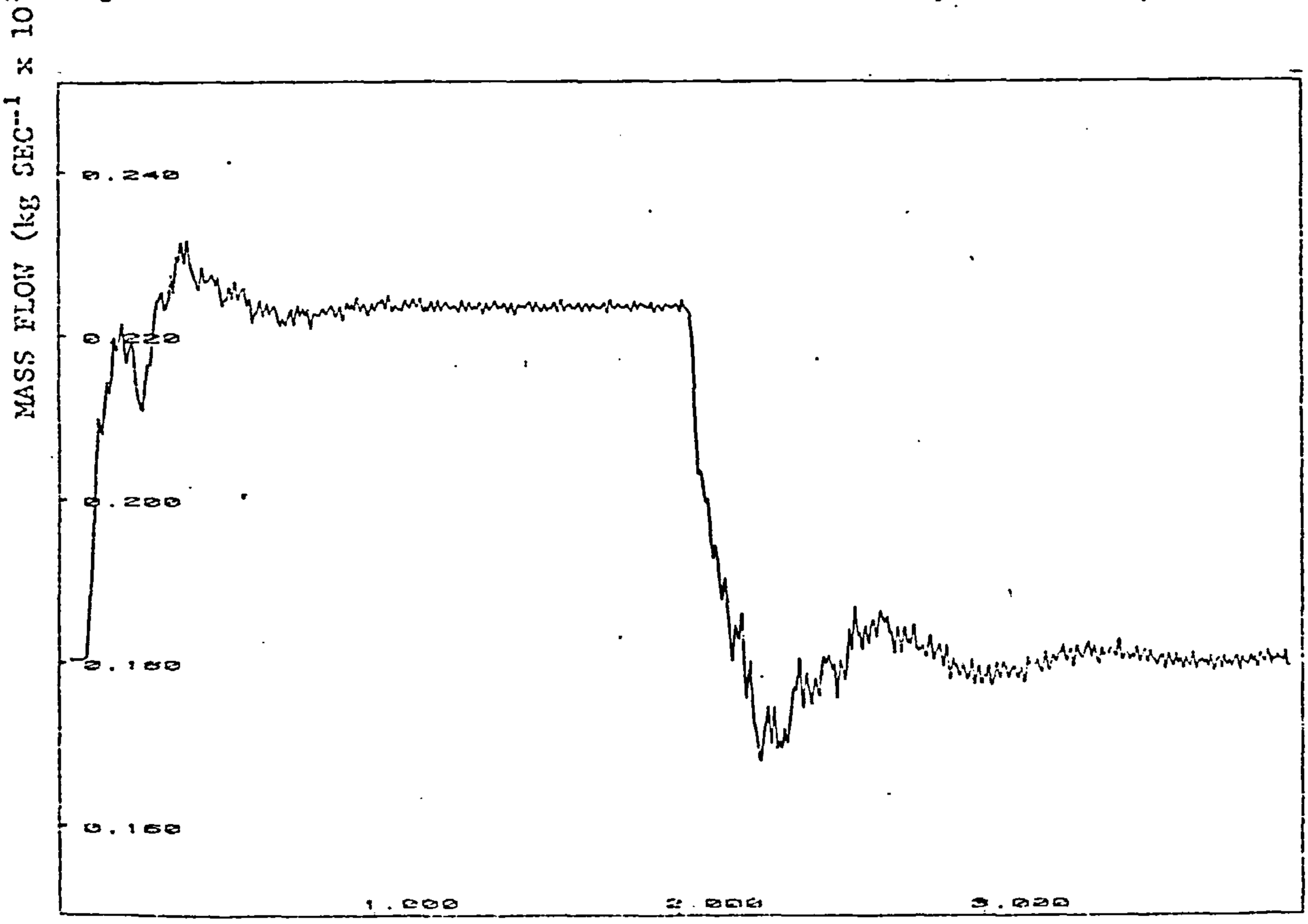

Figure 6.8b Entry mass flow time history due to opening and closing recycle valve. (The valve opens at t = 0.02 sec and closes at t = 2.0 sec).

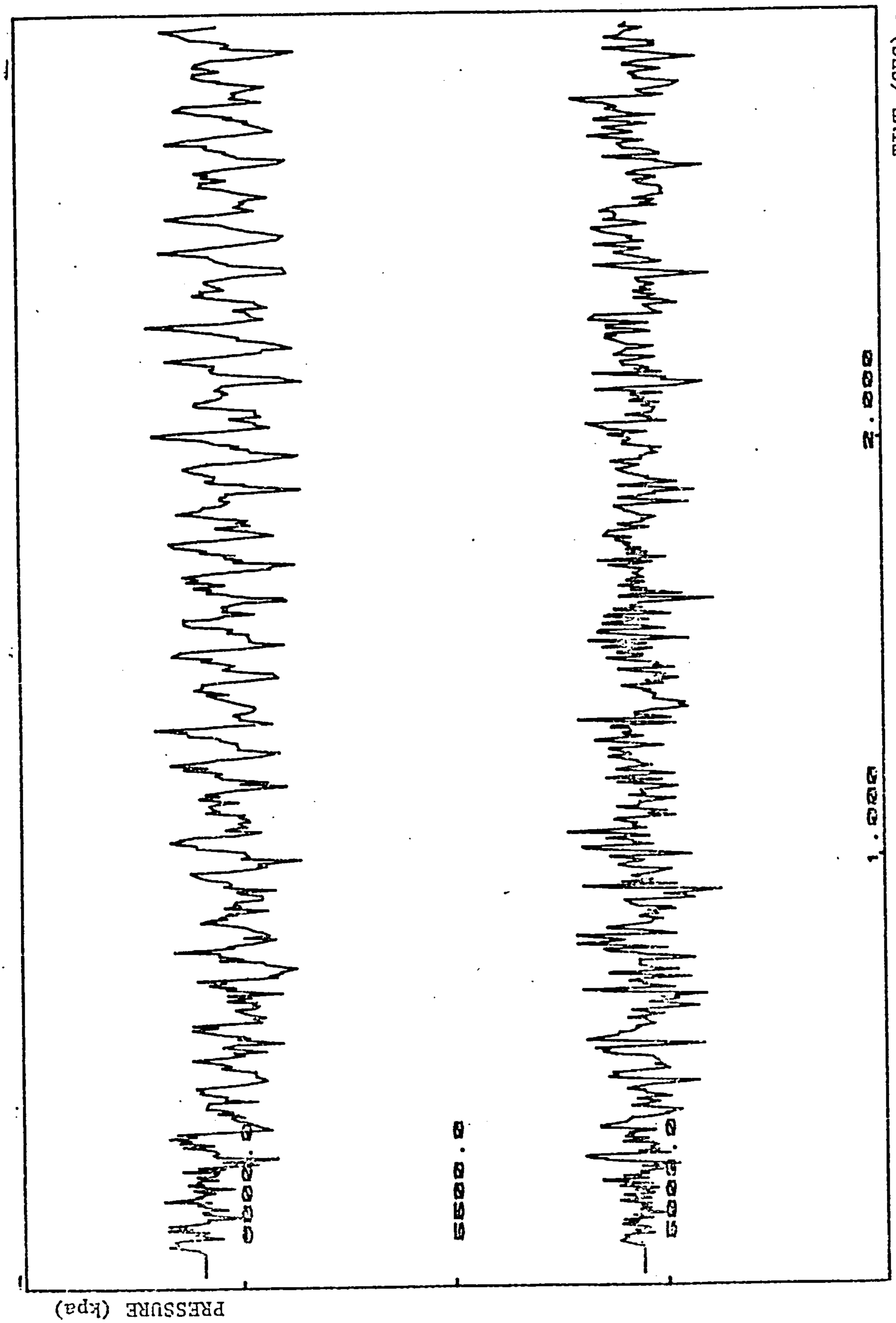

Figure 6.9 Pressure time history across compressor when operating under surge conditions.

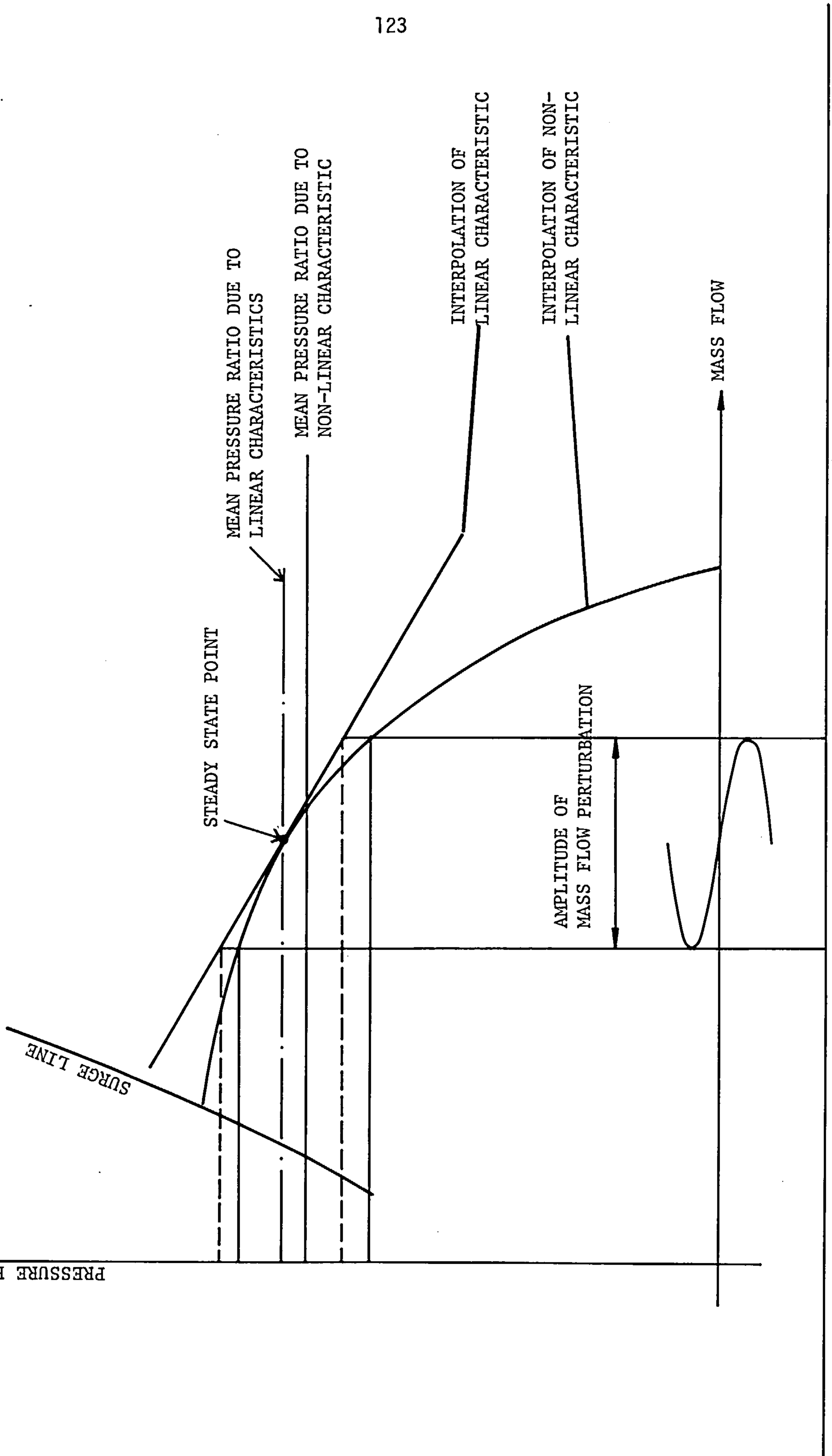

FIGURE 6.10

EFFECT OF PERTURBATIONS WITH LINEAR AND NON-LINEAR CHARACTERISTIC

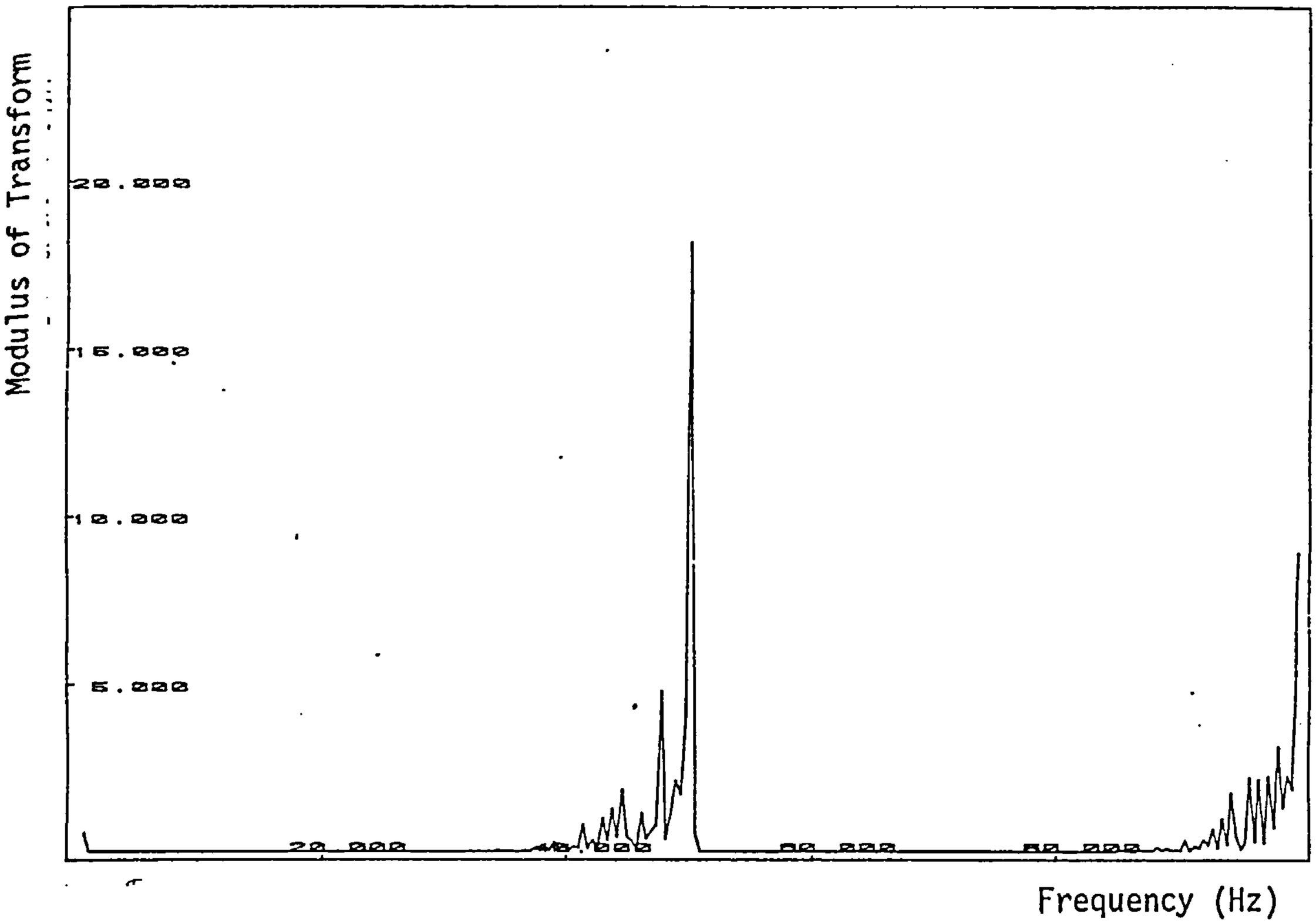

Figure 6.11a Fast Fourier Transform at Compressor Inlet Pressure

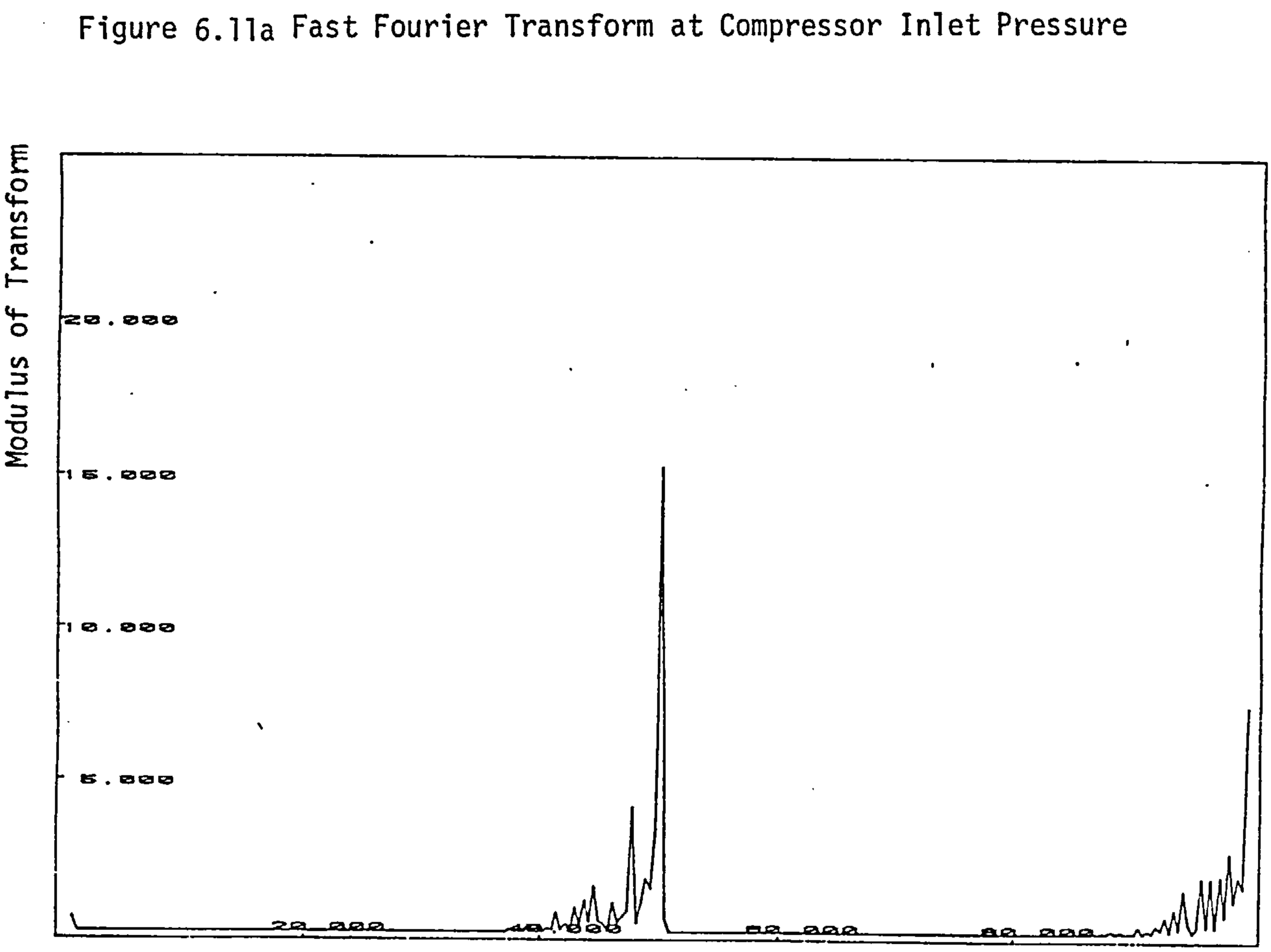

Figure 6.11b Fast Fourier Transform at Compressor Outlet Pressure

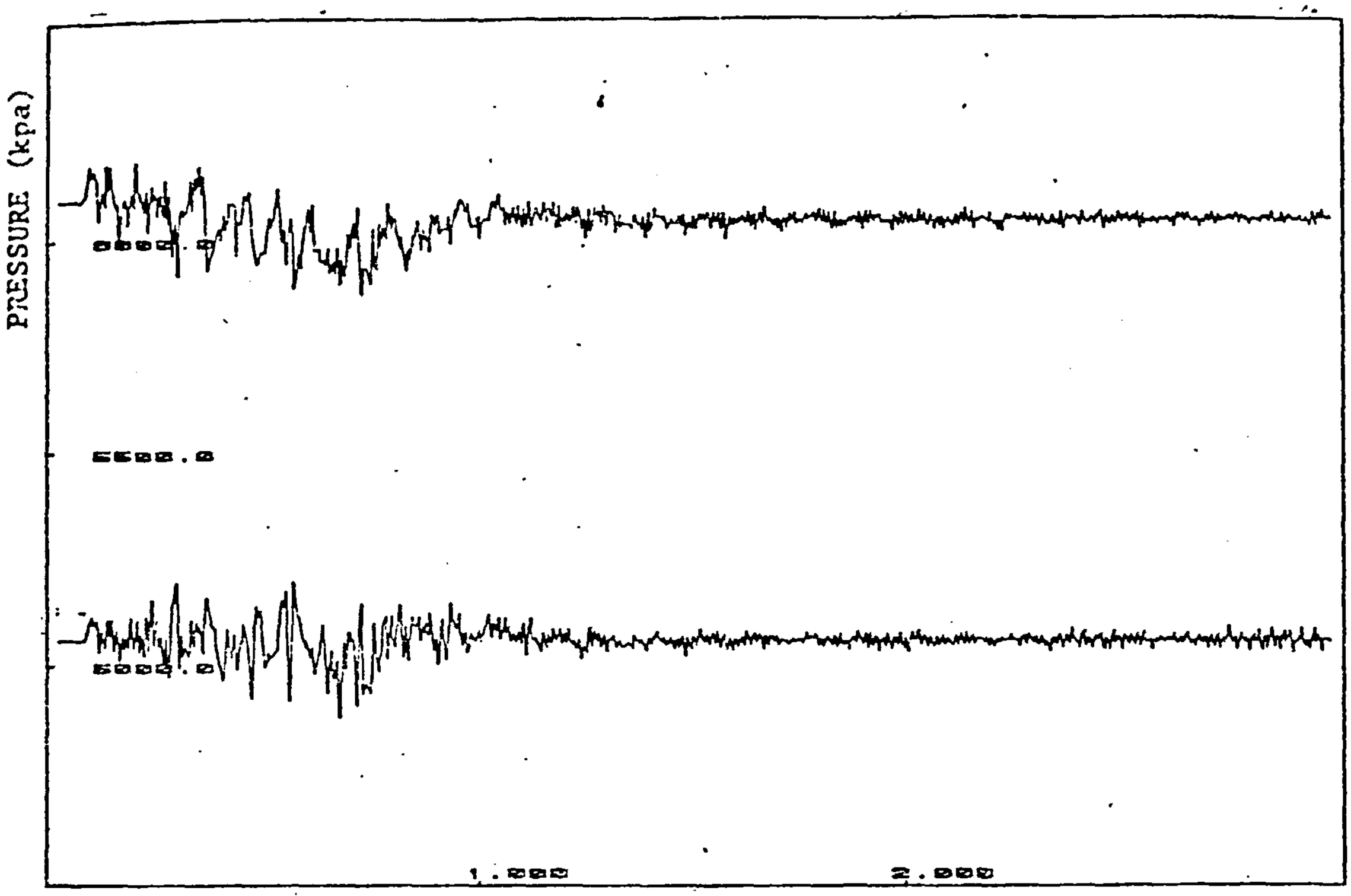

(a) Inlet and Outlet Pressure Time History Across Compressor

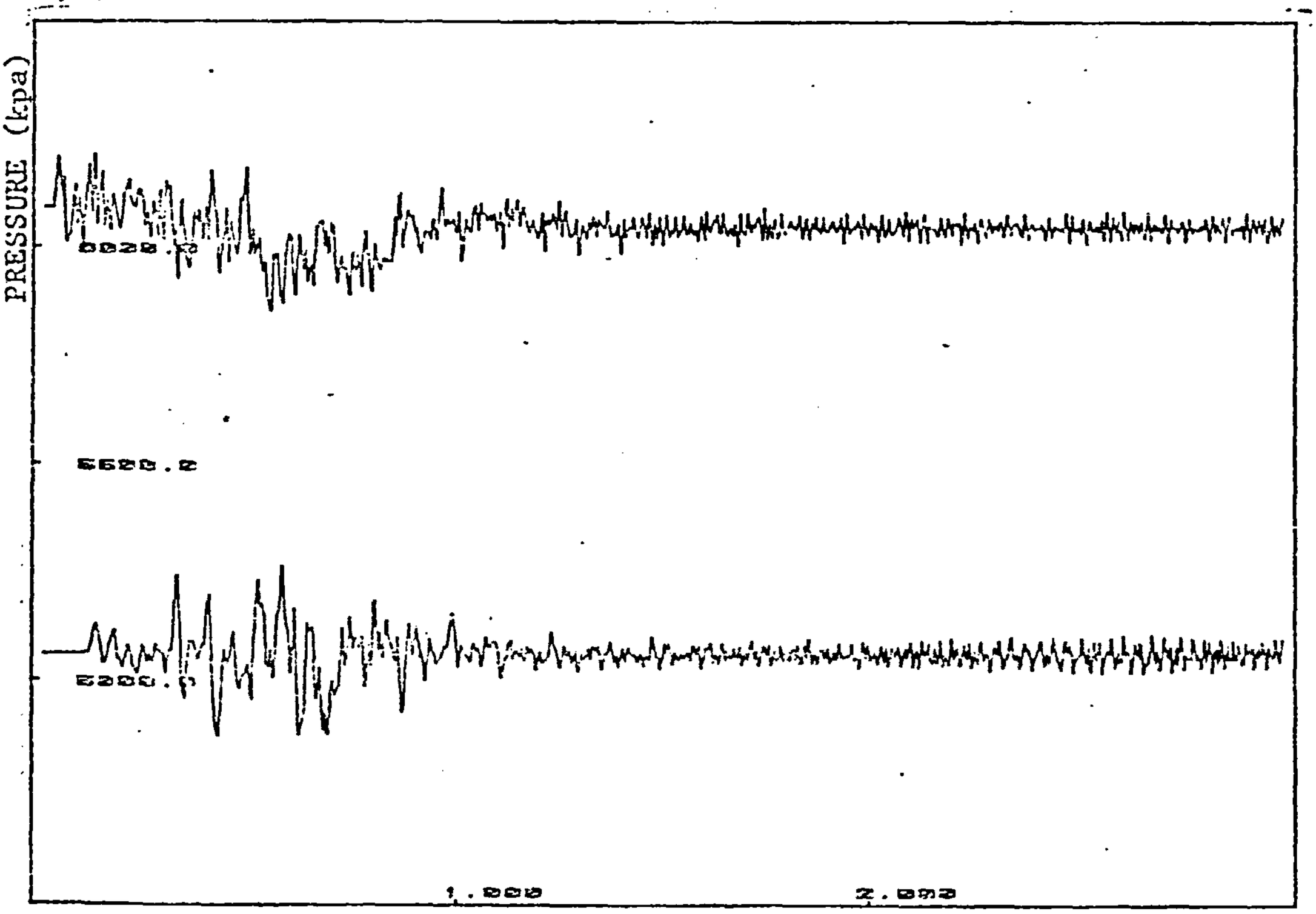

(b) Across non-return valve (element 60, fig. 1).

Figure 6.12 Surge conditions introduced and at t = 0.5 s recycle valve opened to remove compressor from surge.

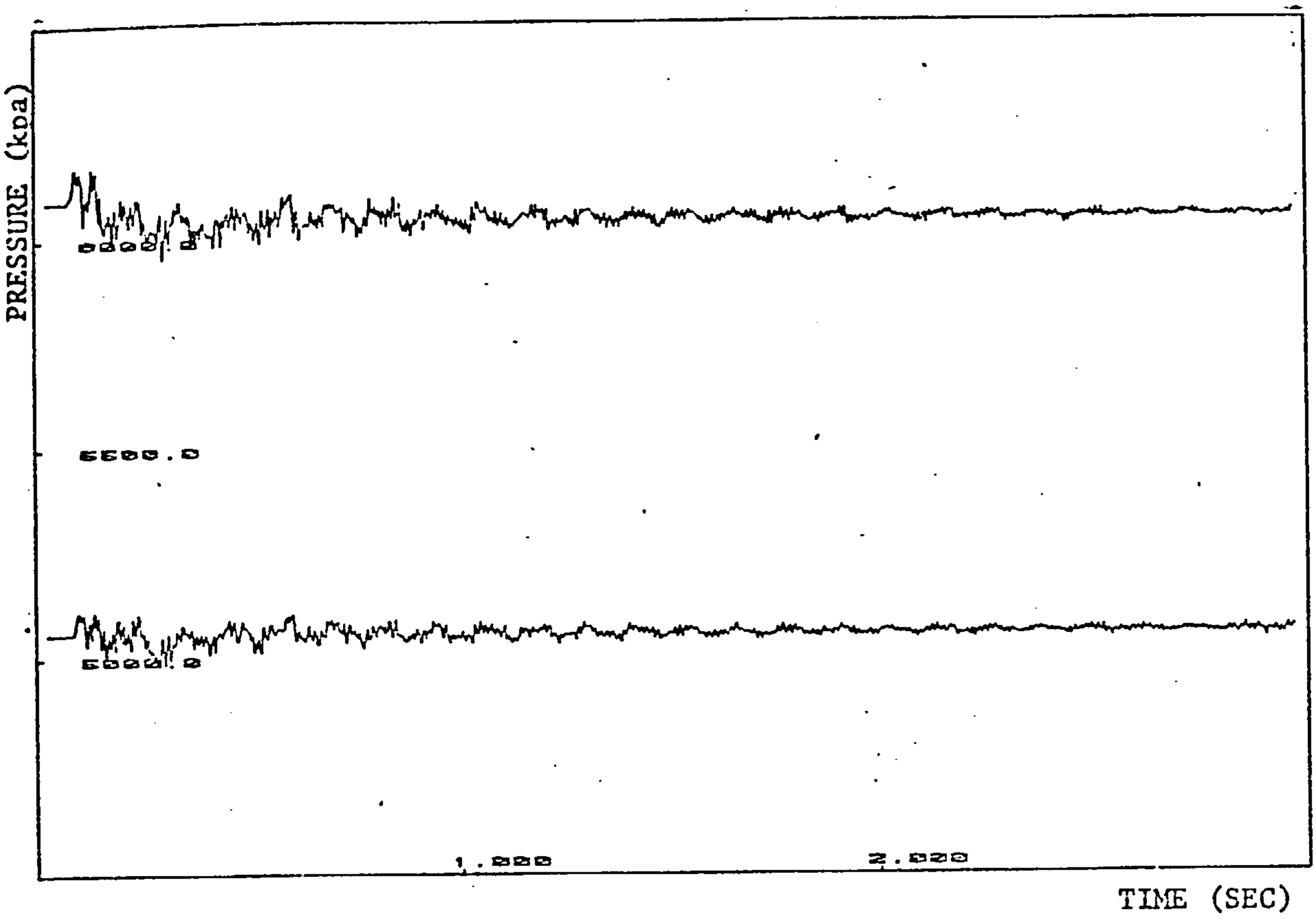

(a) Inlet and Outlet Pressure Time History Across Compressor

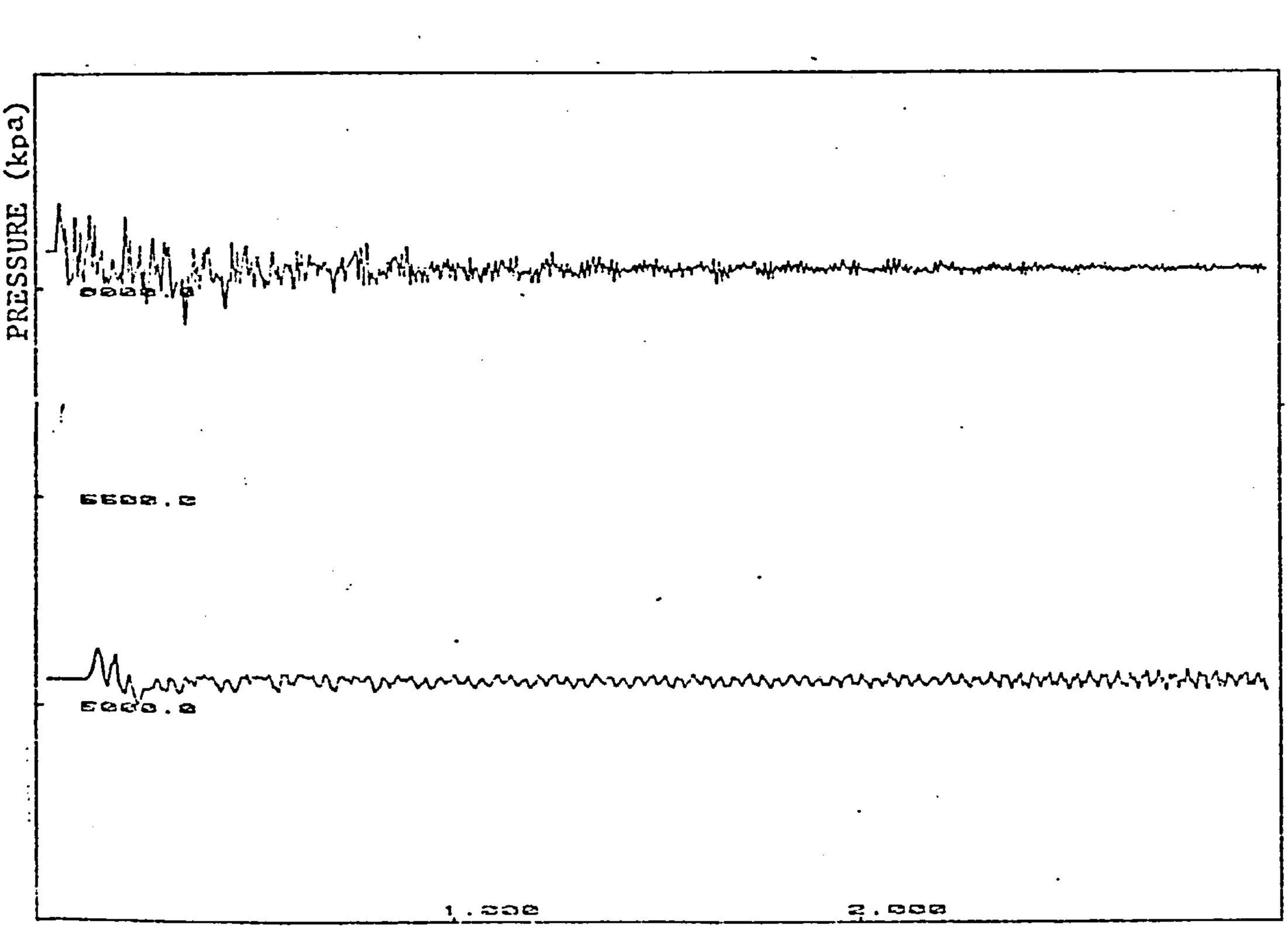

(b) Across non-return valve (element 60, fig. 1).

Figure 6.13 Surge conditions introduced and recycle valve opened by anti-surge controller to remove compressor from surge.

COMPRESSOR CHARACTERISTIC POLYTROPIC HEAD vs VOLUME FLOW RATE

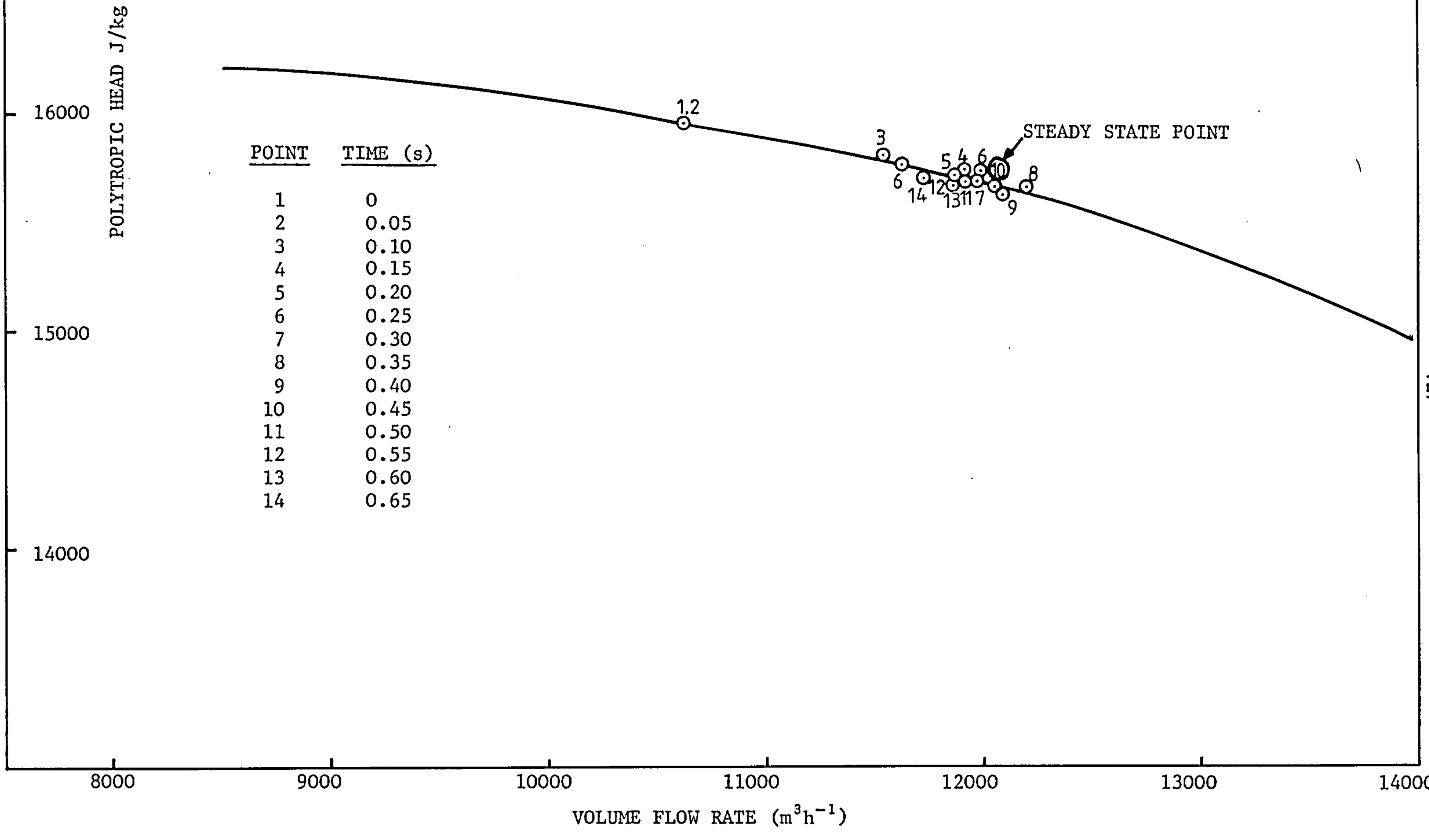

POINT	TIME (s)
1	0
2	0.05
3	0.10
4	0.15
5	0.20
6	0.25
7	0.30
8	0.35
9	0.40
10	0.45
11	0.50
12	0.55
13	0.60
14	0.65

FIGURE 6.14a REPRODUCTION OF CHARACTERISTIC BY HALF OPENED RECYCLE VALVE

COMPRESSOR CHARACTERISTIC POLYTROPIC HEAD vs VOLUME FLOW RATE

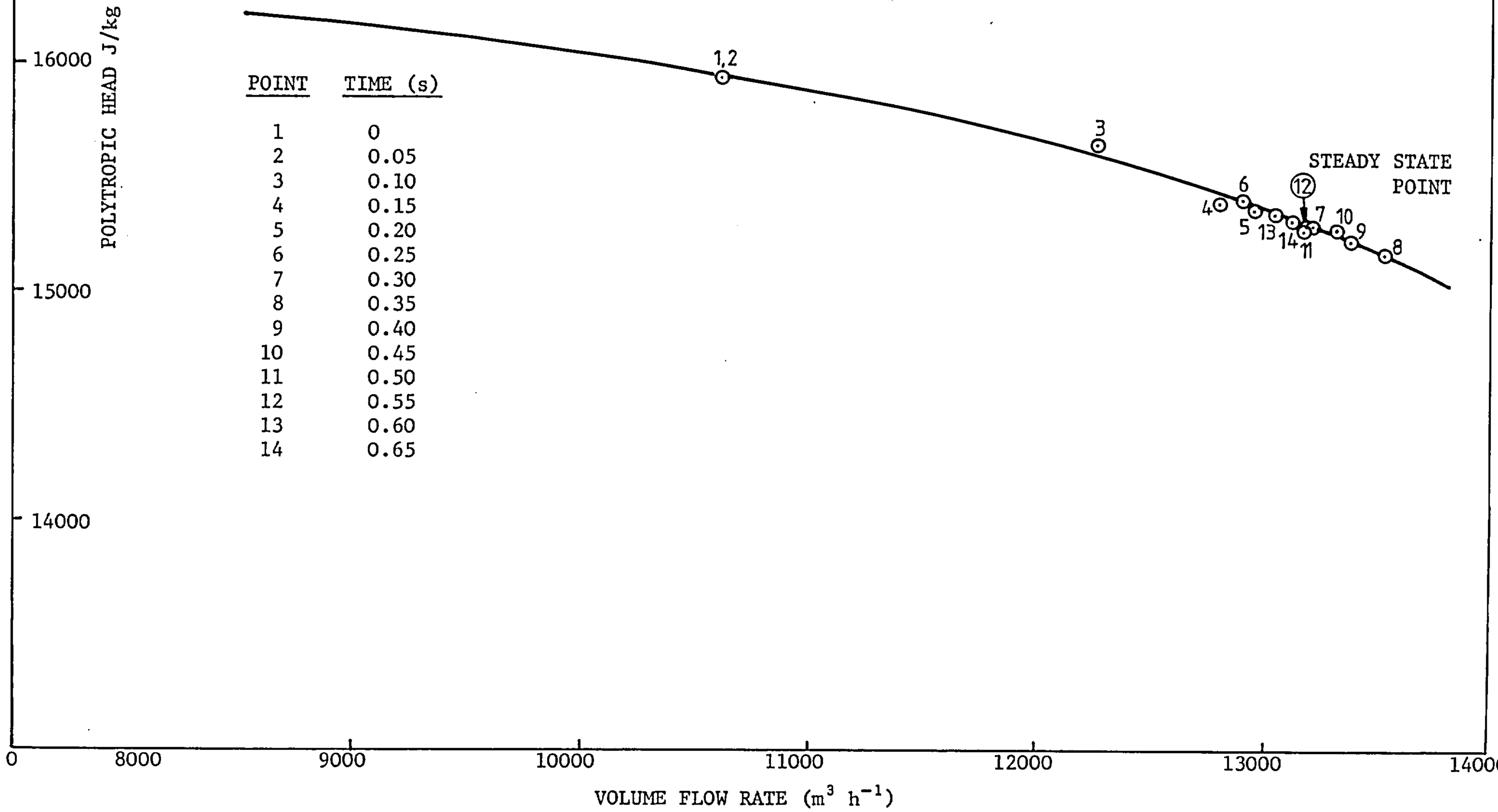

POINT	TIME (s)
1	0
2	0.05
3	0.10
4	0.15
5	0.20
6	0.25
7	0.30
8	0.35
9	0.40
10	0.45
11	0.50
12	0.55
13	0.60
14	0.65

FIGURE 6.14b REPRODUCTION OF CHARACTERISTIC BY FULL OPENED RECYCLE VALVE

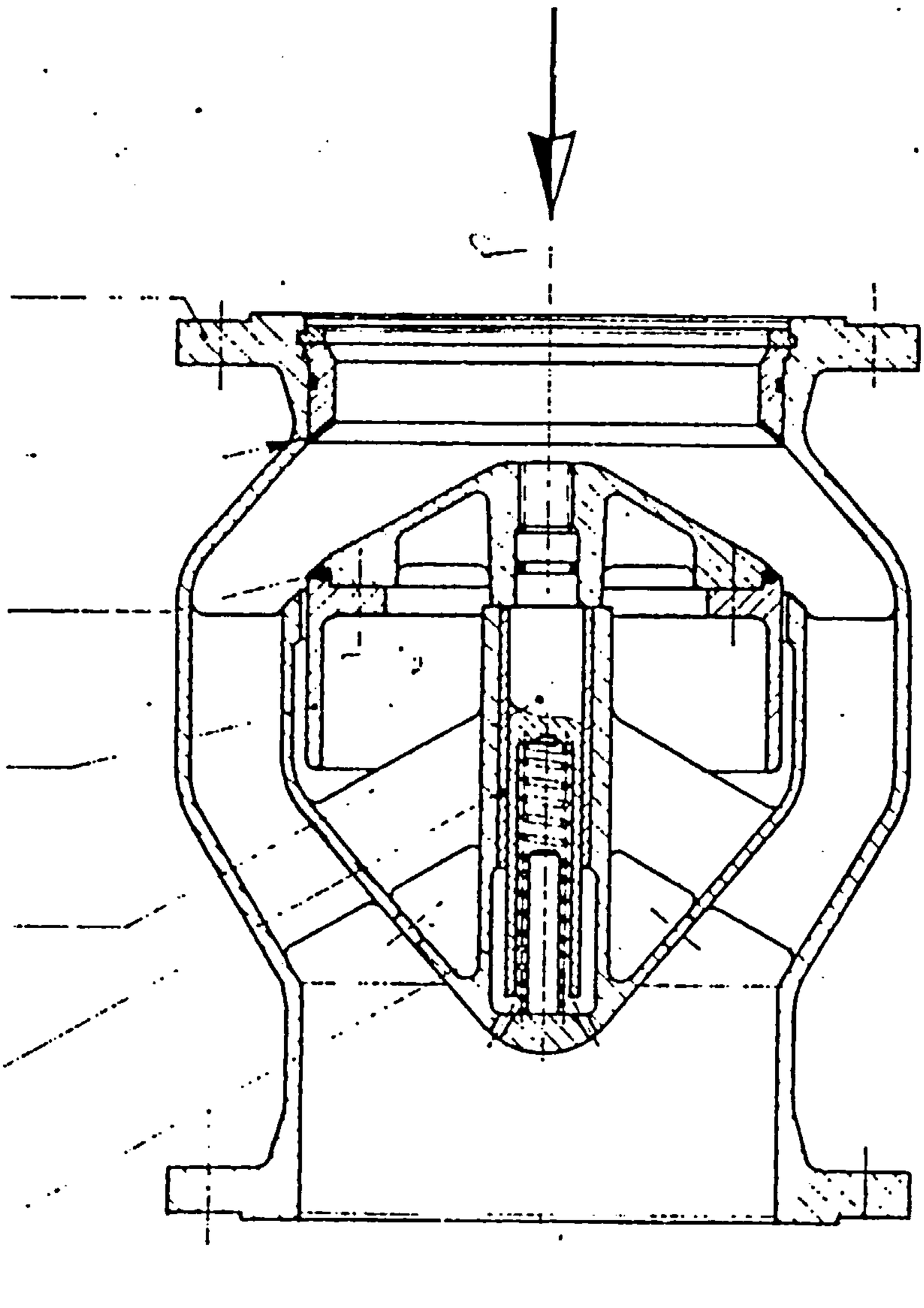

Figure 6.15a Drawing of Non-Return Valve

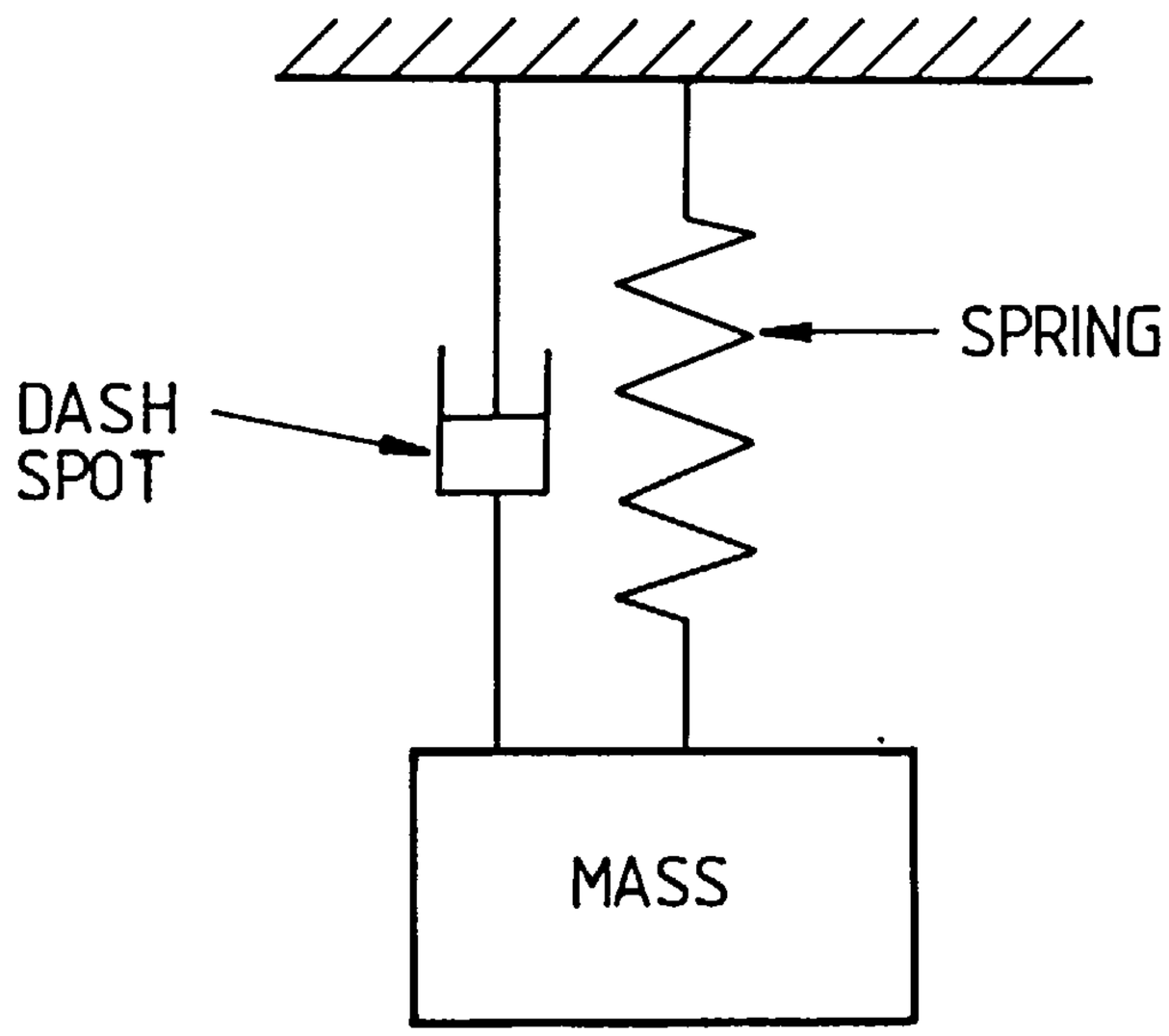

FIG. 6·15b SPRING MASS REPRESENTATION OF NON RETURN VALVE

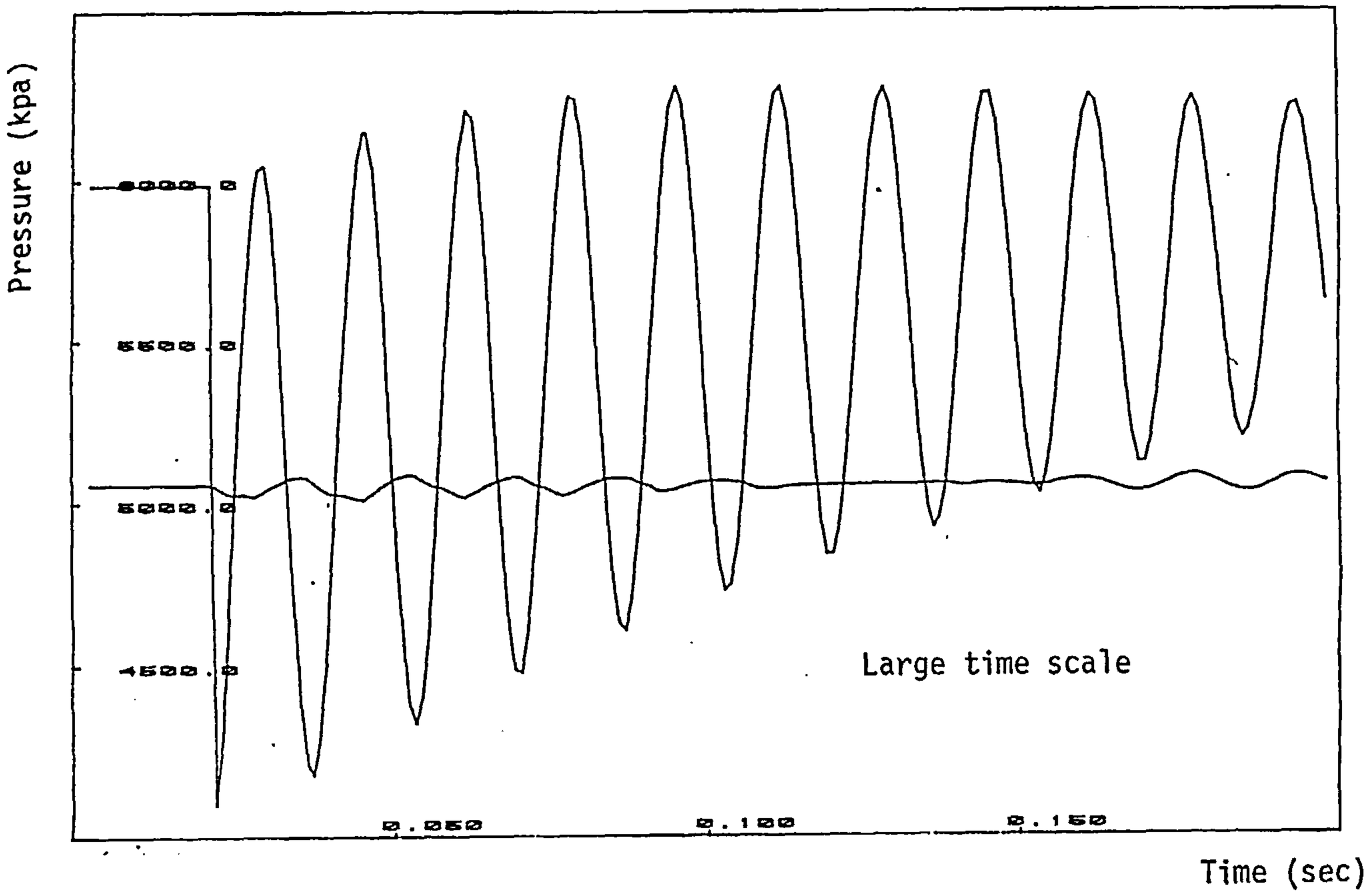

Figure 6.16 Pressures across non-return valve (element 63 fig. 6.3)

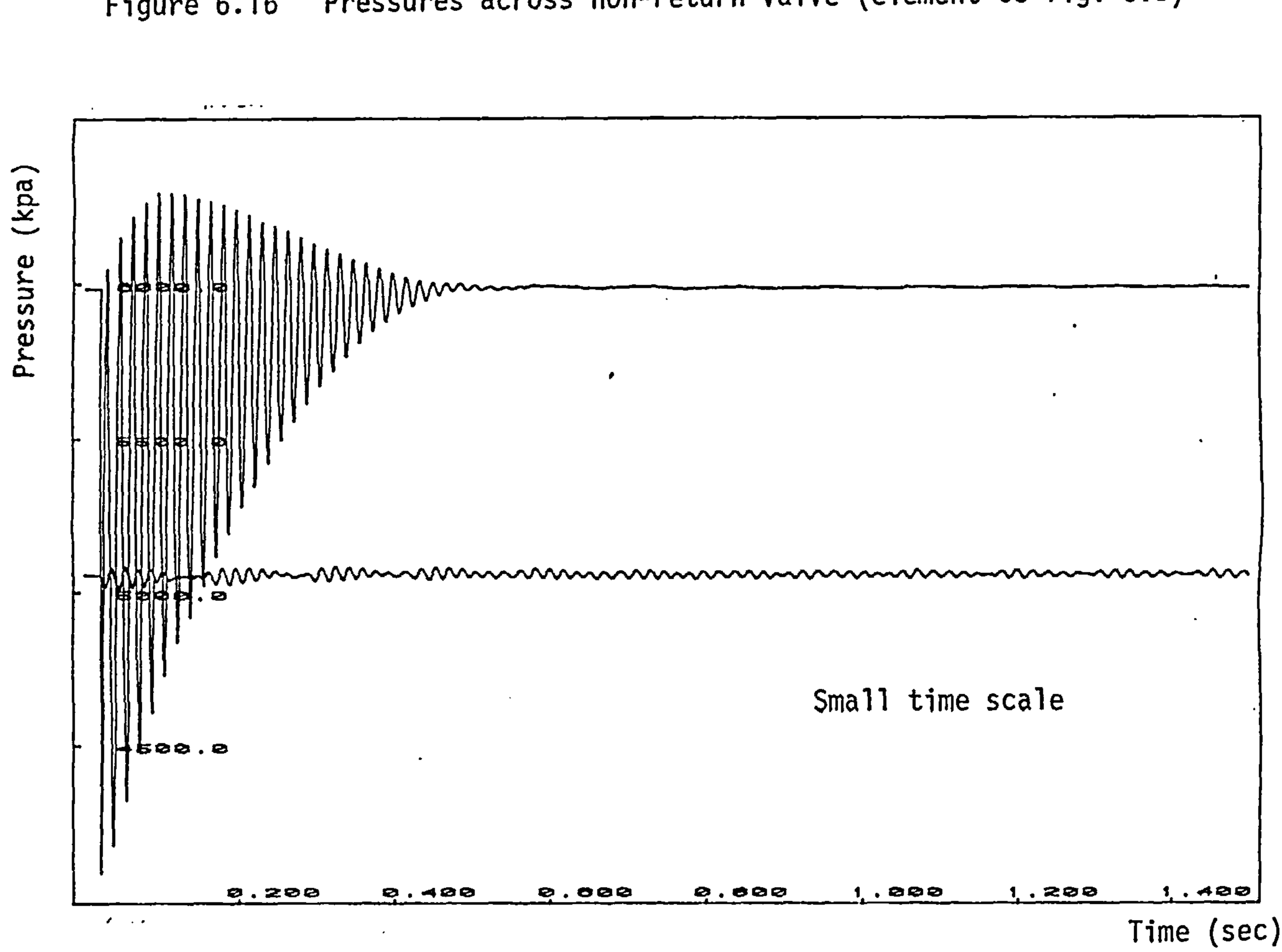

Figure 6.17 Pressures across non-return valve (element 63 fig 6.3)

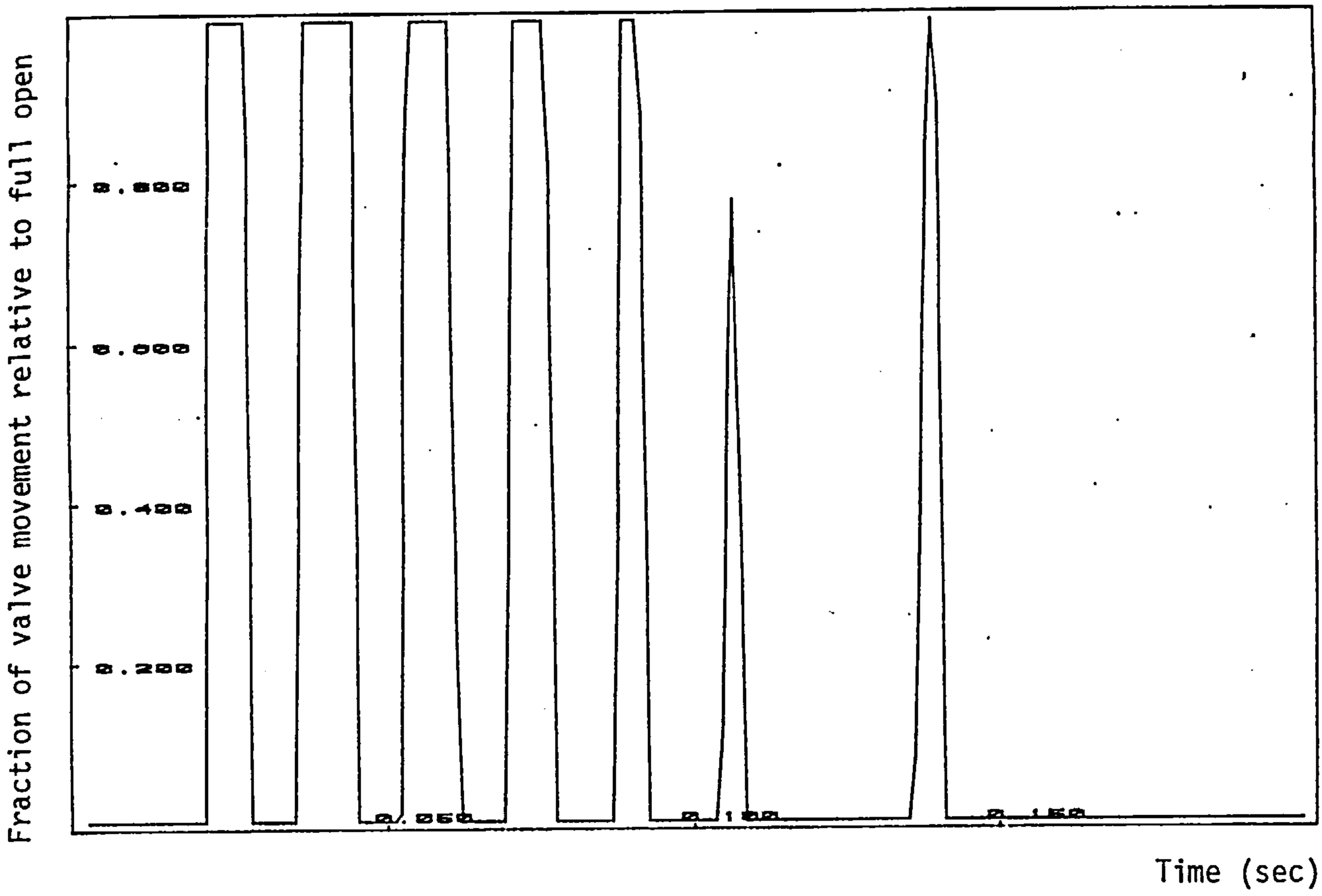

Figure 6.18a Non-Return Valve Movement (element 63 fig. 6.3)

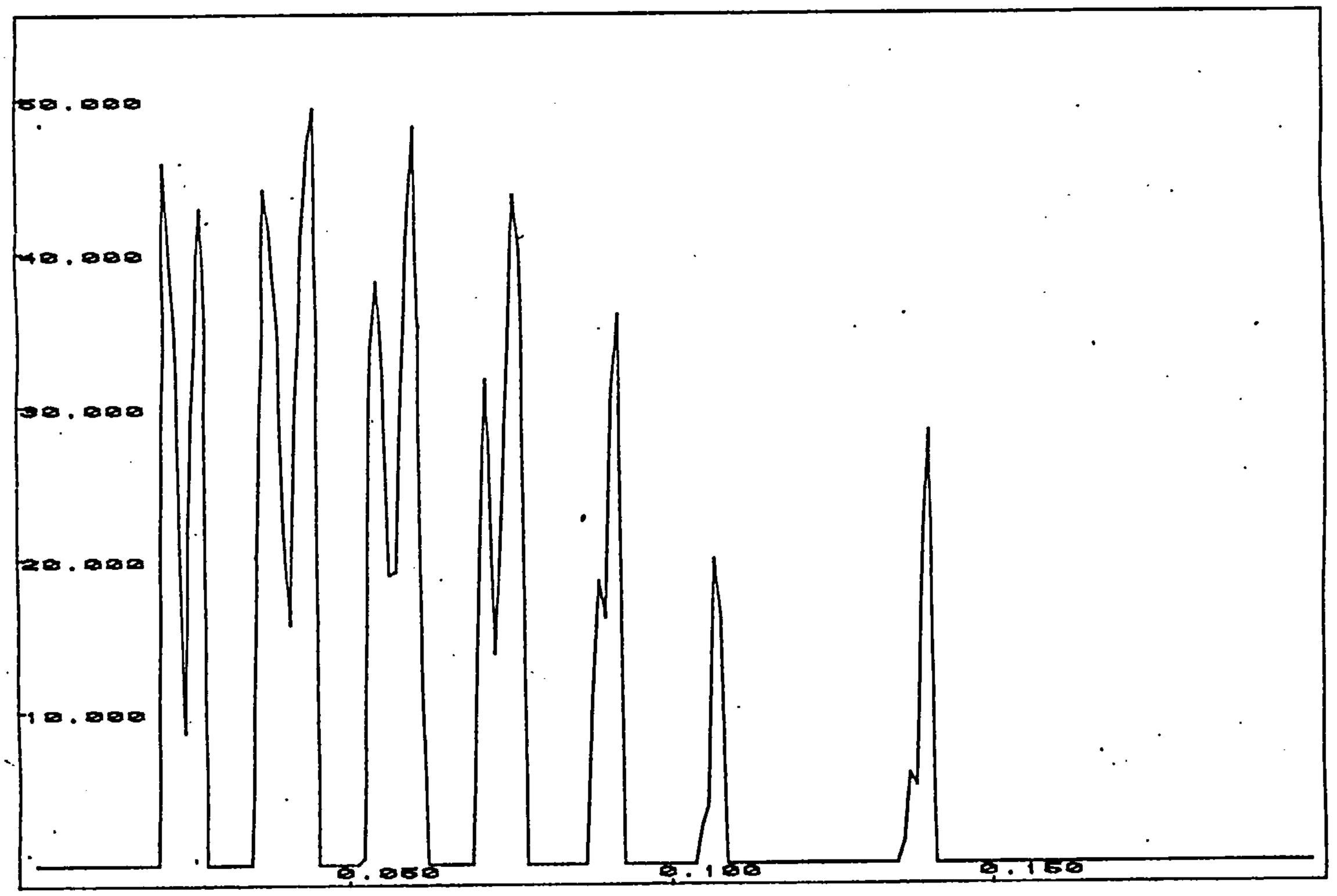

Figure 6.18b Non-Return Valve Entry Mass Flow (element 63 fig.6.3)

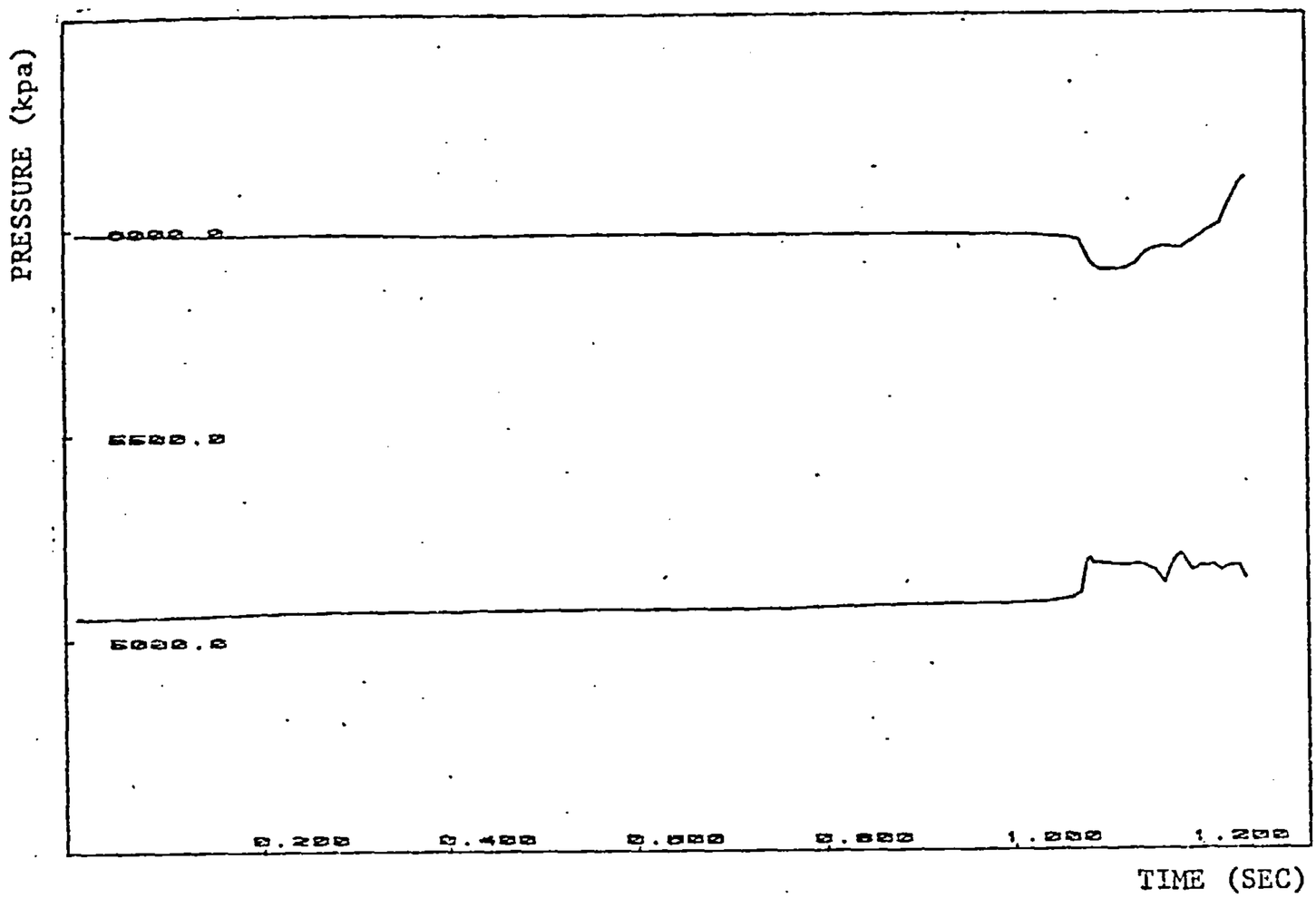

(a) Inlet and Outlet Pressure Time History Across Compressor

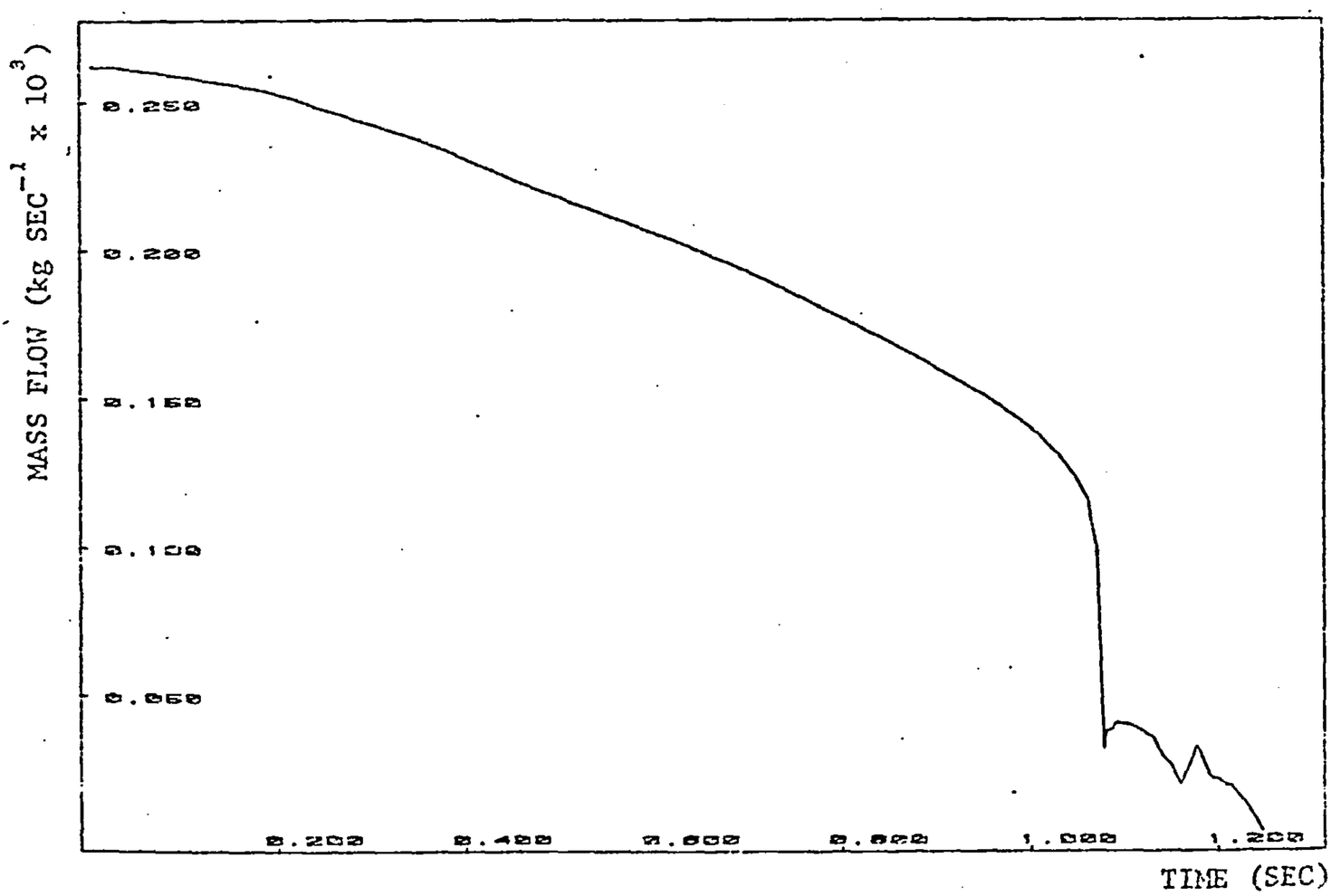

(b) Compressor entry mass flow.

Figure 6.19 Speed transient (speed reduction and impedance boundary condition).

COMPRESSOR CHARACTERISTIC POLYTROPIC HEAD vs VOLUME FLOW RATE

Δ SPEED = 500 RPM/s

POINT	TIME (s)	POINT	TIME (s)
1	0	13	1.2
2	0.1	14	1.3
3	0.2	15	1.4
4	0.3	16	1.5
5	0.4	17	1.6
6	0.5	18	1.7
7	0.6	19	1.8
8	0.7	20	1.9
9	0.8	21	2.0
10	0.9	22	2.1
11	1.0	23	2.2
12	1.1	24	2.3
		25	2.4
		26	2.5
		27	2.6
		28	3.0
		29	3.5

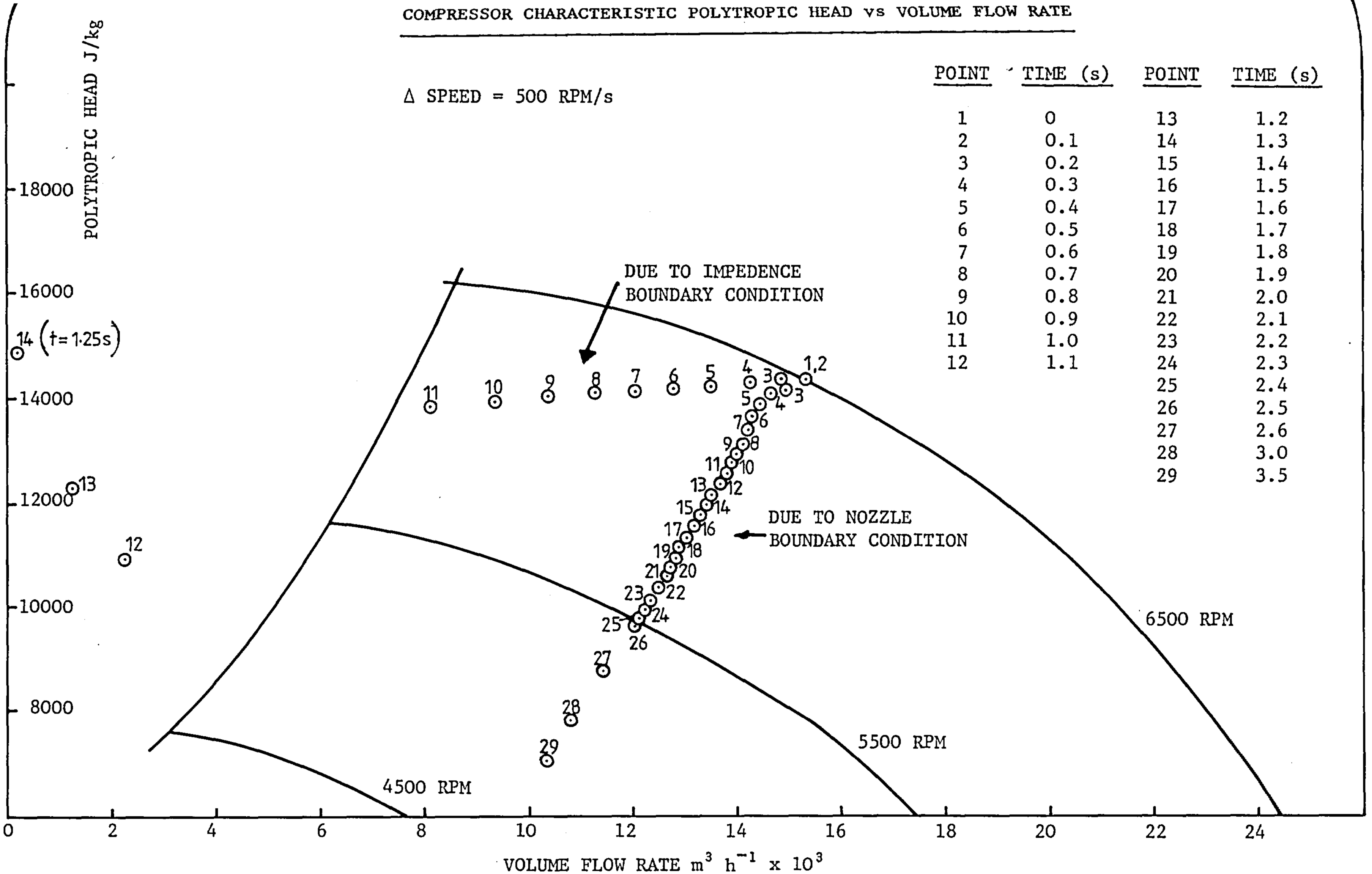

FIGURE 6.20 THE SPEED TRANSIENT REPRESENTED ON CHARACTERISTIC

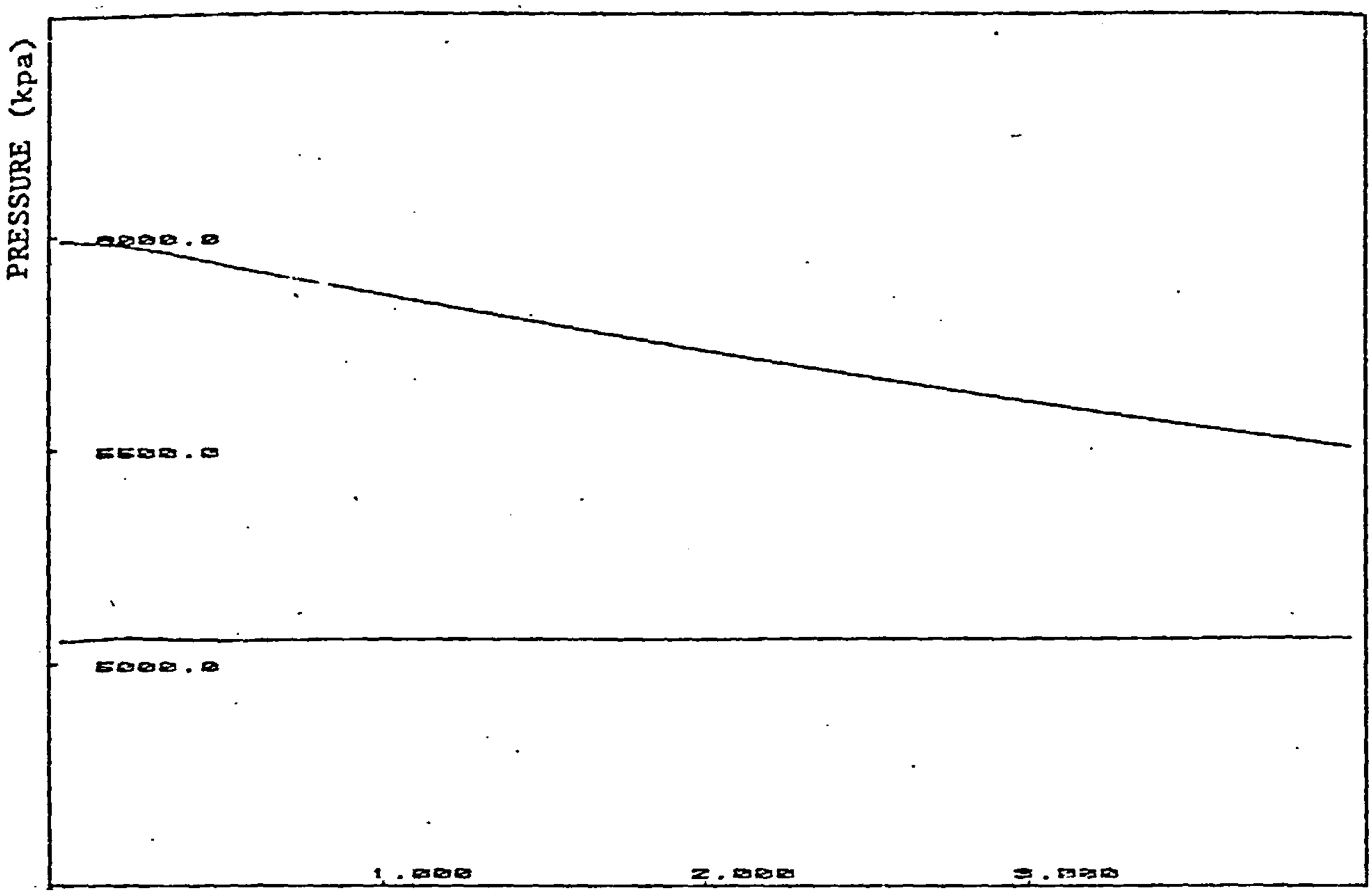

(a) Inlet and Outlet Pressure Time History Across Compressor

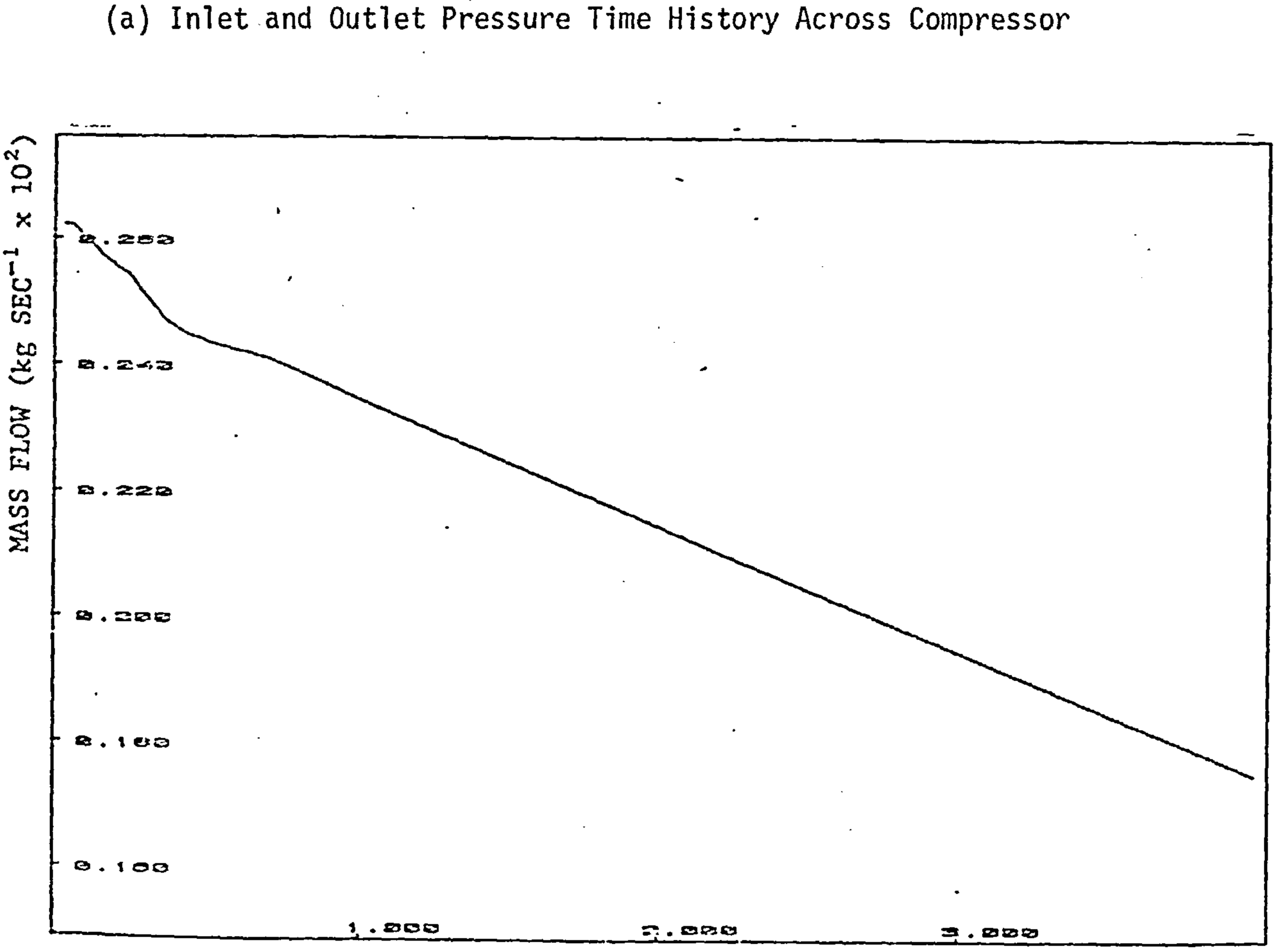

(b) Compressor entry mass flow.

Figure 6.21 Speed transient (speed reduction and nozzle boundary condition)

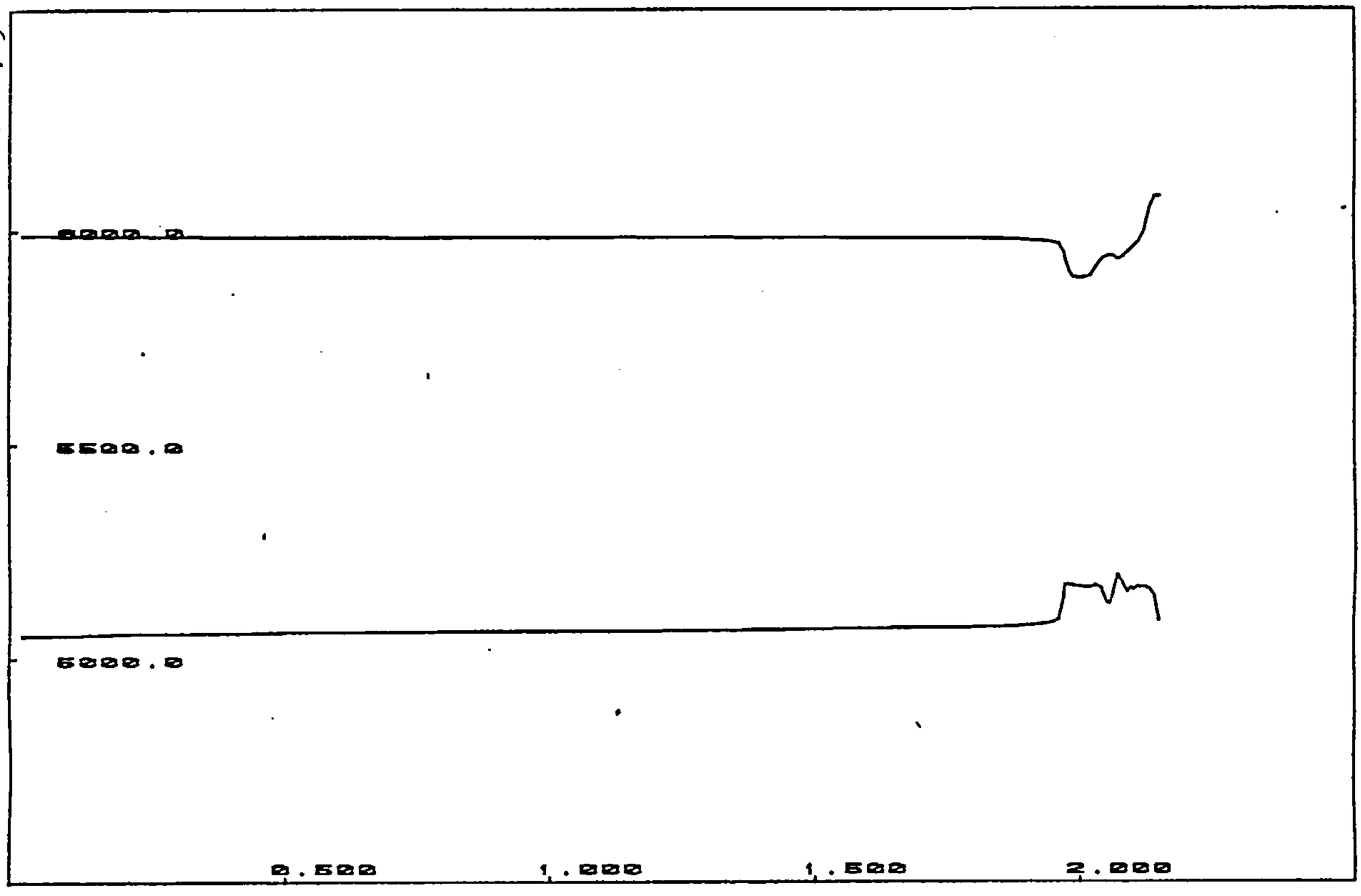

(a) Inlet and Outlet Pressure Time History for Compressor

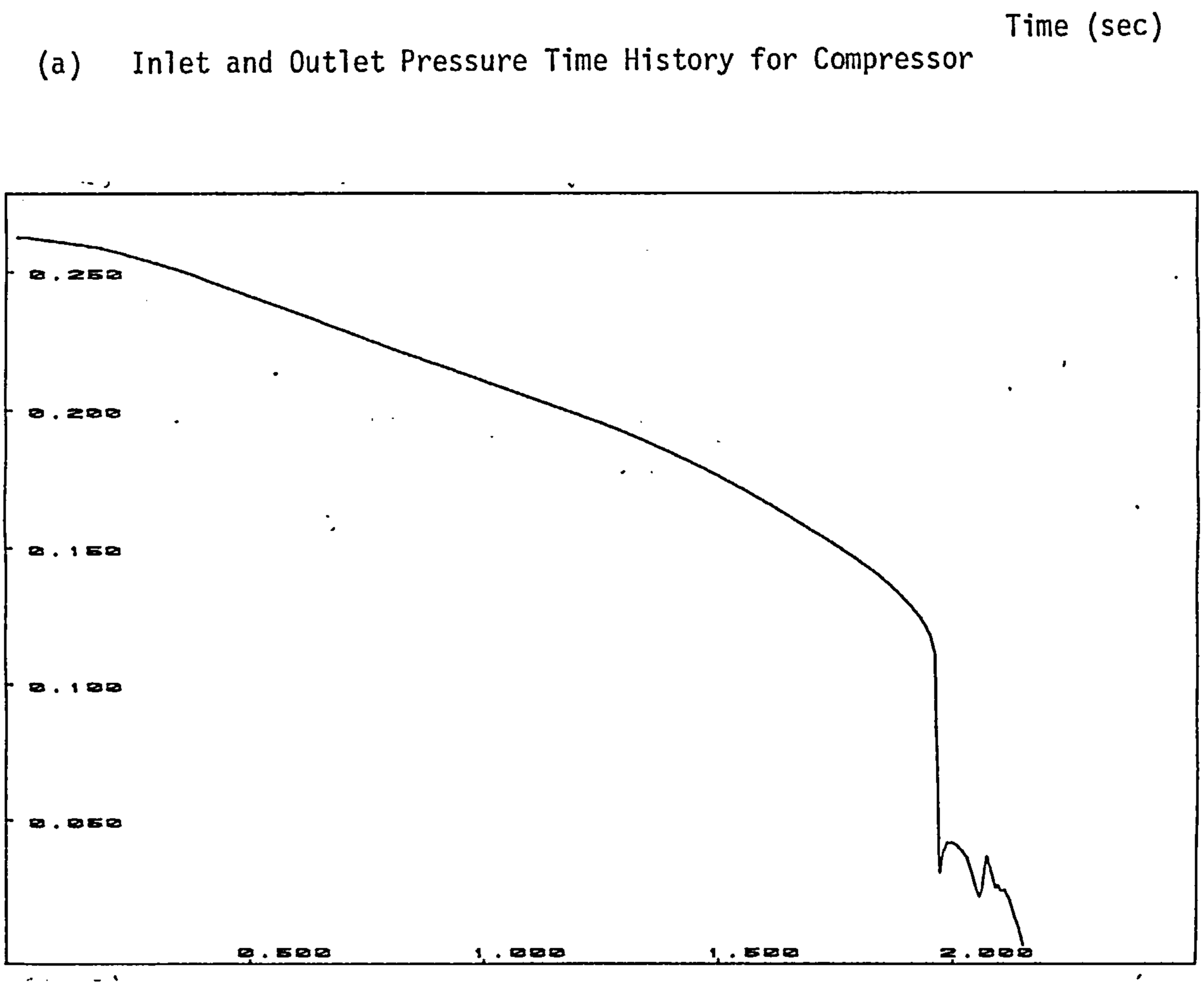

(b) Compressor Entry Mass Flow

Figure 6.22 Speed Transient (Speed Reduction and near Infinite Volume Boundary Condition). Deceleration rate = 25 rpm s^{-1} Small System

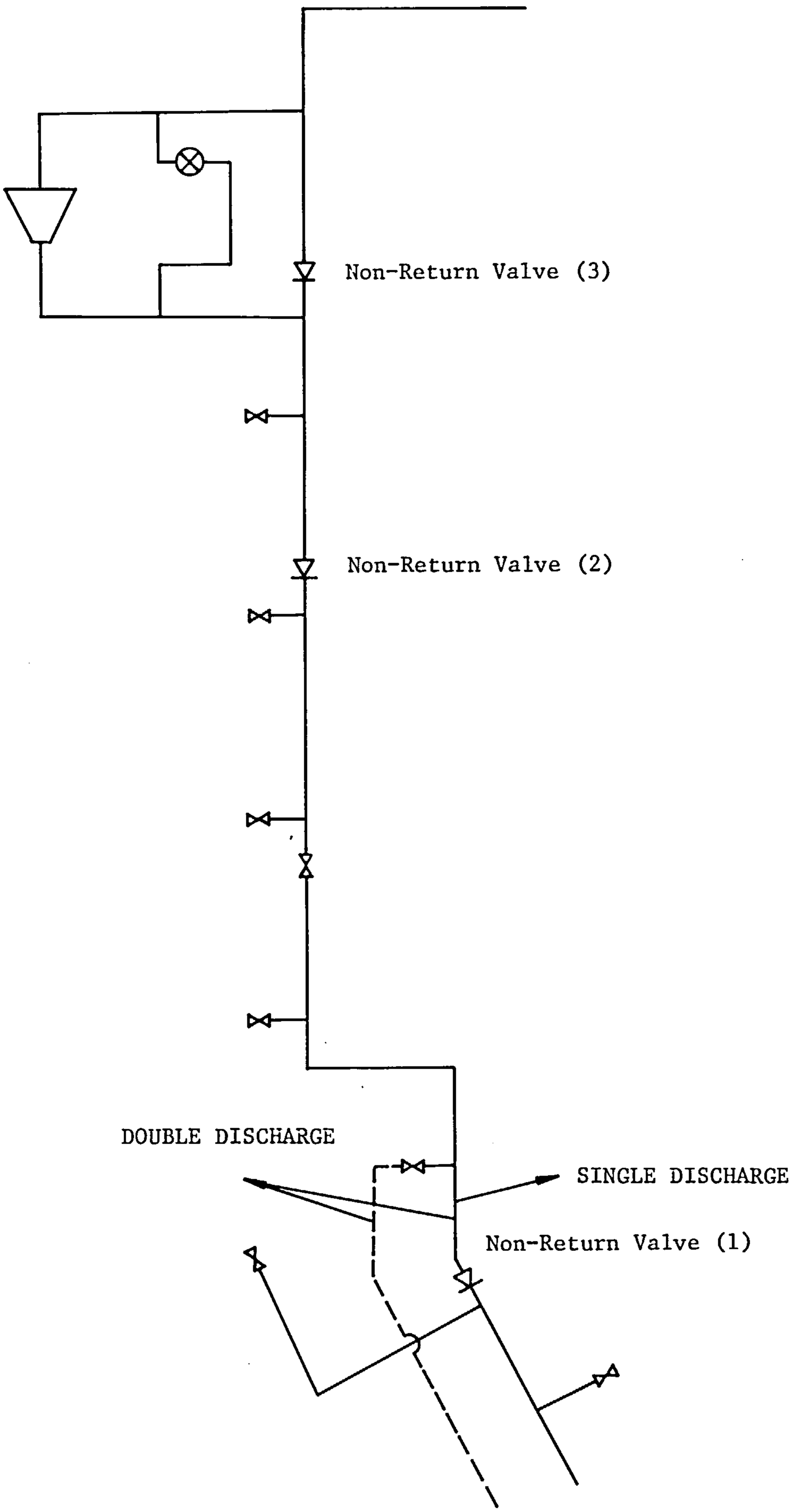

FIGURE 6.23 LARGE SYSTEM (133 ELEMENTS)

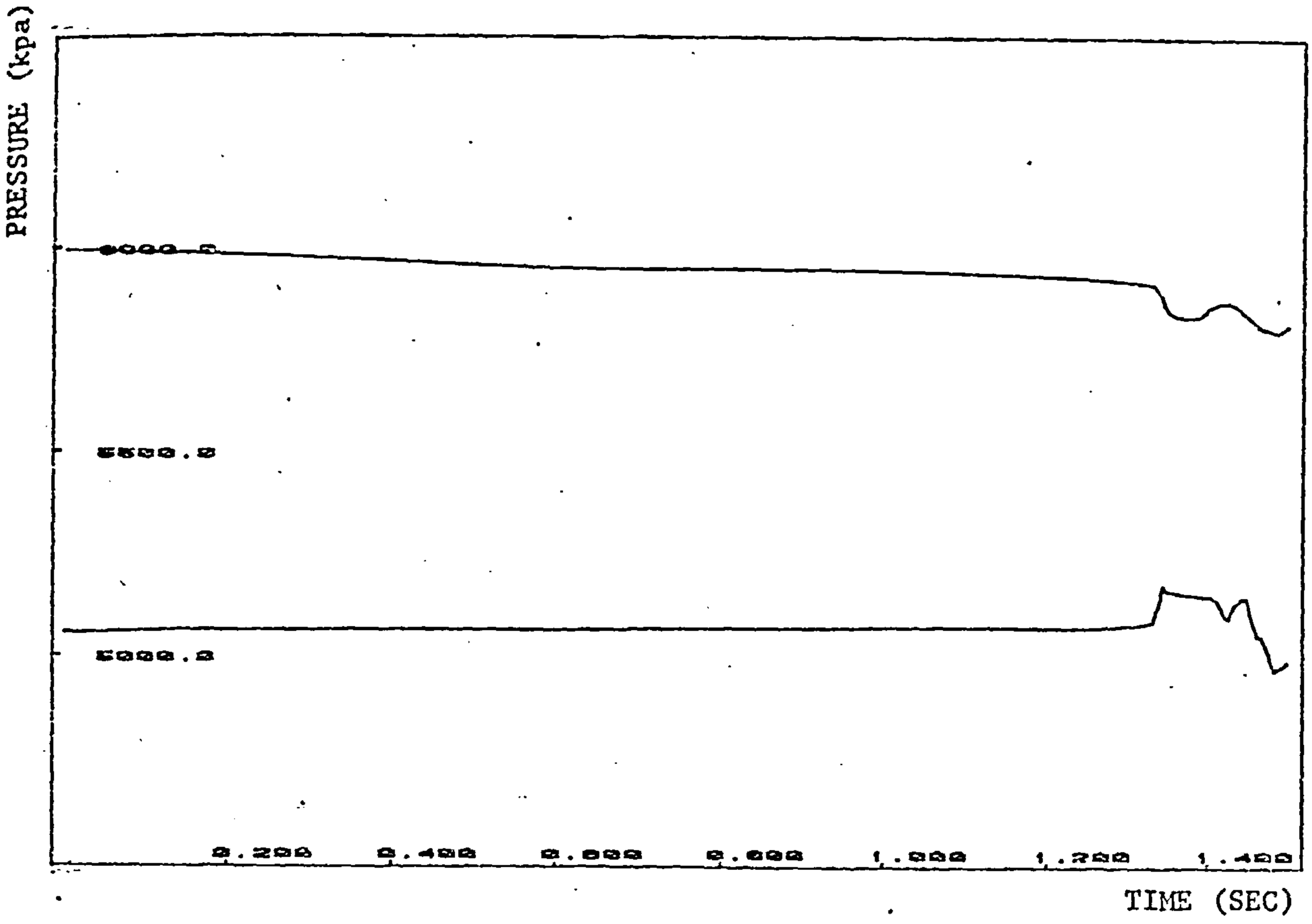

(a) Inlet and Outlet Pressure Time History Across Compressor

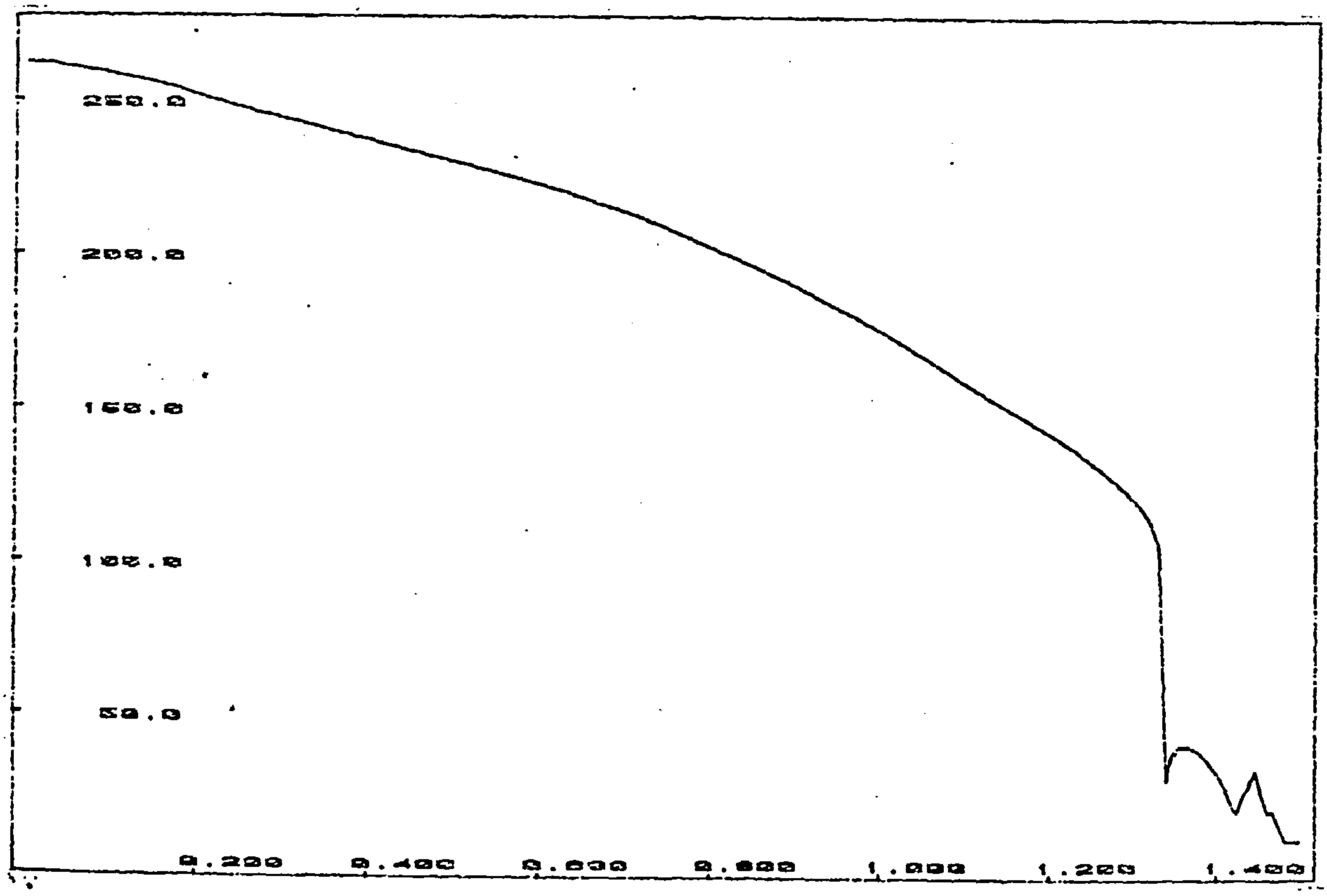

(b) Compressor entry mass flow.

Figure 6.24 Speed transient (speed reduction and near infinite volume boundary condition). Large system 133 elements.

COMPRESSOR CHARACTERISTIC POLYTROPIC HEAD vs VOLUME FLOW RATE

SINGLE DISCHARGE

Δ SPEED = 500 RPM/s

POINT	TIME (s)	POINT	TIME (s)
1	0.0	9	0.8
2	0.1	10	0.9
3	0.2	11	1.0
4	0.3	12	1.1
5	0.4	13	1.2
6	0.5	14	1.3
7	0.6	15	1.4
8	0.7		

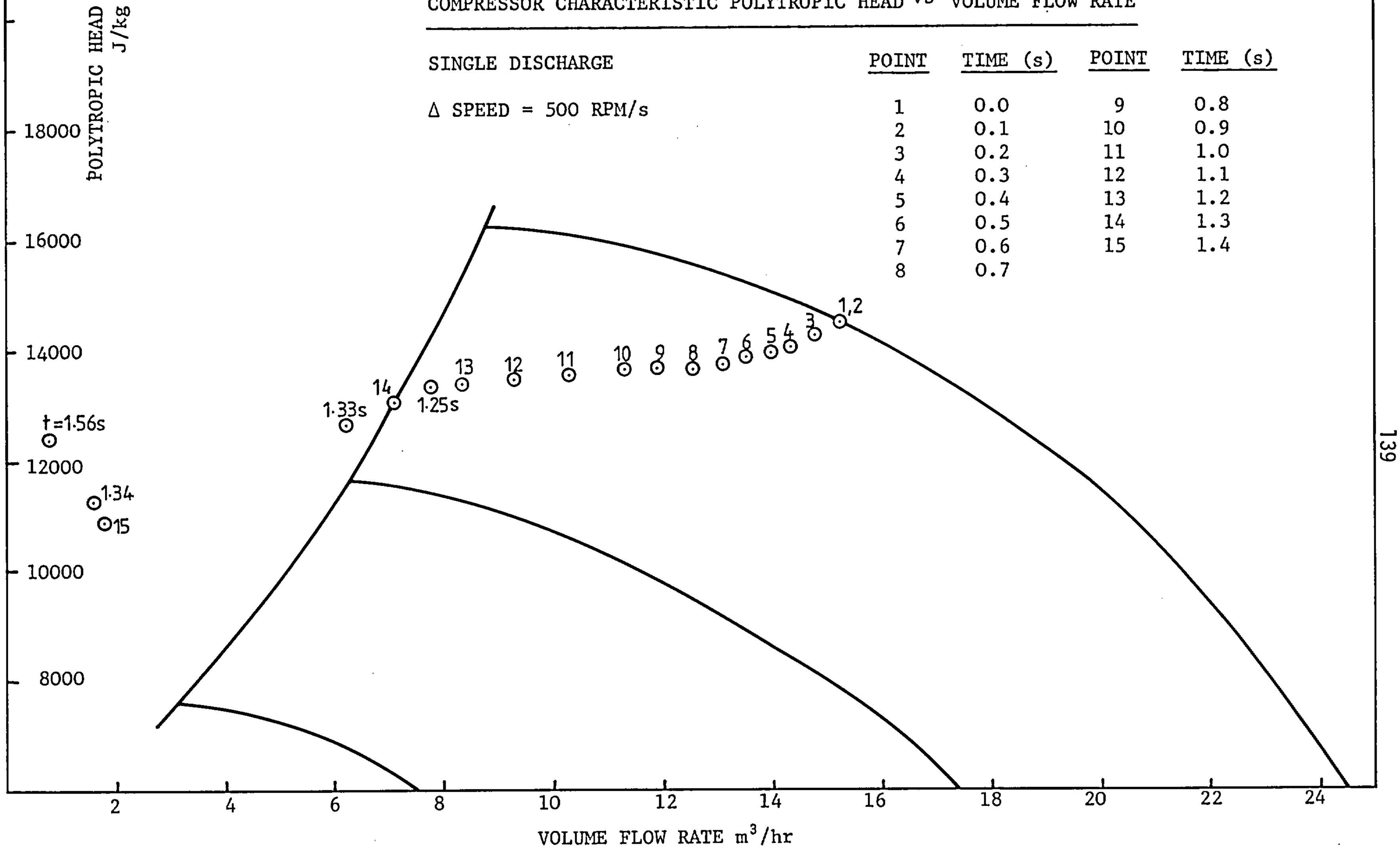

FIGURE 6.25 THE SPEED TRANSIENT REPRESENTED ON CHARACTERISTIC

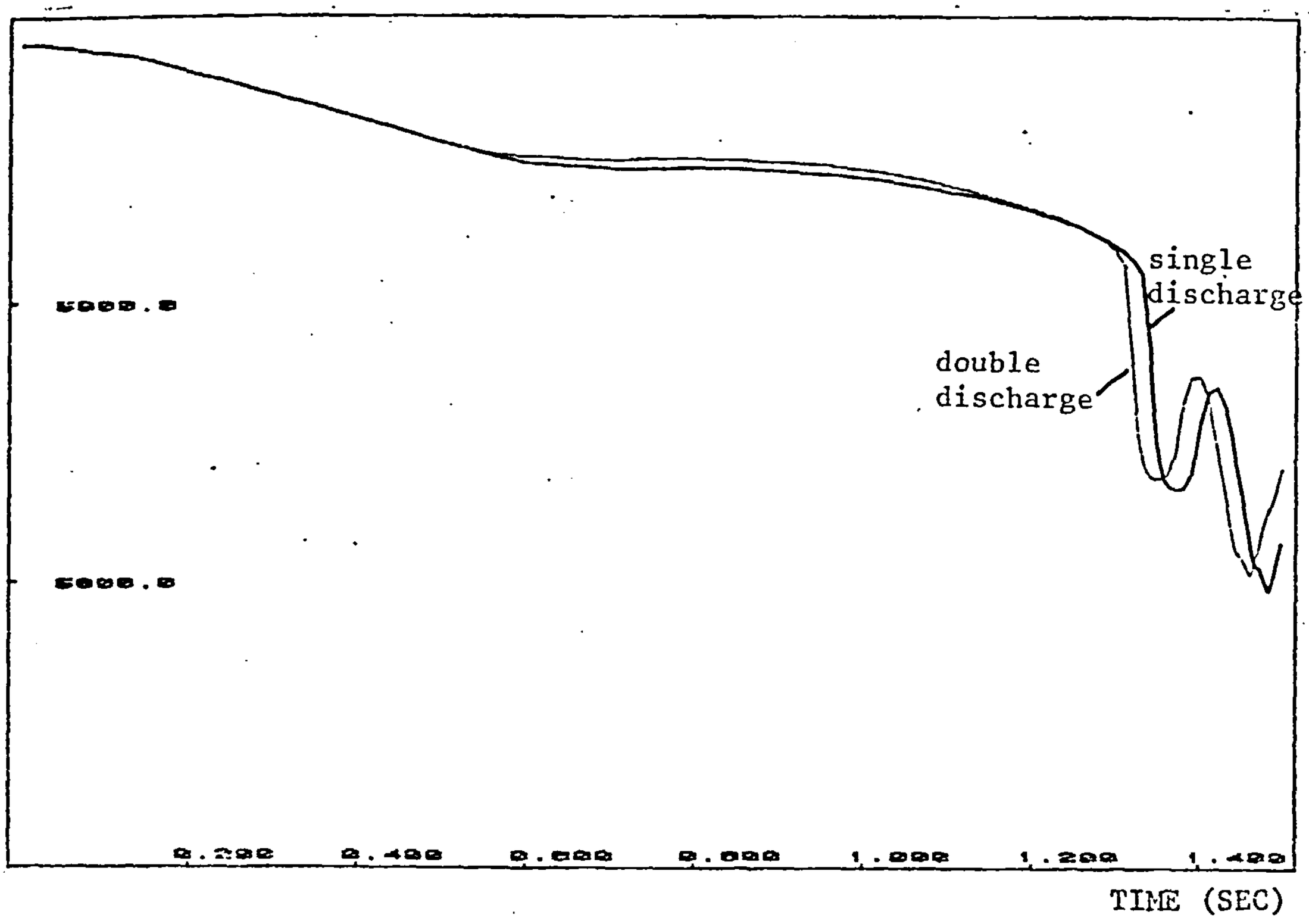

(a) Compressor outlet pressure time history.

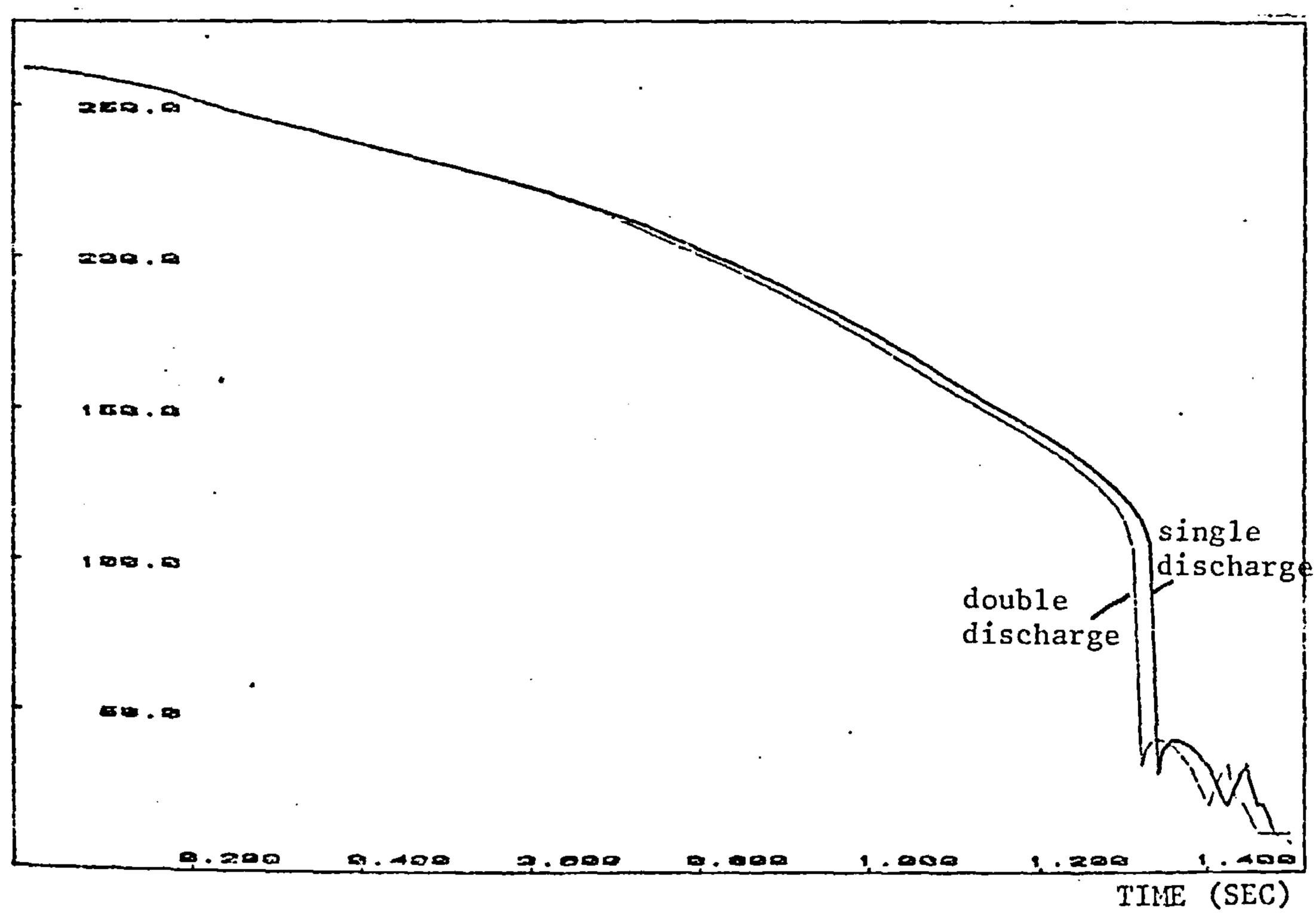

(b) Compressor entry mass flow time history.

Figure 6.26 Speed transient with single and double discharge operation.

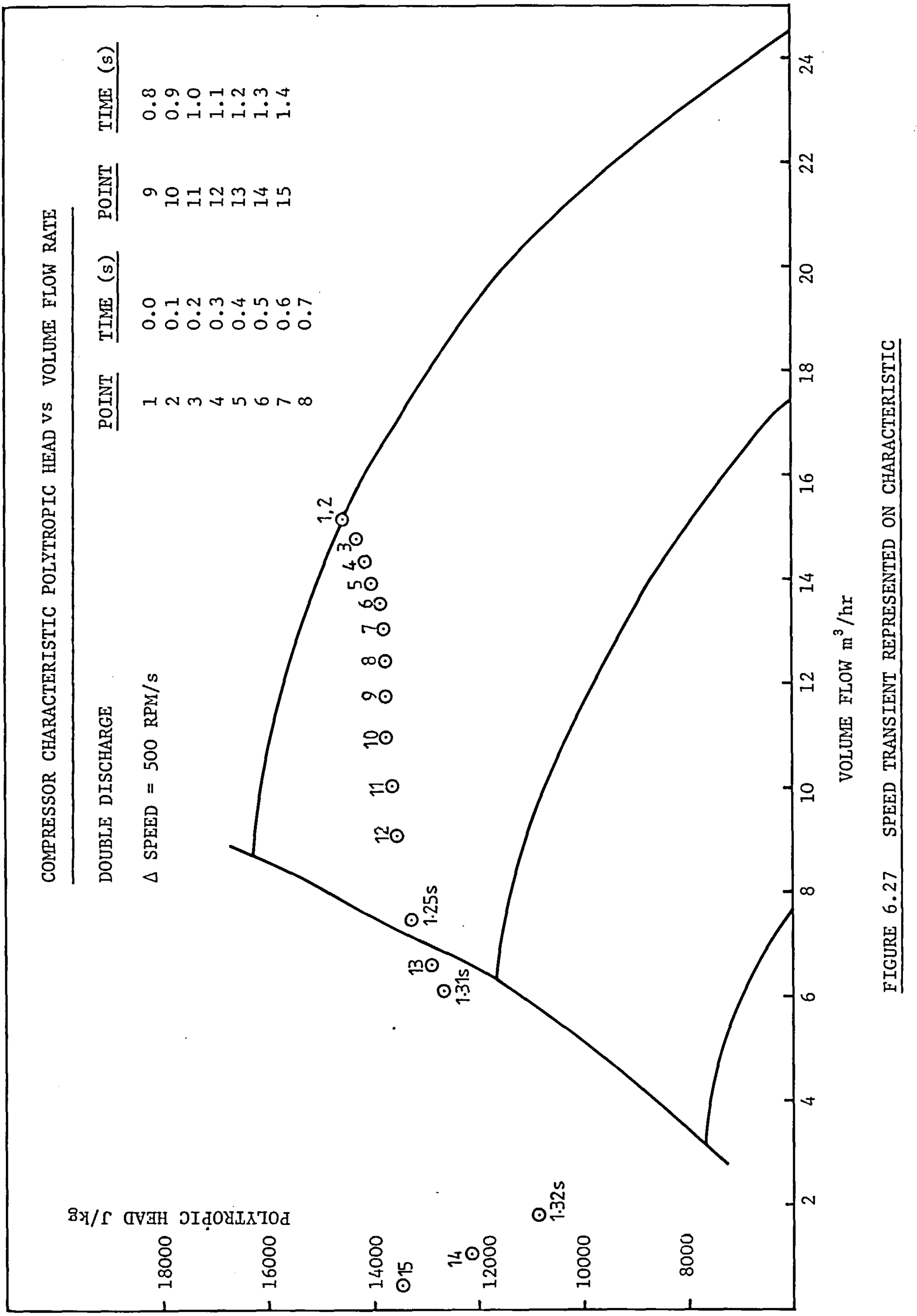

FIGURE 6.27 SPEED TRANSIENT REPRESENTED ON CHARACTERISTIC

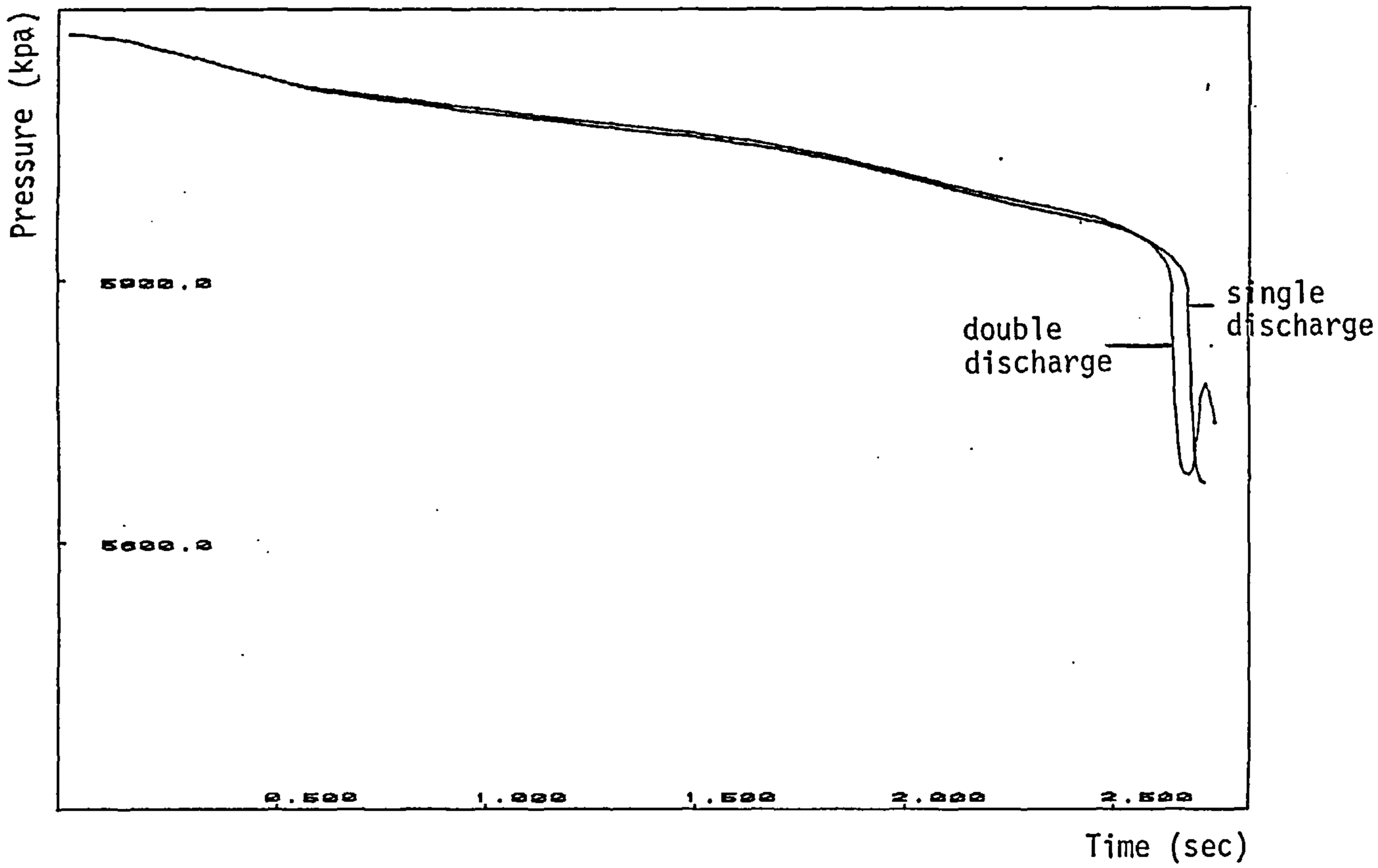

(a) Compressor Outlet Pressure Time History

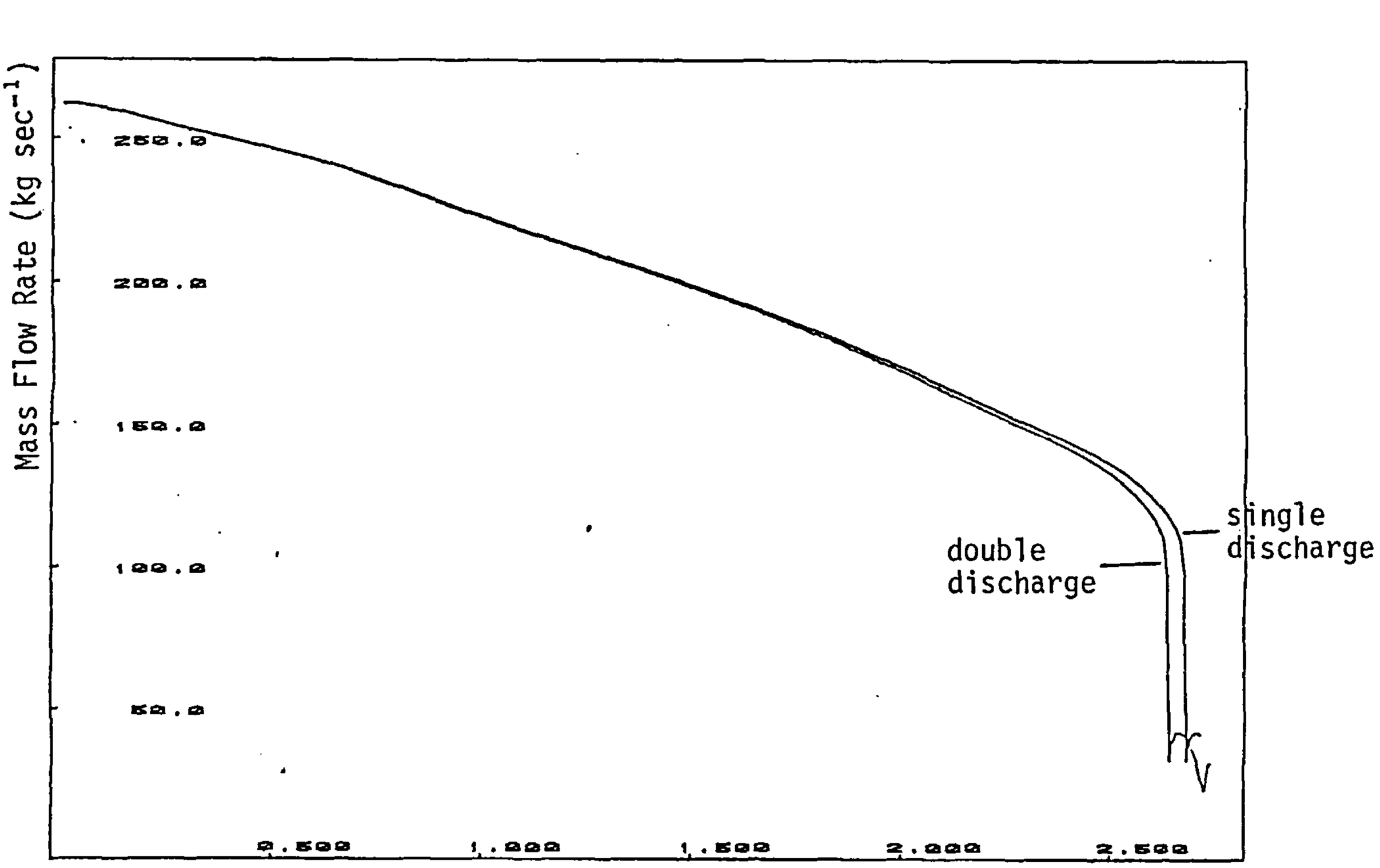

(b) Compressor Entry Mass Flow Time History

Figure 6.28 Speed Transient with Single and Double Discharge Operation. Deceleration = 250 rpm/sec.

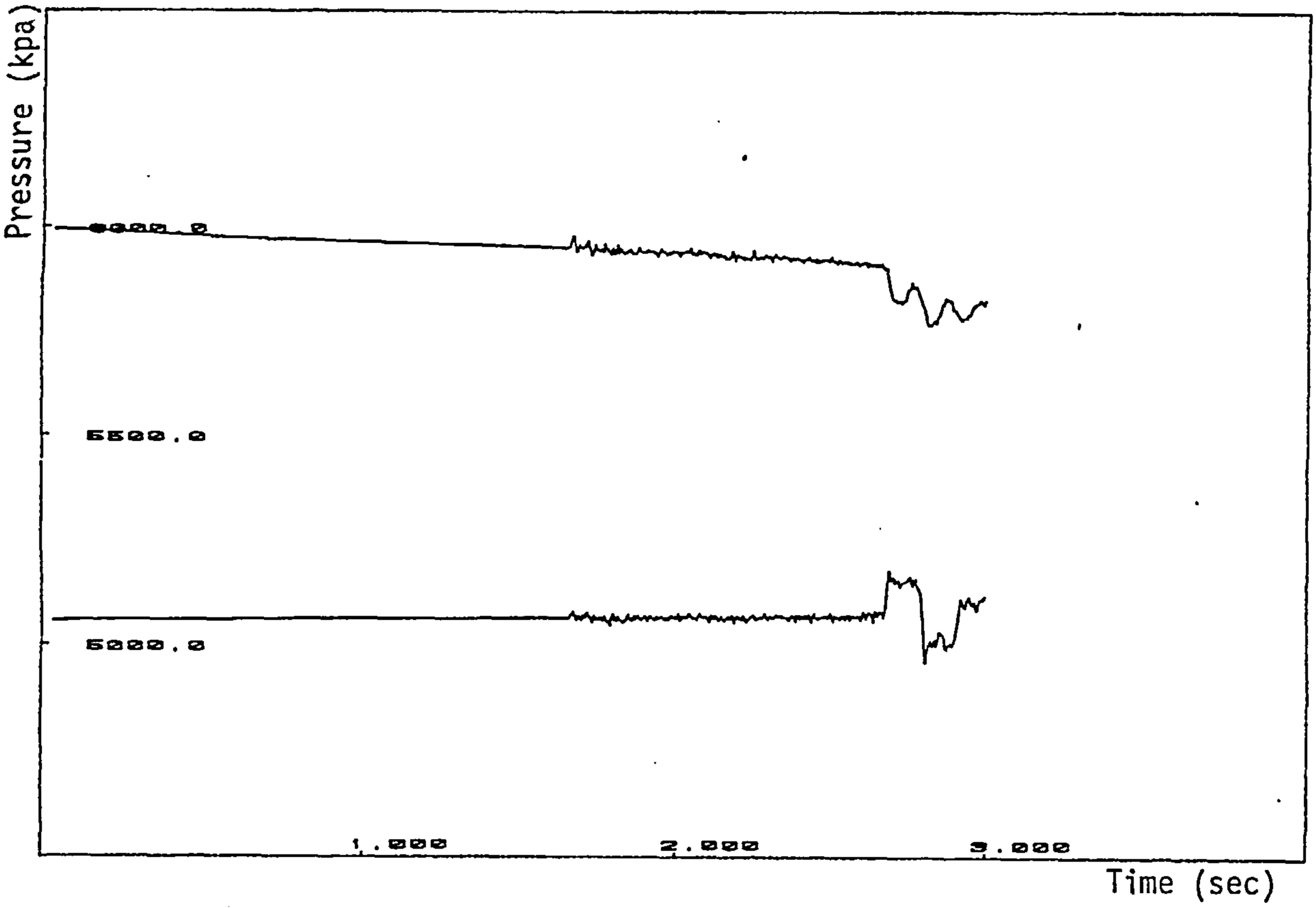

(a) Compressor Inlet and Outlet Pressure Time History

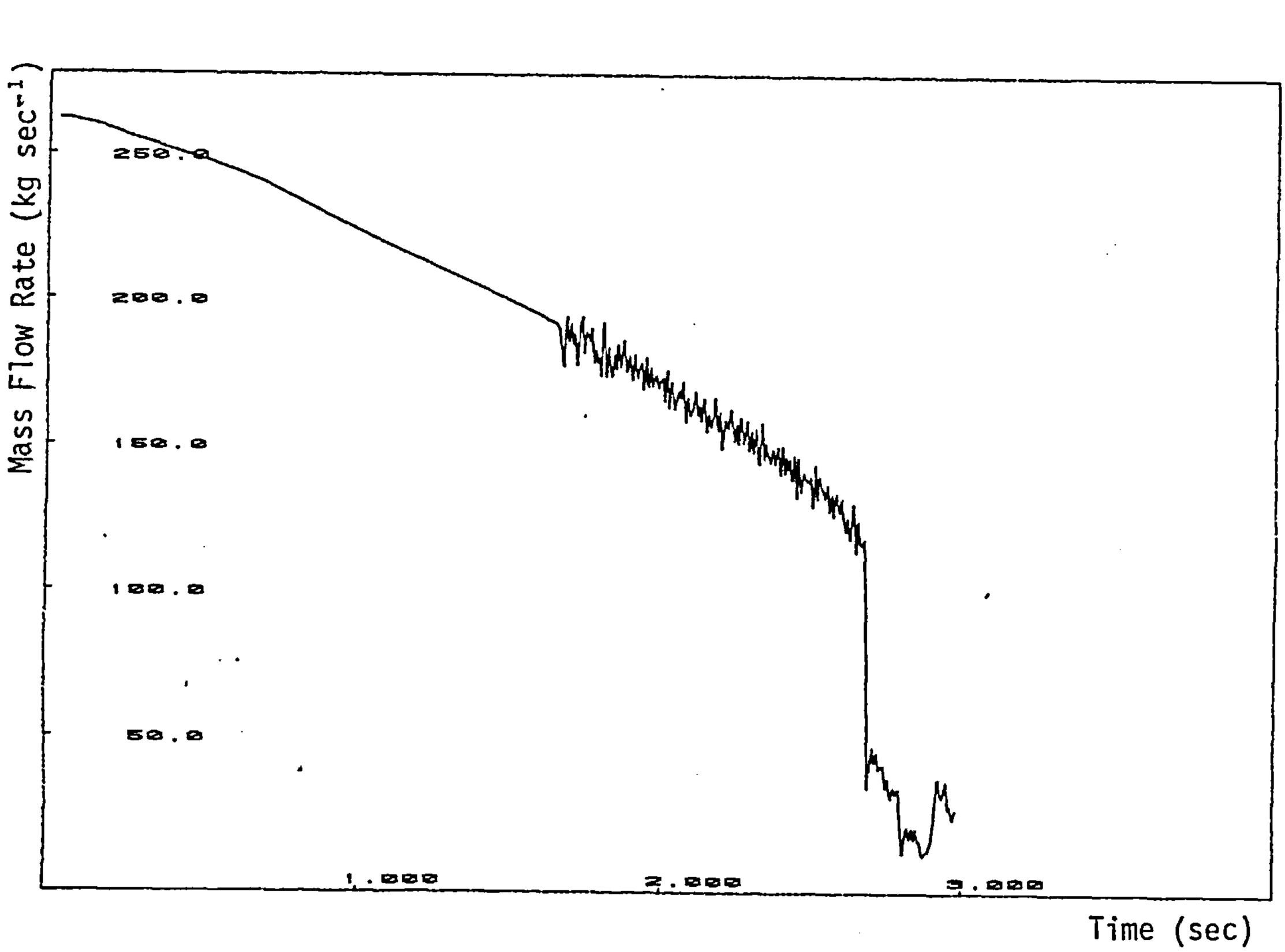

(b) Compressor Entry Mass Flow Time History

Figure 6.29 Speed and Delayed Pulse Transients

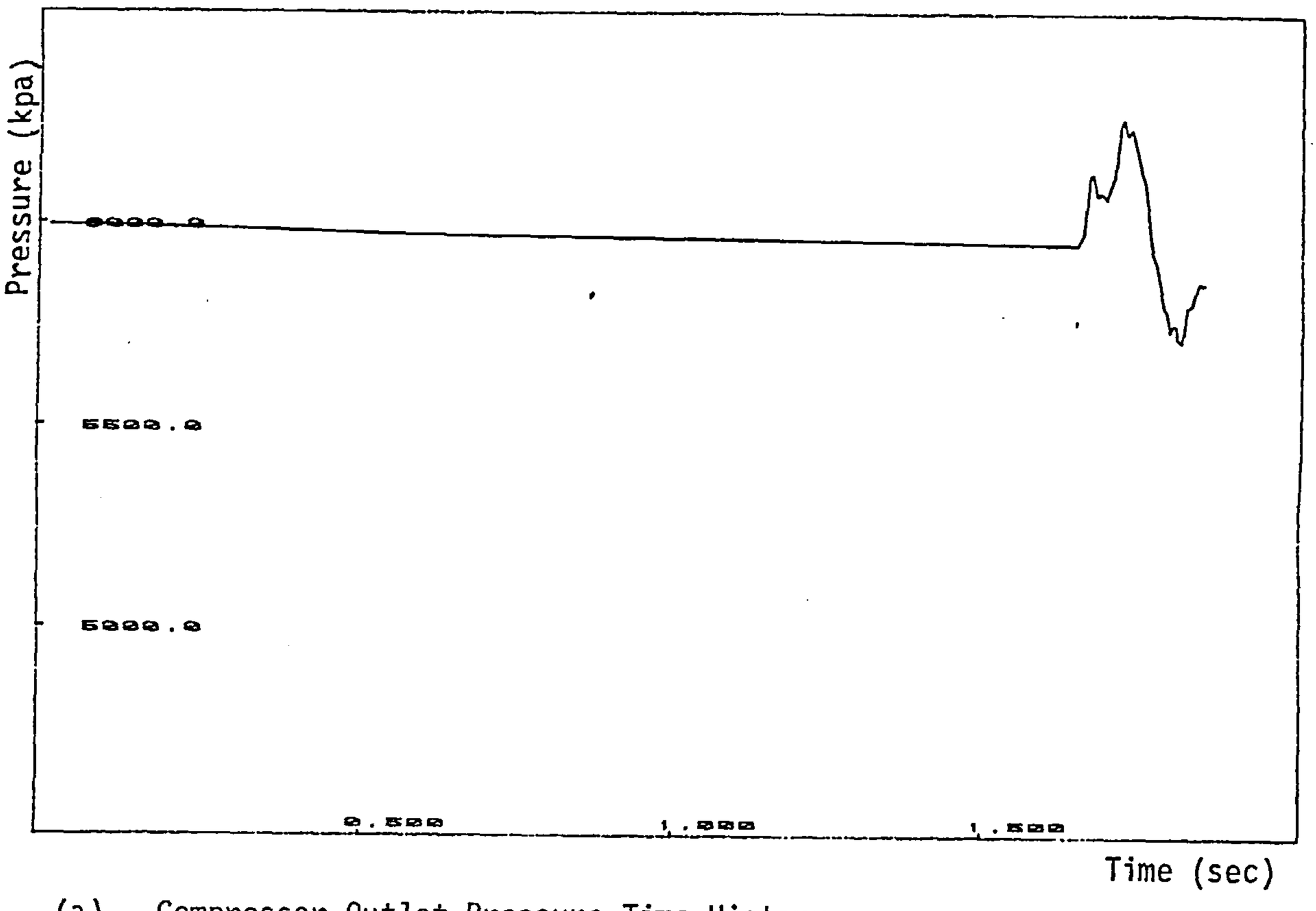

(a) Compressor Outlet Pressure Time History

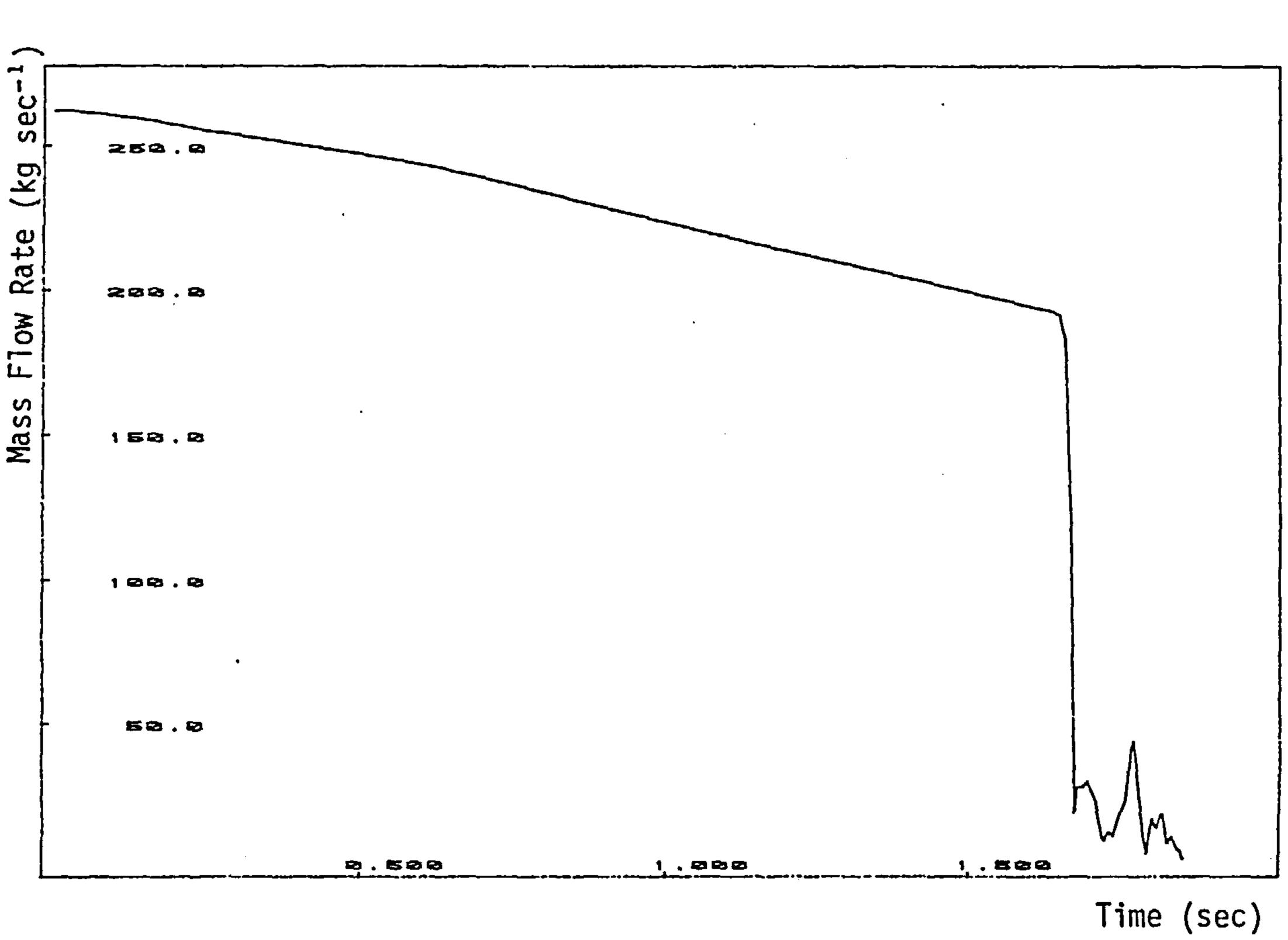

(b) Compressor Entry Mass Flow Time History

Figure 6.30 Speed and Delayed Throttling of Downstream Flow Transient

COMPRESSOR CHARACTERISTIC POLYTROPIC HEAD Vs VOLUME FLOW RATE

△SPEED = -250 R.P.M/s

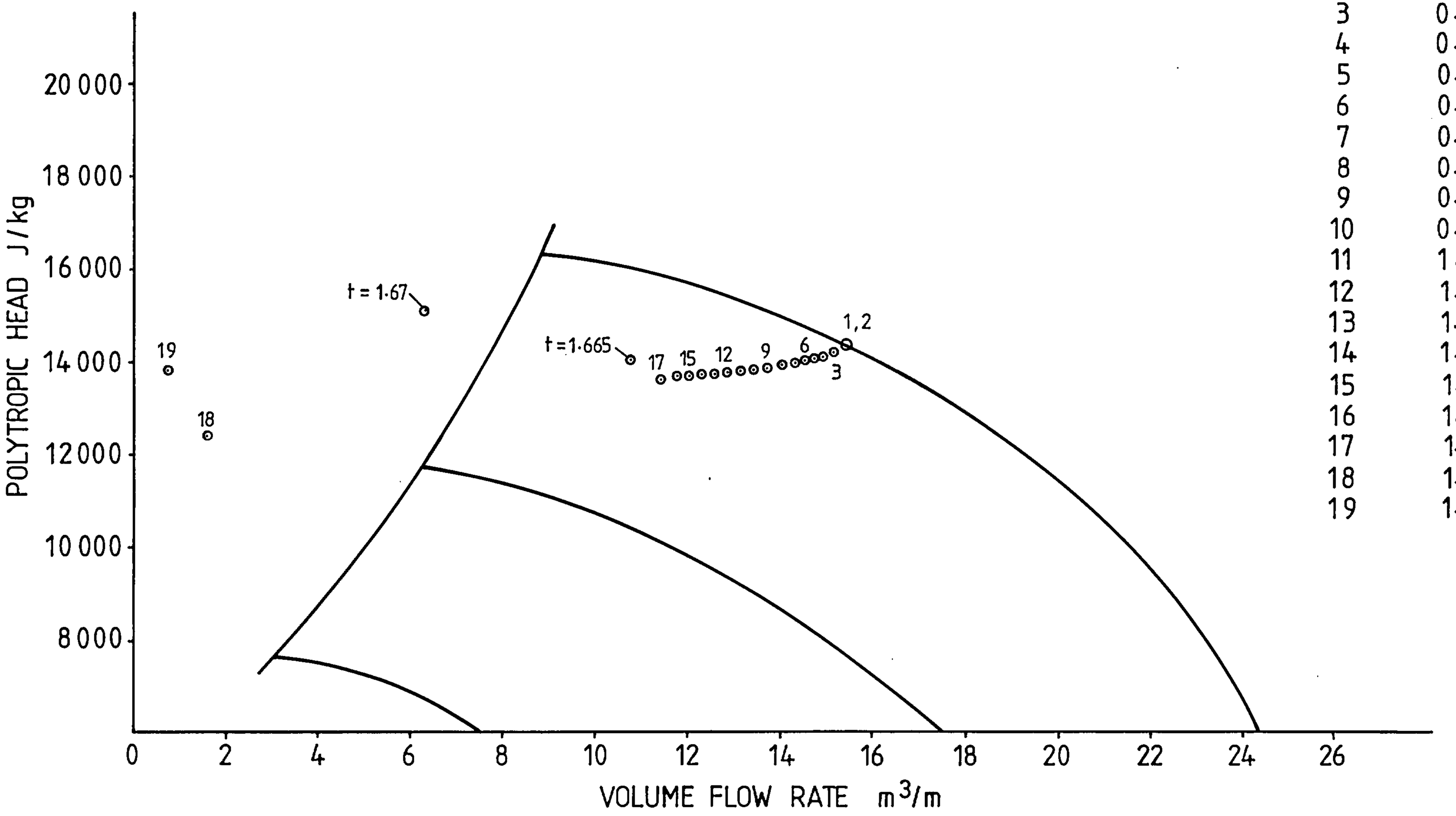

POINT	TIME (S)
1	0·0
2	0·1
3	0·2
4	0·3
5	0·4
6	0·5
7	0·6
8	0·7
9	0·8
10	0·9
11	1·0
12	1·1
13	1·2
14	1·3
15	1·4
16	1·5
17	1·6
18	1·7
19	1·8

FIG. 6·31 Speed and Delayed Pulse Transient Represented on Characteristic

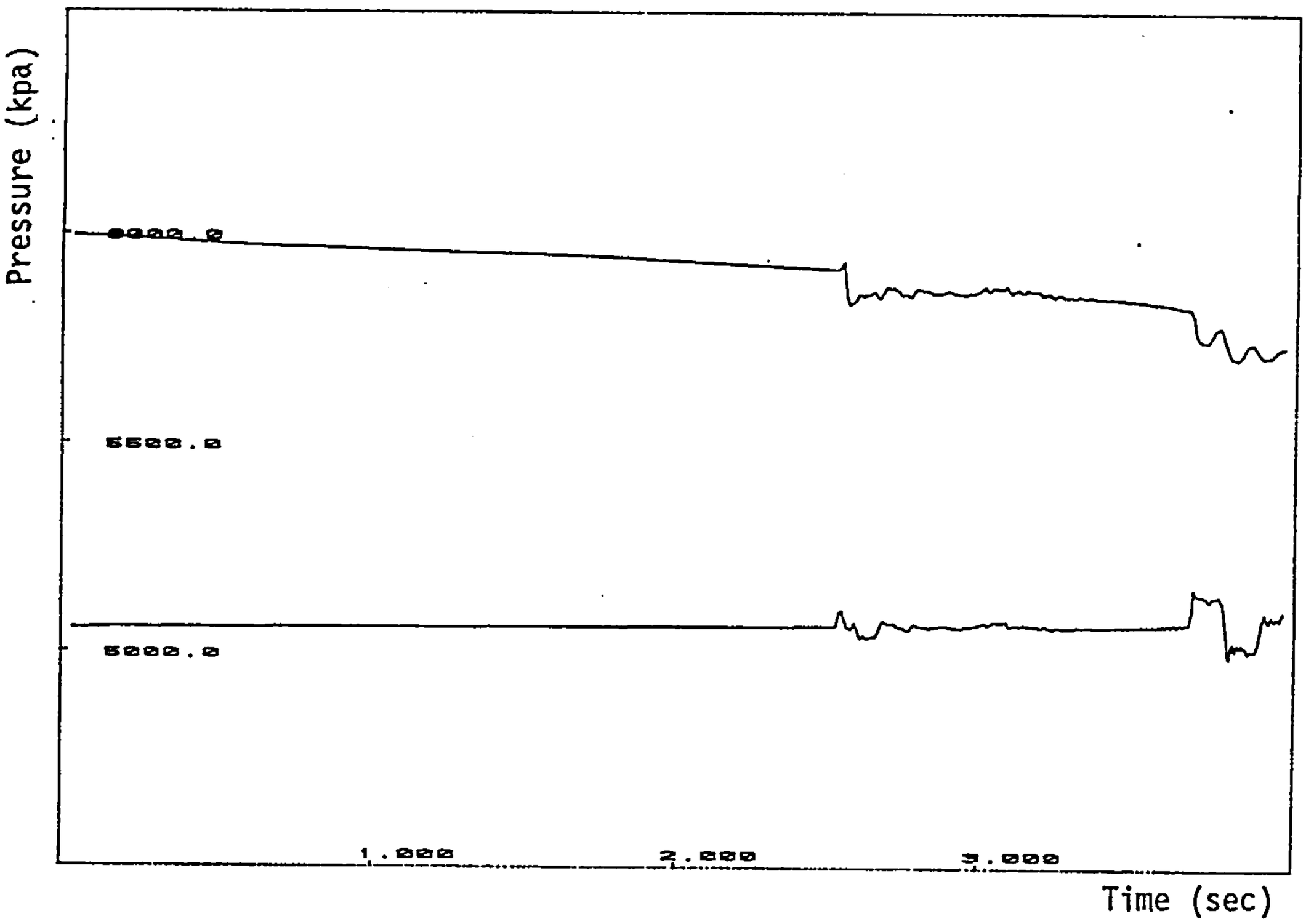

(a) Compressor Inlet and Outlet Pressure Time History

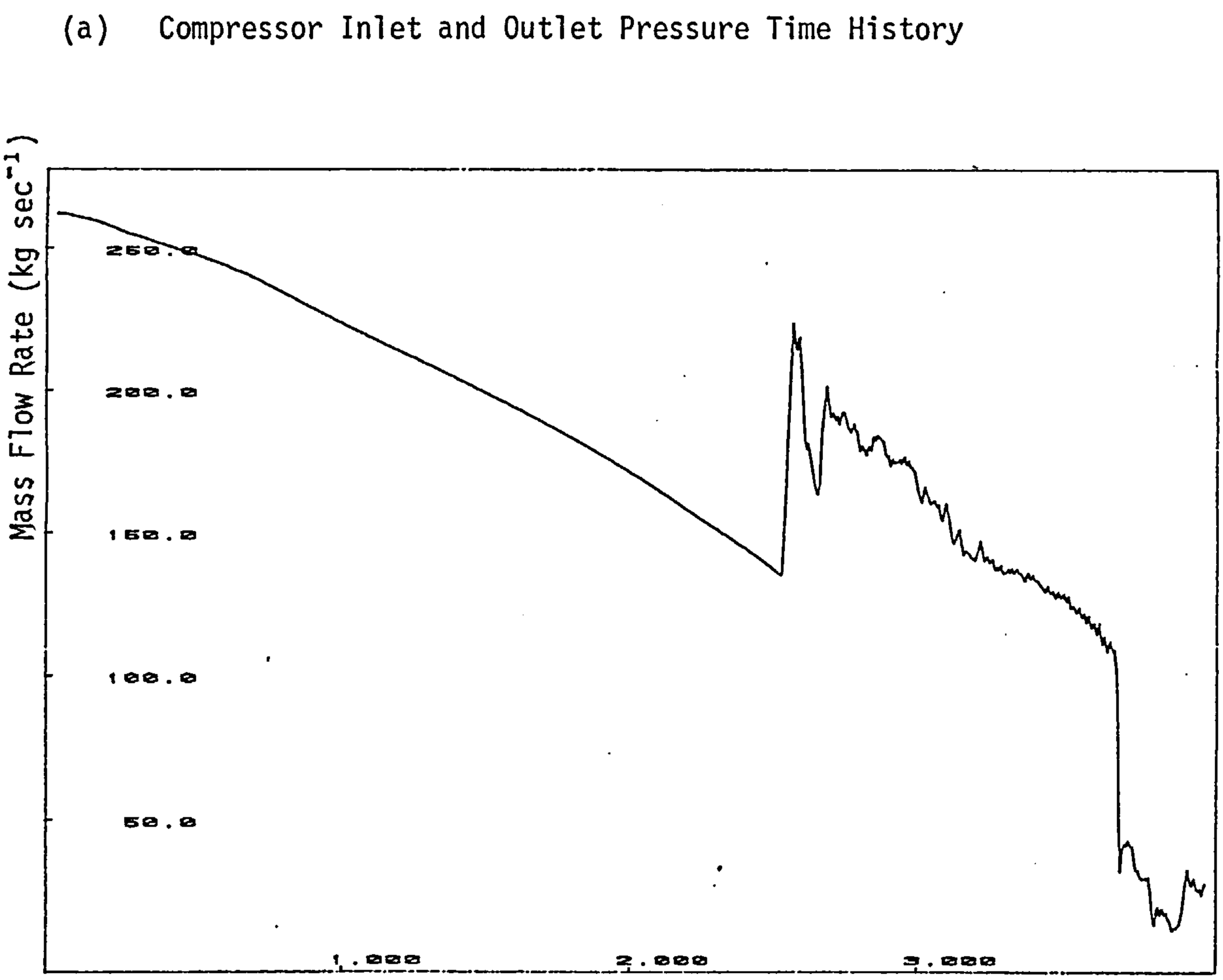

(b) Compressor Entry Mass Flow Time History

Figure 6.32 Speed and Controller Actuation of Recycle Valve. Late Opening of Recycle Valve.

COMPRESSOR CHARACTERISTIC POLYTROPIC HEAD Vs VOLUME FLOW RATE

LATE ACTION OF RECYCLE VALVE

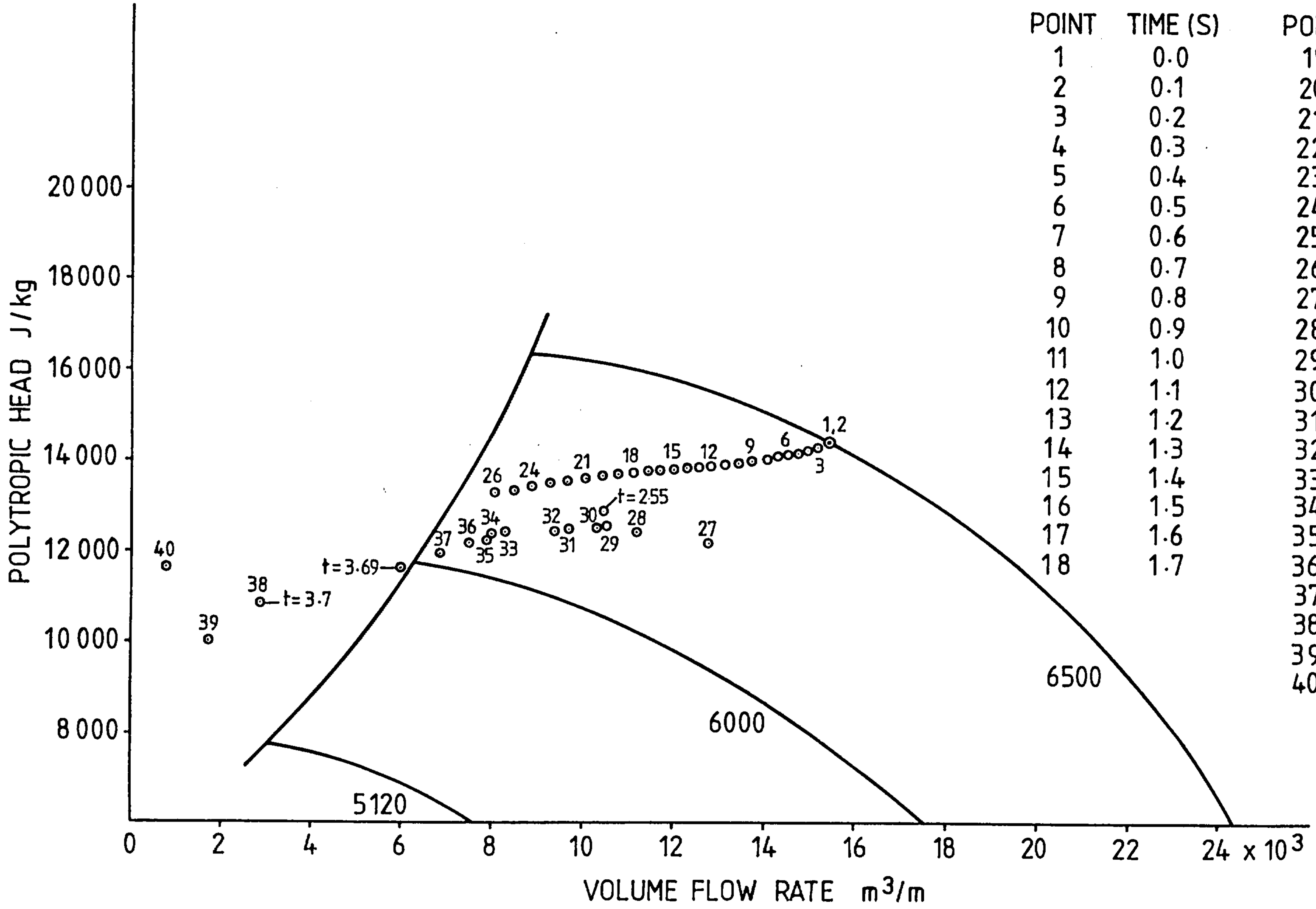

POINT	TIME (S)	POINT	TIME (S)
1	0·0	19	1·8
2	0·1	20	1·9
3	0·2	21	2·0
4	0·3	22	2·1
5	0·4	23	2·2
6	0·5	24	2·3
7	0·6	25	2·4
8	0·7	26	2·5
9	0·8	27	2·6
10	0·9	28	2·7
11	1·0	29	2·8
12	1·1	30	2·9
13	1·2	31	3·0
14	1·3	32	3·1
15	1·4	33	3·2
16	1·5	34	3·3
17	1·6	35	3·4
18	1·7	36	3·5
		37	3·6
		38	3·7
		39	3·8
		40	3·9

FIG. 6.33

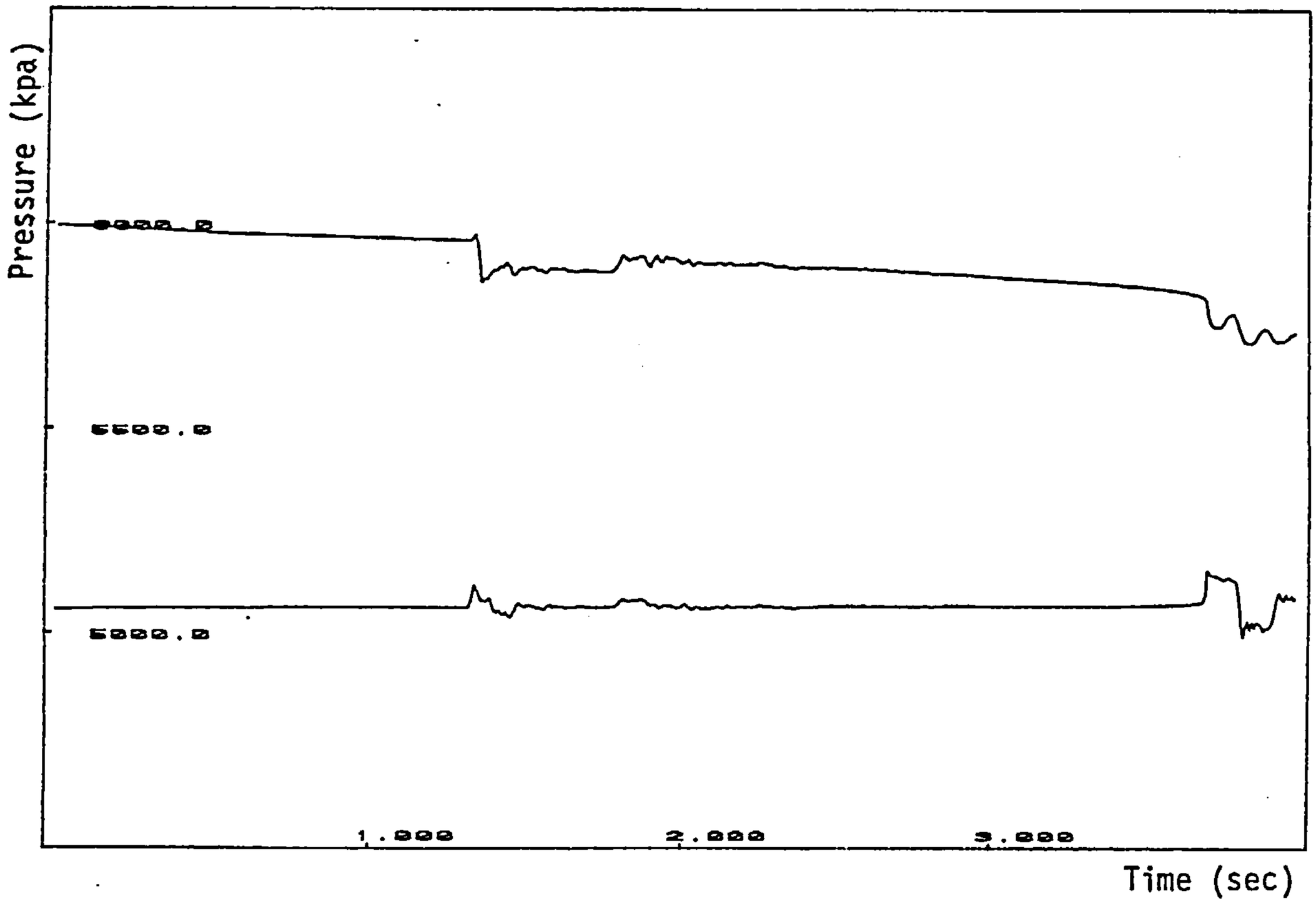

(a) Compressor Inlet and Outlet Pressure Time History

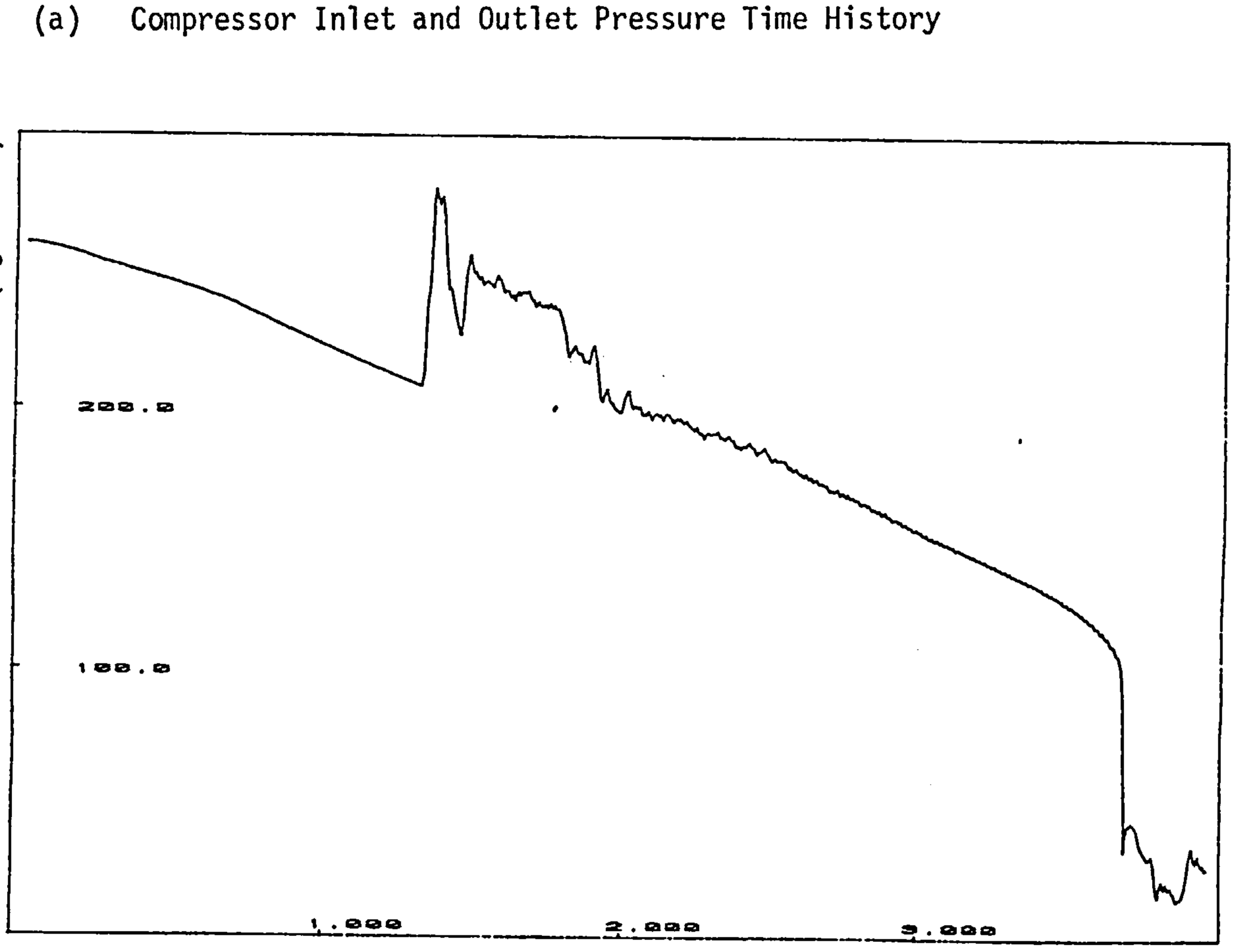

(b) Compressor Entry Mass Flow Time History

Figure 6.34 Speed and Controller Actuation of Recycle Valve. Early Opening.

COMPRESSOR CHARACTERISTIC POLYTROPIC HEAD Vs VOLUME FLOW RATE

△SPEED = -250 R.P.M/s

EARLY ACTION OF RECYCLE VALVE
BY ANTISURGE CONTROLLER

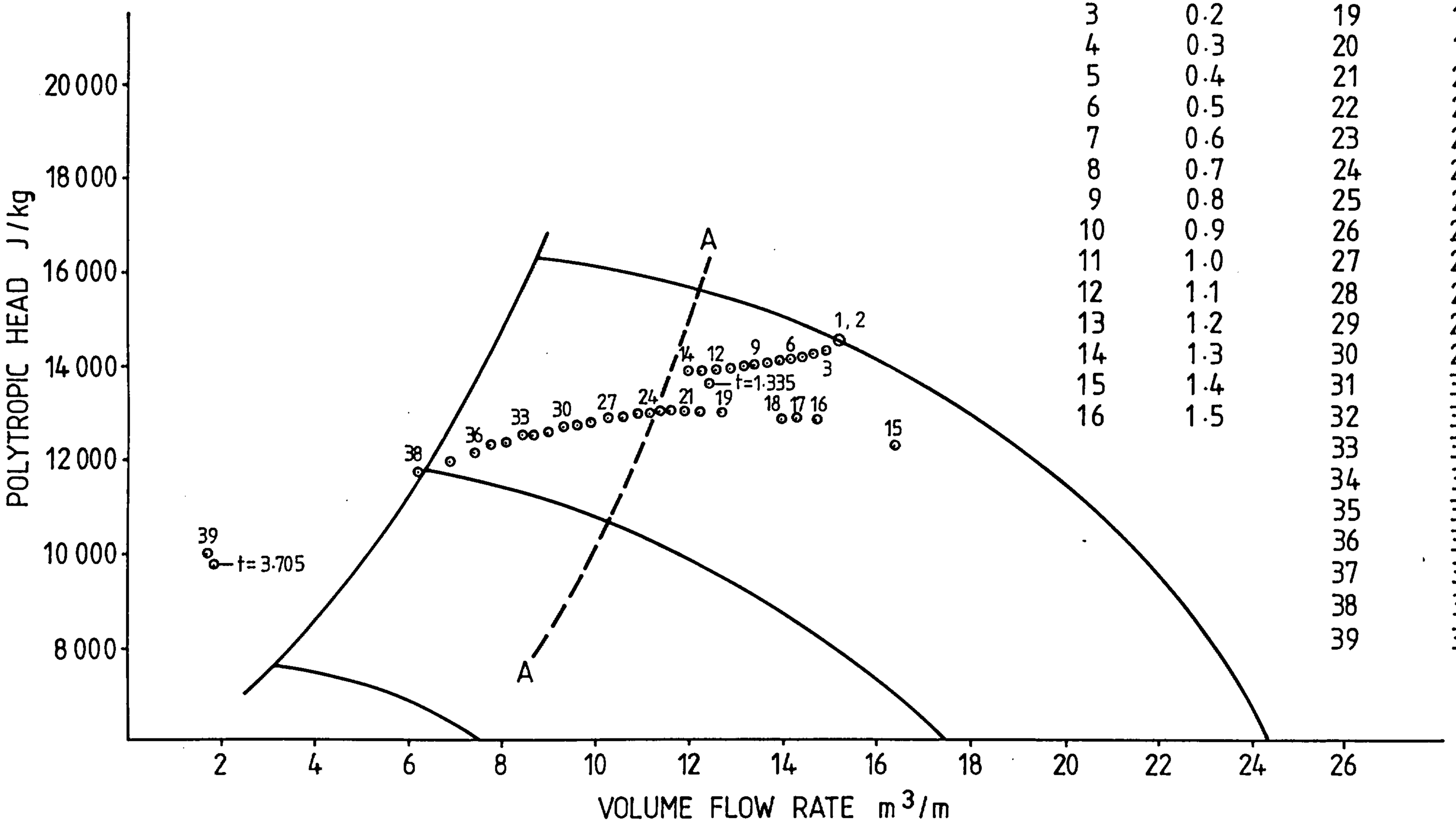

POINT	TIME (S)	POINT	TIME (S)
1	0·0	17	1·6
2	0·1	18	1·7
3	0·2	19	1·8
4	0·3	20	1·9
5	0·4	21	2·0
6	0·5	22	2·1
7	0·6	23	2·2
8	0·7	24	2·3
9	0·8	25	2·4
10	0·9	26	2·5
11	1·0	27	2·6
12	1·1	28	2·7
13	1·2	29	2·8
14	1·3	30	2·9
15	1·4	31	3·0
16	1·5	32	3·1
		33	3·2
		34	3·3
		35	3·4
		36	3·5
		37	3·6
		38	3·7
		39	3·8

FIG. 6·35

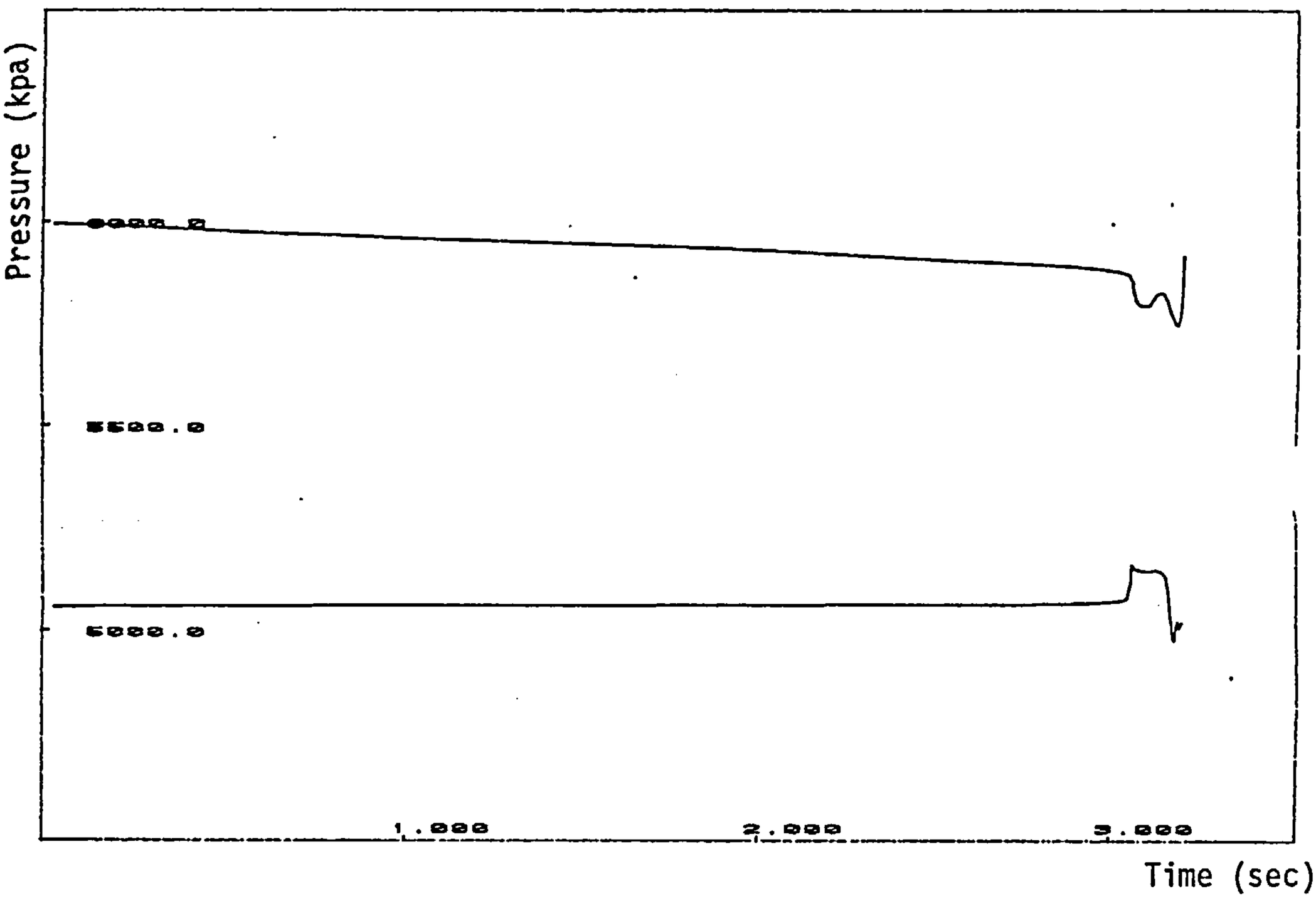

(a) Compressor Inlet and Outlet Pressure Time History

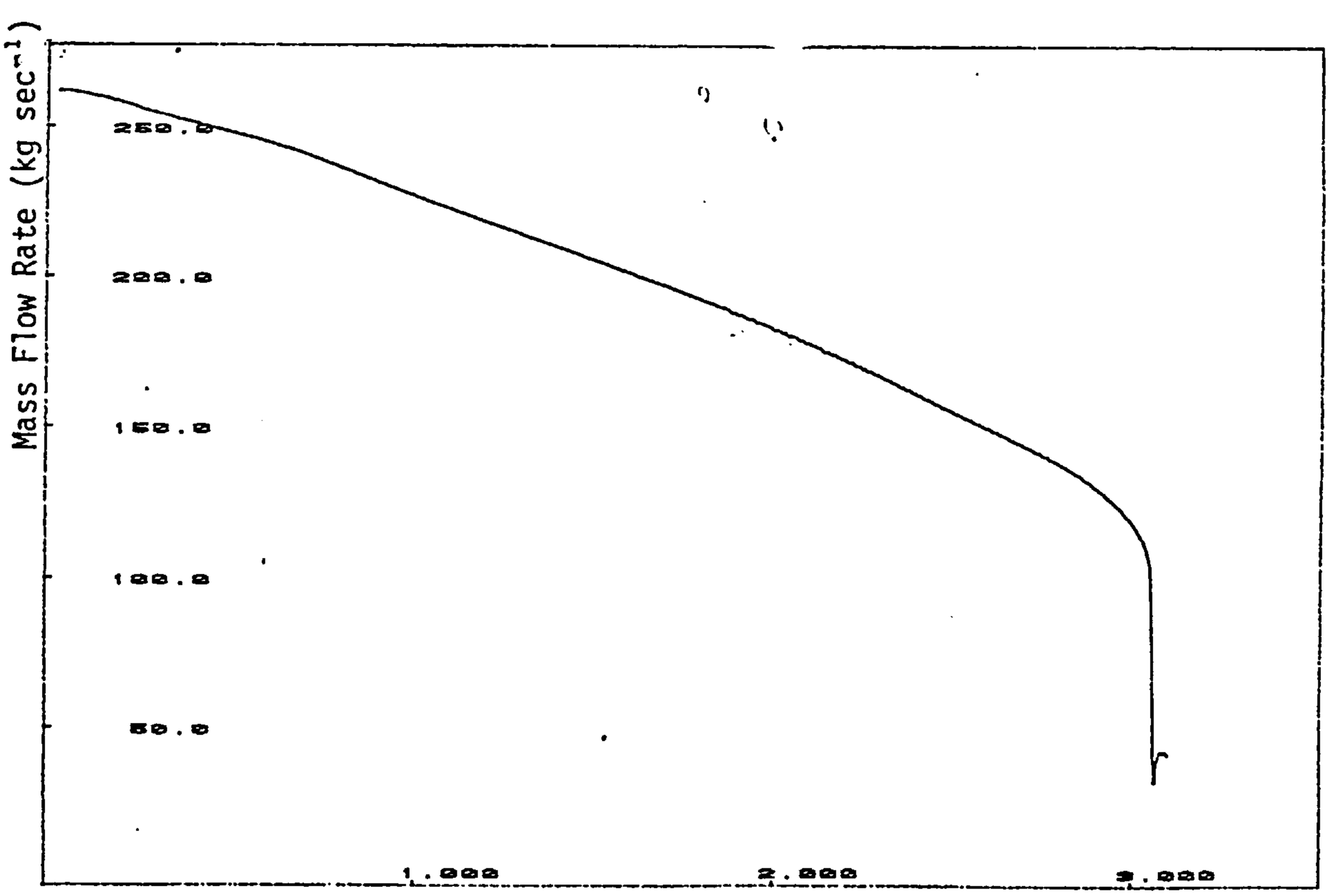

(b) Compressor Entry Mass Flow Time History

Figure 6.36 Speed Transient with both Downstream Discharge Line Non-Return Valves in Place.

COMPRESSOR CHARACTERISTIC POLYTROPIC HEAD Vs VOLUME FLOW RATE

△SPEED = - 250 R.P.M/s

WITH NRV VALUES DOWN STREAM

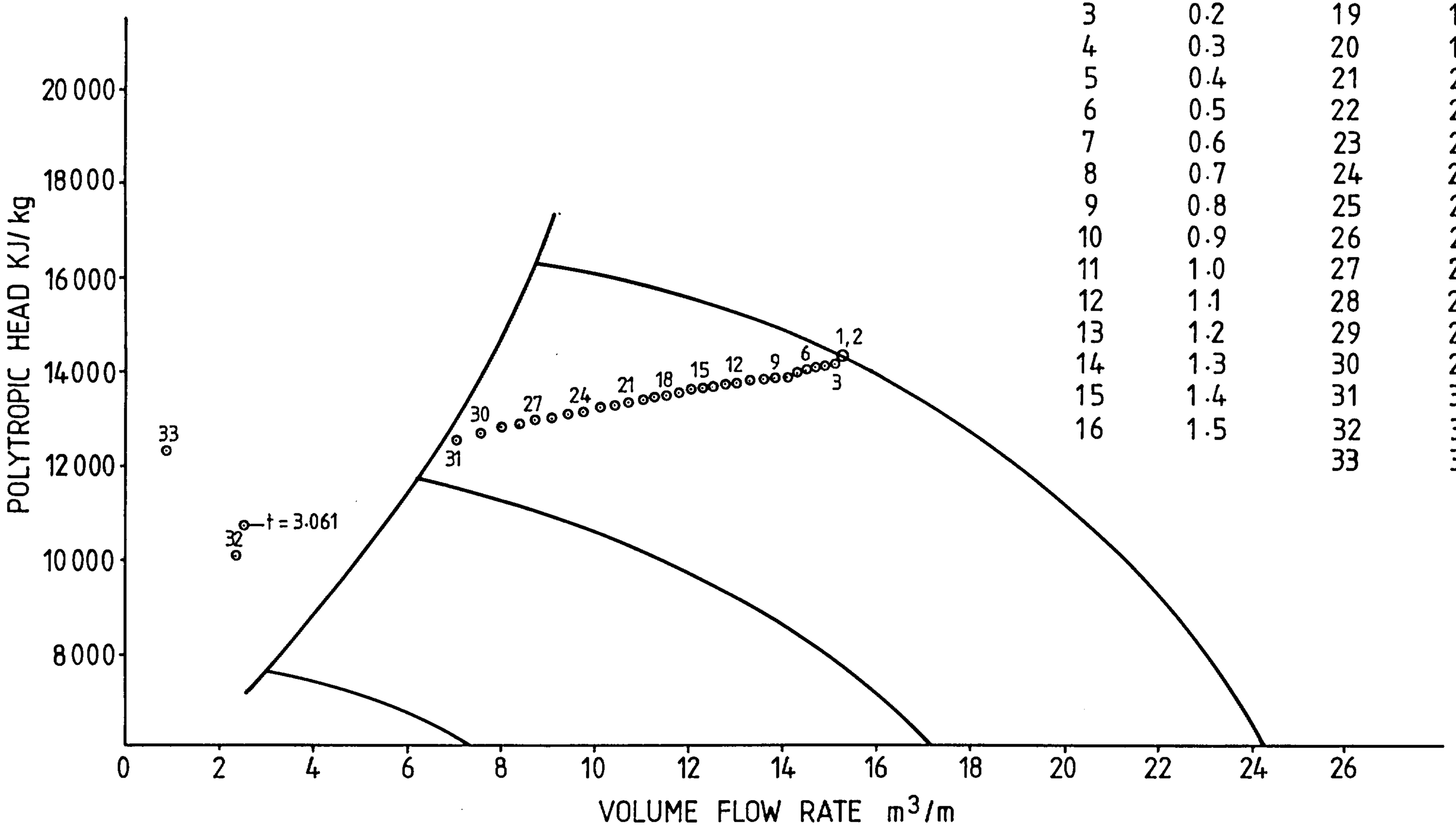

POINT	TIME (S)	POINT	TIME (S)
1	0·0	17	1·6
2	0·1	18	1·7
3	0·2	19	1·8
4	0·3	20	1·9
5	0·4	21	2·0
6	0·5	22	2·1
7	0·6	23	2·2
8	0·7	24	2·3
9	0·8	25	2·4
10	0·9	26	2·5
11	1·0	27	2·6
12	1·1	28	2·7
13	1·2	29	2·8
14	1·3	30	2·9
15	1·4	31	3·0
16	1·5	32	3·1
		33	3·2

FIG. 6·37

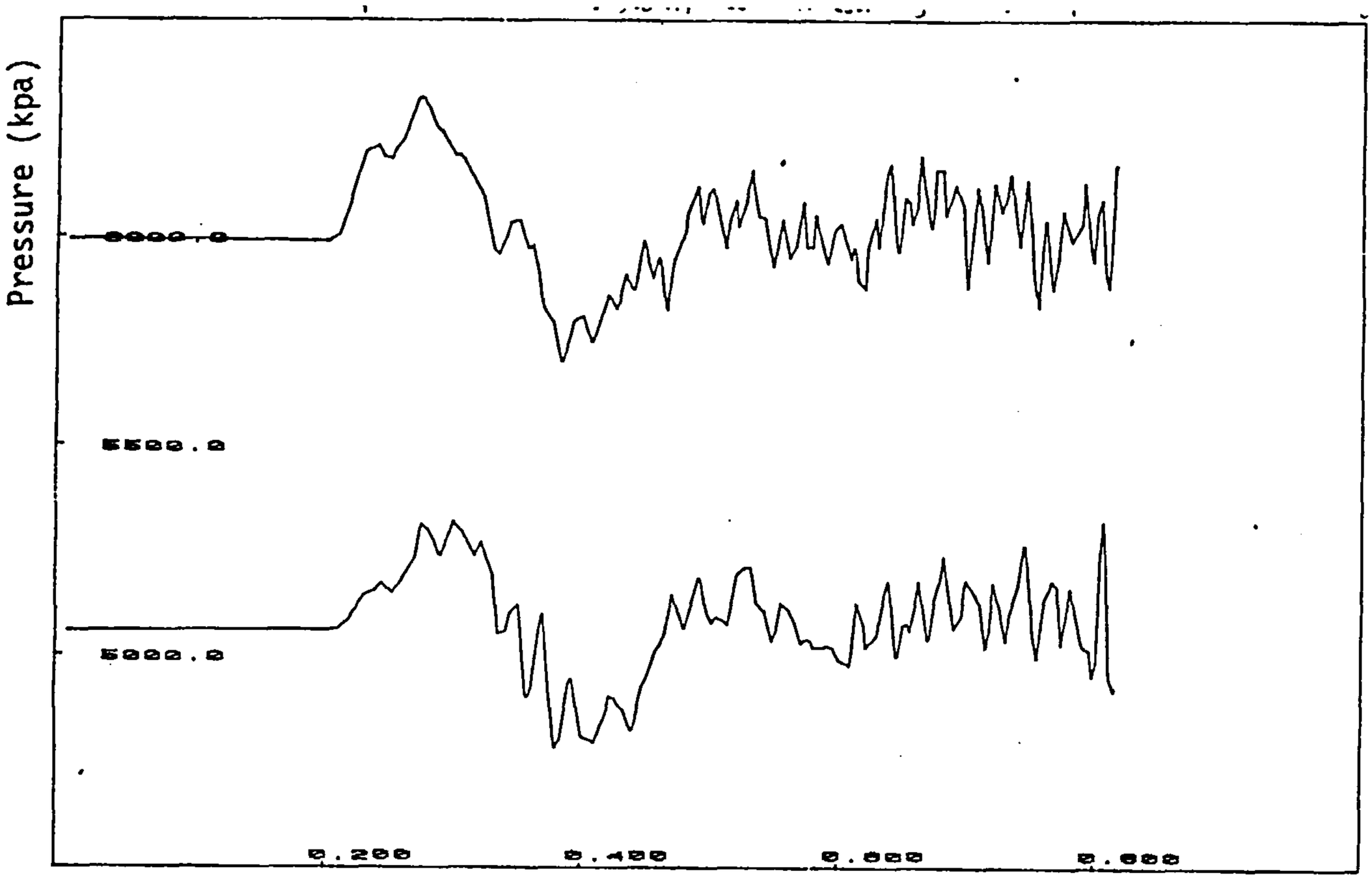

(a) Compressor Inlet and Outlet Pressure Time History

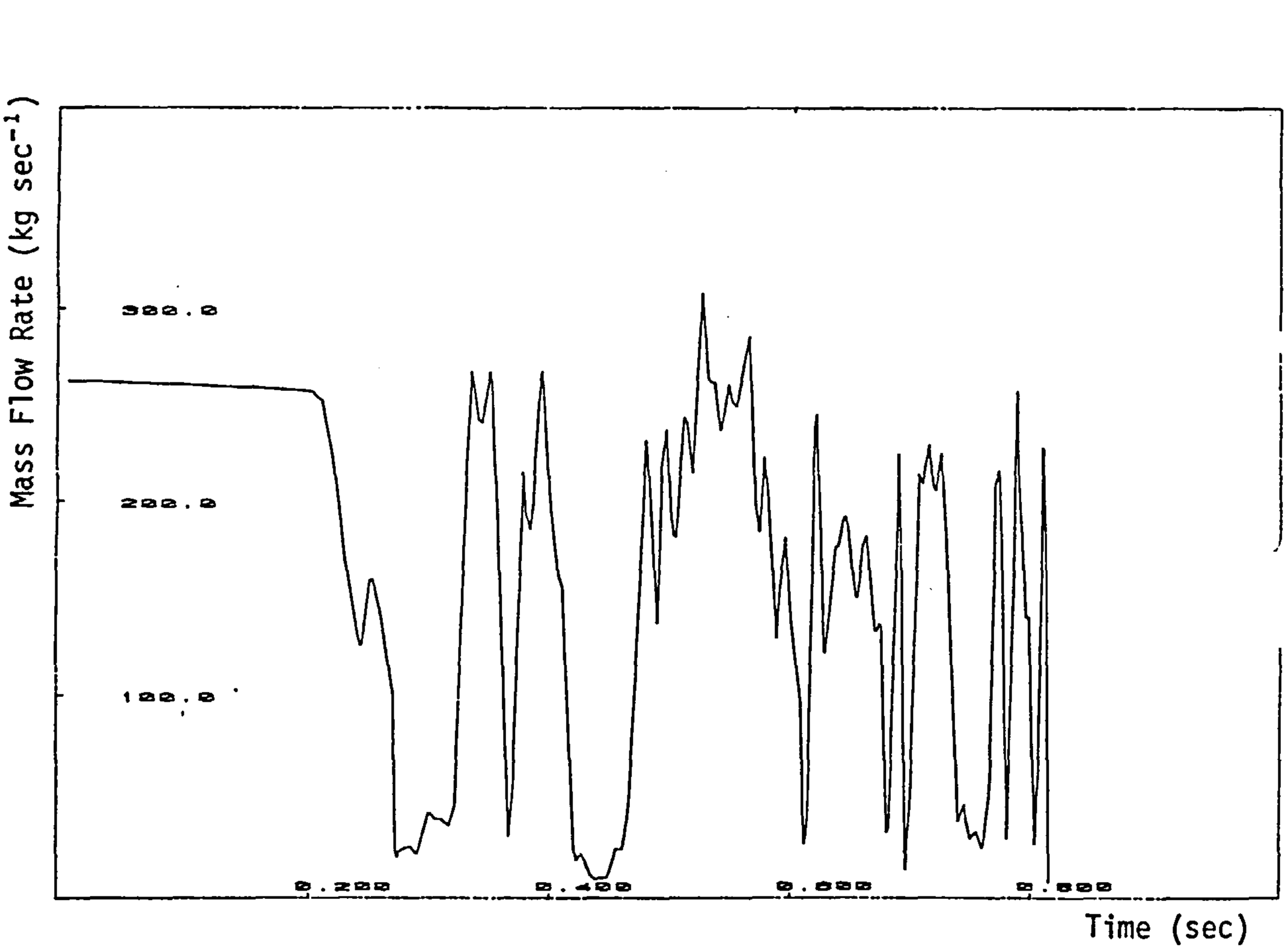

(b) Compressor Entry Mass Flow Time History

Figure 6.38 Speed Transient and Pressure Transient. The Pressure Transient causes the last non-return valve in the discharge line to close.

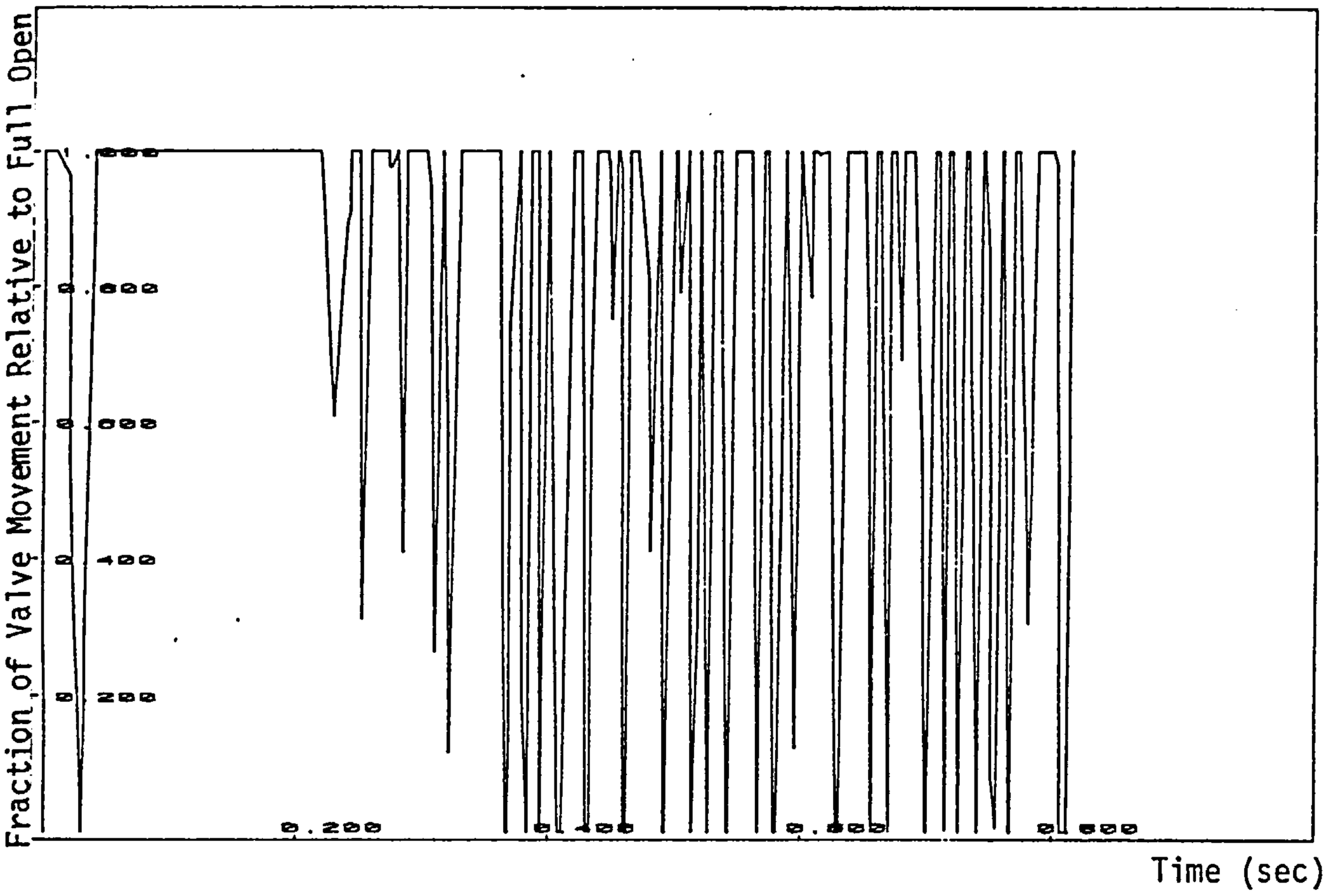

Figure 6.39a Non-Return Valve (1) Movement due to Pressure and Speed Transient

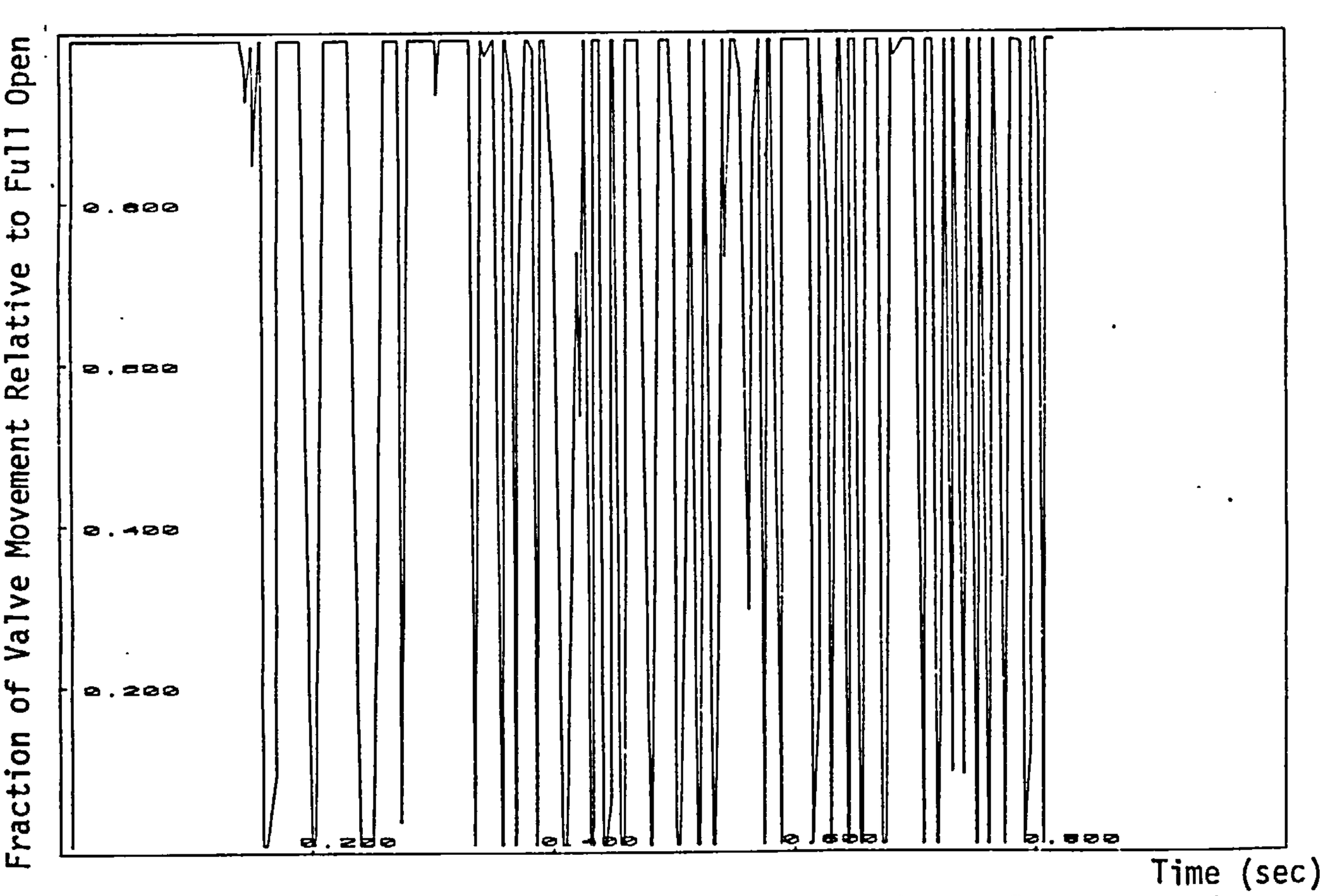

Figure 6.39b Non-Return Valve (2) Movement due to Pressure and Speed Transient

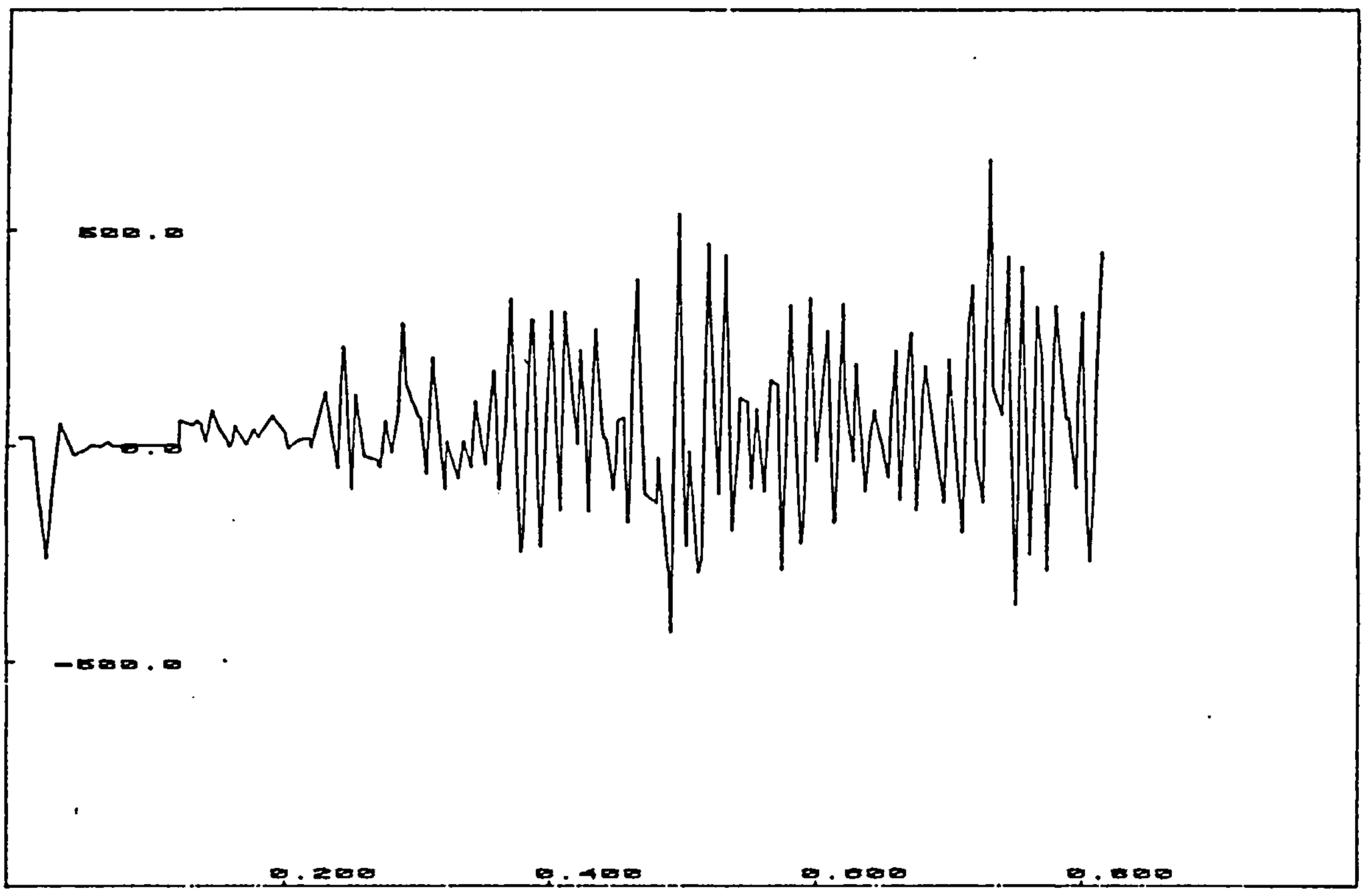

Figure 6.40a Non-Return Valve (1) Pressure Difference Time History due to Speed and Pressure Transient

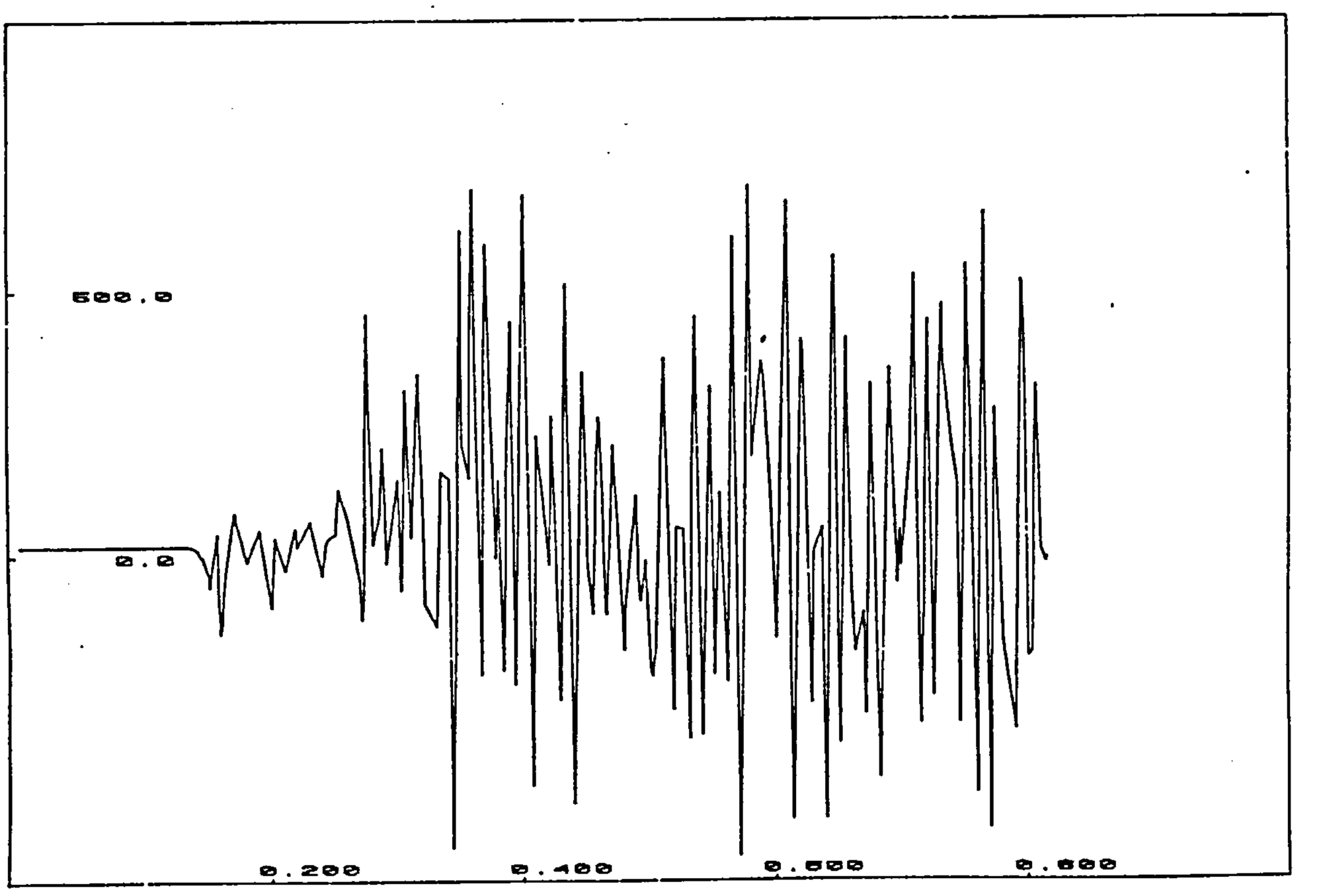

Figure 6.40b Non-Return Valve (2) Pressure Difference Time History due to Speed and Pressure Transient

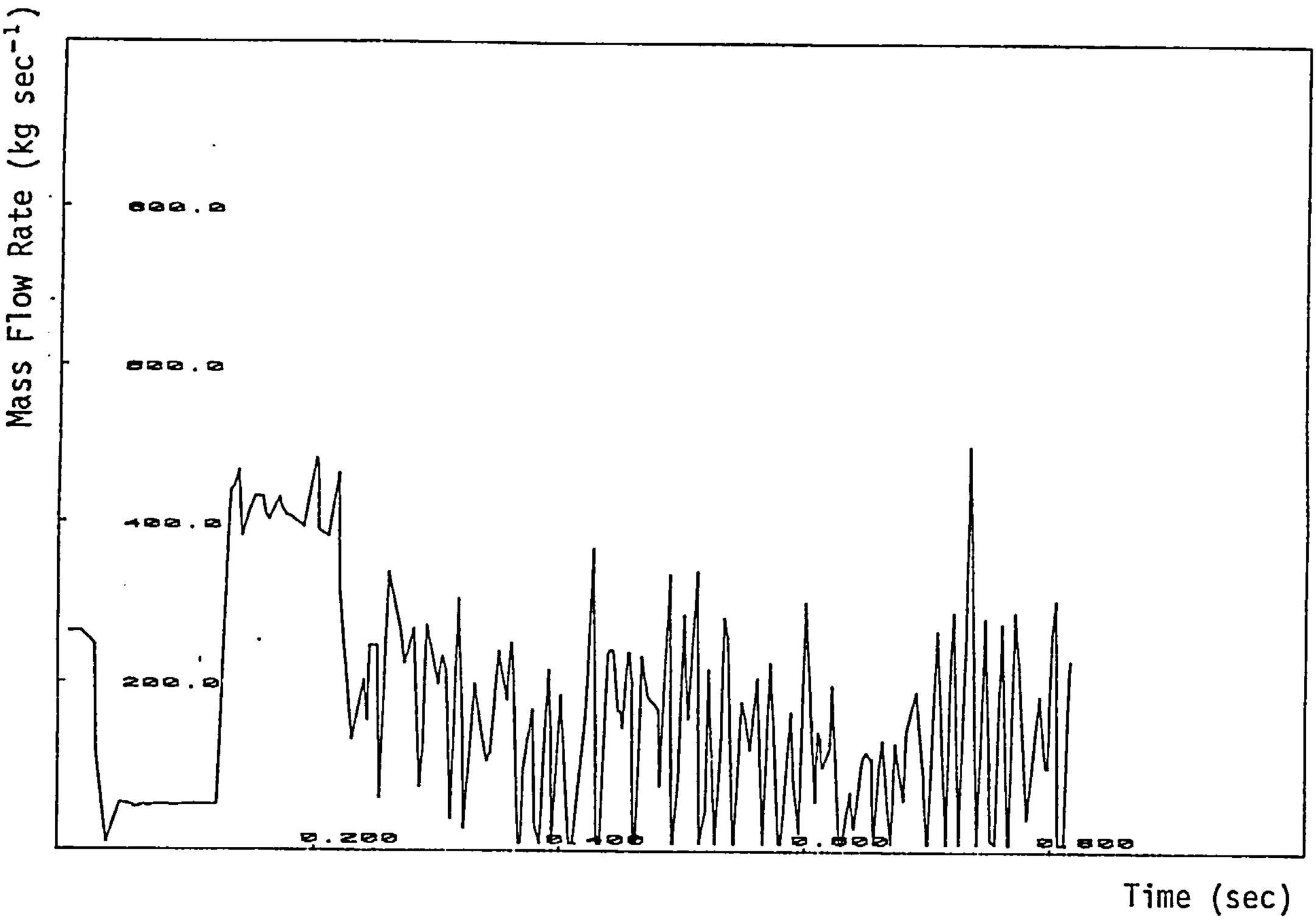

Figure 6.41a Mass Flow Rate Through Non-Return Valve (1) Time History due to Speed and Pressure Transient

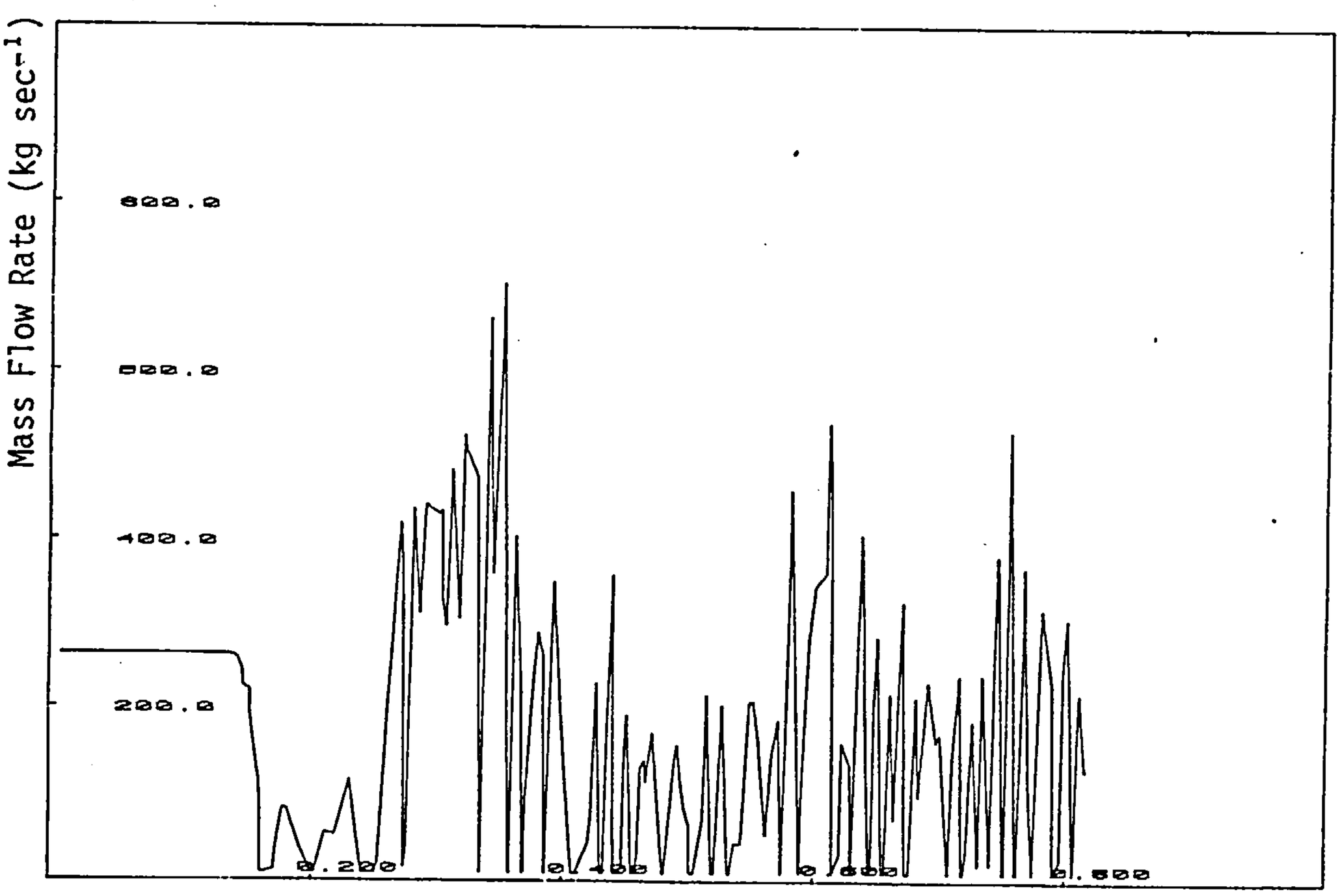

Figure 6.41b Mass Flow Rate Through Non-Return Valve (2) Time History due to Speed and Pressure Transient

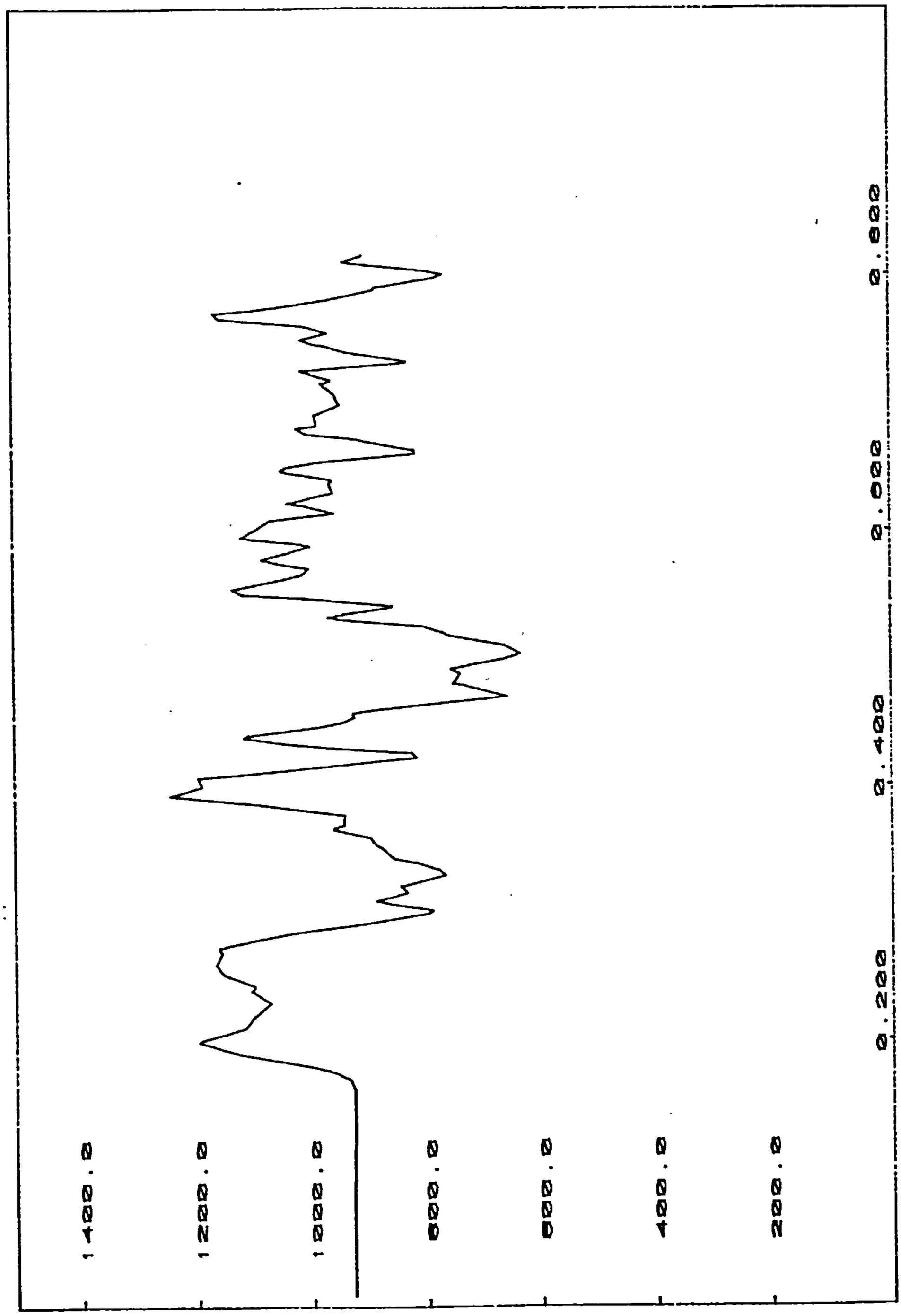

Figure 6.42 Non-

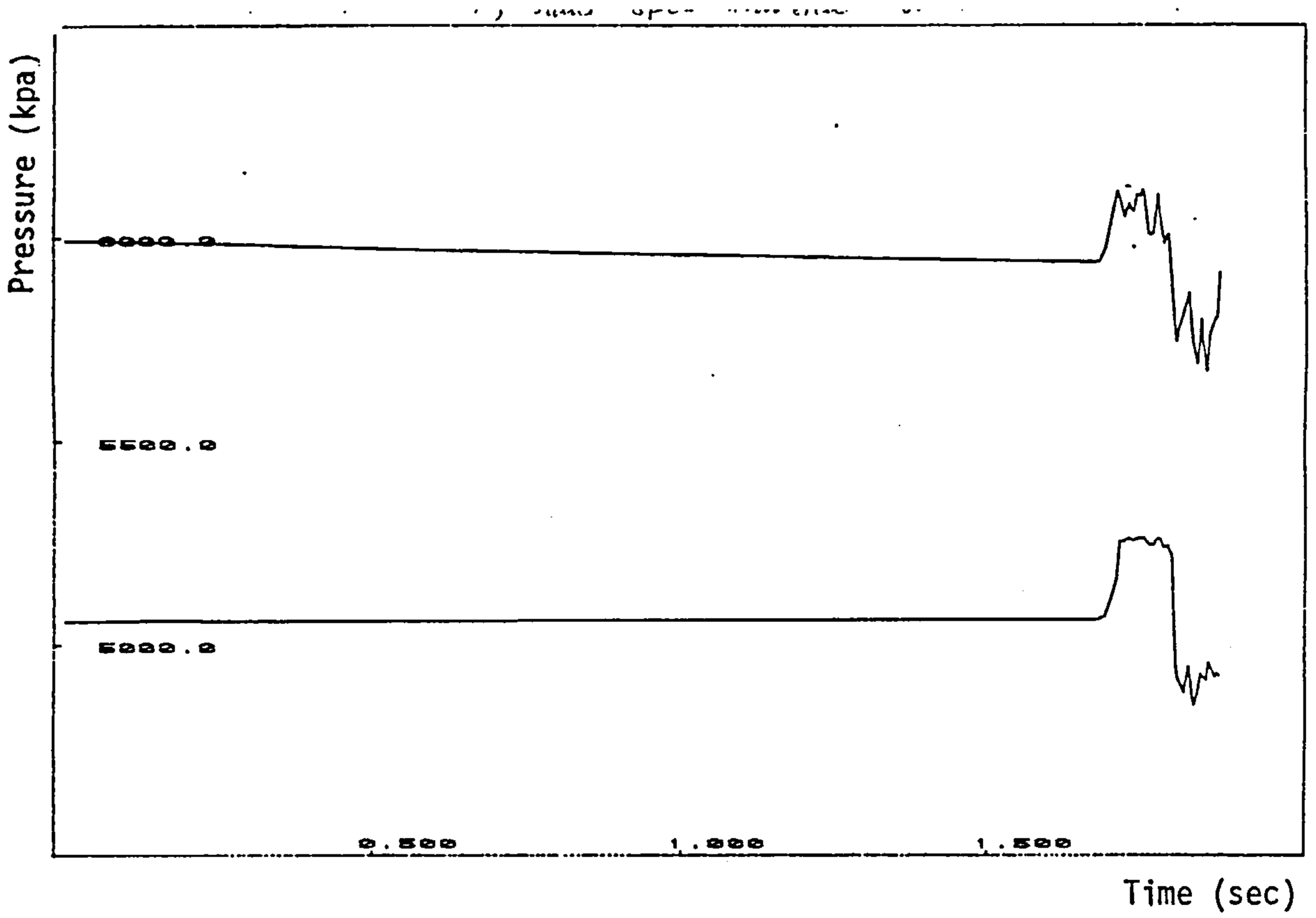

(a) Compressor Inlet and Outlet Pressure Time History

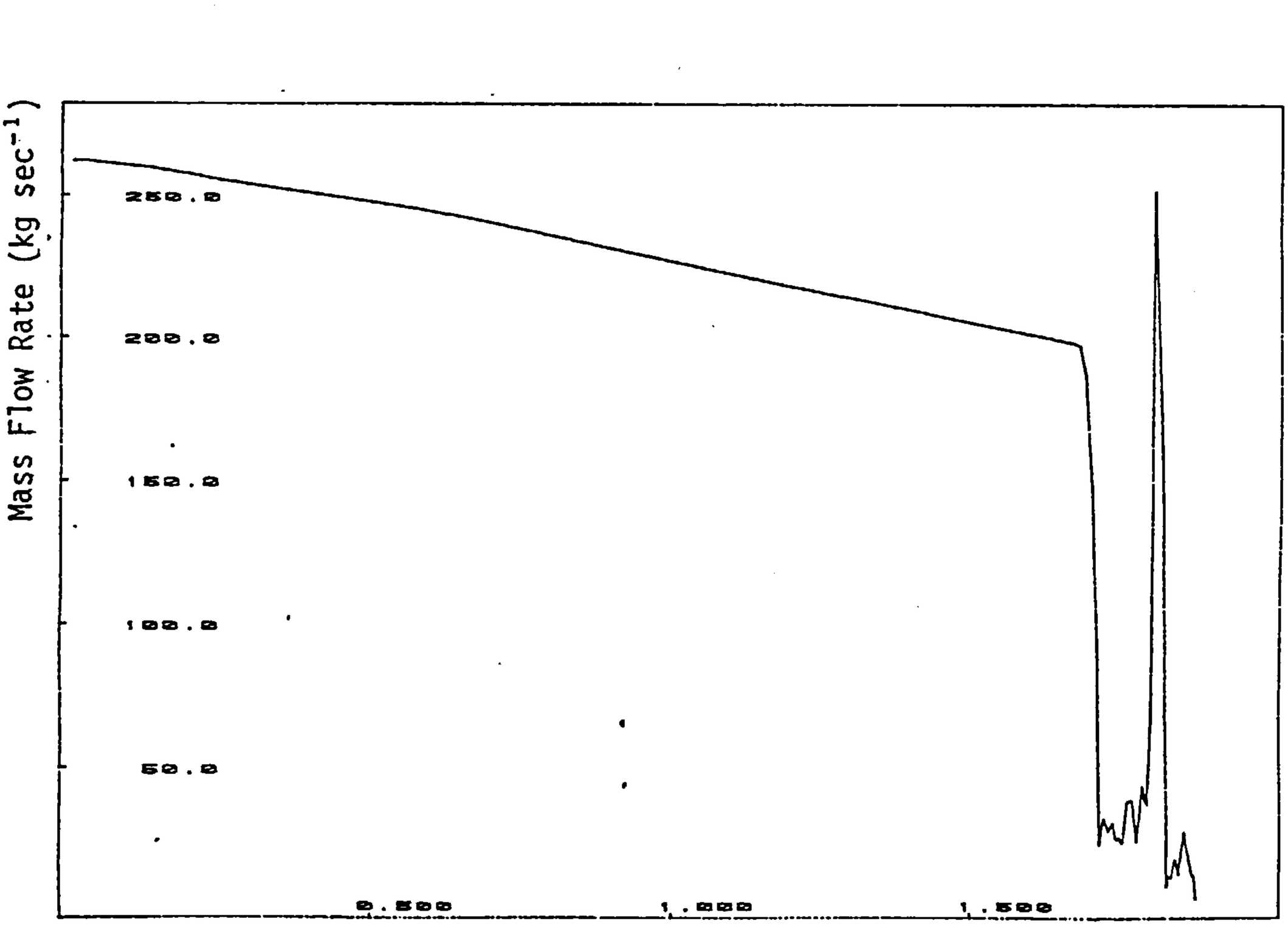

(b) Compressor Entry Mass Flow Time History

Figure 6.43 Speed and Delayed Pressure Transient. The Delayed Pressure Transient Closes Non-Return Valve (1).

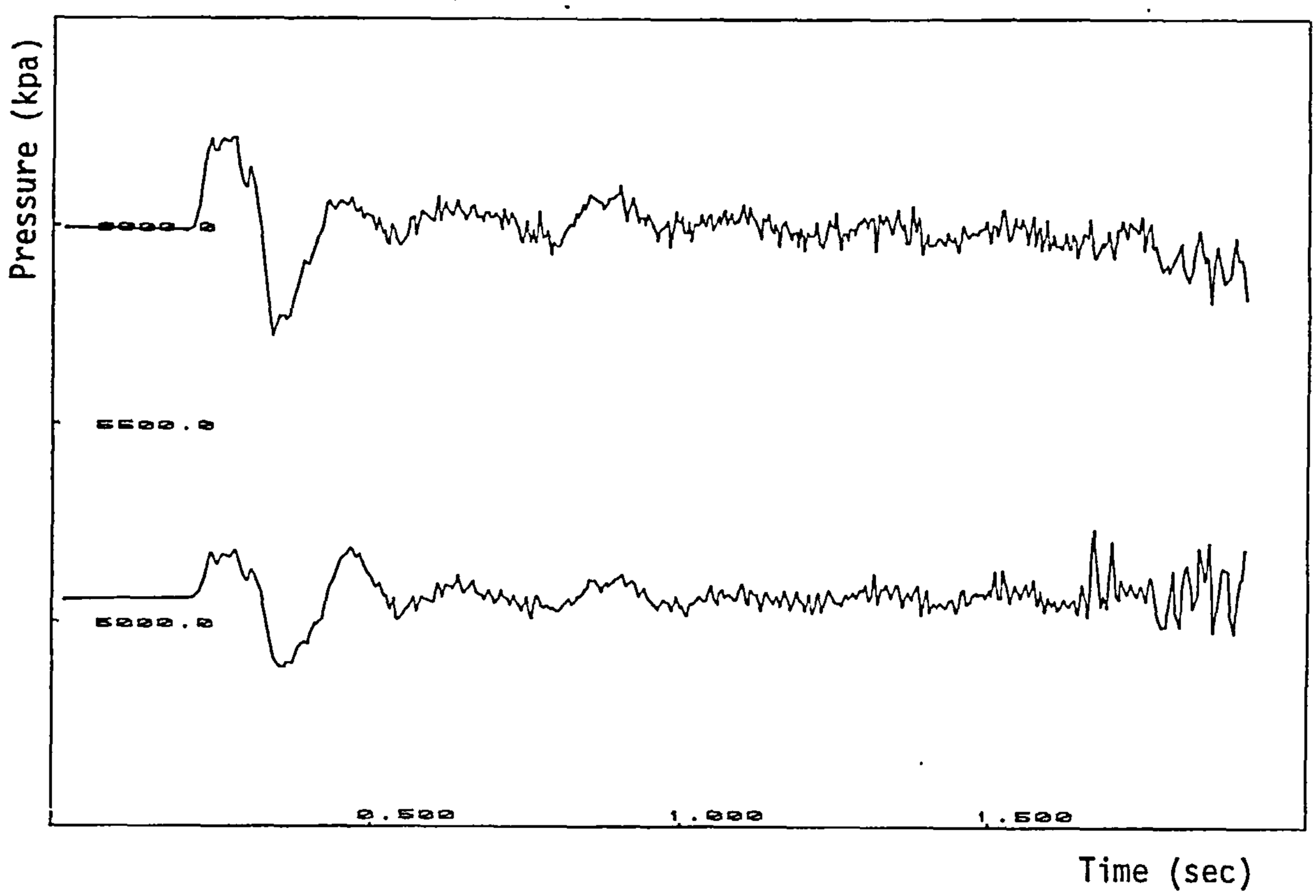

(a) Compressor Inlet and Outlet Pressure Time History

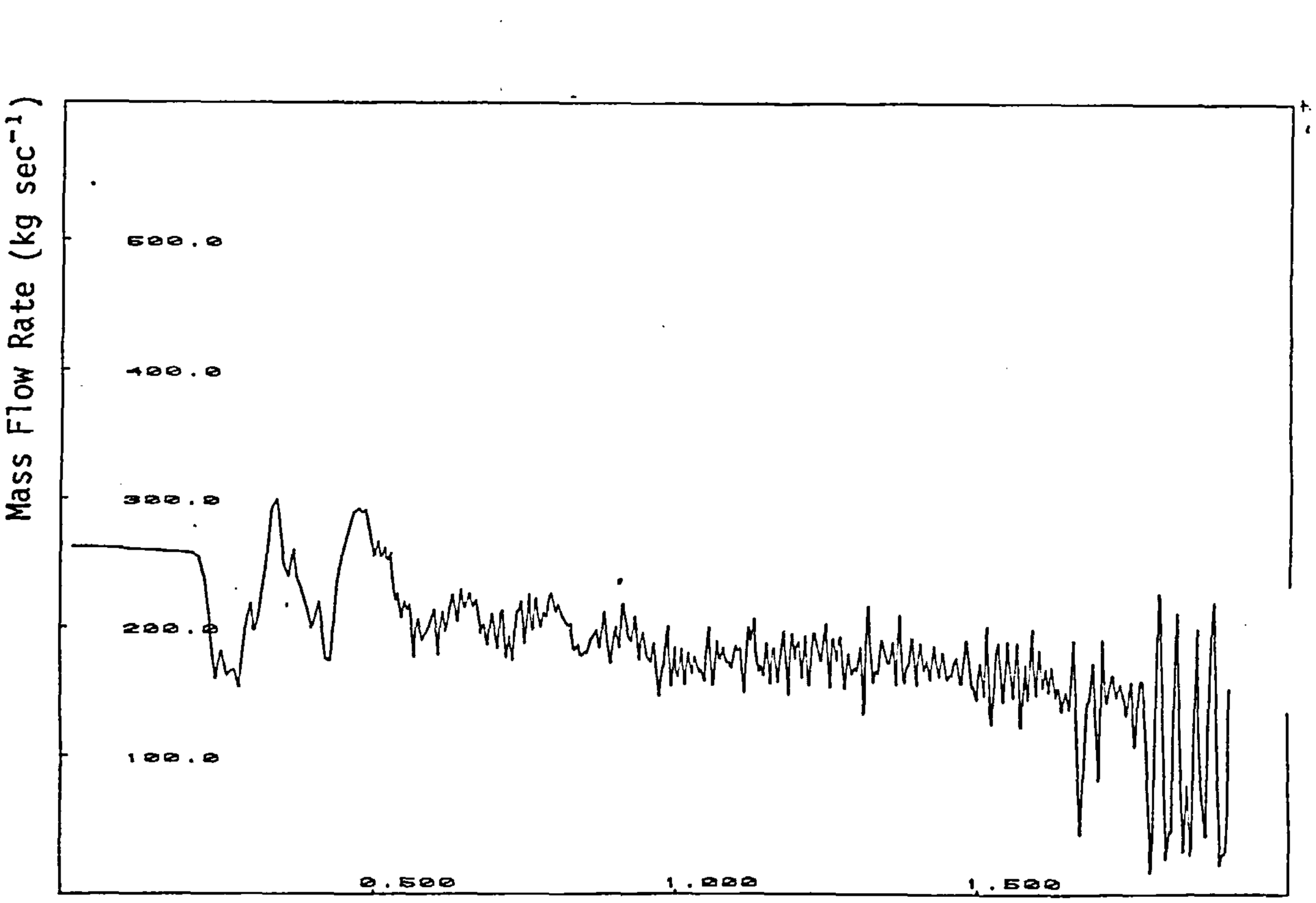

(b) Compressor Entry Mass Flow Time History

Figure 6.44 Speed and Pressure Transient with Non-Return Valves (2) and (3).

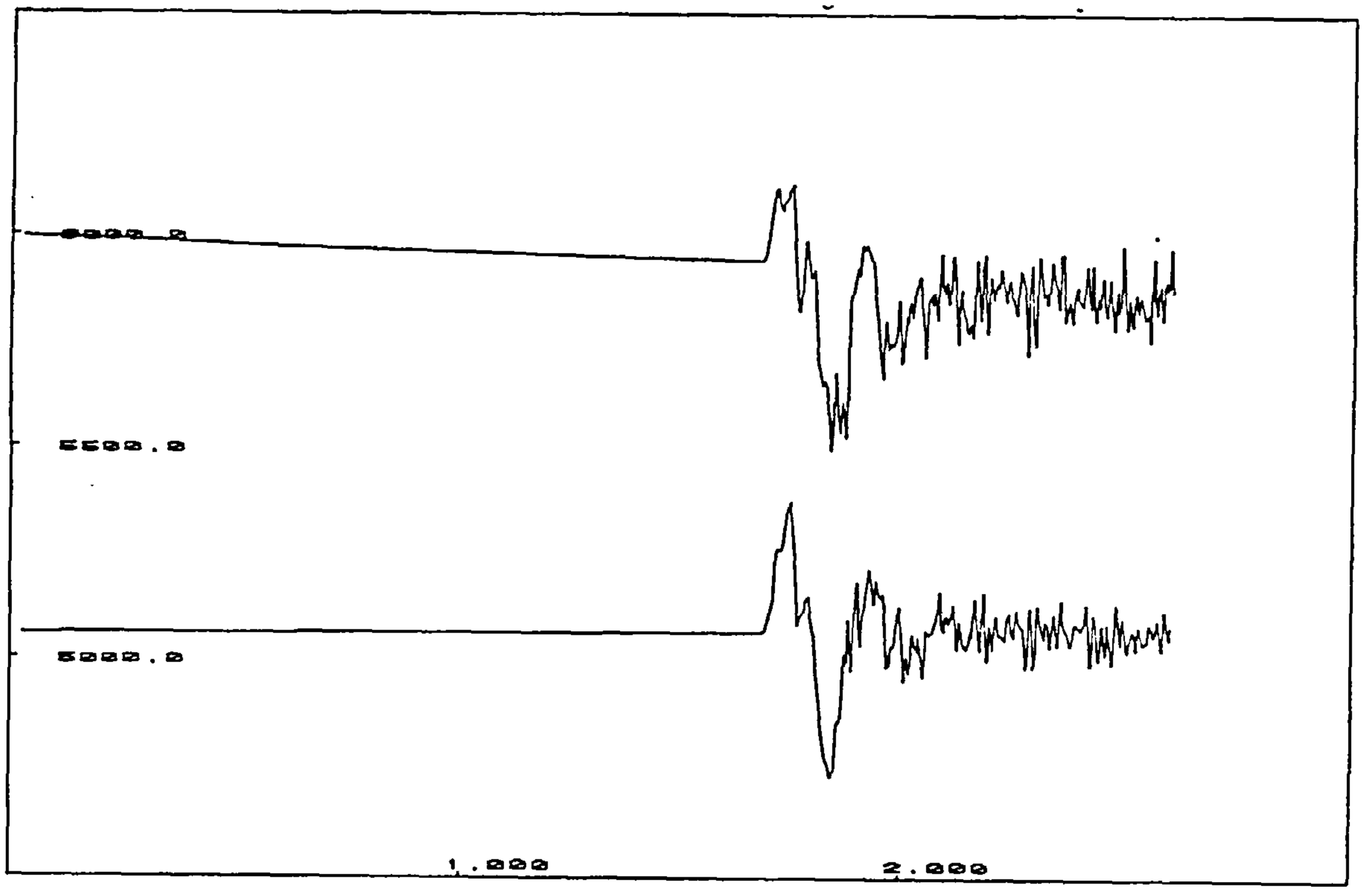

(a) Compressor Inlet and Outlet Pressure Time History

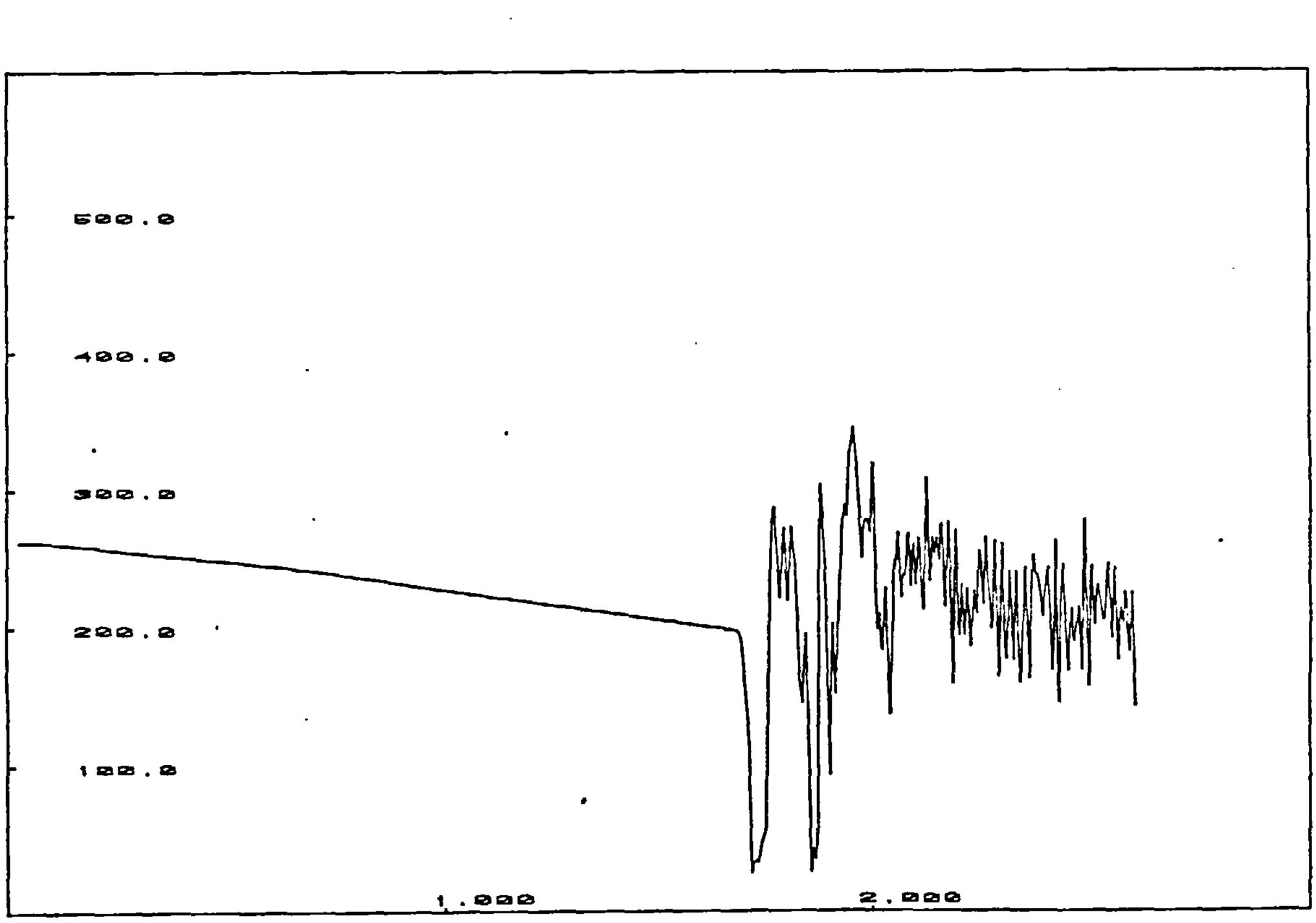

(b) Compressor Mass Flow Time History

Figure 6.45 Speed Transient and the Opening of Recycle Valve to Avoid Surge Conditions.

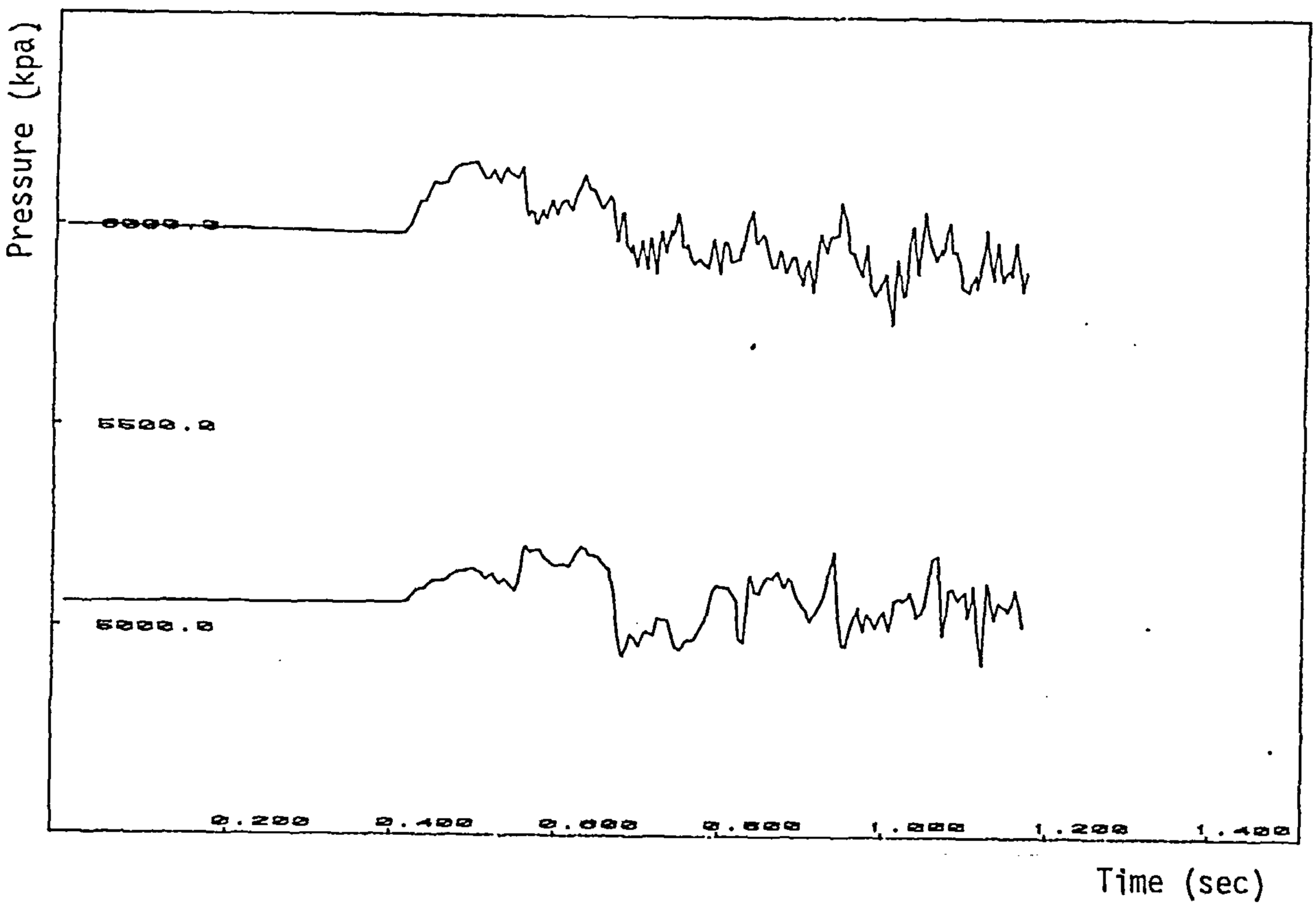

(a) Compressor Inlet and Outlet Pressure Time History

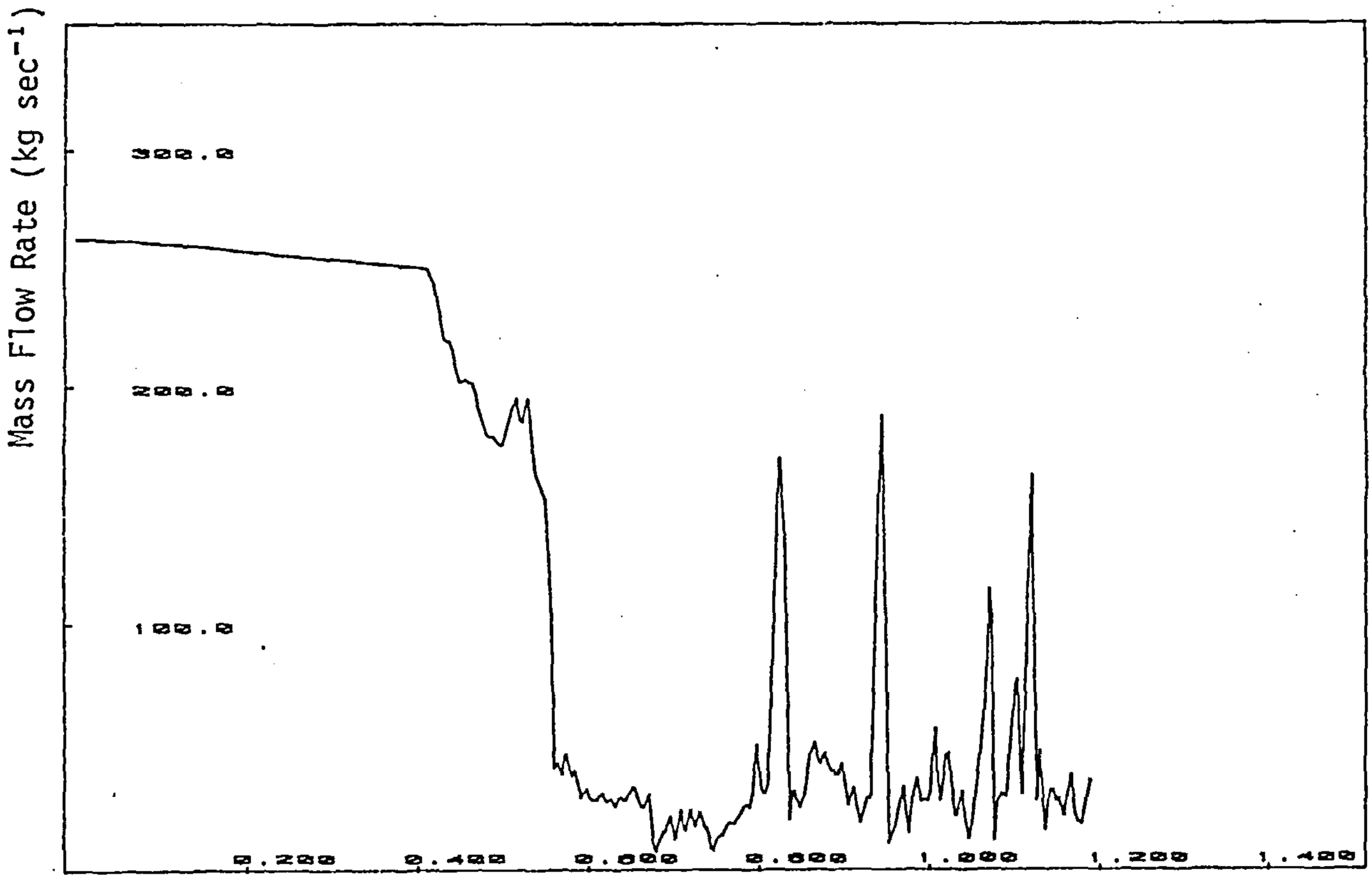

(b) Compressor Mass Flow Time History

Figure 6.46 Speed Transient with Reduced Pressure Loss in Non-Return Valves.

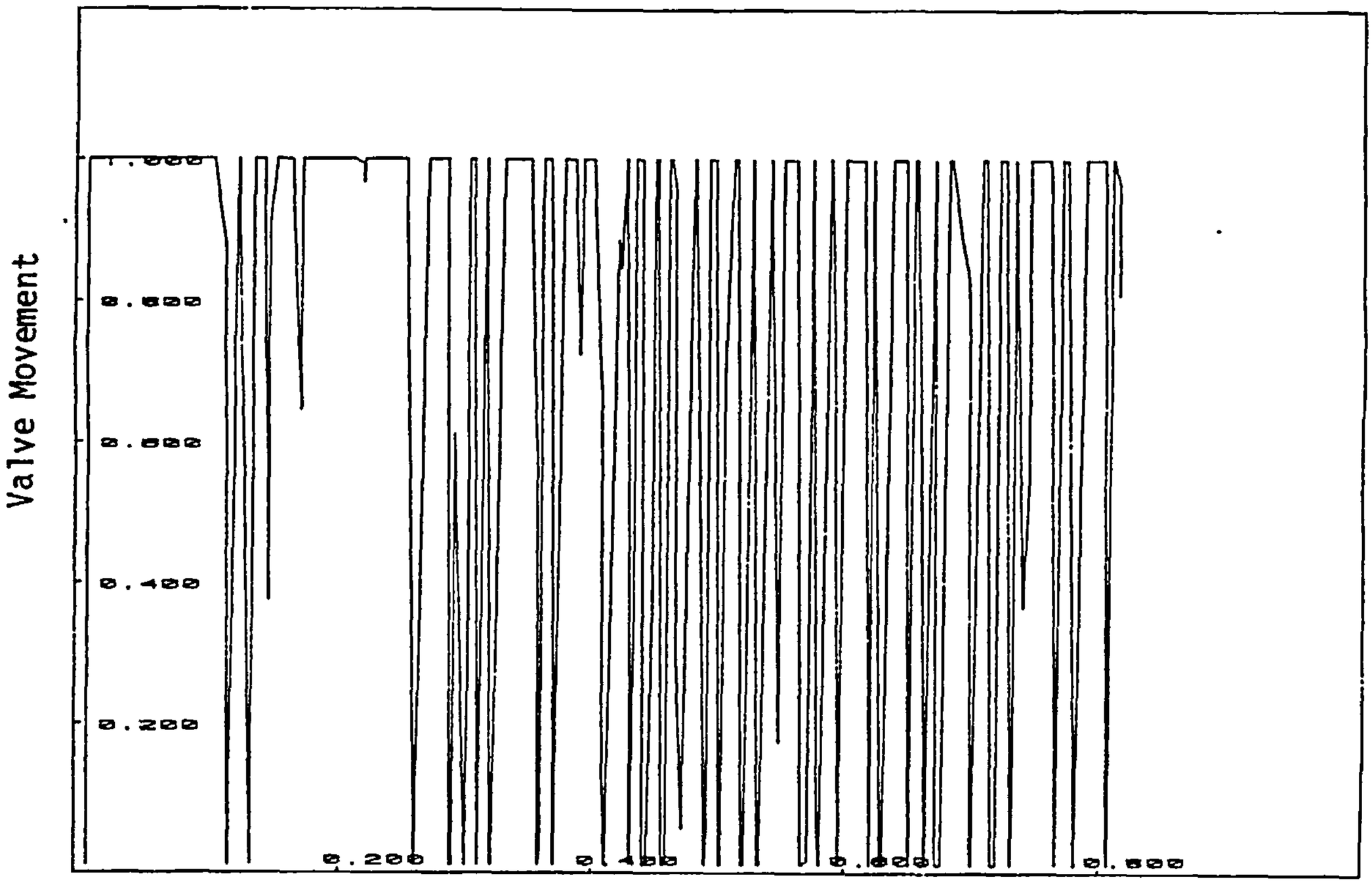

Figure 6.47a Non-Return Valve (1) Movement due to Speed Transient with reduced Pressure Loss in Non-Return Valves

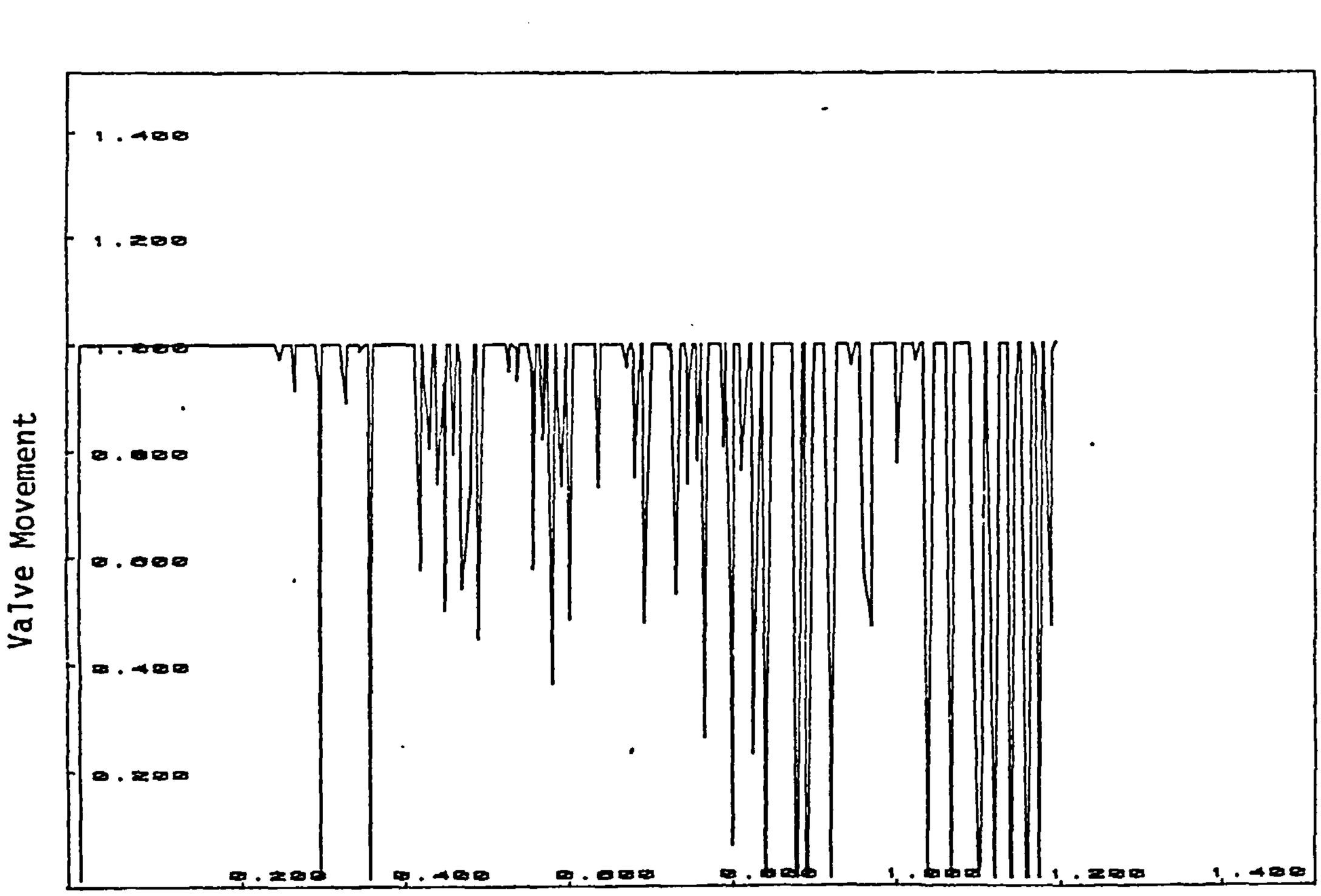

Figure 6.47b Non-Return Valve (2) Movement due to Speed Transient with reduced Pressure Loss in Non-Return Valves

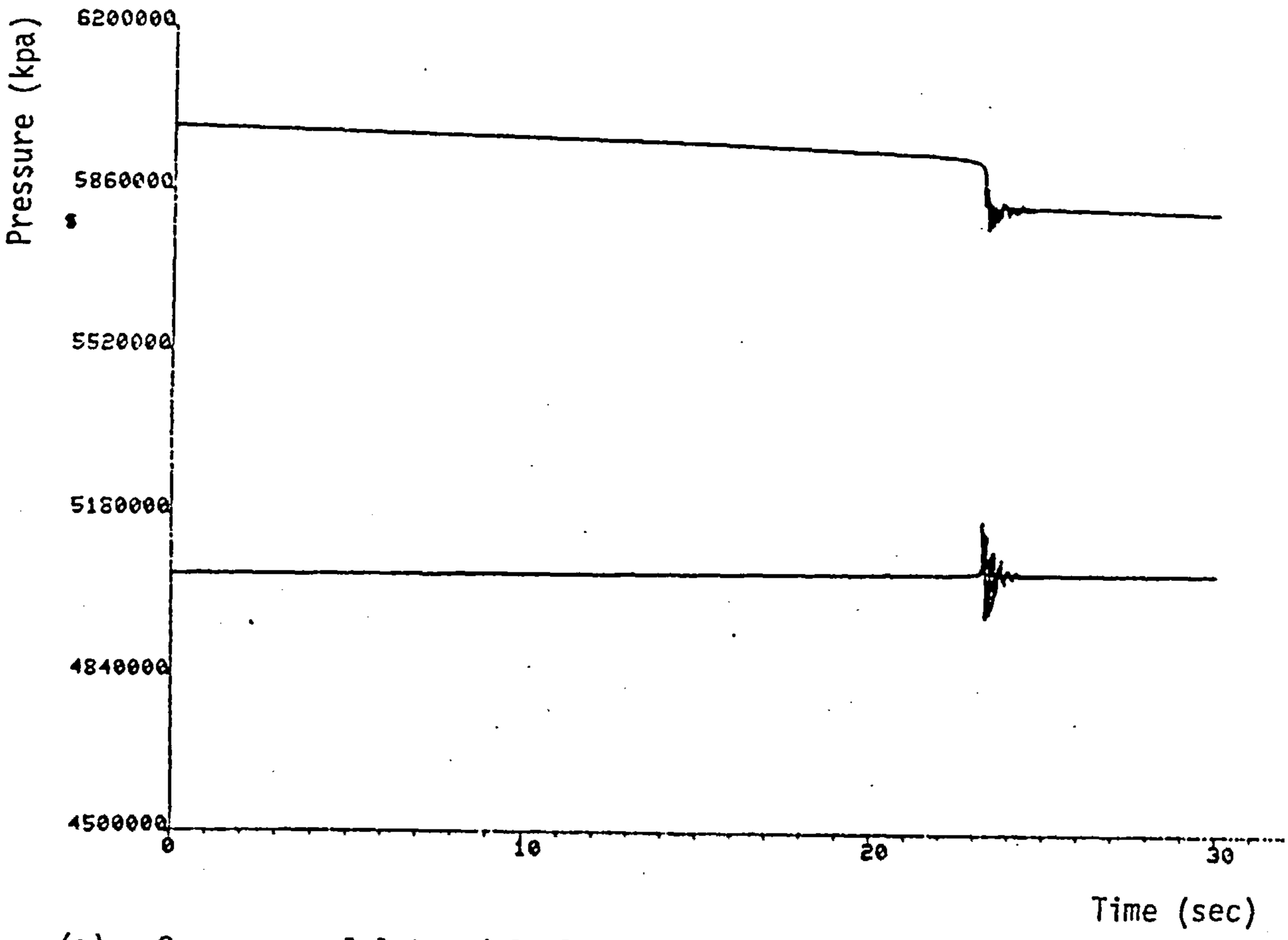

(a) Compressor Inlet and Outlet Pressure Time History

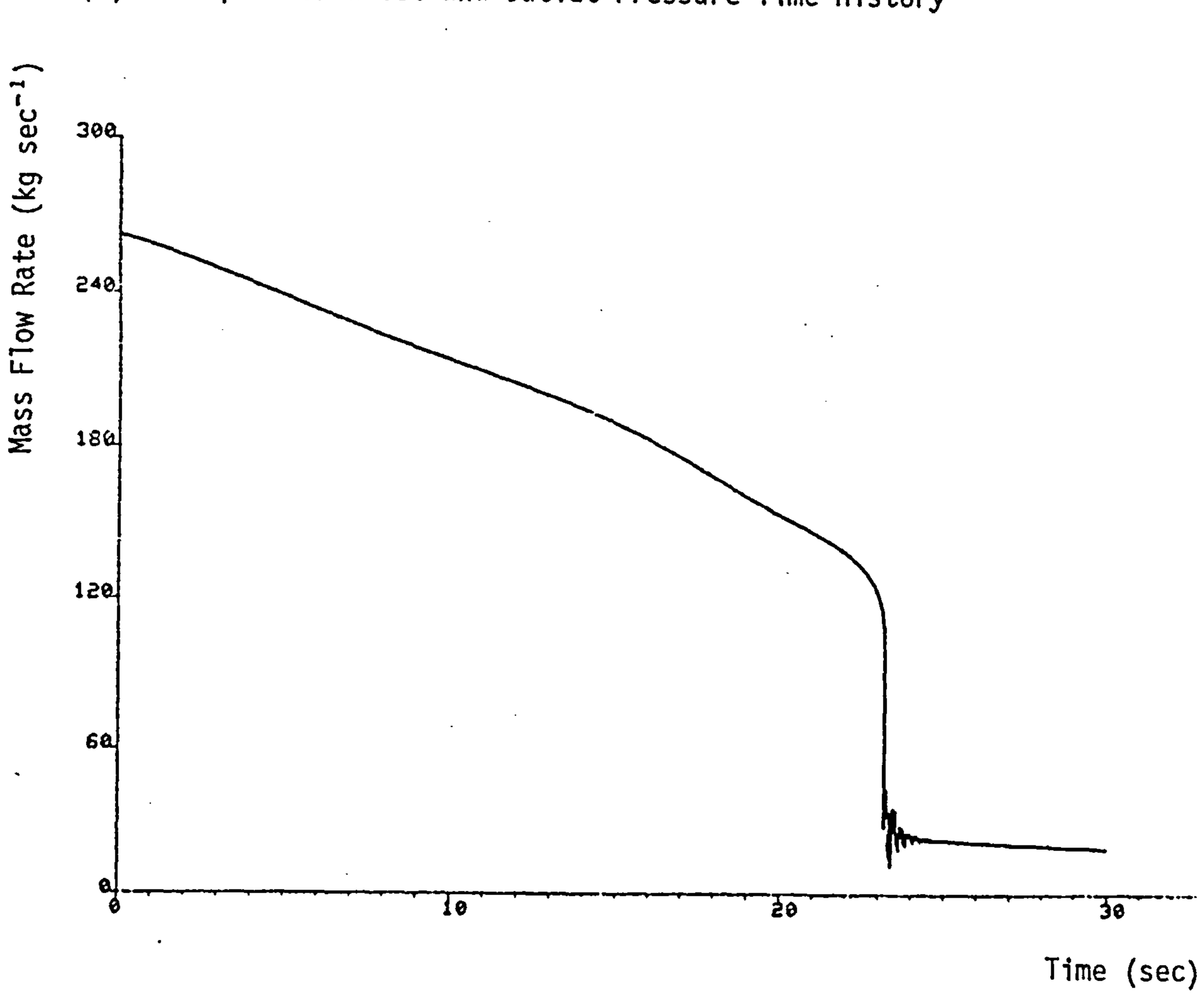

(b) Compressor Entry Mass Flow Time History.

Figure 6.48 Speed Transient (deceleration rate = 25 rpm sec^{-1}) with no Downstream Non-Return Valves.

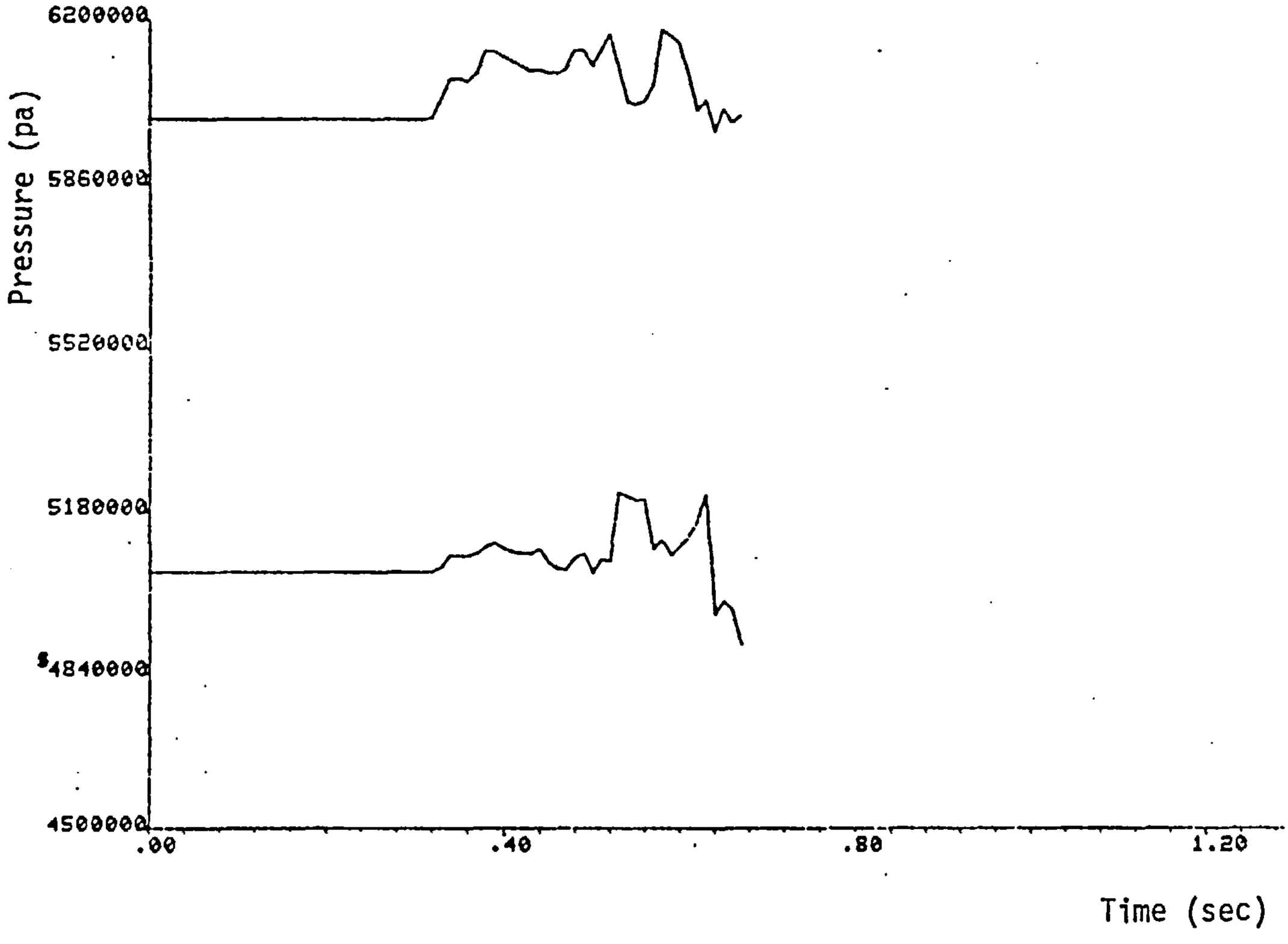

(a) Compressor Inlet and Outlet Pressure Time History

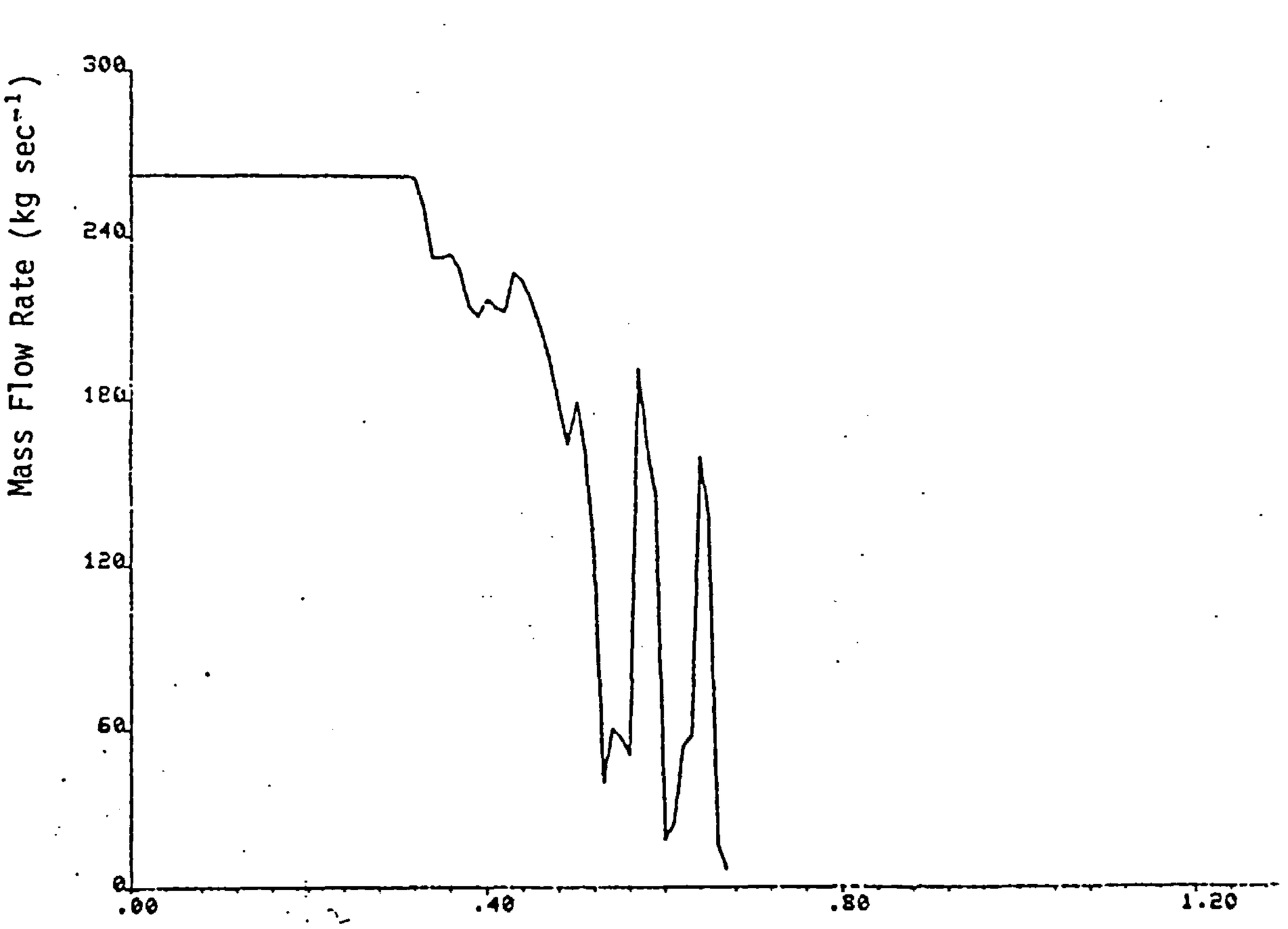

(b) Compressor Entry Mass Flow Time History

Figure 6.49 Speed Transient (deceleration = 25 rpm sec^{-1}) with reduced Pressure Loss in Non-Return Valve

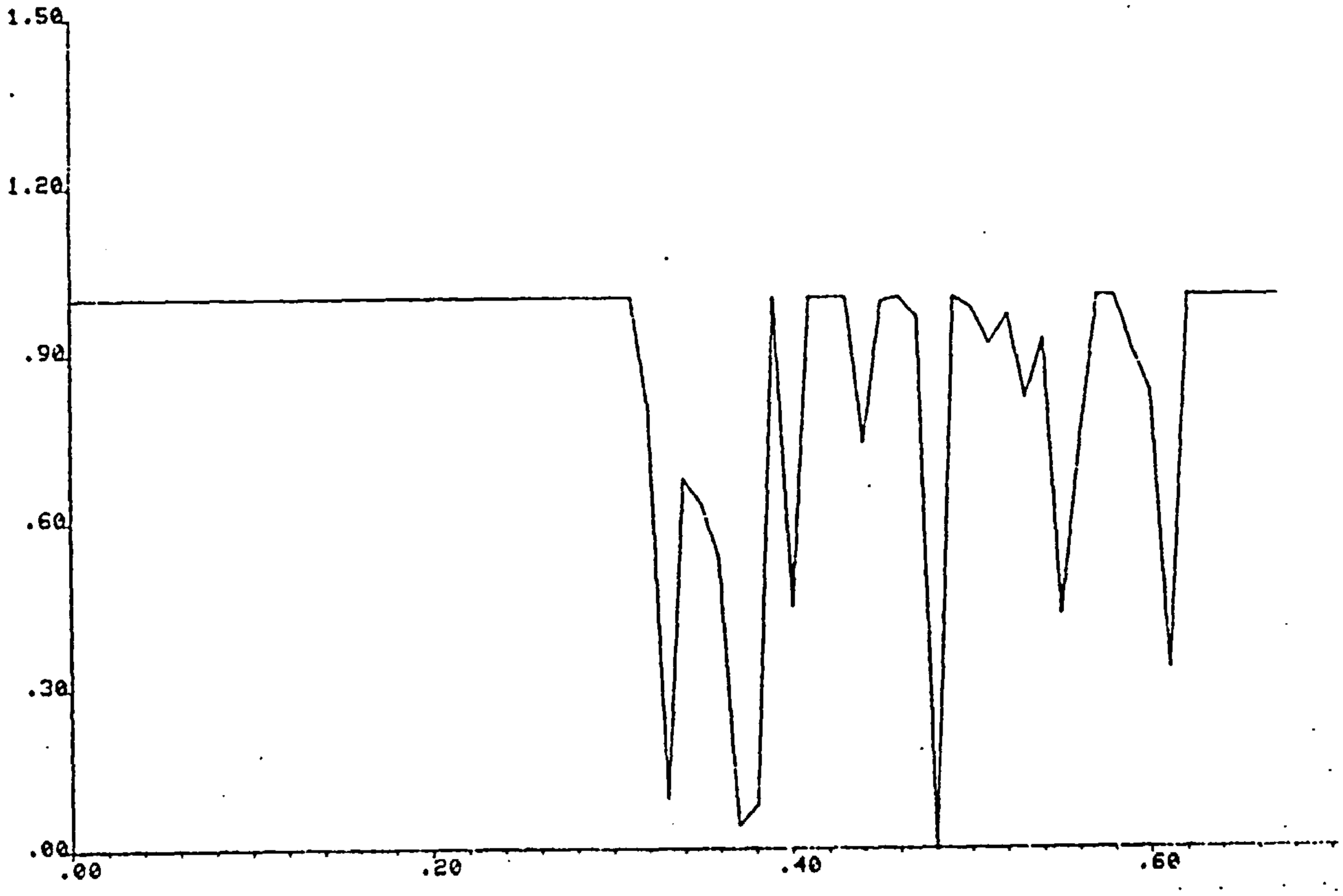

Figure 6.50a Non-Return Valve (1) Movement due to Reduced Pressure Loss in Non-Return Valves. (Deceleration = 25 rpm sec^{-1})

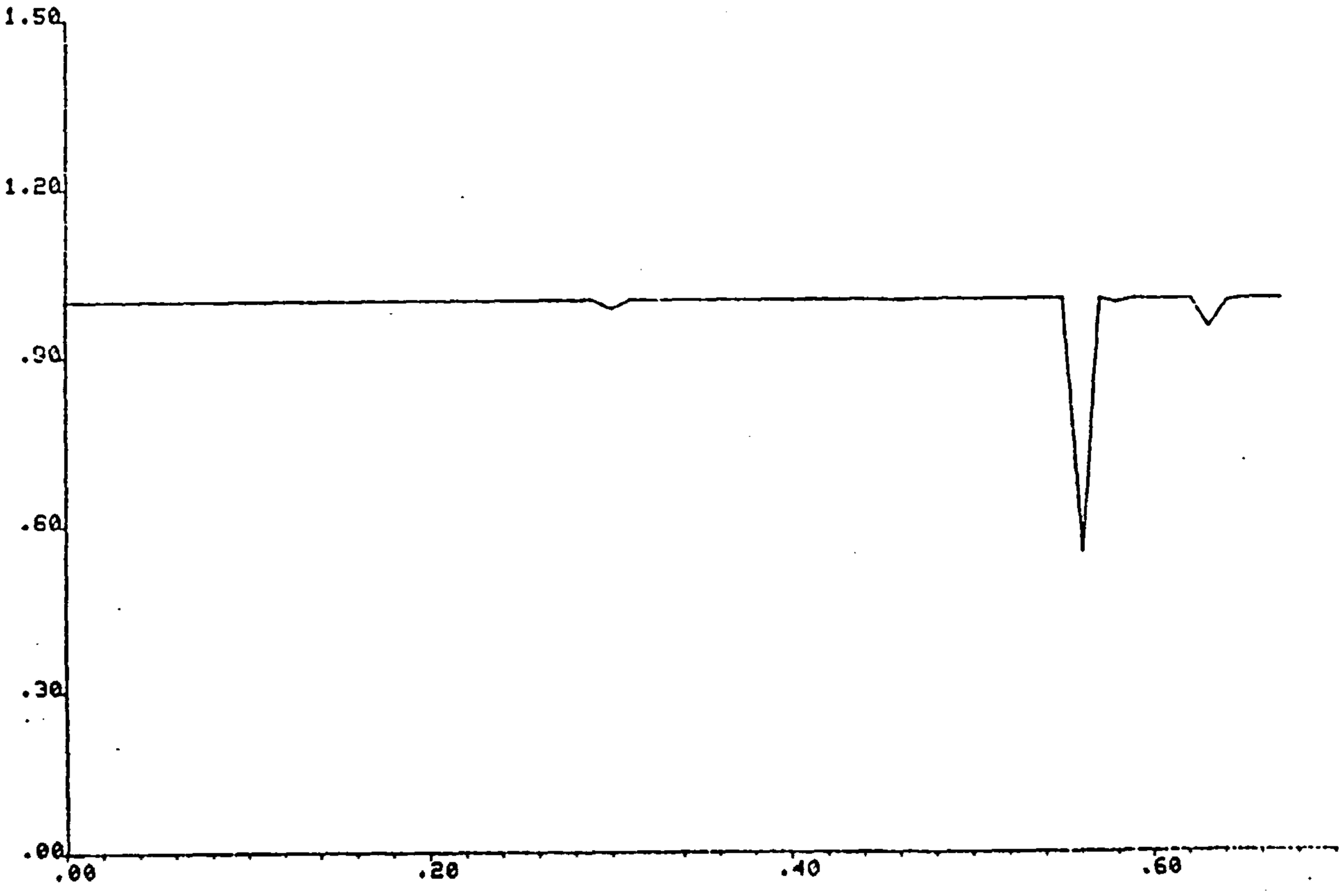

Figure 6.50b Non-Return Valve (2) Movement due to reduced Pressure Loss in Non-Return Valves. (Deceleration = 25 rpm sec^{-1})

COMPRESSOR CHARACTERISTIC POLYTROPIC HEAD Vs VOLUME FLOW RATE
△ SPEED = -25 R.P.M/s
WITH NON-RETURN VALUES DOWNSTEAM

POINT	TIME(S)
1	0.00
2	0.35
3	0.41
4	0.44
5	0.49
6	0.56
7	0.60
8	0.67

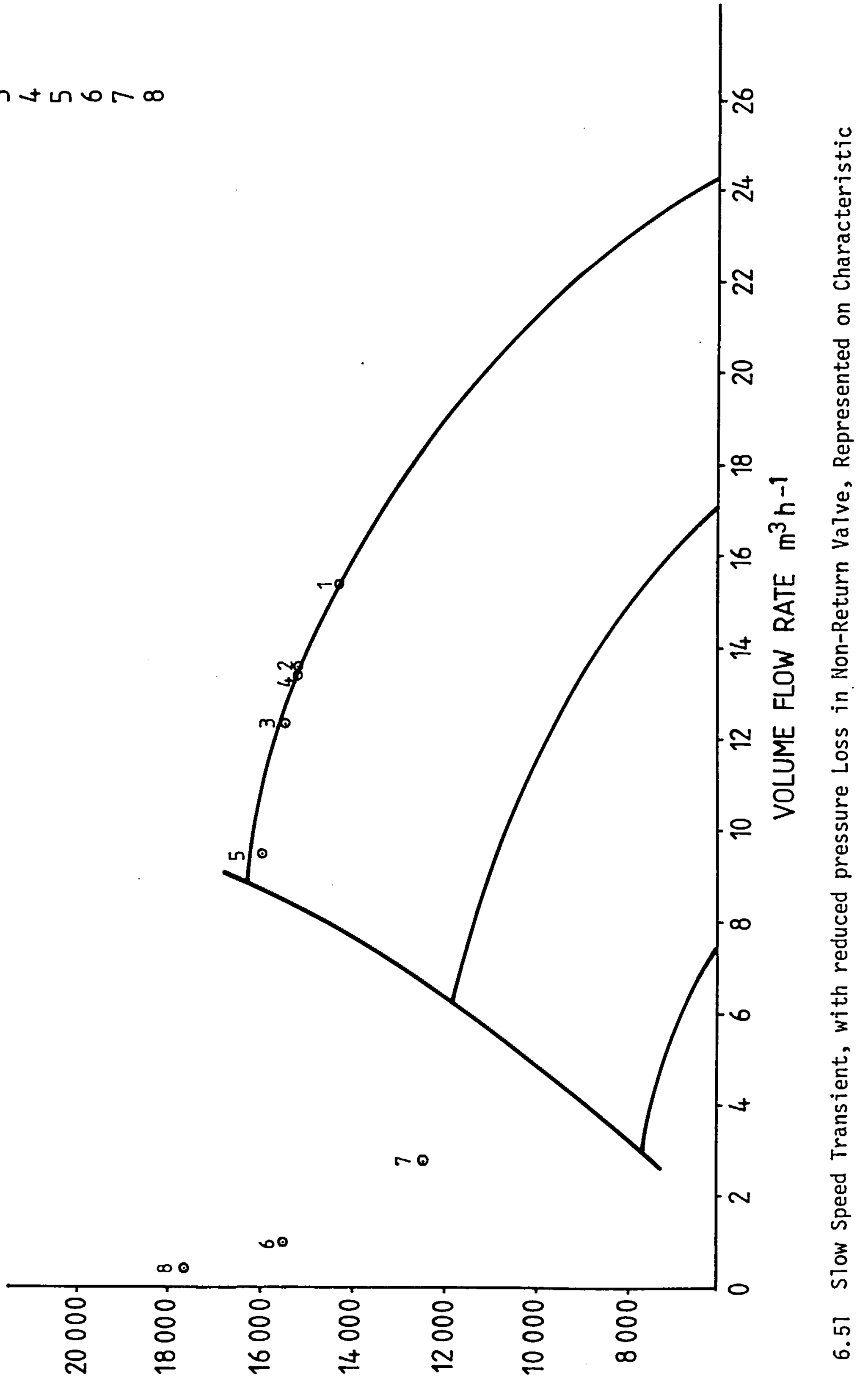

FIG. 6.51 Slow Speed Transient, with reduced pressure Loss in Non-Return Valve, Represented on Characteristic

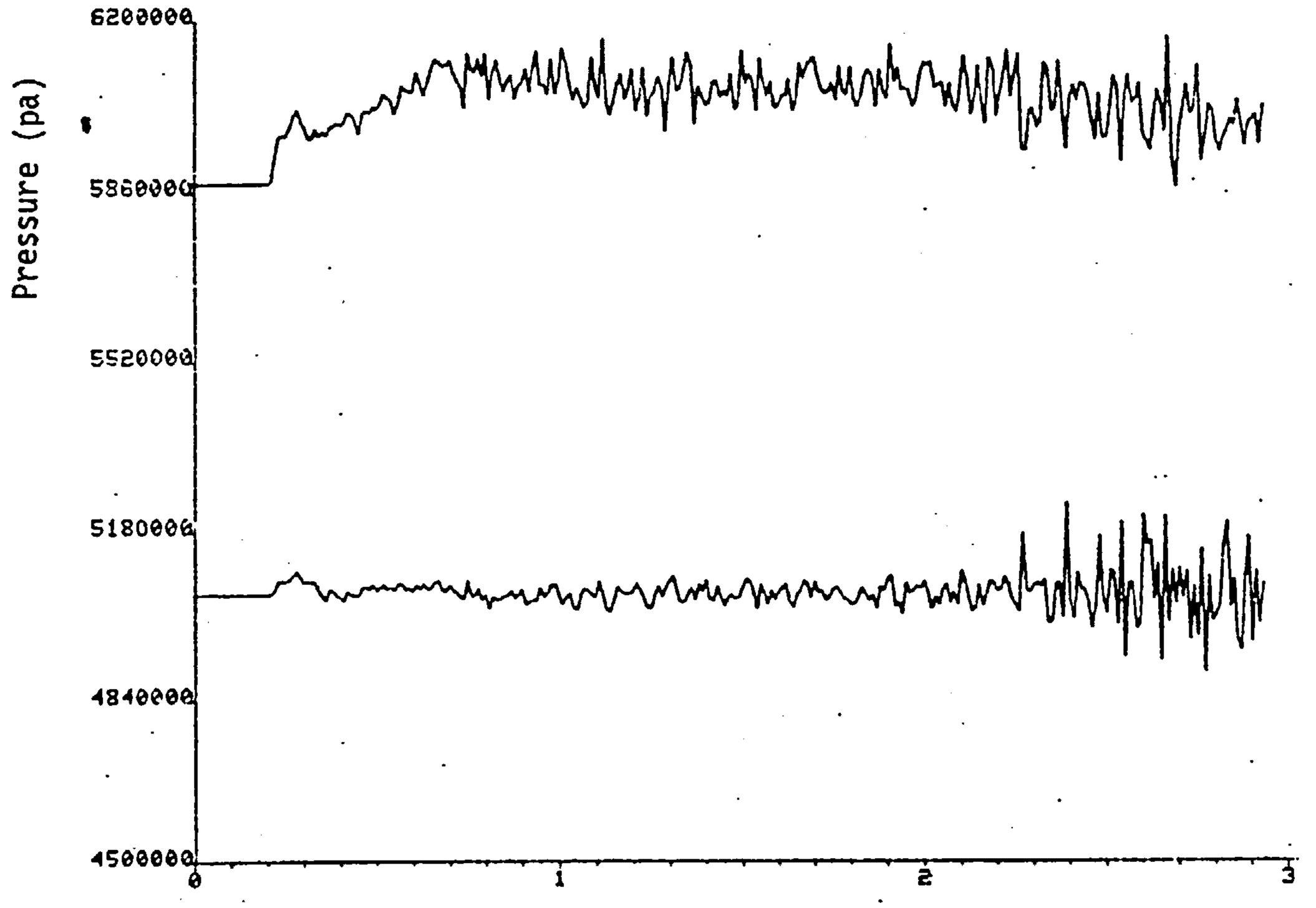

(a) Compressor Inlet and Outlet Pressure Time History

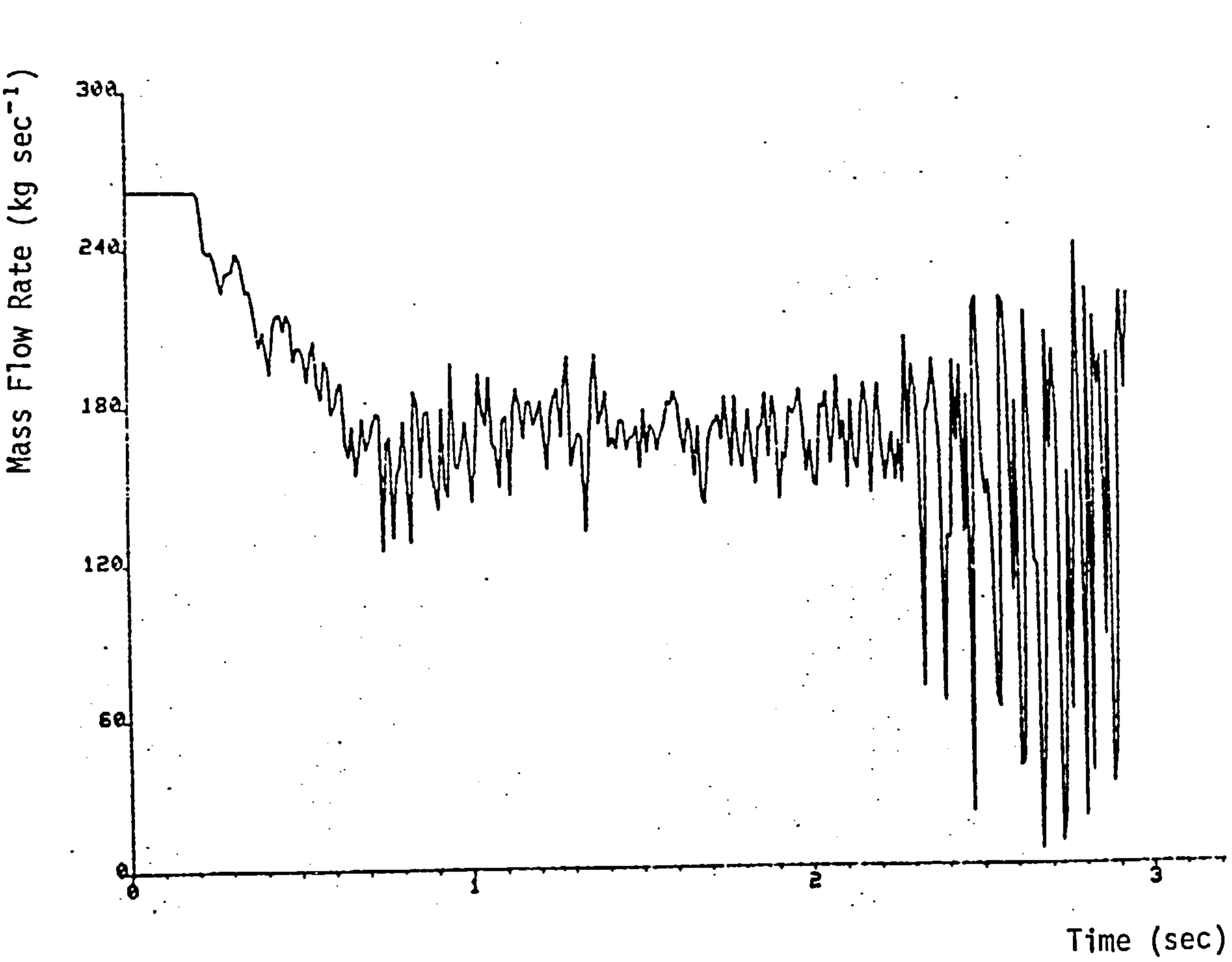

(b) Compressor Entry Mass Flow Time History

Figure 6.52 Speed Transient with Steep Compressor Characteristic and reduced pressure loss in non-return valves.

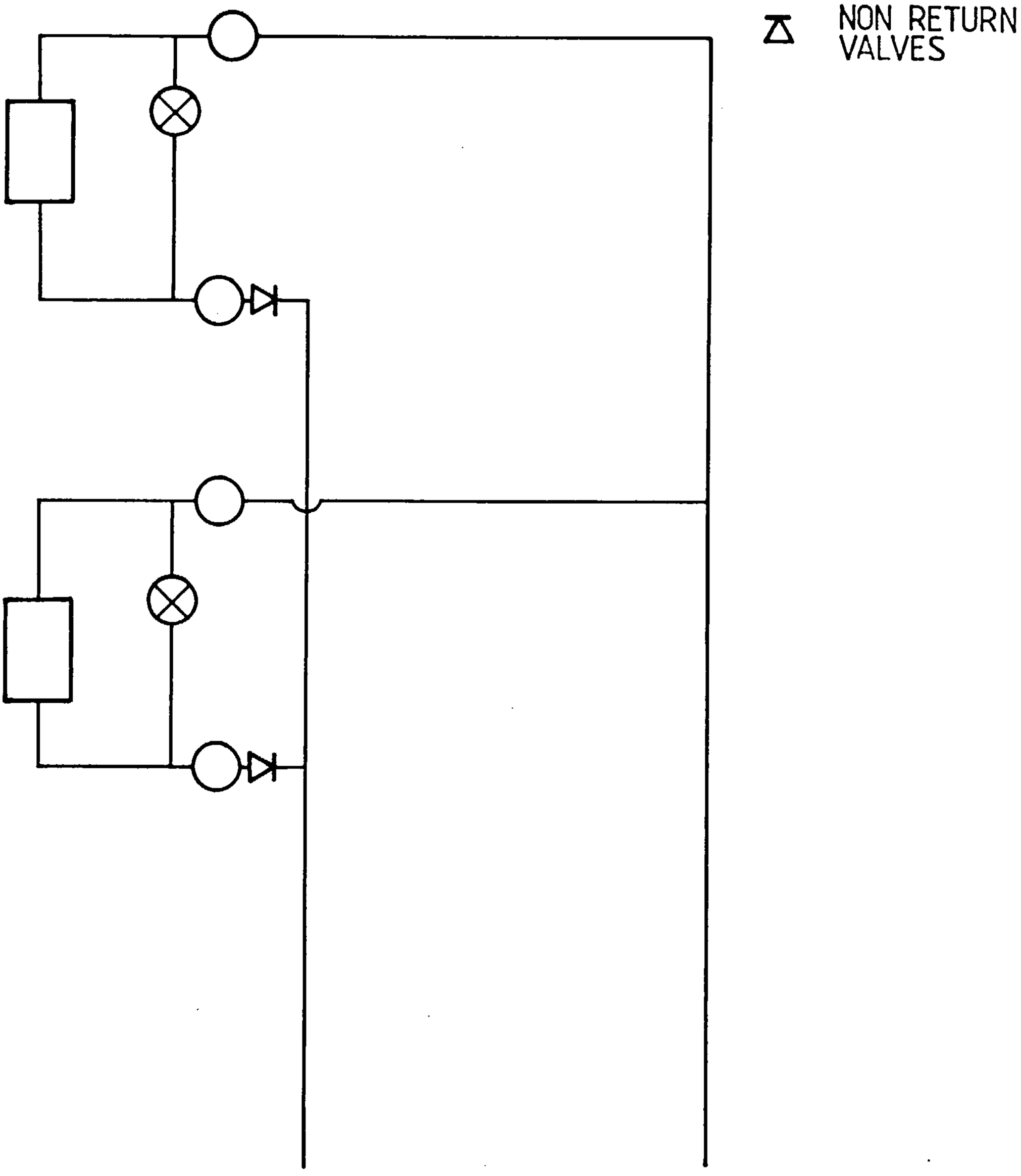

FIG.6·53 PROPOSED LAYOUT OF TRANSMISSION STATION